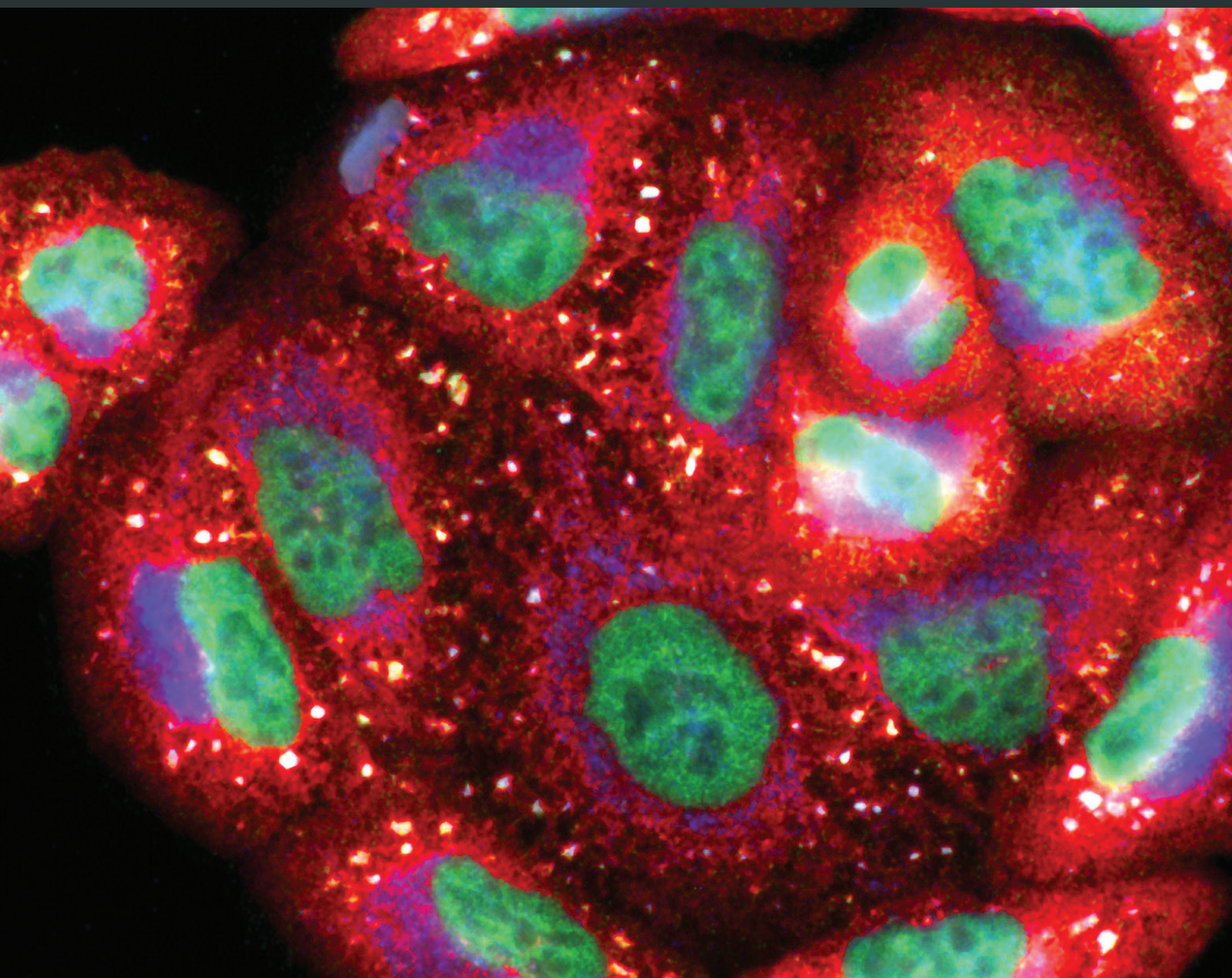


Oxidative Medicine and Cellular Longevity

# Phytochemicals in Cardiovascular and Respiratory Diseases: Evidence in Oxidative Stress and Inflammation

Lead Guest Editor: Raluca M. Pop

Guest Editors: Ada Popolo, Adrian P. Trifa, and Luminita A. Stanciu





---

# **Phytochemicals in Cardiovascular and Respiratory Diseases: Evidence in Oxidative Stress and Inflammation**

## **Phytochemicals in Cardiovascular and Respiratory Diseases: Evidence in Oxidative Stress and Inflammation**

Lead Guest Editor: Raluca M. Pop

Guest Editors: Ada Popolo, Adrian P. Trifa,  
and Luminita A. Stanciu



Copyright © 2018 Hindawi. All rights reserved.

This is a special issue published in “Oxidative Medicine and Cellular Longevity.” All articles are open access articles distributed under the Creative Commons Attribution License, which permits unrestricted use, distribution, and reproduction in any medium, provided the original work is properly cited.



## Editorial Board

Dario Acuña-Castroviejo, Spain  
Fabio Altieri, Italy  
Fernanda Amicarelli, Italy  
José P. Andrade, Portugal  
Cristina Angeloni, Italy  
Antonio Ayala, Spain  
Elena Azzini, Italy  
Peter Backx, Canada  
Damian Bailey, UK  
Grzegorz Bartosz, Poland  
Sander Bekeschus, Germany  
Ji C. Bihl, USA  
Consuelo Borrás, Spain  
Nady Braidy, Australia  
Darrell W. Brann, USA  
Ralf Braun, Germany  
Laura Bravo, Spain  
Vittorio Calabrese, Italy  
Amadou Camara, USA  
Gianluca Carnevale, Italy  
Roberto Carnevale, Italy  
Angel Catalá, Argentina  
Giulio Ceolotto, Italy  
Shao-Yu Chen, USA  
Ferdinando Chiaradonna, Italy  
Zhao Zhong Chong, USA  
Alin Ciobica, Romania  
Ana Cipak Gasparovic, Croatia  
Giuseppe Cirillo, Italy  
Maria R. Ciriolo, Italy  
Massimo Collino, Italy  
Manuela Corte-Real, Portugal  
Mark Crabtree, UK  
Manuela Curcio, Italy  
Andreas Daiber, Germany  
Felipe Dal Pizzol, Brazil  
Francesca Danesi, Italy  
Domenico D'Arca, Italy  
Claudio De Lucia, Italy  
Yolanda de Pablo, Sweden  
Sonia de Pascual-Teresa, Spain  
Cinzia Domenicotti, Italy  
Joël R. Drevet, France  
Grégory Durand, France

Javier Egea, Spain  
Ersin Fadillioglu, Turkey  
Ioannis G. Fatouros, Greece  
Qingping Feng, Canada  
Gianna Ferretti, Italy  
Giuseppe Filomeni, Italy  
Swaran J. S. Flora, India  
Teresa I. Fortoul, Mexico  
Jeferson L. Franco, Brazil  
Rodrigo Franco, USA  
Joaquin Gadea, Spain  
José Luís García-Giménez, Spain  
Gerardo García-Rivas, Mexico  
Janusz Gebicki, Australia  
Alexandros Georgakilas, Greece  
Husam Ghanim, USA  
Eloisa Gitto, Italy  
Daniela Giustarini, Italy  
Saeid Golbidi, Canada  
Aldrin V. Gomes, USA  
Tilman Grune, Germany  
Nicoletta Guaragnella, Italy  
Solomon Habtemariam, UK  
Eva-Maria Hanschmann, Germany  
Tim Hofer, Norway  
John D. Horowitz, Australia  
Silvana Hrelia, Italy  
Stephan Immenschuh, Germany  
Maria G. Isaguliant, Sweden  
Luigi Iuliano, Italy  
Vladimir Jakovljevic, Serbia  
Marianna Jung, USA  
Peeter Karihtala, Finland  
Eric E. Kelley, USA  
Kum Kum Khanna, Australia  
Neelam Khaper, Canada  
Thomas Kietzmann, Finland  
Demetrios Kouretas, Greece  
Andrey V. Kozlov, Austria  
Jean-Claude Lavoie, Canada  
Simon Lees, Canada  
Christopher Horst Lillig, Germany  
Paloma B. Liton, USA  
Ana Lloret, Spain

Lorenzo Loffredo, Italy  
Daniel Lopez-Malo, Spain  
Antonello Lorenzini, Italy  
Nageswara Madamanchi, USA  
Kenneth Maiese, USA  
Marco Malaguti, Italy  
Tullia Maraldi, Italy  
Reiko Matsui, USA  
Juan C. Mayo, Spain  
Steven McNulty, USA  
Antonio Desmond McCarthy, Argentina  
Bruno Meloni, Australia  
Pedro Mena, Italy  
Víctor Manuel Mendoza-Núñez, Mexico  
Maria U Moreno, Spain  
Trevor A. Mori, Australia  
Ryuichi Morishita, Japan  
Fabiana Morroni, Italy  
Luciana Mosca, Italy  
Ange Mouithys-Mickalad, Belgium  
Iordanis Mourouzis, Greece  
Danina Muntean, Romania  
Colin Murdoch, UK  
Pablo Muriel, Mexico  
Ryoji Nagai, Japan  
David Nieman, USA  
Hassan Obied, Australia  
Julio J. Ochoa, Spain  
Pál Pacher, USA  
Pasquale Pagliaro, Italy  
Valentina Pallottini, Italy  
Rosalba Parenti, Italy  
Vassilis Paschalis, Greece  
Daniela Pellegrino, Italy  
Ilaria Peluso, Italy  
Claudia Penna, Italy  
Serafina Perrone, Italy  
Tiziana Persichini, Italy  
Shazib Pervaiz, Singapore  
Vincent Pialoux, France  
Ada Popolo, Italy  
José L. Quiles, Spain  
Walid Rachidi, France  
Zsolt Radak, Hungary



---




Namakkal S. Rajasekaran, USA  
Kota V. Ramana, USA  
Sid D. Ray, USA  
Hamid Reza Rezvani, France  
Alessandra Ricelli, Italy  
Paola Rizzo, Italy  
Francisco J. Romero, Spain  
Joan Roselló-Catafau, Spain  
H. P. Vasantha Rupasinghe, Canada  
Gabriele Saretzki, UK  
Nadja Schroder, Brazil  
Sebastiano Sciarretta, Italy  
Honglian Shi, USA

Cinzia Signorini, Italy  
Mithun Sinha, USA  
Carla Tatone, Italy  
Frank Thévenod, Germany  
Shane Thomas, Australia  
Carlo Tocchetti, Italy  
Angela Trovato Salinaro, Jamaica  
Paolo Tucci, Italy  
Rosa Tundis, Italy  
Giuseppe Valacchi, Italy  
Jeannette Vasquez-Vivar, USA  
Daniele Vergara, Italy  
Victor M. Victor, Spain



László Virág, Hungary  
Natalie Ward, Australia  
Philip Wenzel, Germany  
Anthony R. White, Australia  
Georg T. Wondrak, USA  
Michal Wozniak, Poland  
Sho-ichi Yamagishi, Japan  
Liang-Jun Yan, USA  
Guillermo Zalba, Spain  
Jacek Zielonka, USA  
Mario Zoratti, Italy

## Contents





### **Phytochemicals in Cardiovascular and Respiratory Diseases: Evidence in Oxidative Stress and Inflammation**

Raluca M. Pop , Ada Popolo , Adrian P. Trifa , and Luminita A. Stanciu  
Editorial (3 pages), Article ID 1603872, Volume 2018 (2018)

### **Phytochemical Analysis of Anti-Inflammatory and Antioxidant Effects of *Mahonia aquifolium* Flower and Fruit Extracts**

Andra-Diana Andreicut, Alina Elena Pârvu , Augustin Cătălin Mot, Marcel Pârvu, Eva Fischer Fodor, Adriana Florinela Cătoi , Vasile Feldrihan, Mihai Cecan, and Alexandru Irimie  
Research Article (12 pages), Article ID 2879793, Volume 2018 (2018)

### **Anti-Inflammatory Activity of *Boswellia serrata* Extracts: An *In Vitro* Study on Porcine Aortic Endothelial Cells**

Martina Bertocchi , Gloria Isani , Federica Medici, Giulia Andreani , Irvin Tubon Usca , Paola Roncada, Monica Forni , and Chiara Bernardini   
Research Article (9 pages), Article ID 2504305, Volume 2018 (2018)




### **How Could We Influence Systemic Inflammation in Allergic Rhinitis? The Role of H1 Antihistamines**

Ioana Adriana Muntean, Ioana Corina Bocsan , Nicolae Miron, Anca Dana Buzoianu, and Diana Deleanu  
Research Article (8 pages), Article ID 3718437, Volume 2018 (2018)

### **Ganoderma Triterpenoids Exert Antiatherogenic Effects in Mice by Alleviating Disturbed Flow-Induced Oxidative Stress and Inflammation**

Pei-Ling Hsu, Yung-Ching Lin, Hao Ni, and Fan-E Mo   
Research Article (11 pages), Article ID 3491703, Volume 2018 (2018)


### **Chemerin, Inflammatory, and Nitrooxidative Stress Marker Changes Six Months after Sleeve Gastrectomy**

Adriana Florinela CÔȘtoi , Alina Elena Pârvu , Aurel Mironiuc, Ștefan Chiorescu, Alexandra Crăciun, Ioana Delia Pop , and Cornel CÔȘtoi  
Research Article (7 pages), Article ID 1583212, Volume 2018 (2018)

### **Polyphenolic Compounds, Antioxidant, and Cardioprotective Effects of Pomace Extracts from Fetească Neagră Cultivar**

Ștefania Silvia Balea, Alina Elena Pârvu , Nastasia Pop, Fernando Zamora Marín, and Marcel Pârvu  
Research Article (11 pages), Article ID 8194721, Volume 2018 (2018)

### **SIRT3: A New Regulator of Cardiovascular Diseases**

Wei Sun, Caixia Liu, Qiuhui Chen, Ning Liu, Youyou Yan, and Bin Liu   
Review Article (11 pages), Article ID 7293861, Volume 2018 (2018)

## Editorial

# Phytochemicals in Cardiovascular and Respiratory Diseases: Evidence in Oxidative Stress and Inflammation

Raluca M. Pop<sup>1</sup>, Ada Popolo<sup>2</sup>, Adrian P. Trifa<sup>3</sup>, and Luminita A. Stanciu<sup>4</sup>

<sup>1</sup>Department of Pharmacology, Toxicology and Clinical Pharmacology, “Iuliu Hatieganu” University of Medicine and Pharmacy, Cluj-Napoca, Romania

<sup>2</sup>Department of Pharmacy, University of Salerno, Fisciano, Salerno, Italy

<sup>3</sup>Department of Genetics, “Iuliu Hatieganu” University of Medicine and Pharmacy, Cluj-Napoca, Romania

<sup>4</sup>National Heart and Lung Institute, Imperial College London, London, UK

Correspondence should be addressed to Raluca M. Pop; [raluca\\_parlog@yahoo.com](mailto:raluca_parlog@yahoo.com)

Received 3 June 2018; Accepted 3 June 2018; Published 9 August 2018

Copyright © 2018 Raluca M. Pop et al. This is an open access article distributed under the Creative Commons Attribution License, which permits unrestricted use, distribution, and reproduction in any medium, provided the original work is properly cited.

Cardiovascular and respiratory diseases are amongst the leading cause of mortality worldwide. Within these pathologies, excessive oxidative stress and chronic inflammation are important factors with a role in their pathogenesis. Recent studies suggested that natural compounds can be successfully used in order to prevent, control, or block disease progression by targeting oxidative stress and inflammatory mediators. Therefore, this special issue focused on following aims: (i) to understand the mechanisms of initiation and progression of CVD and respiratory disease within the context of oxidative stress and inflammation and (ii) to highlight phytochemical potential in everyday life, by bringing evidence of their properties related to the oxidation and inflammatory processes from CVD and respiratory diseases.

The collection of the review and original research articles in this special issue is approaching a wide range of topics from supplements used in cardiovascular disease prevention or treatment and regulators of cardiovascular diseases to lifestyle interventions like surgical interventions that can potentially reduce cardiovascular risks. Also, new perspectives regarding allergic rhinitis disease management conditions were discussed.

In the original research article, A.-D. Andreicut et al. investigated the phytochemical composition of the flowers, green fruits, and ripe fruits of *Mahonia aquifolium* (*M. aquifolium*) ethanolic extracts and their

antioxidant and anti-inflammatory properties. The *in vivo* anti-inflammatory and antioxidant effects were investigated using a rat turpentine oil-induced acute inflammation model. The authors proved the antioxidant activity and anti-inflammatory effects of the ethanolic extracts by comparing them to diclofenac. All extracts decreased serum nitric oxide (NOx), total oxidative status (TOS), and 3-nitrotyrosine (3NT) and increased total thiols (SH). The variation of malondialdehyde (MDA) was not influenced by the extracts while TNF- $\alpha$  was also reduced. Total antioxidant reactivity (TAR) was increased only when flower and green fruit ethanolic extracts were used. Finally, the authors support the use of *M. aquifolium* in the prevention of the inflammatory processes.

Ş. S. Balea et al. investigated the effect of phenolic compounds from fresh and fermented pomace extracts, their antioxidant, and cardioprotective properties using the isoprenaline-induced myocardial ischemia model in rats. Taking into account the actual trend of reducing oxidative stress with herbal supplements or functional foods with antioxidant properties, the authors evaluated the grape pomace *in vitro* antioxidant activity using the most frequently used method like DPPH test. Following, they further investigated the grape pomace extracts *in vivo* cardioprotective properties by ECG monitoring and measuring creatine kinase, aspartate transaminase, and alanine transaminase serum levels. The

*in vivo* antioxidant effects were also evaluated measuring TOS, TAR, MDA, SH, GSH, and NOx serum values. They showed that the high total phenolic content in both fresh or fermented grape pomace extracts presented good *in vitro* antioxidant activity, which improved *in vivo* cardiac and oxidative stress parameters. Overall, their findings suggest that grape pomace extract pretreatment may be used as an option for heart preconditioning.

Next, M. Bertocchi et al. investigated the cytotoxicity, anti-inflammatory, and angiogenic activities of *Boswellia serrata* (*B. serrata*) extracts on primary culture of porcine aortic endothelial cells (pAECs). Since *B. serrata* is being used in Ayurvedic medicine to treat different diseases with an inflammatory component, the authors of this study aimed to characterize the active molecules of *B. serrata* extracts and then further to evaluate their possible biological effects. Taking into account the great variability of phytochemical concentration and composition encountered in the commercial products, the authors underlined the importance of this aim which should be a prerequisite for testing any biological effect. Further, the anti-inflammatory and angiogenic properties of *B. serrata* extracts were tested using lipopolysaccharide- (LPS-) induced cytotoxicity by comparison with pure 11-keto- $\beta$ -boswellic acid (KBA), 3-O-acetyl-11-keto- $\beta$ -boswellic acid (AKBA), and  $\beta$ -boswellic acid ( $\beta$ BA), either individually or in different mixtures. They demonstrated that *B. serrata* extracts had a protective effect against LPS inflammatory stimulus in the endothelial cells. In particular, the hydroenzymatic extract presented the best results with cell viability completely restored at all studied doses and was free of cytotoxicity. The comparison of *Boswellia* extracts with the pure BAs suggested that the anti-inflammatory effect of the extracts was also related to the other bioactive molecules like triterpenes from their composition. Importantly, the authors underlined that proliferative stimulation can also occur instead of the protective effect depending on the used formulations. Thus, when used in humans and animals for its cardiovascular health, the concentration and the composition of the bioactive components should be carefully considered.

In their study, P.-L. Hsu et al. investigated the effect of *Ganoderma lucidum* (GL) in atherosclerosis using a carotid-artery-ligation mouse model. Through their article, the authors aimed to bring evidence regarding GL effect in atherosclerosis, still considered as a leading cause of death disease associated with chronic oxidative stress and inflammation. Being widely accepted and used as herbal supplements, especially in the traditional Chinese medicine, GL is commercially cultivated under controlled conditions with known chemical composition. The authors showed that GL protected the carotid artery from disturbed flow-induced atherogenesis, prevented carotid artery ligation-induced neointima formation, alleviated disturbed flow-induced oxidative stress and proatherogenic response in endothelial cells, suppressed oscillating flow-induced inflammatory response in endothelial cells, and protected endothelial cells against oxidative insults while deferred GT treatment effectively inhibited atherogenesis. Thus, their findings provide evidence that *Ganoderma*,

by its triterpenoid composition, possesses atheroprotective effects and could be used to enhance the *Ganoderma* supplement health benefits.

The cardiovascular disease problematic issue was also addressed by W. Sun et al. which investigated the potential role of sirtuin 3 (SIRT3) as a new regulator of cardiovascular diseases. They analyzed recent studies referring to the role of SIRT3 in CVD physiology and pathology, with emphasis on its regulating mechanisms in the cardiac processes. The authors aimed to find its prospects in clinical application. The role of SIRT3 in ischemic heart disease, in hypertrophy and heart failure, in the drug-induced cardiotoxicity, in diabetic cardiomyopathy and cardiac lipotoxicity, and in hypertension was discussed. Its protective effect against CVDs was suggested, emphasizing its important role in cellular energy metabolism, in the oxidative stress processes, and in apoptosis. Also, the components extracted from traditional Chinese medicine which promoted SIRT3-mediated cardioprotective effects were described.

A. F. Cătoi et al. investigated the variations of serum chemerin in patients with laparoscopic sleeve gastrectomy (SG) in order to assess its correlation with the inflammatory and nitrooxidative stress markers. They hypothesized and verified if the increased chemerin levels are changing 6 months after SG and whether these changes are influencing some specific inflammatory markers like high-sensitivity C-reactive protein (hsCRP), tumour necrosis factor alpha (TNF- $\alpha$ ), and nitrooxidative stress (NOx, TOS, TAR, and OSI). They were expecting that these variations could lead to a reduction of the cardiovascular risk. In the end, their study did not confirm significant changes in chemerin levels, neither in other inflammatory and nitrooxidative stress markers, with the exception of hsCRP and OSI levels, further investigations being needed in order to confirm their hypothesis.

Finally, in their study, the allergic rhinitis was approached by I. A. Muntean et al. which is considered an important risk factor for asthma's occurrence. The authors' aims were to target the minimal persistent systemic inflammation in allergic rhinitis investigating the role of H1 antihistamines. Thus the adhesion molecules' profile (intercellular cell adhesion molecule 1 (ICAM-1), vascular cell adhesion molecule 1 (VCAM-1), and E-selectin) was analyzed in patients with allergic rhinitis with focus on H1 antihistamine (desloratadine or levocetirizine) influence on these markers. H1 antihistamine treatment significantly improved the total symptom score and significantly decreased the levels of plasmatic eosinophils and total IgE and the levels of fractionate nitric oxide in exhaled air (FeNO) after 1 month of continuous therapy. Also, the plasmatic levels of ICAM-1 and E-selectin were significantly decreased. This study emphasized the 2nd generation H1 antihistamine anti-inflammatory role, which was demonstrated through CAM plasmatic level reduction, in patients with persistent allergic rhinitis, giving in this way new insights in allergic disease management.

Overall, the papers reported in this special issue highlight the importance of phytochemicals and their role in CVD



prevention. Moreover, the attention is focused on our understanding regarding their use in traditional medicine, on their safety and efficacy which are in strong correlation with plant extract composition and their phytochemical concentrations. New insight on better allergic rhinitis disease management is also provided.

*Raluca M. Pop*  
*Ada Popolo*  
*Adrian P. Trifa*  
*Luminita A. Stanciu*

## Research Article

# Phytochemical Analysis of Anti-Inflammatory and Antioxidant Effects of *Mahonia aquifolium* Flower and Fruit Extracts

Andra-Diana Andreicut,<sup>1</sup> Alina Elena Pârvu ,<sup>1</sup> Augustin Cătălin Mot,<sup>2</sup> Marcel Pârvu,<sup>3</sup> Eva Fischer Fodor,<sup>4,5</sup> Adriana Florinela Cătoi ,<sup>1</sup> Vasile Feldrihan,<sup>6</sup> Mihai Cecan,<sup>7</sup> and Alexandru Irimie<sup>8</sup>

<sup>1</sup>Department of Pathophysiology, Faculty of Medicine, “Iuliu Hațieganu” University of Medicine and Pharmacy, 3-4 Victor Babes Street, RO-400012 Cluj-Napoca, Romania

<sup>2</sup>Department of Chemistry, Faculty of Chemistry and Chemical Engineering, “Babes-Bolyai” University, 11 Arany Janos Street, RO-400028 Cluj-Napoca, Romania

<sup>3</sup>Department of Biology, Faculty of Biology and Geology, “Babes-Bolyai” University, 42 Republicii Street, RO-400015 Cluj-Napoca, Romania

<sup>4</sup>Medfuture Research Center for Advanced Medicine, “Iuliu Hațieganu” University of Medicine and Pharmacy, RO-400012 Cluj-Napoca, Romania

<sup>5</sup>Institute of Oncology “I. Chiricuta”, 34-36 Republicii Street, RO-400015 Cluj-Napoca, Romania

<sup>6</sup>Department of Immunology and Alergology, Faculty of Medicine, “Iuliu Hațieganu” University of Medicine and Pharmacy, 19-21 Croitorilor Street, RO-400162 Cluj-Napoca, Romania

<sup>7</sup>Faculty of Medicine, “Iuliu Hațieganu” University of Medicine and Pharmacy, 8 Babes Street, RO-400012 Cluj-Napoca, Romania

<sup>8</sup>Department of Oncology, Faculty of Medicine, “Iuliu Hațieganu” University of Medicine and Pharmacy, 34-36 Republicii Street, RO-400015 Cluj-Napoca, Romania

Correspondence should be addressed to Alina Elena Pârvu; [parvualinaelena@umfcluj.ro](mailto:parvualinaelena@umfcluj.ro)

Received 21 February 2018; Accepted 7 May 2018; Published 27 June 2018

Academic Editor: Ada Popolo

Copyright © 2018 Andra-Diana Andreicut et al. This is an open access article distributed under the Creative Commons Attribution License, which permits unrestricted use, distribution, and reproduction in any medium, provided the original work is properly cited.

Oxidative stress and inflammation are interlinked processes. The aim of the study was to perform a phytochemical analysis and to evaluate the antioxidant and anti-inflammatory activities of ethanolic *Mahonia aquifolium* flower (MF), green fruit (MGF), and ripe fruit (MRF) extracts. Plant extract chemical composition was evaluated by HPLC. A DPPH test was used for the *in vitro* antioxidant activity. The *in vivo* antioxidant effects and the anti-inflammatory potential were tested on a rat turpentine oil-induced inflammation, by measuring serum nitric oxide (NOx) and TNF-alpha, total oxidative status (TOS), total antioxidant reactivity (TAR), oxidative stress index (OSI), 3-nitrotyrosine (3NT), malondialdehyde (MDA), and total thiols (SH). Extracts were administrated orally in three dilutions (100%, 50%, and 25%) for seven days prior to inflammation. The effects were compared to diclofenac. The HPLC polyphenol and alkaloid analysis revealed chlorogenic acid as the most abundant compound. All extracts had a good *in vitro* antioxidant activity, decreased NOx, TOS, and 3NT, and increased SH. TNF-alpha was reduced, and TAR increased only by MF and MGF. MDA was not influenced. Our findings suggest that *M. aquifolium* has anti-inflammatory and antioxidant effects that support the use in primary prevention of the inflammatory processes.

## 1. Introduction

The relation between antioxidants and degenerative diseases is a topic that focuses the attention of many researchers nowadays [1]. Reactive oxygen species (ROS) result from the

oxidative processes in every living organism, as part of the aerobic metabolism. They are represented by superoxide anion, hydrogen peroxide, and hydroxyl radicals [2]. In small doses, they are useful and play physiological roles and are also involved in signalling processes [3]. When the

antioxidant system is overloaded, ROS will damage proteins, DNA, and lipids [4]. Therefore, it is essential to identify exogenous sources of antioxidants which can reduce ROS effects [5].

Plants represent an important source of protective agents, due to their content of polyphenols, vitamins, fiber, phytosterols, and carotenoids [6]. Polyphenols have both antioxidant and prooxidant properties. The antioxidant activity is due to the scavenging effect of free radicals [7] and ensures the protection of intracellular structures against oxidative stress, favouring cell viability [8].

As prooxidants, polyphenols may stimulate apoptosis and inhibit tumour growth [8]. Polyphenols have good effects on degenerative diseases like cancer, cardiovascular diseases, diabetes, and osteoporosis [9]. As for their effect on the cardiovascular system, polyphenols reduce blood pressure, inflammation, and oxidative markers, they prevent endothelial dysfunction [10], they are antithrombotic, and they act as vasodilators [11]. They also inhibit the proinflammatory activity of cyclooxygenase (COX), lipooxygenase (LOX), and inducible nitric oxide synthase (iNOS) [12]. As protectors for the endothelial function, polyphenols act in the early stages of the atherosclerotic process by reducing LDL oxidation [12].

Genus *Mahonia* is the second largest one from the *Berberidaceae* family. The plants from this genus were used in traditional medicine as a treatment for psoriasis, dermatitis, fungal infections, tuberculosis, dizenteria, and wounds [13]. From all *Mahonia* species, *Mahonia aquifolium* is the most cultivated in Turkey [14]. Due to its high content in alkaloids, *M. aquifolium* has antioxidant, anti-inflammatory, [15, 16], hypoglycemic, hepatoprotective, and hypotensive properties [17]. In the cardiovascular system, *M. aquifolium* alkaloids induce vasodilatation by blocking  $Ca^{2+}$  entrance in the cells [18] and act as  $\alpha$ -1 adrenoreceptor antagonists [19].

A variety of fruits are known for having anti-inflammatory and vasodilatation properties [5]. Fruits from *M. aquifolium* are light yellow and bloom in April, but less information is known about their effects [14]. However, the fruits from a *Mahonia* were used in the treatment of insomnia, tinnitus, and dizziness [20].

Considering all these previous findings, the present work aimed at performing a phytochemical analysis and investigating the antioxidant and anti-inflammatory activity of the ethanolic *M. aquifolium* flower and fruit extracts.

## 2. Materials and Methods

**2.1. Plant Material.** Fresh *Mahonia aquifolium* (Pursh) Nutt. flowers and fruits were purchased from the A. Borza Botanical Garden “Babes-Bolyai” University of Cluj-Napoca, Romania between April and June 2015 and extracted in the Mycology Laboratory of “Babes-Bolyai” University, Cluj-Napoca, Romania, by a modified Squibb repercolation method with 70% ethanol (Merck, Bucuresti, Romania), producing the following extracts of *M. aquifolium*: green fruit extract 1:1 (g:mL) (MGF), ripe fruit extract 1:1 (g:mL) (MRF), and flower extract 1:1 (g:mL) (MF) [21]. The plants

were taxonomically identified and authenticated, and voucher specimens (number 665978) were deposited in the Herbarium of “A. Borza” Botanical Garden, “Babes-Bolyai” University of Cluj-Napoca, Romania.

**2.2. Phytochemical Analysis.** A HPLC-DAD approach was used to separate and quantitatively determine the polyphenols and alkaloids. In the first chromatographic approach, the assays were performed on an Agilent 1200 HPLC system (Waldbronn, Germany) equipped with an online vacuum degasser, quaternary pump, temperature-controlled sample tray, automatic injector, a column thermostat compartment, and a DAD detector. The chromatographic separations were run on a Nucleosil 100 C<sub>18</sub> column (240 mm × 4.6 mm, 5  $\mu$ m particle size) from Macherey-Nagel (Duren, Germany). The injection volume was 5  $\mu$ L (0.2  $\mu$ m filtered extract), the column temperature was set at 25°C, and the flow rate was 1.2 mL/min. Several preliminary tests were employed for method optimization by varying the experimental conditions. The optimum method consisted of a gradient elution using solvent A, 10 mM of ammonium acetate pH 5, and solvent B as acetonitrile. The gradient was as follows: 0–15 min from 8 to 30% B, 15–25 min isocratic at 30% B, 25–35 min from 30% to 85% B, 35–38 min from 85% to 95% B, 38–39 min isocratic at 95% B and 39–39.1 min back to 8% B where it was kept until 40 min. As standards, there were chlorogenic acid, *p*-coumaric acid, ferulic acid, rutin, isoquercitrin, quercetin, berberine, jatrorrhizine, palmatine, and berberine, all of analytical grade purity from different commercially available sources (Sigma-Aldrich, Germany). A calibration curve was constructed for each compound at 11, 22, 44, 88, 175, and 340  $\mu$ g/mL using the area of the peak by integration employed by the Agilent software. The limit of quantification (LOQ) and limit of detection (LOD) were determined by the formulas  $LOQ = (10 \times \text{standard deviation of intercept}) / \text{calibration curve slope}$  and  $LOD = (3.3 \times \text{standard deviation of intercept}) / \text{calibration curve slope}$ , respectively. The UV-Vis detection of the compounds has been accomplished using the DAD detector that measured the entire spectrum in the 210–700 nm region every 1 s, and the chromatograms were monitored at 220, 280, 340, and 425 nm. The identification of the compounds was employed by both chromatographic retention time (with a 0.3 s as tolerance) and spectral similarities (higher than 99.9% was considered as positive) which were done by the built-in software. The chromatograms were exported and the graphs were developed in Excel.

**2.3. In Vitro Antioxidant Effects.** The 1,1-diphenyl-2-picrylhydrazyl (DPPH) free radical scavenging assay was used for the evaluation of the antioxidant capacity of the investigated extracts. Briefly, in 3 mL of each diluted extract, a 1 mL DPPH and 0.1 mM methanol solution was added. Blanks were included replacing extract volumes for acetone/water. After 30 min in the dark and at room temperature, mixture absorbance was measured at 517 nm against a blank. The percentage of the radical scavenging activity of each extract was calculated using the following formula:

percentage of radical scavenging activity (AA%) =  $[(\text{OD control} - \text{OD sample}) / \text{OD control}] \times 100$ . AA% was converted to Trolox equivalents using a calibration curve of Trolox standard solutions (0.5–5  $\mu\text{g/mL}$ ). The concentration required to scavenge 50% of DPPH free radicals (IC<sub>50</sub>) was calculated [22].

**2.4. Experimental Design.** For the present study, 12 groups ( $n = 5$ ) of male albino Wistar rats with body weights between 200 and 250 g were used. They were purchased from the Animal Facility of “Iuliu Hațieganu” University of Medicine and Pharmacy. The rats were kept in common polypropylene cages under controlled conditions (12 h light/dark cycles, at an average temperature of 21–22°C), with free access to a standard pellet diet (Cantacuzino Institute, Bucharest, Romania) and water *ad libitum*. Three ethanolic extracts of *M. aquifolium* were tested: ripe fruits (MRF), green fruits (MGF), and flowers (MF). For seven days, the mentioned extracts were administered orally by gavage (1 mL/animal) in three different dilutions, respectively: 100%, 50%, and 25%. Tap water (1 mL/animal) was administered by gavage for seven days to the animals from the negative control group (CONTROL) and for the positive inflammation group (INFLAM). An anti-inflammatory control group was treated by gavage for seven days with diclofenac (10 mg/kg b.w.) (DICLO) [23]. Inflammation was induced with turpentine oil (6 mL/kg b.w.) administered intramuscularly, in the animals treated with the extracts, as well as in the INFLAM and DICLO groups [24]. To the CONTROL animals, 0.9% saline was injected intramuscularly (i.m.). One day after the inflammation induction, 60 mg/kg b.w. ketamine and 15 mg/kg b.w. xylazine were used to anesthetize the rats [25], blood was withdrawn by retroorbital puncture, and serum was stored at  $-80^\circ\text{C}$  until use. The experiments were performed in triplicate. All the animals were used only once, and they were killed by cervical dislocation immediately after the assay.

**2.5. The Anti-Inflammatory Effect Evaluation.** To evaluate the anti-inflammatory effects of the ethanolic plant extracts, nitric oxide (NO) and TNF- $\alpha$  were measured.

For NO synthesis, the Griess reaction was used as an indirect method which measures total nitrites and nitrates (NO<sub>x</sub>) as previously described [26]. The concentration of serum NO<sub>x</sub> was expressed as nitrite  $\mu\text{mol/L}$  [27].

Serum TNF- $\alpha$  was measured using a rat ELISA kit (MBS175904) that applies the quantitative sandwich enzyme immunoassay technique.

**2.6. The Antioxidant Effect Evaluation.** The total oxidative status (TOS) of the serum was measured using a colorimetric assay [26, 28]. The assay results are expressed in  $\mu\text{mol H}_2\text{O}_2$  equiv./L.

The total antioxidant response (TAR) was measured in serum using a colorimetric assay [26, 29]. The results are expressed as  $\mu\text{mol Trolox equiv./L}$ .

The oxidative stress index (OSI) is the ratio of the TOS to the TAR and it is an indicator of the oxidative stress level

[26, 30]:  $\text{OSI (arbitrary unit)} = \text{TOS } (\mu\text{mol H}_2\text{O}_2 \text{ equiv./L}) / \text{TAR } (\mu\text{mol Trolox equiv./L})$ .

Peroxynitrite formation was assessed indirectly by measuring serum 3-nitrotyrosine (3NT) using a rat ELISA kit (MBS732683) that applies the quantitative sandwich enzyme immunoassay technique.

Malondialdehyde (MDA) was assessed using thiobarbituric acid, as previously described [26, 31]. Serum MDA concentration was expressed as nmol/mL of serum.

Total thiols (SH) were measured using Ellman's reagent [26, 32]. Serum SH concentration was expressed as mmol GSH/mL.

All of the spectroscopic measurements were performed using a Jasco V-530 UV-Vis spectrophotometer (Jasco International Co. Ltd., Tokyo, Japan).

**2.7. Statistical Analysis.** Data are expressed as mean  $\pm$  SD, averaged over at least three independent experiments for normally distributed data. Otherwise, the median, first quartile (Q1), and third quartile (Q3) were reported. Comparisons among groups, in all studied parameters, were analyzed by using the one-way analysis of variance (ANOVA) test and Bonferroni-Holm post hoc test.  $p < 0.05$  was considered statistically significant. Correlations among data obtained were calculated using Pearson's correlation coefficient ( $r$ ). All analyses were performed using the program “Statistical Package for Social Sciences (SPSS) version 16” (SPSS Inc., Chicago, IL, USA).

### 3. Results

**3.1. Phytochemical Analysis.** In the present study, we measured six polyphenols (chlorogenic acid, *p*-coumaric acid, ferulic acid, rutin, isoquercitrin, and quercetin) and four alkaloids (berbamine, jatrorrhizine, palmatine, and berberine) (Table 1, Figure 1). We identified and quantified chlorogenic acid, ferulic acid, and *p*-coumaric acid as hydroxycinnamic acid derivatives (Table 1). Chlorogenic acid was found in the highest concentration in MF ( $2013 \pm 2 \mu\text{g/mL}$ ), followed by MGF ( $1763 \pm 7 \mu\text{g/mL}$ ) and MRF ( $944 \pm 22 \mu\text{g/mL}$ ). We could quantify *p*-coumaric acid only in MF ( $7.2 \pm 0.1 \mu\text{g/mL}$ ) and MRF ( $4.5 \pm 2.0 \mu\text{g/mL}$ ). MF was richer in *p*-coumaric acid ( $10.0 \pm 0.3 \mu\text{g/mL}$ ) than MRF ( $7.8 \pm 0.0 \mu\text{g/mL}$ ) and MGF ( $5.6 \pm 0.2 \mu\text{g/mL}$ ) were. In all ethanolic extracts, we identified two flavonoid glycosides, namely rutin and isoquercitrin. Rutin was more abundant in MF ( $73 \pm 1.6 \mu\text{g/mL}$ ) than in MRF ( $26.1 \pm 0.0 \mu\text{g/mL}$ ) and MGF ( $12.9 \pm 0.0 \mu\text{g/mL}$ ). Isoquercitrin was higher in MGF ( $37.3 \pm 0.2 \mu\text{g/mL}$ ) than in MF ( $29.7 \pm 0.7 \mu\text{g/mL}$ ) and MRF ( $32.4 \pm 0.3 \mu\text{g/mL}$ ). In MF, MGF, and MRF, the tested alkaloids were in concentrations under LOD.

**3.2. In Vitro Antioxidant Activity.** The ethanolic extracts of *M. aquifolium* had a good DPPH radical scavenging activity (Table 2). Trolox IC<sub>50</sub> was 11.2  $\mu\text{g/mL}$ . Considering that an antioxidant activity with an IC<sub>50</sub> between 50 and 100  $\mu\text{g/mL}$  is good and one that has between 100 and 200  $\mu\text{g/mL}$  is weak, MF IC<sub>50</sub> (60.82  $\mu\text{g/mL}$ ) and MGF IC<sub>50</sub> (81.6  $\mu\text{g/mL}$ )



TABLE 1: HPLC analysis of the *M. aquifolium* flower, green fruit, and ripe fruit extracts.

Number	Compounds	$t_{\text{elution}}$ (min)	$R^2$	LOD ( $\mu\text{g/mL}$ )	LOQ ( $\mu\text{g/mL}$ )	Sample1 MF ( $\mu\text{g/mL}$ )	Sample2 MRF ( $\mu\text{g/mL}$ )	Sample3 MGF ( $\mu\text{g/mL}$ )
1	Chlorogenic ac.	5.41	0.9991	3.2	9.8	2013 $\pm$ 2	944 $\pm$ 22	1763 $\pm$ 7
2	<i>p</i> -Coumaric ac.	9.17	0.9999	1.3	4.0	7.2 $\pm$ 0.1	4.5 $\pm$ 2.0	<LOQ
3	Ferulic ac.	10.07	0.9998	1.4	4.2	10.0 $\pm$ 0.3	7.8 $\pm$ 0.	5.6 $\pm$ 0.2
4	Rutin	14.55	0.9996	2.7	8.1	73 $\pm$ 1.6	26.1 $\pm$ 0.0	12.9 $\pm$ 0.0
5	Isoquercitrin	15.34	0.9995	1.7	5.2	29.7 $\pm$ 0.7	32.4 $\pm$ 0.3	37.3 $\pm$ 0.2
6	Quercetin	24.1	0.9949	13.7	41.6	<LOD	<LOD	<LOD
7	Berberine	25.5	0.9997	2.4	7.3	<LOD	<LOD	<LOD
8	Jatrorrhizine	30.57	0.9994	2.7	8.3	<LOD	<LOD	<LOD
9	Palmatine	34.96	0.9998	1.7	5.2	<LOD	<LOD	<LOD
10	Berberine	36.08	0.9996	2.1	6.4	<LOD	<LOD	<LOD

MF—*M. aquifolium* flowers, MGF—*M. aquifolium* green fruits, MRF—*M. aquifolium* ripe fruits, LOD—limit of detection, LOQ—limit of quantification, and  $R^2$ —coefficient of determination for the calibration curves (at six levels of concentrations). Indicated intervals represent the average  $\pm$  standard deviation ( $n = 3$ ).

mL) had a good antioxidant activity and MRF IC<sub>50</sub> (135.74  $\mu\text{g/mL}$ ) has a weak antioxidant activity.

**3.3. In Vivo Anti-Inflammatory and Antioxidant Effects.** TNF- $\alpha$  was increased in the inflammation group ( $p < 0.01$ ). TNF- $\alpha$  was reduced exclusively by MGF50 and MF25 ( $p < 0.05$ ) and no significant effect was found for the rest of the tested extracts ( $p > 0.05$ ) (Table 3).

NOx was significantly increased in the inflammation group ( $p < 0.01$ ) and an important reduction was found in the group where diclofenac was administered ( $p < 0.01$ ). Compared to the inflammation group, MRF extracts reduced NOx significantly ( $p < 0.01$ ), MRF100 being the most efficient. MRF effects were comparable to that of diclofenac ( $p > 0.05$ ). There was no significant inhibitory activity on NOx in all MF dilutions ( $p > 0.05$ ). From the MGF samples, only MGF50 had a small inhibitory effect on NOx ( $p < 0.05$ ) (Table 3).

TOS analysis showed that inflammation caused an important increase ( $p < 0.01$ ) and diclofenac caused a significant reduction ( $p < 0.001$ ). All MGF extracts reduced TOS ( $p < 0.01$ ), but not as much as diclofenac ( $p > 0.05$ ). MRF extracts did not influence TOS significantly ( $p > 0.05$ ). MF reduced TOS, but only MF100 had a significant inhibitory effect ( $p < 0.01$ ).

TAR was reduced in the inflammation group ( $p < 0.05$ ), and it was slightly increased when diclofenac was administered ( $p < 0.05$ ). MGF increased TAR, MGF25 being the better stimulator ( $p < 0.001$ ). The MGF effect was as good as that of diclofenac ( $p > 0.05$ ). MF100 and MF50 increased TAR ( $p < 0.05$ ), but this effect was smaller than diclofenac ( $p < 0.001$ ). MRF extracts had no significant effects on TAR ( $p > 0.05$ ) (Table 4).

OSI was increased in the inflammation group ( $p < 0.01$ ) and decreased when diclofenac was administered ( $p < 0.01$ ). Only MF100 extracts decreased OSI ( $p < 0.05$ ), but the effect was smaller than that of diclofenac ( $p < 0.05$ ). MGF extracts were good inhibitors of OSI ( $p < 0.01$ ), but the effect was smaller than that of diclofenac ( $p > 0.05$ ). The MRF extract had no significant effect on OSI ( $p > 0.05$ ) (Table 4).

3NT was increased in the inflammation group ( $p < 0.01$ ) and was reduced significantly after diclofenac ( $p < 0.001$ ). MGF were also good inhibitors of 3NT, MGF100 being more efficient ( $p < 0.001$ ) than MGF50 ( $p < 0.01$ ) and MGF25 ( $p < 0.05$ ). From the MRF, only MRF25 reduced 3NT ( $p < 0.001$ ). MF extracts decreased 3NT significantly ( $p < 0.01$ ) (Table 4). MDA production was significantly increased in the inflammation group ( $p < 0.001$ ), and diclofenac treatment caused an important decrease of MDA ( $p < 0.001$ ). Only MRF100 ( $p < 0.01$ ) and MRF50 ( $p < 0.05$ ) reduced MDA. MF and MGF did not influence significantly the production of MDA ( $p > 0.05$ ) (Table 4).

Inflammation caused a reduction of SH ( $p < 0.001$ ), and diclofenac caused an important increase ( $p < 0.01$ ). SH was increased by all *M. aquifolium* extracts ( $p < 0.01 - 0.001$ ), and the effects were better than the effect of diclofenac (Table 4).

## 4. Discussion

In the present study, a phytochemical analysis of the ethanolic *M. aquifolium* flower, green fruit, and ripe fruit extracts, was performed for the first time. The antioxidant activity and anti-inflammatory effects were proved.

From the three hydroxycinnamic acid derivatives measured in the ethanolic *M. aquifolium* extracts, the main component was chlorogenic acid. MF had a higher content of chlorogenic acid than MGF and MRF. This was an important result because chlorogenic acid improves the risk of cardiovascular and associated diseases by reducing the levels of free fatty acids and triglycerides [33]. Due to its antioxidant properties, chlorogenic acid also has a protective role in cardiovascular diseases by increasing NO production [34]. In hypertension, it has a vasodilator effect and reduces ROS production [35]. Chlorogenic acid also inhibits platelet aggregation and reduces blood viscosity [36].

Ferulic acid was found in much lesser concentrations. It was higher in MF than in MRF and MGF. Ferulic acid has antioxidant properties [37, 38] by scavenging ROS and activating DNA repair [39]. It interferes with insulin,



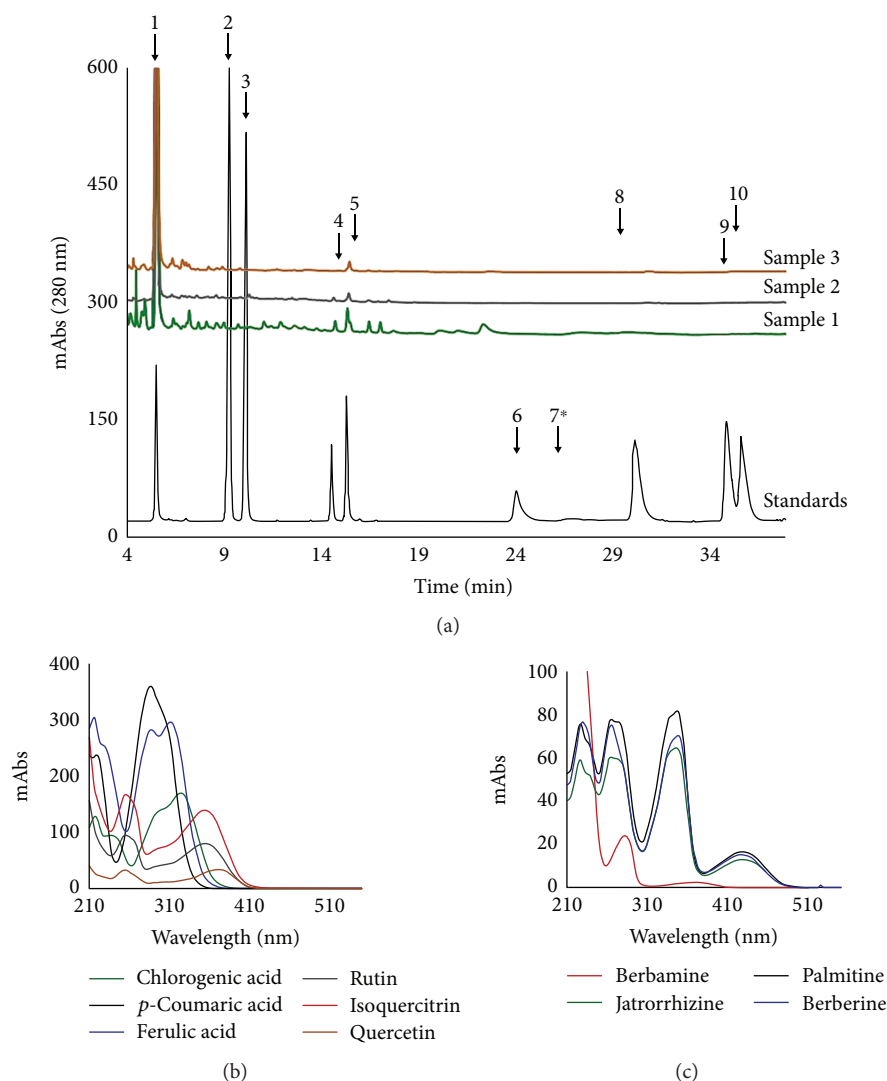


FIGURE 1: (a) Chromatograms at 280 nm of the *M. aquifolium* flower, green fruit, and ripe fruit extracts. The ten standards are indicated by arrows and numbers. Berbamine (7\*) is barely visible in the 280 nm chromatogram, but it is much better detected and quantified separately from the 220 nm chromatogram. (b) HPLC-DAD registered absorption molecular spectra in the UV-vis domain for the polyphenolic standards at 350  $\mu\text{g/mL}$ . (c) HPLC-DAD registered absorption molecular spectra in the UV-vis domain for the alkaloid standards at 350  $\mu\text{g/mL}$ . 1—Chlorogenic acid, 2—*p*-coumaric acid, 3—ferulic acid, 4—rutin, 5—isoquercitrin, 6—quercetin, 7—berbamine, 8—jatrorrhizine, 9—palmitine, and 10—berberine. Sample 1—*Mahonia aquifolium* flowers, sample 2—*Mahonia aquifolium* ripe fruits, and sample 3—*Mahonia aquifolium* green fruits.

TABLE 2: *In vitro* DPPH radical scavenging activity of *M. aquifolium* flower, green fruit, and ripe fruit extracts.

MGF		MRF		MF	
( $\mu\text{g/mL}$ )	(AA%)	( $\mu\text{g/mL}$ )	(AA%)	( $\mu\text{g/mL}$ )	(AA%)
750	94.6	1000	83.1	375	88
562.5	86.65	750	73.13	250	79.95
375	76.65	500	67.82	125	65.6
187.5	65.17	250	61		

MGF—*M. aquifolium* green fruits, MRF—*M. aquifolium* ripe fruits, MF—*M. aquifolium* flowers, and AA%—percentage of radical scavenging activity.

ghrelin, and leptin to prevent weight gain and the accumulation of intra-abdominal fat [40]. Ferulic acid also has anti-inflammatory, anticancer, and cardioprotective effects [41]. Due to its antioxidant properties, it is beneficial in epilepsy [42] and other chronic neurological conditions [43]. It is also an antidepressant [44], and it improves memory [45].

The *p*-coumaric acid was found only in MRF and MF. It is a phenolic acid with antioxidant [46], anti-inflammatory, cardioprotective [47], hepatoprotective, and nephroprotective properties [48]. It reduces the lipoprotein peroxidation process and reduces the free radicals [46, 49]. The *p*-coumaric acid has anticancer activity by inducing apoptosis and cell cycle arrest [48].

TABLE 3: *In vivo* anti-inflammatory effects of *M. aquifolium* flower, green fruit, and ripe fruit extracts.

	NOx ( $\mu\text{mol/L}$ )	TNF (pg/mL)
CONTROL	48,489 $\pm$ 12,975	116,634 $\pm$ 0.678
INFLAM	75,234 $\pm$ 12,136**	140,594 $\pm$ 15,960***
DICLO	52,318 $\pm$ 5389**	127,228 $\pm$ 10,332
MGF100%	72,406 $\pm$ 9292*	143,564 $\pm$ 16,419
MGF50%	57,473 $\pm$ 9110*	118,317 $\pm$ 13,854*
MGF25%	62,686 $\pm$ 10,155*	133,168 $\pm$ 15,522
MRF100%	46,898 $\pm$ 6766***	130,941 $\pm$ 17,836
MRF50%	53,172 $\pm$ 3981**	146,287 $\pm$ 15,092
MRF25%	53,526 $\pm$ 7582**	121,782 $\pm$ 15,522
MF100%	59,623 $\pm$ 10,224*	132,178 $\pm$ 21,138
MF50%	69,638 $\pm$ 7507	129,951 $\pm$ 16,419
MF25%	62,421 $\pm$ 7539	115,842 $\pm$ 10,632*

3NT—3-nitrotyrosine; *M. aquifolium*: MGF—green fruits, MRF—ripe fruits, and MF—flowers; \* $p < 0.05$ , \*\* $p < 0.01$ , and \*\*\* $p < 0.001$ .

From the three measured flavonoid glycosides, only rutin and isoquercitrin were found in MF, MGF, and MRF. Quercetin was under the LOD.

Rutin is a flavonoid with antioxidant, anti-inflammatory, antidiabetic, and antiobesity properties [50, 51]. Due to its antioxidant capacity, rutin has cardioprotective effects, reducing LDH, CK-MB, ROS, and apoptosis [52, 53]. Rutin protects against endothelial damage and reduces the occurrence of chronic complications in type 2 diabetes [42, 54]. The higher level of rutin concentration in MF was correlated with a good DPPH scavenging activity. Isoquercitrin is a glycosylated flavonoid [55] with a strong antioxidant activity due to its capacity to scavenge free radicals [56] and to inhibit arginase, favouring NO production [57]. This phenolic compound has anticancer [58] and antiapoptotic effects [59].

The isoquinoline alkaloids are the major subclass of alkaloids of the genus *Mahonia* [26]. The previously identified alkaloids belong to three major classes: protoberberines, aporphines, and bisbenzylisoquinolines. Berberine is the most widely distributed alkaloid in the *Mahonia* species [60], but other protoberberines, including palmatine, jatrorrhizine, berbamine, columbamine, and coptisine were also found in these species [20]. The analysis of *M. aquifolium* extracts looked for the presence of berberine, palmatine, jatrorrhizine, and berbamine but due to the trace amounts of these alkaloids they were under LOD.

The phytochemical analyses suggested the possible anti-inflammatory and antioxidant effects of the *M. aquifolium* fruit and flower extracts.

The *in vitro* antioxidant activity was assessed with the DPPH test. MF and MGF proved to have a good antioxidant effect, but MRF had just a weak antioxidant activity. For MF, DPPH correlated with the high chlorogenic acid, ferulic acid, and rutin content and for MGF with the high chlorogenic acid and isoquercitrin content.

Furthermore, the present study evaluated the *in vivo* anti-inflammatory and antioxidant effects in an experimental rat

acute inflammation induced by turpentine oil, a nonantigenic inflammatory stimulus [61] that activates inflammatory cytokines and NO release. High serum levels of TNF alpha and NOx were positive markers of the inflammatory response. Only MF and MGF proved to have important anti-inflammatory effects by reducing TNF alpha.

NO is the product with the smallest molecular mass secreted in the mammalian cells. It has a high chemical reactivity and a short lifetime and specificity [62]. NO is generated by 3 isoforms of NOS, respectively, inducible NOS (iNOS), neuronal NOS (nNOS), and endothelial NOS (eNOS) [63]. The nNOS and eNOS are expressed constitutively and produce small quantities of NO. The iNOS is expressed after immunological and inflammatory stimuli and acts like a protector agent [64]. Low levels of NO induce normal physiological signalling, leading to antioxidant reactions. In intermediate concentrations, NO stimulates anti-inflammatory and immunosuppressive responses, has antiapoptotic, progrowth, and angiogenic effects. High NO levels have antiproliferative effects and induce cell cycle delay. Moreover, if there is a prolonged NO increase, it may induce apoptosis [65]. When iNOS is synthesised in high quantities, NO also reacts fast with superoxide anion and will form peroxynitrite (ONOO<sup>-</sup>), a nonradical reactive species responsible for most of the NO pathological effects [66–68]. Previous studies suggest that plants play an important anti-inflammatory role, because they inhibit NO synthesis [24]. In the present study, only MRF100 proved to have important anti-inflammatory effects by reducing NO synthesis and it was comparable with that induced by diclofenac. Treatment with MGF had a weak inhibitory effect, and MF had no important effect upon NOx. Because the MRF effect on NOx was not correlated with the *in vitro* DPPH test, it may be presumed that the antioxidant activity was not significantly involved. In some human diseases, antioxidant therapy failure was called the antioxidant paradox [69]. Due to the fact that overproduction of ROS can induce an inflammatory response, and inflammatory mediators can induce an oxidative stress, it was generally accepted that oxidation and inflammation are interlinked processes [70]. The latest explanation of antioxidant therapy failure comes from the finding that antioxidants do not inhibit oxidative stress and the associated inflammation at the same time [71].

Oxidative stress is destructive and it represents the dysbalance between antioxidants and oxidants, in favour of the last ones [72, 73]. The most important oxidants are the reactive oxygen species (ROS), which include superoxide anion, hydrogen peroxide, and hydroxyl radicals [2]. In small to moderate concentrations, ROS have physiologic roles [3], acting as signalling molecules, being involved in cell growth, intercellular adhesion, cellular differentiation, and apoptosis [73, 74]. In high concentrations, ROS are highly reactive molecules that may damage proteins, lipids, and DNA [2, 3, 75] and favour atherosclerosis, cancer, and ageing [76]. The measurement of the stable markers in circulation during oxidative stress [77–79] is a helpful way to appreciate plant extract effects. The oxidative stress biomarkers may be classified as molecules that are modified by interactions with ROS (e.g., DNA, lipids, proteins and carbohydrates)

TABLE 4: *In vivo* antioxidant effects of *M. aquifolium* flower, green fruit, and ripe fruit extracts.

	( $\mu\text{mol H}_2\text{O}_2$ TOS equiv./L)	(mmol TA Trolox R equiv./L)	OSI	3NT	MD (nmol A MDA/L)	(mmol SH GSH/L)
CONTROL	29.58 $\pm$ 1.85	1.09 $\pm$ 0.001	27.13 $\pm$ 1.67	0.34 $\pm$ 0.06	4.31 $\pm$ 0.89	0.67 $\pm$ 0.09
INFLAM	41.58 $\pm$ 6.55**	1.08 $\pm$ 0.0007*	38.20 $\pm$ 6.009**	0.67 $\pm$ 0.18**	7.62 $\pm$ 0.62***	0.42 $\pm$ 0.06**
DICLO	24.92 $\pm$ 3.02***	1.08 $\pm$ 0.0004*	22.87 $\pm$ 2.77***	0.29 $\pm$ 0.02***	5.49 $\pm$ 0.72***	0.56 $\pm$ 0.05**
MGF100%	26.19 $\pm$ 7.37**	1.09 $\pm$ 0.0011**	24.03 $\pm$ 6.74**	0.29 $\pm$ 0.04***	6.90 $\pm$ 0.47	0.66 $\pm$ 0.11**
MGF50%	32.09 $\pm$ 5.63*	1.09 $\pm$ 0.0006**	29.45 $\pm$ 5.15*	0.32 $\pm$ 0.02**	6.97 $\pm$ 0.54	0.67 $\pm$ 0.10**
MGF25%	30.60 $\pm$ 4.59**	1.09 $\pm$ 0.0008***	28.07 $\pm$ 4.19**	0.38 $\pm$ 0.14*	6.90 $\pm$ 0.47	0.59 $\pm$ 0.11**
MRF100%	39.21 $\pm$ 5.31	1.08 $\pm$ 0.0008	36.02 $\pm$ 4.86	0.41 $\pm$ 0.27	6.00 $\pm$ 0.66**	0.77 $\pm$ 0.14**
MRF50%	34.49 $\pm$ 6.64	1.08 $\pm$ 0.0006	31.70 $\pm$ 6.10	0.42 $\pm$ 0.26	6.54 $\pm$ 0.86*	0.83 $\pm$ 0.20**
MRF25%	34.85 $\pm$ 7.85	1.08 $\pm$ 0.0003	32.03 $\pm$ 7.21	0.29 $\pm$ 0.03***	7.73 $\pm$ 0.29	0.67 $\pm$ 0.14**
MF100%	30.18 $\pm$ 4.74**	1.08 $\pm$ 0.0003*	27.76 $\pm$ 4.36**	0.32 $\pm$ 0.06**	7.15 $\pm$ 0.97	0.66 $\pm$ 0.10**
MF50%	39.65 $\pm$ 4.51	1.08 $\pm$ 0.001	36.43 $\pm$ 4.12	0.45 $\pm$ 0.25	7.12 $\pm$ 0.82	0.77 $\pm$ 0.05**
MF25%	32.79 $\pm$ 6.77	1.08 $\pm$ 0.001	30.12 $\pm$ 6.21	0.28 $\pm$ 0.03***	7.68 $\pm$ 0.97	0.75 $\pm$ 0.14**

TOS—total oxidative status, TAR—total antioxidant reactivity, OSI—oxidative stress index, 3NT—3-nitrotyrosine, MDA—malondialdehyde, SH—total thiols, MGF—*M. aquifolium* green fruits, MRF—*M. aquifolium* ripe fruits, and MF—*M. aquifolium* flowers; \*  $p < 0.05$ , \*\*  $p < 0.01$ , and \*\*\*  $p < 0.001$ .

and molecules of the antioxidant system that change in response to increased redox stress [77]. For total oxidative status (TOS) evaluation, diverse methods were developed [28]. In our study, serum TOS was higher in the inflammation group. MF and MGF lowered serum TOS more than MRF. These results positively correlated with the DPPH test.

The antioxidant mechanisms are given in terms of the capacity to scavenge free radicals, to chelate metals, and to act in a synergic manner with other antioxidants. There are two groups of methods used for the determination of the total antioxidant capacity: those based on single-electron transfer monitored spectrophotometrically by a color change due to the free radical reduction, and those based on hydrogen atom transfer measured by the elimination of peroxy radicals [80]. The antioxidant capacity of the plasma is represented by the thiol groups of proteins and uric acid [81]. Serum TAR [82] was lower in the inflammation group, and only the treatments with MF and MGF extracts increased TAR. In these extracts, we found higher levels of chlorogenic acid, rutin, and isoquercitrin, compounds known to have antioxidant activities.

OSI assesses the global oxidant/antioxidant balance in the living organisms [83]. It was decreased by the MGF and MF treatments, and this was correlated positively with TOS and negatively to TAR.

3NT is a product of protein tyrosine nitration mediated by peroxynitrite anion and nitrogen dioxide. Therefore, it is a good marker of oxidative cell injury and inflammation, as well as NO production [84]. Increased oxidative stress increases ROS and 3NT and consumes NO. Increased levels of 3NT were associated with atherosclerosis [85] and observed in patients with coronary dysfunction, as well as after the removal of the cardiovascular risk factors and normalization of C reactive protein [77]. All tested *M. aquifolium* extracts reduced 3NT, but MF and MGF were more effective than MRF. The inhibitory effect on 3NT was correlated positively with TOS reduction and negatively with TAR elevation. These results could be explained by the better MF and MGF *in vitro* DPPH tests.

Malondialdehyde (MDA) results from arachidonic acid, a polyunsaturated fatty acid, and it is a secondary product of lipid peroxidation [86]. Aldehydes are toxic because they interact with DNA and proteins favouring mutations, which are risk factors for cancer, atherosclerosis, and other cardiovascular diseases [87]. The link between MDA and atherosclerosis is its reaction with lipoproteins and the formation of arterial foam cells [88, 89]. Collagen has a high reactivity for MDA, and this will increase heart and vessel rigidity [87]. High levels of MDA were correlated also with myocardial infarction [90], cardiovascular complications of haemodialysis, diabetes, preeclampsia [87], congestive heart failure, and with the severity of the disease [91]. Only treatment with MRF decreased MDA, and it was negatively correlated with TAR.

Protein thiol groups are important determinants of the total antioxidant capacity. They contain a sulfhydryl group which can transform into disulfide bonds when oxidized by the oxygen molecules. This reaction is reversible, so the

disulfide bonds can turn back into thiols [92]. The chemical versatility allows them to participate in different processes like signalling, antioxidant defence, and structural stabilization [93]. Studies show that albumin, the most thiol-abundant protein, is implied in the reduction of blood pressure and cardiovascular risk [94]. All tested *M. aquifolium* ethanolic extracts increased serum SH, proving that these extracts may improve the antioxidant defence.

## 5. Conclusion

Considering the study results, we concluded that *M. aquifolium* flower, green fruit, and ripe fruit ethanol extracts have good *in vitro* and *in vivo* antioxidant activities, and good anti-inflammatory effects. The efficiency varies with plant organ phytochemical composition. *M. aquifolium* flower, green fruit, and ripe fruit extracts may be considered for therapeutic interventions needing simultaneous antioxidant and anti-inflammatory effects.

## Data Availability

The data sets for this manuscript will not be publicly available until an associated PhD thesis is published. Requests to access these data sets should be directed to Andra-Diana Andreicut at andra\_cecan@yahoo.com.

## Ethical Approval

The study protocol was approved by the Institutional Animal Ethical Committee (IAEC) of the “Iuliu Hațieganu” University of Medicine and Pharmacy, Cluj-Napoca, Romania (number 18/13.12.2016).

## Conflicts of Interest

None of the authors has any conflict of interest that could affect the performance of the work or the interpretation of the data.

## Authors' Contributions

Andra-Diana Andreicut, Alexandru Irimie, Alina Elena Pârvu, and Marcel Pârvu contributed to the study conception and design, and interpreted the data. Augustin Cătălin Mot was responsible for the phytochemical analysis. Andra-Diana Andreicut and Mihai Cekan were responsible for the experimental study. Adriana Florinelă Cătoi was responsible for data acquisition and statistical analysis. Eva Fischer Fodor and Vasile Feldrihan performed biochemical and ELISA tests. All authors have reviewed and approved the final submitted version.

## Acknowledgments

The study was partly supported by research grants from the “Iuliu Hațieganu” University of Medicine and Pharmacy, Cluj-Napoca, Romania (PCD 7690/19/15.04.2016; PCD 2017 1300/12/13.01.2017).



## References

- [1] I. C. Jeung, D. Jee, C.-R. Rho, and S. Kang, "Melissa officinalis L. extracts protect human retinal pigment epithelial cells against oxidative stress-induced apoptosis," *International Journal of Medical Sciences*, vol. 13, no. 2, pp. 139–146, 2016.
- [2] M. Schieber and N. S. Chandel, "ROS function in redox signaling and oxidative stress," *Current Biology*, vol. 24, no. 10, pp. R453–R462, 2014.
- [3] P. Poprac, K. Jomova, M. Simunkova, V. Kollar, C. J. Rhodes, and M. Valko, "Targeting free radicals in oxidative stress-related human diseases," *Trends in Pharmacological Sciences*, vol. 38, no. 7, pp. 592–607, 2017.
- [4] M. Shoaib, S. W. Ali Shah, N. Ali et al., "In vitro enzyme inhibition potentials and antioxidant activity of synthetic flavone derivatives," *Journal of Chemistry*, vol. 2015, Article ID 516878, 7 pages, 2015.
- [5] K. Pyrkosz-Biardzka, A. Z. Kucharska, A. Sokół-Łętowska, P. Strugała, and J. Gabrielska, "A comprehensive study on antioxidant properties of crude extracts from fruits of *Berberis vulgaris* L., *Cornus mas* L. and *Mahonia aquifolium* Nutt," *Polish Journal of Food and Nutrition Sciences*, vol. 64, no. 2, pp. 91–99, 2014.
- [6] G. Williamson and C. Manach, "Bioavailability and bioefficacy of polyphenols in humans. II. Review of 93 intervention studies," *The American Journal of Clinical Nutrition*, vol. 81, no. 1, pp. 243S–255S, 2005.
- [7] K. D. Croft, "The chemistry and biological effects of flavonoids and phenolic acids," *Annals of the New York Academy of Sciences*, vol. 854, no. 1, pp. 435–442, 1998.
- [8] A. Scalbert, I. T. Johnson, and M. Saltmarsh, "Polyphenols: antioxidants and beyond," *The American Journal of Clinical Nutrition*, vol. 81, no. 1, pp. 215S–217S, 2005.
- [9] A. Scalbert, C. Manach, C. Morand, C. Rémésy, and L. Jiménez, "Dietary polyphenols and the prevention of diseases," *Critical Reviews in Food Science and Nutrition*, vol. 45, no. 4, pp. 287–306, 2005.
- [10] A. Tresserra-Rimbau, E. B. Rimm, A. Medina-Remón et al., "Polyphenol intake and mortality risk: a re-analysis of the PRE-DIMED trial," *BMC Medicine*, vol. 12, no. 1, pp. 1–11, 2014.
- [11] Y. S. Velioglu, G. Mazza, L. Gao, and B. D. Oomah, "Antioxidant activity and total phenolics in selected fruits, vegetables, and grain products," *Journal of Agricultural and Food Chemistry*, vol. 46, no. 10, pp. 4113–4117, 1998.
- [12] H. E. R. Christy Tangney, "NIH public access," *Current Atherosclerosis Reports*, vol. 6, no. 9, pp. 2166–2171, 2008.
- [13] A. D. Damjanović, G. Zdunić, K. Šavikin et al., "Evaluation of the anti-cancer potential of *Mahonia aquifolium* extracts via apoptosis and anti-angiogenesis," *Bangladesh Journal of Pharmacology*, vol. 11, no. 3, pp. 741–749, 2016.
- [14] H. Coklar and M. Akbulut, "Anthocyanins and phenolic compounds of *Mahonia aquifolium* berries and their contributions to antioxidant activity," *Journal of Functional Foods*, vol. 35, pp. 166–174, 2017.
- [15] B. S. Wong, Y. C. Hsiao, T. W. Lin et al., "The in vitro and in vivo apoptotic effects of *Mahonia oiwakensis* on human lung cancer cells," *Chemico-Biological Interactions*, vol. 180, no. 2, pp. 165–174, 2009.
- [16] K. Gunduz, "Morphological and phytochemical properties of *Mahonia aquifolium* from Turkey," *Pakistan Journal of Agricultural Sciences*, vol. 50, no. 3, pp. 439–443, 2013.
- [17] A. Singh, V. Bajpai, S. Kumar, A. K. Singh Rawat, and B. Kumar, "Analysis of isoquinoline alkaloids from *Mahonia leschenaultia* and *Mahonia napaulensis* roots using UHPLC-Orbitrap-MS<sup>n</sup> and UHPLC-QqQ<sup>LIT</sup>-MS/MS," *Journal of Pharmaceutical Analysis*, vol. 7, no. 2, pp. 77–86, 2017.
- [18] Ružena Sotníková, D. Košťálová, and Štefánia Vaverková, "Effect of bisbenzylisoquinoline alkaloids from *Mahonia aquifolium* on the isolated rat aorta," *General Pharmacology: The Vascular System*, vol. 25, no. 7, pp. 1405–1410, 1994.
- [19] R. Sotníková, V. Kettmann, D. Košťálová, and E. Táborská, "Relaxant properties of some aporphine alkaloids from *Mahonia aquifolium*," *Methods and Findings in Experimental and Clinical Pharmacology*, vol. 19, no. 9, pp. 589–597, 1997.
- [20] J. M. He and Q. Mu, "The medicinal uses of the genus *Mahonia* in traditional Chinese medicine: an ethnopharmacological, phytochemical and pharmacological review," *Journal of Ethnopharmacology*, vol. 175, pp. 668–683, 2015.
- [21] A. E. Parvu, M. Parvu, L. Vlase, P. Miclea, A. C. Mot, and R. Silaghi-Dumitrescu, "Anti-inflammatory effects of *Allium schoenoprasum* L. leaves," *Journal of Physiology and Pharmacology*, vol. 65, no. 2, 2014.
- [22] D. Benedec, D. Hanganu, I. Oniga et al., "Achillea schurii flowers: chemical, antioxidant, and antimicrobial investigations," *Molecules*, vol. 21, no. 8, 2016.
- [23] R. P. Barcelos, G. Bresciani, M. J. Cuevas, S. Martínez-Flórez, F. A. A. Soares, and J. González-Gallego, "Diclofenac pretreatment modulates exercise-induced inflammation in skeletal muscle of rats through the TLR4/NF-κB pathway," *Applied Physiology, Nutrition, and Metabolism*, vol. 42, no. 7, pp. 757–764, 2017.
- [24] A. E. Pârvu, Ș. Țălu, M. A. Taulescu et al., "Fractal analysis of ibuprofen effect on experimental dog peri-implantitis," *Implant Dentistry*, vol. 23, no. 3, pp. 295–304, 2014.
- [25] J. N. Francischi, T. I. C. Frade, M. P. A. d. Almeida, B. F. G. d. Queiroz, and Y. S. Bakhle, "Ketamine-xylazine anaesthesia and orofacial administration of substance P: a lethal combination in rats," *Neuropeptides*, vol. 62, pp. 21–26, 2017.
- [26] A. D. Andreicuț, A. E. Pârvu, A. C. Moț et al., "Anti-inflammatory and antioxidant effects of *Mahonia aquifolium* leaves and bark extracts," *Farmacia*, vol. 66, no. 1, 2018.
- [27] K. M. Miranda, M. G. Espey, and D. A. Wink, "A rapid, simple spectrophotometric method for simultaneous detection of nitrate and nitrite," *Nitric Oxide*, vol. 5, no. 1, pp. 62–71, 2001.
- [28] O. Erel, "A new automated colorimetric method for measuring total oxidant status," *Clinical Biochemistry*, vol. 38, no. 12, pp. 1103–1111, 2005.
- [29] O. Erel, "A novel automated direct measurement method for total antioxidant capacity using a new generation, more stable ABTS radical cation," *Clinical Biochemistry*, vol. 37, no. 4, pp. 277–285, 2004.
- [30] M. Harma, M. Harma, and O. Erel, "Increased oxidative stress in patients with hydatidiform mole," *Swiss Medical Weekly*, vol. 133, no. 41–42, pp. 563–566, 2003.
- [31] H. H. Draper, E. J. Squires, H. Mahmoodi, J. Wu, S. Agarwal, and M. Hadley, "A comparative evaluation of thiobarbituric acid methods for the determination of malondialdehyde in biological materials," *Free Radical Biology & Medicine*, vol. 15, no. 4, pp. 353–363, 1993.
- [32] D. Mitev, H. Gradeva, Z. Stoyanova et al., "Evaluation of thiol compounds and lipid peroxidative products in plasma of



- patients with COPD,” *Trakia Journal of Sciences*, vol. 8, pp. 306–314, 2010.
- [33] H. V. Sudeep, V. K. D. Patel, and S. K., “Biomechanism of chlorogenic acid complex mediated plasma free fatty acid metabolism in rat liver,” *BMC Complementary and Alternative Medicine*, vol. 16, no. 1, pp. 274–278, 2016.
  - [34] R. Jiang, J. M. Hodgson, E. Mas, K. D. Croft, and N. C. Ward, “Chlorogenic acid improves *ex vivo* vessel function and protects endothelial cells against HOCl-induced oxidative damage, via increased production of nitric oxide and induction of Hmox-1,” *The Journal of Nutritional Biochemistry*, vol. 27, pp. 53–60, 2016.
  - [35] M. S. M. Tsang, D. Jiao, B. Chan et al., “Anti-inflammatory activities of pentaherbs formula, berberine, gallic acid and chlorogenic acid in atopic dermatitis-like skin inflammation,” *Molecules*, vol. 21, no. 4, 2016.
  - [36] M. Zhang and X. Hu, “Mechanism of chlorogenic acid treatment on femoral head necrosis and its protection of osteoblasts,” *Biomedical Reports*, vol. 5, no. 1, pp. 57–62, 2016.
  - [37] F. H. Lin, J. Y. Lin, R. D. Gupta et al., “Ferulic acid stabilizes a solution of vitamins C and E and doubles its photoprotection of skin,” *The Journal of Investigative Dermatology*, vol. 125, no. 4, pp. 826–832, 2005.
  - [38] R. Sultana, “Ferulic acid ethyl ester as a potential therapy in neurodegenerative disorders,” *Biochimica et Biophysica Acta (BBA) - Molecular Basis of Disease*, vol. 1822, no. 5, pp. 748–752, 2012.
  - [39] U. Das, K. Manna, A. Khan et al., “Ferulic acid (FA) abrogates  $\gamma$ -radiation induced oxidative stress and DNA damage by up-regulating nuclear translocation of Nrf2 and activation of NHEJ pathway,” *Free Radical Research*, vol. 51, no. 1, pp. 47–63, 2016.
  - [40] T. S. de Melo, P. R. Lima, K. M. M. B. Carvalho et al., “Ferulic acid lowers body weight and visceral fat accumulation via modulation of enzymatic, hormonal and inflammatory changes in a mouse model of high-fat diet-induced obesity,” *Brazilian Journal of Medical and Biological Research*, vol. 50, article e5630, pp. 1–8, 2017.
  - [41] S. Ghosh, P. Basak, S. Dutta, S. Chowdhury, and P. C. Sil, “New insights into the ameliorative effects of ferulic acid in pathophysiological conditions,” *Food and Chemical Toxicology*, vol. 103, pp. 41–55, 2017.
  - [42] J. F. Aitken, K. M. Loomes, I. Riba-Garcia et al., “Rutin suppresses human-amylin/hIAPP misfolding and oligomer formation *in-vitro*, and ameliorates diabetes and its impacts in human-amylin/hIAPP transgenic mice,” *Biochemical and Biophysical Research Communications*, vol. 482, no. 4, pp. 625–631, 2017.
  - [43] T. Asano, H. Matsuzaki, N. Iwata et al., “Protective effects of ferulic acid against chronic cerebral hypoperfusion-induced swallowing dysfunction in rats,” *International Journal of Molecular Sciences*, vol. 18, no. 3, 2017.
  - [44] Y. M. Liu, C. Y. Hu, J. D. Shen, S. H. Wu, Y. C. Li, and L. T. Yi, “Elevation of synaptic protein is associated with the antidepressant-like effects of ferulic acid in a chronic model of depression,” *Physiology & Behavior*, vol. 169, pp. 184–188, 2017.
  - [45] E. Mhillaj, S. Catino, F. M. Miceli et al., “Ferulic acid improves cognitive skills through the activation of the heme oxygenase system in the rat,” *Molecular Neurobiology*, vol. 55, no. 2, pp. 905–916, 2018.
  - [46] I. Kiliç and Y. Yeşiloğlu, “Spectroscopic studies on the antioxidant activity of *p*-coumaric acid,” *Spectrochimica Acta Part A: Molecular and Biomolecular Spectroscopy*, vol. 115, pp. 719–724, 2013.
  - [47] I. Aguilar-Hernández, N. K. Afseth, T. López-Luke, F. F. Contreras-Torres, J. P. Wold, and N. Ornelas-Soto, “Surface enhanced Raman spectroscopy of phenolic antioxidants: a systematic evaluation of ferulic acid, *p*-coumaric acid, caffeic acid and sinapic acid,” *Vibrational Spectroscopy*, vol. 89, pp. 113–122, 2017.
  - [48] S. H. Sharma, D. R. Chellappan, P. Chinnaswamy, and S. Nagarajan, “Protective effect of *p*-coumaric acid against 1,2 dimethylhydrazine induced colonic preneoplastic lesions in experimental rats,” *Biomedicine & Pharmacotherapy*, vol. 94, pp. 577–588, 2017.
  - [49] S. A. Heleno, A. Martins, M. J. R. P. Queiroz, and I. C. F. R. Ferreira, “Bioactivity of phenolic acids: metabolites *versus* parent compounds: a review,” *Food Chemistry*, vol. 173, pp. 501–513, 2015.
  - [50] E. H. Aksu, F. M. Kandemir, M. Özkaraca, A. D. Ömür, S. Küçükler, and S. Çomaklı, “Rutin ameliorates cisplatin-induced reproductive damage via suppression of oxidative stress and apoptosis in adult male rats,” *Andrologia*, vol. 49, no. 1, 2017.
  - [51] X. Yuan, G. Wei, Y. You et al., “Rutin ameliorates obesity through brown fat activation,” *The FASEB Journal*, vol. 31, no. 1, pp. 333–345, 2017.
  - [52] F. Imam, N. O. Al-Harbi, M. M. Al-Harbia et al., “Rutin attenuates carfilzomib-induced cardiotoxicity through inhibition of NF- $\kappa$ B, hypertrophic gene expression and oxidative stress,” *Cardiovascular Toxicology*, vol. 17, no. 1, pp. 58–66, 2017.
  - [53] Y. Wang, Y. Zhang, B. Sun, Q. Tong, and L. Ren, “Rutin protects against pirarubicin-induced cardiotoxicity through TGF- $\beta$ 1-p38 MAPK signaling pathway,” *Evidence-based Complementary and Alternative Medicine*, vol. 2017, Article ID 1759385, 10 pages, 2017.
  - [54] W. Wang, Q. H. Wu, Y. Sui, Y. Wang, and X. Qiu, “Rutin protects endothelial dysfunction by disturbing Nox4 and ROS-sensitive NLRP3 inflammasome,” *Biomedicine & Pharmacotherapy*, vol. 86, pp. 32–40, 2017.
  - [55] A. Kotsiou, N. Seferos, H. G. Mikail, and C. Tesseromatis, “Pleiotropic activity of *Hypericum perforatum* L,” *Journal of Medicinal Plants Studies*, vol. 4, no. 4, pp. 256–258, 2016.
  - [56] P. Wu, F. Li, J. Zhang, B. Yang, Z. Ji, and W. Chen, “Phytochemical compositions of extract from peel of hawthorn fruit, and its antioxidant capacity, cell growth inhibition, and acetylcholinesterase inhibitory activity,” *BMC Complementary and Alternative Medicine*, vol. 17, no. 1, pp. 151–157, 2017.
  - [57] S. F. Akomolafe, G. Oboh, S. I. Oyeleye, and A. A. Boligon, “Aqueous extract from *Ficus capensis* leaves inhibits key enzymes linked to erectile dysfunction and prevent oxidative stress in rats’ penile tissue,” *NFS Journal*, vol. 4, pp. 15–21, 2016.
  - [58] D.-H. Kim, J.-H. Cho, and Y.-J. Cho, “Anti-inflammatory activity of extracts from ultra-fine ground *Saururus chinensis* leaves in lipopolysaccharide-stimulated Raw 264.7 cells,” *Journal of Applied Biological Chemistry*, vol. 59, no. 1, pp. 37–43, 2016.
  - [59] Y. Liang, J. Li, Q. Lin et al., “Research progress on signaling pathway-associated oxidative stress in endothelial cells,” *Oxidative Medicine and Cellular Longevity*, vol. 2017, Article ID 7156941, 8 pages, 2017.

- [60] S. Gu, B. Cao, R. Sun et al., "A metabolomic and pharmacokinetic study on the mechanism underlying the lipid-lowering effect of orally administered berberine," *Molecular BioSystems*, vol. 11, no. 2, pp. 463–474, 2015.
- [61] V. G. N. V. Prasad, C. Vivek, P. Anand Kumar, P. Ravi Kumar, and G. S. Rao, "Turpentine oil induced inflammation decreases absorption and increases distribution of phenacetin without altering its elimination process in rats," *European Journal of Drug Metabolism and Pharmacokinetics*, vol. 40, no. 1, pp. 23–28, 2015.
- [62] J. Lei, Y. Vodovotz, E. Tzeng, and T. R. Billiar, "Nitric oxide, a protective molecule in the cardiovascular system," *Nitric Oxide*, vol. 35, pp. 175–185, 2013.
- [63] S. Yuan, R. P. Patel, and C. G. Kevil, "Working with nitric oxide and hydrogen sulfide in biological systems," *American Journal of Physiology-Lung Cellular and Molecular Physiology*, vol. 308, no. 5, pp. L403–L415, 2015.
- [64] A. Predonzani, B. Cali, A. H. Agnellini, and B. Molon, "Spotlights on immunological effects of reactive nitrogen species: when inflammation says nitric oxide," *World Journal of Experimental Medicine*, vol. 5, no. 2, pp. 64–76, 2015.
- [65] D. D. Thomas, J. L. Heinecke, L. A. Ridnour et al., "Signaling and stress: the redox landscape in NOS2 biology," *Free Radical Biology & Medicine*, vol. 87, no. 301, pp. 204–225, 2015.
- [66] C. P. Bondonno, K. D. Croft, N. Ward, M. J. Considine, and J. M. Hodgson, "Dietary flavonoids and nitrate: effects on nitric oxide and vascular function," *Nutrition Reviews*, vol. 73, no. 4, pp. 216–235, 2015.
- [67] J. Lorin, M. Zeller, J. C. Guillard, Y. Cottin, C. Vergely, and L. Rochette, "Arginine and nitric oxide synthase: regulatory mechanisms and cardiovascular aspects," *Molecular Nutrition & Food Research*, vol. 58, no. 1, pp. 101–116, 2014.
- [68] H.-J. Hsieh, C.-A. Liu, B. Huang, A. H. H. Tseng, and D. Wang, "Shear-induced endothelial mechanotransduction: the interplay between reactive oxygen species (ROS) and nitric oxide (NO) and the pathophysiological implications," *Journal of Biomedical Science*, vol. 21, no. 1, pp. 3–15, 2014.
- [69] B. Halliwell, "The antioxidant paradox: less paradoxical now?," *British Journal of Clinical Pharmacology*, vol. 75, no. 3, pp. 637–644, 2013.
- [70] M. E. Bauer and M. D. I. Fuente, "The role of oxidative and inflammatory stress and persistent viral infections in immunosenescence," *Mechanisms of Ageing and Development*, vol. 158, pp. 27–37, 2016.
- [71] S. K. Biswas, "Does the interdependence between oxidative stress and inflammation explain the antioxidant paradox?," *Oxidative Medicine and Cellular Longevity*, vol. 2016, Article ID 5698931, 9 pages, 2016.
- [72] H. Sies, "Physiological Society symposium: impaired endothelial and smooth muscle cell function in oxidative stress oxidative stress: oxidants and antioxidants," *Experimental Physiology*, vol. 82, pp. 291–295, 1997.
- [73] T. Finkel, "Oxidant signals and oxidative stress," *Current Opinion in Cell Biology*, vol. 15, no. 2, pp. 247–254, 2003.
- [74] M. Mittal, M. R. Siddiqui, K. Tran, S. P. Reddy, and A. B. Malik, "Reactive oxygen species in inflammation and tissue injury," *Antioxidants & Redox Signaling*, vol. 20, no. 7, pp. 1126–1167, 2014.
- [75] K. Sevgi, B. Tepe, and C. Sarikurkcu, "Antioxidant and DNA damage protection potentials of selected phenolic acids," *Food and Chemical Toxicology*, vol. 77, pp. 12–21, 2015.
- [76] G. L. Milne, S. C. Sanchez, E. S. Musiek, and J. D. Morrow, "Quantification of F<sub>2</sub>-isoprostanes as a biomarker of oxidative stress," *Nature Protocols*, vol. 2, no. 1, pp. 221–226, 2007.
- [77] E. Ho, K. Karimi Galougahi, C.-C. Liu, R. Bhindi, and G. A. Figtree, "Biological markers of oxidative stress: applications to cardiovascular research and practice," *Redox Biology*, vol. 1, no. 1, pp. 483–491, 2013.
- [78] A. F. Cătoi, A. Părvu, R. F. Galea, I. D. Pop, A. Mureșan, and C. Cătoi, "Nitric oxide, oxidant status and antioxidant response in morbidly obese patients: the impact of 1-year surgical weight loss," *Obesity Surgery*, vol. 23, no. 11, pp. 1858–1863, 2013.
- [79] A. F. Cătoi, A. Părvu, A. Mureșan, and L. Busetto, "Metabolic mechanisms in obesity and type 2 diabetes: insights from bariatric/metabolic surgery," *Obesity Facts*, vol. 8, no. 6, pp. 350–363, 2015.
- [80] M. T. Barcia, P. B. Pertuzatti, V. C. Bochi, I. Hermosín-Gutiérrez, and H. T. Godoy, "Vinification by-products and their phenolic compounds," *American Journal of Food Science and Technology*, vol. 3, no. 4A, pp. 18–23, 2015.
- [81] A. Ghiselli, M. Serafini, F. Natella, and C. Scaccini, "Total antioxidant capacity as a tool to assess redox status: critical view and experimental data," *Free Radical Biology & Medicine*, vol. 29, no. 11, pp. 1106–1114, 2000.
- [82] O. Erel, "A novel automated method to measure total antioxidant response against potent free radical reactions," *Clinical Biochemistry*, vol. 37, no. 2, pp. 112–119, 2004.
- [83] F. K. Yalcin, M. Er, H. C. Hasanoglu et al., "Deteriorations of pulmonary function, elevated carbon monoxide levels and increased oxidative stress amongst water-pipe smokers," *International Journal of Occupational Medicine and Environmental Health*, vol. 30, no. 5, pp. 731–742, 2017.
- [84] D. A. Butterfield, T. Reed, and R. Sultana, "Roles of 3-nitrotyrosine- and 4-hydroxynonenal-modified brain proteins in the progression and pathogenesis of Alzheimer's disease," *Free Radical Research*, vol. 45, no. 1, pp. 59–72, 2010.
- [85] M. H. Shishehbor, R. J. Aviles, M. L. Brennan et al., "Association of nitrotyrosine levels with cardiovascular disease and modulation by statin therapy," *JAMA*, vol. 289, no. 13, pp. 1675–1680, 2003.
- [86] D. Tsikas, "Assessment of lipid peroxidation by measuring malondialdehyde (MDA) and relatives in biological samples: analytical and biological challenges," *Analytical Biochemistry*, vol. 524, pp. 13–30, 2017.
- [87] D. Del Rio, A. J. Stewart, and N. Pellegrini, "A review of recent studies on malondialdehyde as toxic molecule and biological marker of oxidative stress," *Nutrition, Metabolism, and Cardiovascular Diseases*, vol. 15, no. 4, pp. 316–328, 2005.
- [88] K. Uchida, "Forum. Role of oxidation in atherosclerosis. Role of reactive aldehyde in cardiovascular diseases," *Free Radical Biology & Medicine*, vol. 28, no. 12, pp. 1685–1696, 2000.
- [89] A. G. Pirinccioglu, D. Gökalp, M. Pirinccioglu, G. Kizil, and M. Kizil, "Malondialdehyde (MDA) and protein carbonyl (PCO) levels as biomarkers of oxidative stress in subjects with familial hypercholesterolemia," *Clinical Biochemistry*, vol. 43, no. 15, pp. 1220–1224, 2010.
- [90] M. Boaz, Z. Matas, A. Biro et al., "Serum malondialdehyde and prevalent cardiovascular disease in hemodialysis," *Kidney International*, vol. 56, no. 3, pp. 1078–1083, 1999.
- [91] M. C. Polidori, K. Savino, G. Alunni et al., "Plasma lipophilic antioxidants and malondialdehyde in congestive heart failure

- patients: relationship to disease severity," *Free Radical Biology and Medicine*, vol. 32, no. 2, pp. 148–152, 2002.
- [92] A. Elbay, O. F. Ozer, M. Altinisik et al., "A novel tool reflecting the role of oxidative stress in the cataracts: thiol/disulfide homeostasis," *Scandinavian Journal of Clinical and Laboratory Investigation*, vol. 77, no. 3, pp. 223–227, 2017.
- [93] J. L. Gilmore, X. Yi, L. Quan, and A. V. Kabanov, "Novel nano-materials for clinical neuroscience," *Journal of Neuroimmune Pharmacology*, vol. 3, no. 2, pp. 83–94, 2008.
- [94] M. Prakash, M. S. Shetty, P. Tilak, and N. Anwar, "Total thiols: biomedical importance and their alteration in various disorders," *Online Journal of Health and Allied Sciences*, vol. 8, no. 2, pp. 1–9, 2009.

## Research Article

# Anti-Inflammatory Activity of *Boswellia serrata* Extracts: An *In Vitro* Study on Porcine Aortic Endothelial Cells

Martina Bertocchi , Gloria Isani , Federica Medici, Giulia Andreani ,  
Irvin Tubon Usca , Paola Roncada, Monica Forni , and Chiara Bernardini 

Department of Veterinary Medical Sciences-DIMEVET, University of Bologna, Ozzano Emilia, Bologna 40064, Italy

Correspondence should be addressed to Gloria Isani; [gloria.isani@unibo.it](mailto:gloria.isani@unibo.it)

Received 21 February 2018; Accepted 11 April 2018; Published 25 June 2018

Academic Editor: Raluca M. Pop

Copyright © 2018 Martina Bertocchi et al. This is an open access article distributed under the Creative Commons Attribution License, which permits unrestricted use, distribution, and reproduction in any medium, provided the original work is properly cited.

This study is aimed at investigating the cytotoxicity, anti-inflammatory, and angiogenic activities of two *Boswellia serrata* extracts on primary culture of porcine aortic endothelial cells (pAECs). Chemical characterization of a dry extract (extract A) and a hydroenzymatic extract (extract G) of *B. serrata* was performed by HPLC using pure boswellic acids (BAs) as standard. In cultured pAECs, extract G improved cell viability, following LPS challenge, in a dose-dependent manner and did not show any toxic effect. On the other hand, extract A was toxic at higher doses and restored pAEC viability after LPS challenge only at lower doses. Pure BAs, used at the same concentrations as those determined in the phytoextracts, did not contrast LPS-induced cytotoxicity. Extract A showed proangiogenic properties at the lowest dose, and the same result was observed using pure AKBA at the corresponding concentration, whereas extract G did not show any effect on the migration capacity of endothelial cells. In conclusion, an anti-inflammatory activity of *B. serrata* extracts on endothelial cells was reported, though cytotoxicity or proliferative stimulation can occur instead of a protective effect, depending on the dose and the formulation.

## 1. Introduction

The endothelium, uniquely positioned at the interface between the vascular wall and the blood, regulates multiple functions such as maintenance of normal vascular tone, modulation of coagulation, and immune responses [1]. It is widely demonstrated that the exposure of endothelial cells to proinflammatory stressors results in the production of molecules correlated with a proadhesive, prothrombotic, and proinflammatory phenotype that contributes to vascular disorders [2, 3], including cardiovascular diseases (CVDs).

Since ancient times, the extracts from the oleo-gum resin of *Boswellia serrata* Roxb. ex Colebr. (family *Burseraceae*), also identified as Indian frankincense or Salai Guggal, have been used in traditional Ayurvedic medicine for the treatment of inflammatory diseases, including osteoarthritis and chronic bowel diseases [4–8].

The oleo-gum resin, obtained by incision of the bark, is composed by essential oil (5–9%), mucopolysaccharides

(21–22%), and pure resin (65–85%), containing tetracyclic and pentacyclic triterpene acids, of which boswellic acids (BAs) are the most important bioactive molecules [4, 9, 10]. In particular, 11-keto- $\beta$ -boswellic acid (KBA) and 3-O-acetyl-11-keto- $\beta$ -boswellic acid (AKBA) were proposed to act as inhibitors of 5-lipoxygenase (5-LO) [11, 12]. Recently, other components of the phytocomplex, such as  $\beta$ -boswellic acid ( $\beta$ BA), have been suggested as anti-inflammatory molecules, acting through inhibition of serine protease cathepsin G (catG) and microsomal prostaglandin E synthase (mPGES) [9].

Differences in the relative amount of BAs and other components of the phytocomplex are related to the existence of different species of the genus *Boswellia*, to environmental conditions (e.g., soil composition, season, and air humidity), and to the extraction procedure [13] leading to herbal products of different composition and quality. In a previous study, seven *B. serrata* extracts were compared for their AKBA content and antioxidant power, highlighting wide variations



[14]. In particular, one of the extracts obtained by bioliquefaction based on enzyme biocatalysis (hydroenzymatic extract) [15] showed interesting peculiarities. A lower content of AKBA and antioxidant power but higher activity in *ex vivo* tests on peripheral blood mononuclear cells (PBMCs) was determined in comparison with the dry extract [14]. In recent years, attention has also been focused on the role of other BAs, namely, KBA and  $\beta$ BA [16, 17], suggesting a possible pharmacological activity also for these BAs. Preliminary data showed wide variability in the concentration of BAs in different extracts [18]; therefore, the present research is aimed at deepening the chemical characterization of the two extracts previously studied, focusing on HPLC quantification of KBA and  $\beta$ BA. The effect of different formulations will be evaluated in comparison with the individual pure BAs in an interesting *in vitro* model: primary culture of porcine aortic endothelial cells (pAECs). With pig as an excellent model for translational medicine in the cardiovascular field [19, 20], we have previously isolated and cultured endothelial cells from thoracic aortas [21]. These primary cultures maintain a stable phenotype, and they prove to be an excellent model of study for the vascular response to different stressors [22, 23]. Therefore, pAECs were chosen as an ideal *in vitro* model to study the anti-inflammatory and angiogenic properties of the two *B. serrata* extracts in comparison with pure AKBA, KBA, and  $\beta$ BA, either individually or mixed together.

## 2. Materials and Methods

**2.1. Chemicals and Reagents.** Human endothelial SFM medium, heat-inactivated fetal bovine serum (FBS), antibiotic-antimycotic, and Dulbecco's phosphate-buffered saline (DPBS) were purchased from Gibco-Life technologies (Carlsbad CA, USA). Dimethyl sulfoxide (DMSO), trypsin EDTA solution, lipopolysaccharide (LPS) (*E. coli* 055: B5), glycerol, methanol, phosphoric acid, acetonitrile, and AKBA (batch number BCBN2928V and CAS number 67416-61-9) were purchased from Sigma-Aldrich Co. (St Louis, MO, USA). KBA and  $\beta$ BA (batch numbers 15020106 and 15010405 and CAS numbers 17019-92-0 and 631-69-6, resp.) were obtained from PhytoPlan (Heidelberg, Germany). Six out of seven samples (extracts A–F) are dry extracts of *B. serrata* oleo-gum resin. The powder is insoluble in water but soluble in methanol and dimethyl sulfoxide (DMSO). Extract G is an aqueous extract obtained by a process of bioliquefaction based on enzyme biocatalysis [15]. Briefly, the gum resin from *B. serrata* was suspended in water (1 : 10 *w/v*) and subjected to enzymatic digestion by xylanase,  $\alpha$ -amylase, and glucosidase for 24 hours. One ml of hydroenzymatic extract is obtained from 145 mg of *B. serrata* resin (145 mg resin/ml).

**2.2. Qualitative and Quantitative Characterization of *B. serrata* Extracts.** Qualitative and quantitative analyses of *B. serrata* extracts were performed by a reversed-phase high-performance liquid chromatography (HPLC) method using the HPLC system (Beckman Coulter, Brea, CA, USA), comprising a 116 pump, a 507 automatic autosampler, a UV-Diode Array 168 detector, and integration software 32 Karat as reported by Beghelli et al. [14]. Seven samples (A–G) were

analyzed for KBA and  $\beta$ BA concentrations and were prepared by dissolving extracts in methanol. KBA and  $\beta$ BA standard stock solutions were prepared by dissolving 5 mg of analytical standard in methanol (5 mL). The calibration curves were obtained by analyzing six serial dilutions (50 ppm, 25 ppm, 10 ppm, 5 ppm, 2.5 ppm, and 1 ppm) of the stock solution and by plotting the peak area measured at 260 nm against KBA concentrations and at 210 nm against  $\beta$ BA concentrations. The following equations of the curves were obtained:

$$\begin{aligned} \text{KBA} &= 77361x + 44918, r^2 = 0.999, \\ \beta\text{BA} &= 26532x + 721.54, r^2 = 0.999. \end{aligned} \quad (1)$$

The KBA and  $\beta$ BA peaks in the samples were identified on the basis of the retention time on the chromatogram at 260 nm and 210 nm, respectively. All measurements were performed in triplicate and data were reported as mean  $\pm$  SD.

**2.3. Cell Culture and Treatment.** Porcine aortic endothelial cells (pAECs) were isolated and maintained as previously described by Bernardini et al. [21]. All experiments were performed with cells from the third to the eighth passage. The first seeding after thawing was always performed in T-25 tissue culture flasks ( $3 \times 10^5$  cells/flask) (T-25, BD Falcon, Franklin Lakes, NJ, USA), and successive experiments were conducted in 24-well plates (scratch test) or 96-well plates (cell viability) with confluent cultures. Cells were cultured in human endothelial SFM medium, added with FBS (5%) and antimicrobial/antimycotic solution (1x) in a 5% CO<sub>2</sub> atmosphere at 38.5°C. Extract A was dissolved in DMSO at 10 mg dry extract/ml (stock solution) and then diluted in culture medium to obtain four doses containing 0.1, 1, 10, and 100  $\mu$ g of dry extract/ml, respectively. Extract G, which is an aqueous solution, was directly diluted in culture medium to obtain four doses referring to 2.4, 24, 240, and 2400  $\mu$ g of resin/ml. These doses were chosen and normalized on the basis of AKBA concentration in extracts as reported in [14]: for both extracts, the lowest dose contained 3.8 ng/ml of AKBA and the highest dose contained 3.8  $\mu$ g/ml of AKBA.

Pure analytical grade BAs (KBA, AKBA, and  $\beta$ BA) were dissolved in methanol (stock solution 1 mg/ml) and then in culture medium to obtain the required concentrations. Two doses were chosen: *low*, corresponding to 3.8 ng/ml AKBA, 3 ng/ml KBA, and 8 ng/ml  $\beta$ BA, and *high*, corresponding to 380 ng/ml AKBA, 300 ng/ml KBA, and 800 ng/ml  $\beta$ BA. For each treatment, the same concentration of the specific vehicle was used as control.

**2.4. Effect of *B. serrata* Extracts on pAEC Viability.** pAECs were seeded in a 96-well plate ( $6 \times 10^3$  cells/well) and exposed to four increasing doses of *B. serrata* extracts for 24 h. Cell viability was measured using tetrazolium salt (MTT assay). The formazan absorbance was measured at a wavelength of 570 nm, using Infinite® F50/Robotic absorbance microplate readers from TECAN (Life Sciences). The background absorbance of multiwell plates at 690 nm was also measured and subtracted from the 570 nm measurements.



**2.5. Effect of *B. serrata* Extracts on LPS-Induced pAEC Death.** pAECs seeded in a 96-well plate ( $6 \times 10^3$  cells/cm<sup>2</sup>) were exposed to lipopolysaccharide (LPS) (25 µg/ml) for 24 h either in the presence or in the absence of extracts A and G or pure BAs at the concentrations reported above. Cell viability was evaluated by MTT assay.

**2.6. Effect of *B. serrata* Extracts on pAEC Migration Capacity.** pAECs were seeded in a 24-well plate ( $4 \times 10^4$  cells/well). When cells reached confluence, a wound was induced scratching the surface by a pipette tip, then the detached cells were removed by washing with DPBS. Complete medium containing low and high doses of extract A (0.1 µg dry extract/ml and 10 µg dry extract/ml) and extract G (2.4 µg resin/ml and 240 µg resin/ml) and pure BAs at low (3 ng/ml KBA, 3.8 ng/ml AKBA, and 8 ng/ml βBA) and high (300 ng/ml KBA, 380 ng/ml AKBA, and 800 ng/ml βBA) concentrations were added. Microscopic phase-contrast pictures and three measurements of the damaged areas were taken immediately after the scratches (T0) and after 6 h (T1) and 24 h (T2). Images were acquired using a Nikon epifluorescence microscope equipped with digital camera (Nikon, Yokohama, Japan).

**2.7. Statistical Analysis.** Each treatment was replicated three times (migration capacity) or eight times (cell viability and LPS challenge). Data were analyzed with a one-way analysis of variance (ANOVA) followed by the Tukey post hoc comparison test or Student's *t*-test. Differences of at least  $p < 0.05$  were considered significant. Statistical analysis was carried out using R software (<http://www.R-project.org>).

### 3. Results

**3.1. KBA and βBA Quantification by HPLC-DAD Analysis.** Representative chromatograms of KBA, AKBA, and βBA analytical standards as well as extracts A and G analyzed at 210 and 260 nm are reported in Figure 1.

Both extracts presented two major peaks at 260 nm: the first one, at Rt of 13.2 min, identified as KBA by the use of the analytical standard, and the second one, at Rt of 26 min, previously identified as AKBA. Other components of the *B. serrata* phytocomplex were only visualized at 210 nm, and the peak at Rt of 49 min was identified as βBA by the use of the analytical standard. KBA, AKBA, and βBA concentrations, calculated based on the peak area and the calibration curve, are shown in Table 1.

Quantitative and qualitative differences were present. The concentrations of BAs in extract G were two orders of magnitude lower than in extract A, and the chromatogram of extract G was characterized by a major number of peaks resolved at 210 nm. Data on KBA and βBA concentrations in other additional five dry extracts (B–F) are reported in Table S1 in the Supplementary Material.

**3.2. Effect of *B. serrata* Extracts on pAEC Viability.** Extract A was cytotoxic at higher concentrations, resulting in a reduction in cell viability of 12 and 47%, respectively, while lower concentrations did not affect cell viability (Figure 2(a)). Extract G did not show any toxic effect on

pAECs (Figure 2(b)). In the presence of pure BAs, a significant ( $p < 0.05$ ) cytotoxic effect was detected at the concentrations studied (Figure 2(c)). Only AKBA presented a dose-dependent effect.

**3.3. Effect of *B. serrata* Extracts on LPS-Induced pAEC Death.** LPS challenge determined a significant 30% reduction of cell viability. Extract A significantly ( $p < 0.05$ ) reduced the cytotoxicity induced by LPS at the lower concentrations (Figure 3(a)). The highest concentration elicited a significant exacerbation of LPS cytotoxicity resulting in 70% reduction of cell viability, while the lowest concentration showed a significant proliferative effect, resulting in a 40% increase in cell viability. Extract G significantly ( $p < 0.05$ ) restored pAEC viability after LPS treatment at all the concentrations analyzed (Figure 3(b)), without a dose-dependent effect. None of pure BAs, individually or mixed together, was able to contrast LPS cytotoxicity (Figure 3(c)).

**3.4. Effect of *B. serrata* Extracts on pAEC Migration Capacity.** Extract A reduced the damaged area at T1 (6 h) and restored completely the monolayer at T2 (24 h) at the lower concentration, while at 10 µg dry extract/ml no significant effect on cell proliferation was measured (Figure 4(a)). The incubation with extract G did not determine the recovery of the damage (Figure 4(b)). Pure BAs showed a significant wound-healing effect at the end of the incubation at the lower concentration (Figure 4(c)). In particular, AKBA at 3.8 ng/ml completely restored the monolayer.

### 4. Discussion

The gum resin obtained from *B. serrata*, used in Ayurvedic medicine for the treatment of a variety of diseases, is considered a promising natural source of anti-inflammatory molecules, in particular BAs [4, 9].

The quantification of these active molecules is a prerequisite for testing any biological effect of a phytoextract from *B. serrata*. Therefore, the first aim of this study was to better characterize the BA profile through the quantification of KBA and βBA in addition to AKBA. The concentrations of BAs determined in extract A are in the range of those reported by other authors [24–26]. AKBA and KBA are used as markers to ensure the quality of *B. serrata* dry extracts, but their concentrations show wide variability in commercial products, which in general claim 65% of BAs. In general, BAs represent only a percentage of total organic acids, whose concentrations are determined by unspecific titration methods and, as a consequence, the claimed content of 65% BAs is absolutely unrealistic as recently pointed out also by other authors [24, 25]. Very low percentages of KBA and βBA were found in extract G compared to extract A. This aqueous extract was also characterized by low AKBA and low polyphenol concentrations [14], confirming again the importance of the extraction procedure on the phytocomplex composition.

To evaluate the possible biological effects of these different formulations, extracts A and G, normalized on the basis of AKBA content, were used for *in vitro* analyses to assess

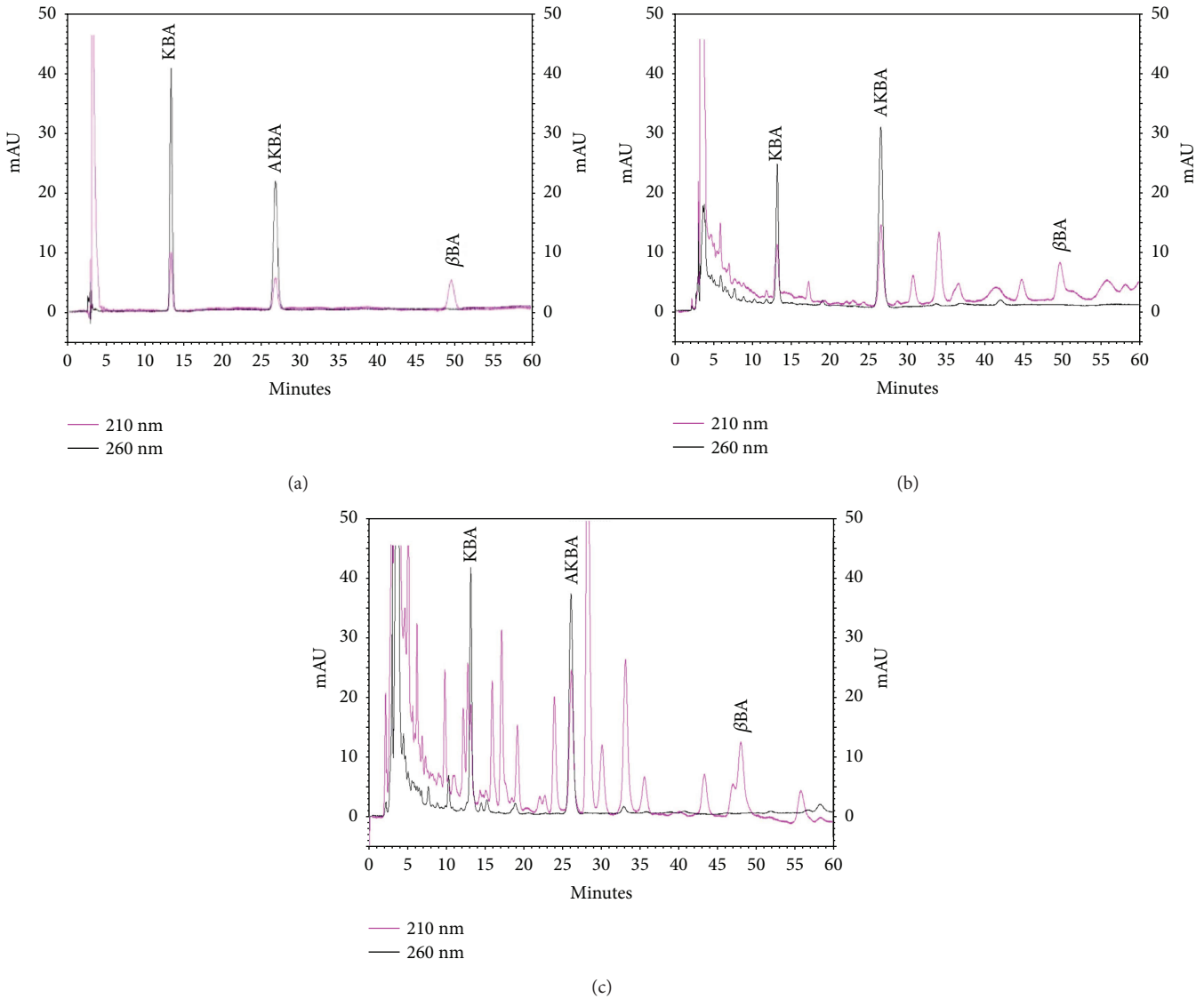


FIGURE 1: Representative chromatograms of pure analytical grade BAs (KBA, AKBA, and  $\beta$ BA) (25 ppm each) (a), extract A (b), and extract G (c) at 210 (pink chromatogram) and 260 nm (black chromatogram).

TABLE 1: KBA,  $\beta$ BA, and AKBA quantification in *Boswellia serrata* extracts. Data are reported as mean  $\pm$  SD ( $n = 3$ ). Concentration is expressed in mg/g of dry extract (extract A) or mg/ml of hydroenzymatic extract (extract G). For each BA, significant differences between extracts are indicated by \* ( $p < 0.05$ , Student's  $t$ -test) and by \*\* ( $p < 0.001$ , Student's  $t$ -test).

Extract	KBA <sup>§</sup>	$\beta$ BA	AKBA <sup>§</sup>
A	15.86 $\pm$ 0.56**	33.53 $\pm$ 7.23*	38.30 $\pm$ 1.01**
G	0.19 $\pm$ 0.02	0.50 $\pm$ 0.03	0.29 $\pm$ 0.04

<sup>§</sup>Data of AKBA concentrations are reported in Beghelli et al. [14].

cytotoxicity, anti-inflammatory activity, and angiogenic properties in comparison with pure BAs. Cytotoxic effects of *B. serrata* dry extracts and BAs were reported in several studies in different cancer cell lines, such as leukemia cells, prostate cancer cells, and gastrointestinal cancer cells [7, 27–30]. As regards the biochemical mechanism

of cell death, Liu et al. [31] reported that BAs are able to induce apoptosis in Hep-G2 cells through the activation of caspase-8, while Bhushan et al. [32] found that a triterpenoid derived from BAs induced apoptosis in HL-60 cells through the activation of Bcl-2 and caspase-3.

The anti-inflammatory activity of *Boswellia* extracts was demonstrated in microvascular endothelial cells by preventing TNF $\alpha$ -induced expression and activity of MMP-3, MMP-10, and MMP-12 [33]. Moreover, previous studies have shown that *B. serrata* extracts and BAs antagonize the inflammatory effect of LPS in human and mouse macrophages, monocytes, and PBMCs [34–36]. Our results demonstrated for the first time the protective effect of *B. serrata* extracts against LPS inflammatory stimulus in endothelial cells. In particular, extract G was the most effective, restoring completely cell viability at all the doses studied without any cytotoxicity. On the contrary, increasing concentrations of extract A lead to opposite results ranging

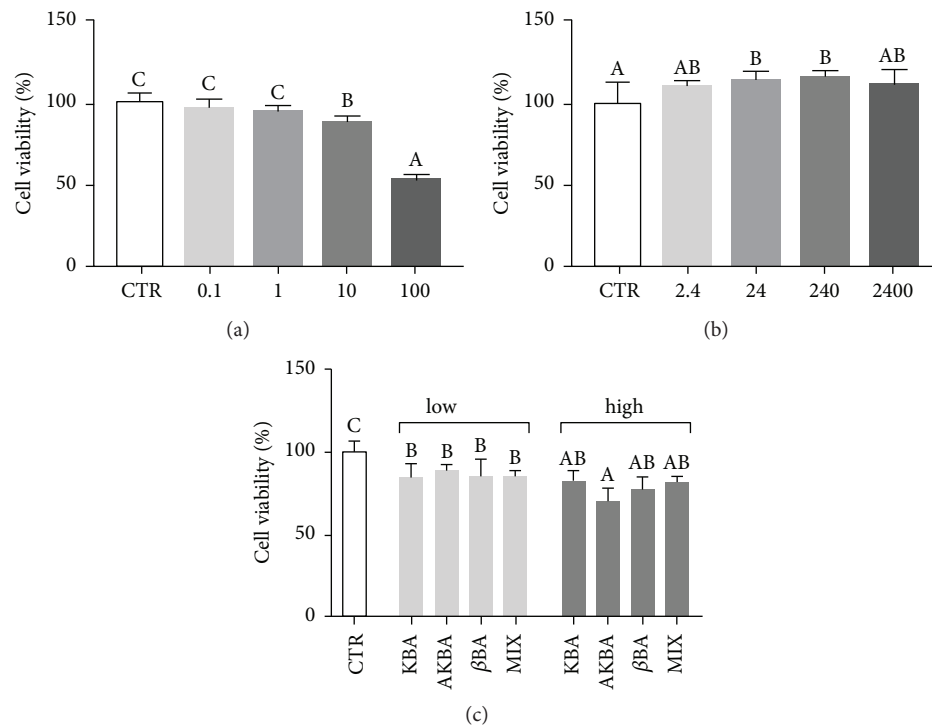


FIGURE 2: Effect of increasing doses of *B. serrata* extract A (0.1, 1, 10, and 100  $\mu\text{g}$  dry extract/ml) (a), extract G (2.4, 24, 240, and 2400  $\mu\text{g}$  resin/ml) (b), and pure BAs (low, corresponding to 3.8 ng/ml AKBA, 3 ng/ml KBA, and 8 ng/ml  $\beta$ BA, and high, corresponding to 380 ng/ml AKBA, 300 ng/ml KBA, and 800 ng/ml  $\beta$ BA) (c) on pAECs. Cell viability was measured by MTT assay. Data are reported as mean  $\pm$  SD of 8 independent replicates. Different letters above the bars indicate significant differences ( $p < 0.05$  ANOVA post hoc Tukey's test).

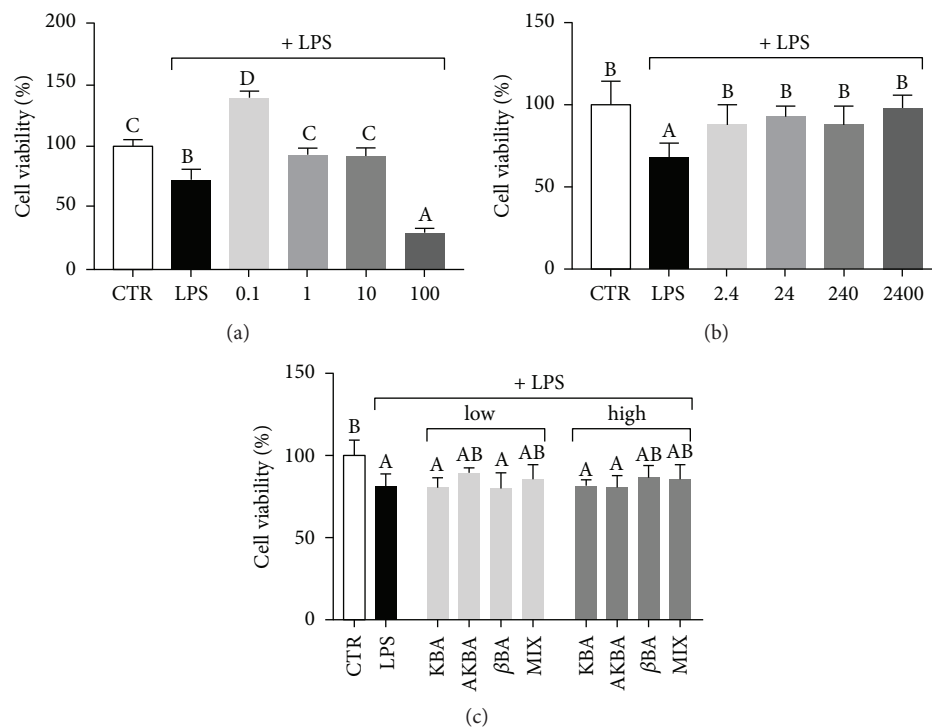


FIGURE 3: Effect of increasing doses of *B. serrata* extract A (0.1, 1, 10, and 100  $\mu\text{g}$  dry extract/ml) (a), extract G (2.4, 24, 240, and 2400  $\mu\text{g}$  resin/ml) (b), and pure BAs (low, corresponding to 3.8 ng/ml AKBA, 3 ng/ml KBA, and 8 ng/ml  $\beta$ BA, and high, corresponding to 380 ng/ml AKBA, 300 ng/ml KBA, and 800 ng/ml  $\beta$ BA) (c) on pAEC viability, in the presence of LPS (25  $\mu\text{g}/\text{ml}$ ), measured by MTT assay. Data are reported as mean  $\pm$  SD of 8 independent replicates. Different letters above the bars indicate significant differences ( $p < 0.05$  ANOVA post hoc Tukey's test).

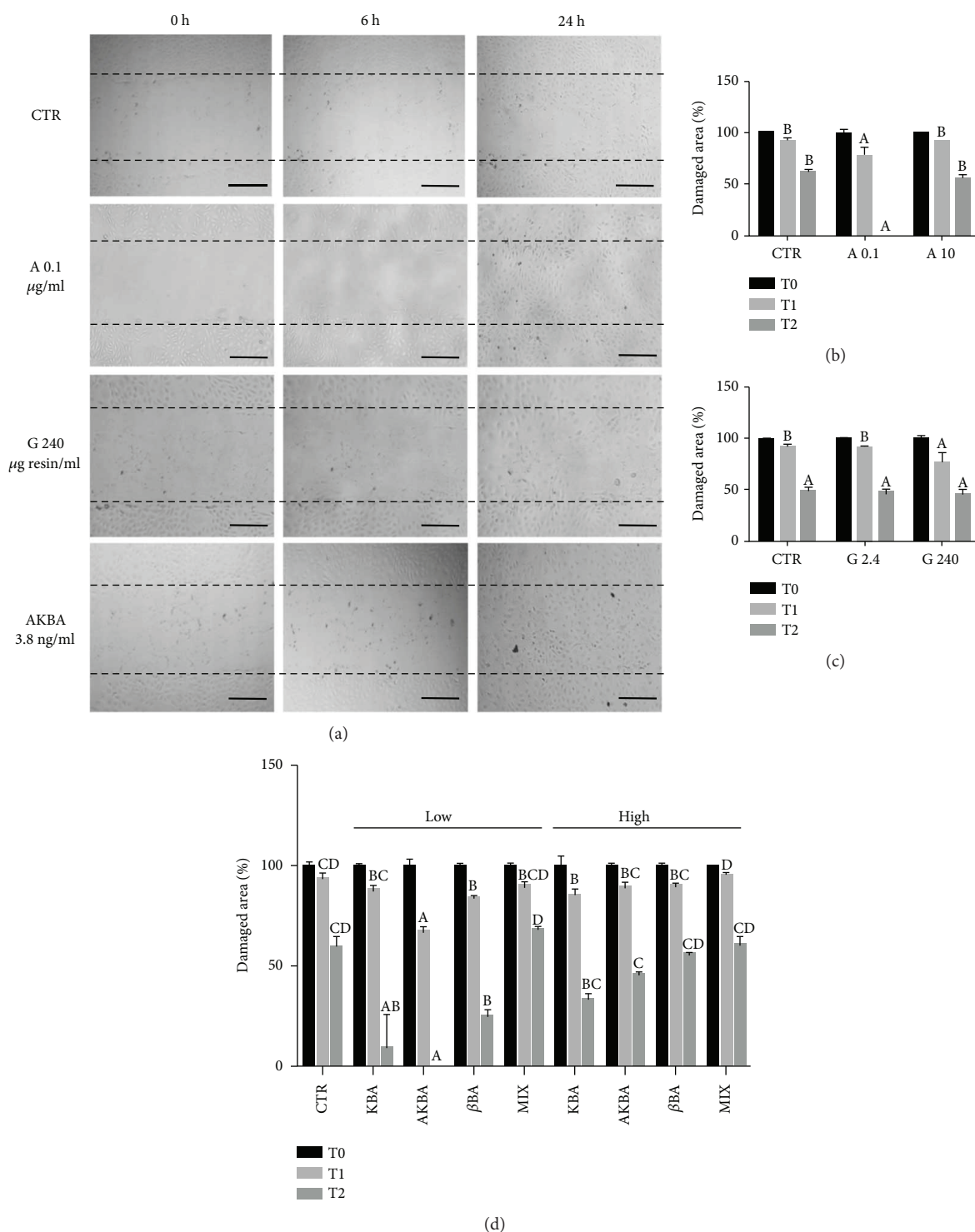


FIGURE 4: Effect of *B. serrata* extracts on pAEC migration capacity. Cells were scratch wounded and then treated with extracts A and G and pure BAs. Photographs were recorded at 0 h (T0), 6 h (T1), and 24 h (T2) after scratching. (a) Representative microscopic phase-contrast pictures showing the size of the scratch wound in different treatment groups compared with control. Scale bar, 200  $\mu\text{m}$ . The extent of the damaged area (%) is reported for treatment with extract A (0.1 and 10  $\mu\text{g}$  dry extract/ml) (b), extract G (2.4 and 240  $\mu\text{g}$  resin/ml) (c), and pure BAs (*low*, corresponding to 3 ng/ml KBA, 3.8 ng/ml AKBA, and 8 ng/ml  $\beta\text{BA}$ , and *high*, corresponding to 300 ng/ml KBA, 380 ng/ml AKBA, and 800 ng/ml  $\beta\text{BA}$ ) (d). Data are reported as mean of 3 replicates  $\pm$  SD. Inside each experimental time (T1 and T2), different letters above the bars indicate significant differences among treatments ( $p < 0.05$ , ANOVA post hoc Tukey's test).

from hyperproliferative effect (the lowest dose) to cytotoxic effect (the highest dose). Interestingly, in our model the use of pure KBA,  $\beta$ BA, and AKBA, either individually or mixed together, failed to protect endothelial cells from LPS toxicity and are only partially in accord with data reported by Henkel et al. [35]. In a cell-free assay, those authors suggested a direct molecular interaction between LPS and BAs lacking the keto moiety, in particular  $\beta$ BA, underlying the anti-inflammatory effect of *Boswellia* extracts.

Our results support the hypothesis that the anti-inflammatory effect of *Boswellia* extracts is not strictly dependent on the presence of the most studied BAs, but it can be related to other bioactive molecules. Other triterpenes, as incensole, could be considered interesting candidates for the pharmacological properties of frankincense, accordingly to suggestions previously reported by other authors [9, 37, 38]. Beyond these bioactive terpenes, the gum resin does contain polysaccharides. These molecules are likely to be minor components in dry extract A, whereas they can be more concentrated in extract G, due to the different polarity of the extraction medium. A water-soluble fraction extracted from the gum resin of *B. serrata* containing galactose, arabinose, and D-glucuronic acid was suggested to act as a potent enhancer of humoral and cell-mediated immune response [39], while the potential anti-inflammatory activity of these polysaccharides has not yet been explored. We cannot exclude that the polysaccharide fraction present in extract G can develop additional modulatory effects on pAECs.

The migration ability of endothelial cells is critical in the physiological and pathological angiogenesis [40]. Our results obtained with an *in vitro* model of physiological angiogenesis showed proangiogenic activity of extract A at the lowest concentration, in agreement with a proliferative effect of the same dose recorded in LPS challenge. In addition, incubation with pure AKBA at the same concentration as that measured in extract A determined the same proangiogenic effect, indicating a possible involvement of this BA in promoting angiogenesis. In contrast, incubation in the presence of extract G containing the same concentrations of AKBA did not show any effect on endothelial cell migration capacity, indicating one more time the existence of complex molecular interactions, which can modify the biological effect of the phytoextract. Contrasting results are also reported in literature. Lulli et al. [41] observed that AKBA reduced proliferation, migration, and tube formation in human retinal microvascular endothelial cells (HRMECs) stimulated with exogenous vascular endothelial growth factor (VEGF). On the other hand, Wang et al. [17] reported that  $\beta$ -BA can attenuate endothelial cell injury in a blood stasis model and protect human umbilical vein endothelial cells (HUEVCs) against cell death induced by oxygen and glucose deprivation. Different regulation pathways could be involved in the repairing activity of *Boswellia* extracts, and further investigations will be necessary to explain why different formulations determine different effects on endothelial cells pathophysiology.

How extracts of *B. serrata* gum resin should modulate the cardiovascular system has been scarcely investigated, so far. Kokkiripati et al. [42] reported that antioxidant

and antithrombotic activities of extracts from *B. serrata* gum resin determined the inhibition of human monocytic cell activation and platelet aggregation. However, recently Siemoneit et al. [43] pointed out the complex agonizing and antagonizing effects of BAs on human platelet aggregation and prompted for careful evaluation of *B. serrata* extract safety in cardiovascular disease-risk patients.

In conclusion, our results demonstrate that different formulations (e.g., dry and hydroenzymatic extracts) obtained from the same botanical species show significantly different biological effects on endothelial cells. The anti-inflammatory activity of *B. serrata* extracts on endothelial cells suggests a potential pharmaceutical application for cardiovascular health, though cytotoxicity or proliferative stimulation can occur instead of a protective effect, depending on the dose and the formulation. This aspect should be carefully considered when these herbal products are used in human and animal phytotherapy.

## Disclosure

Preliminary data has been presented as a poster at the 21th Congress Phytopharm 2017, Graz, Austria, 2–5 July 2017.

## Conflicts of Interest

The authors declare that there is no conflict of interest regarding the publication of this paper.

## Acknowledgments

The authors greatly acknowledge Phenbiox Srl (Calderara di Reno, Bologna, Italy) and Dr. Maurizio Scozzoli for providing the *Boswellia serrata* hydroenzymatic and dry extracts, respectively, and Dr. Alberto Altafini for technical assistance. The authors are grateful to Università di Bologna and Fondazione Cassa di Risparmio di Imola for their financial support.

## Supplementary Materials

Table S1: the concentrations of the two boswellic acids analyzed and discussed in the manuscript in five additional dry extracts of *Boswellia serrata*. The table has been added to emphasize the variability of boswellic acid concentration in different dry extracts obtained from the same botanical species. (*Supplementary Materials*)

## References

- [1] W. C. Aird, "Endothelium and haemostasis," *Hämostaseologie*, vol. 35, no. 1, pp. 11–16, 2015.
- [2] T. Aki, N. Egashira, M. Hama et al., "Characteristics of gabexate mesilate-induced cell injury in porcine aorta endothelial cells," *Society*, vol. 106, no. 3, pp. 415–422, 2008.
- [3] S. Jamwal and S. Sharma, "Vascular endothelium dysfunction: a conservative target in metabolic disorders," *Inflammation Research*, vol. 67, no. 5, pp. 391–405, 2018.
- [4] H. P. T. Ammon, "Boswellic acids in chronic inflammatory diseases," *Planta Medica*, vol. 72, no. 12, pp. 1100–1116, 2006.



- [5] H. P. T. Ammon, "Boswellic acids and their role in chronic inflammatory diseases," in *Anti-Inflammatory Nutraceuticals and Chronic Diseases*, S. C. Gupta, S. Prasad, and B. B. Aggarwal, Eds., pp. 291–327, Cham: Springer International Publishing, Switzerland, 2016.
- [6] I. Gupta, A. Parihar, P. Malhotra et al., "Effects of gum resin of *Boswellia serrata* in patients with chronic colitis," *Planta Medica*, vol. 67, no. 5, pp. 391–395, 2001.
- [7] M. A. Khan, R. Ali, R. Parveen, A. K. Najmi, and S. Ahmad, "Pharmacological evidences for cytotoxic and antitumor properties of Boswellic acids from *Boswellia serrata*," *Journal of Ethnopharmacology*, vol. 191, pp. 315–323, 2016.
- [8] K. Sengupta, K. V. Alluri, A. Satish et al., "A double blind, randomized, placebo controlled study of the efficacy and safety of 5-Loxin® for treatment of osteoarthritis of the knee," *Arthritis Research & Therapy*, vol. 10, no. 4, article R85, 2008.
- [9] M. Abdel-Tawab, O. Werz, and M. Schubert-Zsilavecz, "Boswellia serrata," *Clinical Pharmacokinetics*, vol. 50, no. 6, pp. 349–369, 2011.
- [10] A. R. M. Al-Yasiry and B. Kiczorowska, "Frankincense - therapeutic properties," *Postępy Higieny i Medycyny Doświadczalnej*, vol. 70, pp. 380–391, 2016.
- [11] H. P. T. Ammon, "Modulation of the immune system by *Boswellia serrata* extracts and boswellic acids," *Phytomedicine*, vol. 17, no. 11, pp. 862–867, 2010.
- [12] H. Hussain, A. Al-Harrasi, R. Csuk et al., "Therapeutic potential of boswellic acids: a patent review (1990-2015)," *Expert Opinion on Therapeutic Patents*, vol. 27, no. 1, pp. 81–90, 2017.
- [13] M. Gupta, P. K. Rout, L. N. Misra et al., "Chemical composition and bioactivity of *Boswellia serrata* Roxb. essential oil in relation to geographical variation," *Plant Biosystems - An International Journal Dealing with all Aspects of Plant Biology*, vol. 151, no. 4, pp. 623–629, 2017.
- [14] D. Beghelli, G. Isani, P. Roncada et al., "Antioxidant and ex vivo immune system regulatory properties of *Boswellia serrata* extracts," *Oxidative Medicine and Cellular Longevity*, vol. 2017, Article ID 7468064, 10 pages, 2017.
- [15] L. Setti and D. Zanichelli, "Biorefinery as a bio-refinery's approach for the production of natural bioactive compounds for functional cosmetics," in *Waste Recovery: Strategies, Techniques and Applications in Europe*, L. Morselli, F. Passarini, and I. Vassura, Eds., pp. 122–128, Franco Angeli, Milan, Italy, 2009.
- [16] Y. Ding, M. Chen, M. Wang, Y. Li, and A. Wen, "Posttreatment with 11-keto- $\beta$ -boswellic acid ameliorates cerebral ischemia-reperfusion injury: Nrf2/HO-1 pathway as a potential mechanism," *Molecular Neurobiology*, vol. 52, no. 3, pp. 1430–1439, 2015.
- [17] M. Wang, M. Chen, Y. Ding et al., "Pretreatment with  $\beta$ -boswellic acid improves blood stasis induced endothelial dysfunction: role of eNOS activation," *Scientific Reports*, vol. 5, no. 1, article 15357, 2015.
- [18] M. Bertocchi, F. Medici, C. Bernardini et al., "Characterization of *Boswellia serrata* extracts and evaluation of their effects on porcine aortic endothelial cells," in *Reviews on Clinical Pharmacology and Drug Therapy (The 21th International Congress Phytopharm 2017)*, vol. 15, p. 42, Graz, Austria, July 2017.
- [19] C. Zaragoza, C. Gomez-Guerrero, J. L. Martin-Ventura et al., "Animal models of cardiovascular diseases," *Journal of Biomedicine & Biotechnology*, vol. 2011, Article ID 497841, 13 pages, 2011.
- [20] C. Perleberg, A. Kind, and A. Schnieke, "Genetically engineered pigs as models for human disease," *Disease Models & Mechanisms*, vol. 11, no. 1, article dmm030783, 2018.
- [21] C. Bernardini, A. Zannoni, M. E. Turba et al., "Heat shock protein 70, heat shock protein 32, and vascular endothelial growth factor production and their effects on lipopolysaccharide-induced apoptosis in porcine aortic endothelial cells," *Cell Stress & Chaperones*, vol. 10, no. 4, pp. 340–348, 2005.
- [22] C. Bernardini, A. Zannoni, M. L. Bacci, and M. Forni, "Protective effect of carbon monoxide pre-conditioning on LPS-induced endothelial cell stress," *Cell Stress and Chaperones*, vol. 15, no. 2, pp. 219–224, 2010.
- [23] G. Botelho, C. Bernardini, A. Zannoni, V. Ventrella, M. L. Bacci, and M. Forni, "Effect of tributyltin on mammalian endothelial cell integrity," *Comparative Biochemistry and Physiology Part C: Toxicology & Pharmacology*, vol. 176–177, pp. 79–86, 2015.
- [24] G. Mannino, A. Occhipinti, and M. Maffei, "Quantitative determination of 3-O-acetyl-11-keto- $\beta$ -boswellic acid (AKBA) and other boswellic acids in *Boswellia sacra* Flueck (syn. *B. carteri* Birdw) and *Boswellia serrata* Roxb," *Molecules*, vol. 21, no. 10, p. 1329, 2016.
- [25] J. Meins, C. Artaria, A. Riva, P. Morazzoni, M. Schubert-Zsilavecz, and M. Abdel-Tawab, "Survey on the quality of the top-selling European and American botanical dietary supplements containing boswellic acids," *Planta Medica*, vol. 82, no. 6, pp. 573–579, 2016.
- [26] E. Ranzato, S. Martinotti, A. Volante, A. Tava, M. A. Masini, and B. Burlando, "The major *Boswellia serrata* active 3-acetyl-11-keto- $\beta$ -boswellic acid strengthens interleukin-1 $\alpha$  upregulation of matrix metalloproteinase-9 via JNK MAP kinase activation," *Phytomedicine*, vol. 36, pp. 176–182, 2017.
- [27] Y. Shao, C.-T. Ho, C.-K. Chin, V. Badmaev, W. Ma, and M.-T. Huang, "Inhibitory activity of boswellic acids from *Boswellia serrata* against human leukemia HL-60 cells in culture," *Planta Medica*, vol. 64, no. 4, pp. 328–331, 1998.
- [28] M. Lu, L. Xia, H. Hua, and Y. Jing, "Acetyl-keto-B-boswellic acid induces apoptosis through a death receptor 5-mediated pathway in prostate cancer cells," *Cancer Research*, vol. 68, no. 4, pp. 1180–1186, 2008.
- [29] J.-J. Liu, B. Huang, and S. C. Hooi, "Acetyl-keto- $\beta$ -boswellic acid inhibits cellular proliferation through a p21-dependent pathway in colon cancer cells," *British Journal of Pharmacology*, vol. 148, no. 8, pp. 1099–1107, 2006.
- [30] B. Park, S. Prasad, V. Yadav, B. Sung, and B. B. Aggarwal, "Boswellic acid suppresses growth and metastasis of human pancreatic tumors in an orthotopic nude mouse model through modulation of multiple targets," *PLoS One*, vol. 6, no. 10, article e26943, 2011.
- [31] J.-J. Liu, A. Nilsson, S. Oredsson, V. Badmaev, and R.-D. Duan, "Keto- and acetyl-keto-boswellic acids inhibit proliferation and induce apoptosis in Hep G2 cells via a caspase-8 dependent pathway," *International Journal of Molecular Medicine*, vol. 10, no. 4, pp. 501–505, 2002.
- [32] S. Bhushan, A. Kumar, F. Malik et al., "A triterpenediol from *Boswellia serrata* induces apoptosis through both the intrinsic and extrinsic apoptotic pathways in human leukemia HL-60 cells," *Apoptosis*, vol. 12, no. 10, pp. 1911–1926, 2007.
- [33] S. Roy, S. Khanna, A. V. Krishnaraju et al., "Regulation of vascular responses to inflammation: inducible matrix metalloproteinase-3 expression in human microvascular endothelial cells is sensitive to antiinflammatory Boswellia,"

- Antioxidants & Redox Signaling*, vol. 8, no. 3-4, pp. 653–660, 2006.
- [34] C. Cuaz-Perolin, L. Billiet, E. Bauge et al., “Antiinflammatory and antiatherogenic effects of the NF- $\kappa$ B inhibitor acetyl-11-keto- $\beta$ -boswellic acid in LPS-challenged ApoE-/- mice,” *Arteriosclerosis, Thrombosis, and Vascular Biology*, vol. 28, no. 2, pp. 272–277, 2008.
- [35] A. Henkel, N. Kather, B. Mönch, H. Northoff, J. Jauch, and O. Werz, “Boswellic acids from frankincense inhibit lipopolysaccharide functionality through direct molecular interference,” *Biochemical Pharmacology*, vol. 83, no. 1, pp. 115–121, 2012.
- [36] T. Syrovets, B. Buchele, C. Krauss, Y. Laumonnier, and T. Simmet, “Acetyl-boswellic acids inhibit lipopolysaccharide-mediated TNF- $\alpha$  induction in monocytes by direct interaction with I $\kappa$ B kinases,” *Journal of Immunology*, vol. 174, no. 1, pp. 498–506, 2005.
- [37] A. Moussaieff, E. Shohami, Y. Kashman et al., “Incensole acetate, a novel anti-inflammatory compound isolated from *Boswellia* resin, inhibits nuclear factor- $\kappa$ B activation,” *Molecular Pharmacology*, vol. 72, no. 6, pp. 1657–1664, 2007.
- [38] B. Gayathri, N. Manjula, K. S. Vinaykumar, B. S. Lakshmi, and A. Balakrishnan, “Pure compound from *Boswellia serrata* extract exhibits anti-inflammatory property in human PBMCs and mouse macrophages through inhibition of TNF $\alpha$ , IL-1 $\beta$ , NO and MAP kinases,” *International Immunopharmacology*, vol. 7, no. 4, pp. 473–482, 2007.
- [39] A. Gupta, A. Khajuria, J. Singh, S. Singh, K. A. Suri, and G. N. Qazi, “Immunological adjuvant effect of *Boswellia serrata* (BOS 2000) on specific antibody and cellular response to ovalbumin in mice,” *International Immunopharmacology*, vol. 11, no. 8, pp. 968–975, 2011.
- [40] A. M. Mahecha and H. Wang, “The influence of vascular endothelial growth factor-A and matrix metalloproteinase-2 and -9 in angiogenesis, metastasis, and prognosis of endometrial cancer,” *OncoTargets and Therapy*, vol. 10, pp. 4617–4624, 2017.
- [41] M. Lulli, M. Cammalleri, I. Fornaciari, G. Casini, and M. Dal Monte, “Acetyl-11-keto- $\beta$ -boswellic acid reduces retinal angiogenesis in a mouse model of oxygen-induced retinopathy,” *Experimental Eye Research*, vol. 135, pp. 67–80, 2015.
- [42] P. K. Kokkiripati, L. M. Bhakshu, S. Marri et al., “Gum resin of *Boswellia serrata* inhibited human monocytic (THP-1) cell activation and platelet aggregation,” *Journal of Ethnopharmacology*, vol. 137, no. 1, pp. 893–901, 2011.
- [43] U. Siemoneit, L. Tausch, D. Poeckel et al., “Defined structure-activity relationships of boswellic acids determine modulation of Ca<sup>2+</sup> mobilization and aggregation of human platelets by *Boswellia serrata* extracts,” *Planta Medica*, vol. 83, no. 12/13, pp. 1020–1027, 2017.

## Research Article

# How Could We Influence Systemic Inflammation in Allergic Rhinitis? The Role of H1 Antihistamines

Ioana Adriana Muntean,<sup>1</sup> Ioana Corina Bocsan ,<sup>2</sup> Nicolae Miron,<sup>3</sup> Anca Dana Buzoianu,<sup>2</sup> and Diana Deleanu<sup>1</sup>

<sup>1</sup>Department of Allergy and Immunology, “Iuliu Hatieganu” University of Medicine and Pharmacy, Cluj Napoca, Romania

<sup>2</sup>Department of Pharmacology, Toxicology and Clinical Pharmacology, “Iuliu Hatieganu” University of Medicine and Pharmacy, Cluj Napoca, Romania

<sup>3</sup>Department of Clinical Immunology, Sahlgrenska University Hospital, Göteborg, Sweden

Correspondence should be addressed to Ioana Corina Bocsan; [corinabocsan@yahoo.com](mailto:corinabocsan@yahoo.com)

Received 17 February 2018; Revised 13 April 2018; Accepted 15 May 2018; Published 12 June 2018

Academic Editor: Ada Popolo

Copyright © 2018 Ioana Adriana Muntean et al. This is an open access article distributed under the Creative Commons Attribution License, which permits unrestricted use, distribution, and reproduction in any medium, provided the original work is properly cited.

The aim of the study was the analysis of adhesion molecules' profile (ICAM-1, VCAM-1, and E-selectin) in patients with allergic rhinitis and the influence of H1 antihistamines on those markers. Seventy-nine patients with persistent allergic rhinitis (PAR) and 30 healthy volunteers were included in the study. The patients with PAR were treated with desloratadine 5 mg/day or levocetirizine 5 mg/day for 4 weeks. The clinical (rhinitis symptoms and total symptoms score (TSS), type of sensitization) and biological evaluation (total IgE, eosinophils, ICAM-1, VCAM-1, and E-selectin) as well as fractionate nitric oxide in exhaled air (FeNO) measurement was performed before and after treatment. The plasmatic levels of ICAM-1, VCAM-1, total IgE, and eosinophils and FeNO were significantly increased in patients with PAR compared to healthy volunteers. H1 antihistamines significantly improved TSS, with no differences between the investigated drugs. There was a significant decrease of eosinophils, total IgE, and FeNO after treatment. H1 antihistamines significantly decreased the plasmatic levels of ICAM-1 and E-selectin but not VCAM-1 compared to basal values. There is no difference between levocetirizine and desloratadine in the reduction of CAMs. A systemic inflammation characterized by increased levels of CAMs is present in patients with PAR. H1 antihistamines improve symptoms and reduce CAMs and FeNO levels after 1 month of treatment. H1 antihistamines might reduce the systemic inflammation which could be responsible to asthma occurrence in patients with PAR.

## 1. Introduction

Allergic rhinitis (AR) is an IgE-mediated immune response characterized by an inflammatory process of the nasal mucosa [1]. Now, allergic rhinitis is considered the most prevalent clinical manifestation of allergy, affecting 20–30% of the general population worldwide [1, 2]. AR is also a risk factor for asthma's occurrence; more than 25% of patients with persistent allergic rhinitis (PAR) may develop asthma over time [3].

The immune response to allergen exposure involves several cells and mediators. Immediately after allergen exposure, in the early phase of allergic inflammation there is an immediate release of mast cell products, including histamine. The

released mediators generate a specific inflammatory network, which favours the expression and activation of certain cellular adhesion molecules (CAM) [4, 5]. The activation of CAMs favours the migration of proinflammatory cells such as eosinophils and neutrophils in the nasal mucosa [5, 6]. Late-phase immune response is characterized by release of various cytokines, chemokines, and other mediators, mainly produced by TH2 cells and granulocytes, which changes cellular components, with a predominant influx of TH2 cells and eosinophils [5, 6].

Vascular cell adhesion molecule 1 (VCAM-1) and intercellular cell adhesion molecule 1 (ICAM-1) belong to the immunoglobulin superfamily. Both are expressed mainly on endothelial cells [7, 8]. Proinflammatory cytokines like IL-1

and TNF- $\alpha$  enhance the expression of both CAMs, while Th2 cytokines significantly enhance VCAM-1 expression [9]. ICAM-1 and VCAM-1 are involved in transendothelial migration and adhesion of leukocytes, including eosinophils [6, 10], contributing in the maintenance of late immune response in the nasal mucosa.

E-selectin is a CAM expressed on the endothelial cell, mediating the rapid low-affinity adhesion of leukocytes to endothelial cells. The level of E-selectin is higher in the early stage of inflammation in the vascular endothelium [8, 9]. E-selectin is an important CAM in the initiation and organization of allergic inflammation.

H1 antihistamines are the first therapeutic option in all forms of allergic rhinitis [1]. Their main effect is related to blockade of H1 receptors, mediating their antiallergic action. Further research found that the new-generation H1 antihistamines have also an anti-inflammatory effect, decreasing the number of inflammatory cells recruited in the tissue and diminishing the expression of CAMs [11–15].

The aim of the study was the analysis of CAMs' evolution under 1-month treatment with levocetirizine and desloratadine, two H1 antihistamines from second generation in patients with PAR under continuous natural exposure to allergens. Secondarily, we also characterized the plasmatic levels of CAMs (ICAM-1, VCAM-1, and E-selectin) in patients with PAR.

## 2. Material and Method

**2.1. Patients and Clinical Evaluation.** In the present study, we performed a post hoc analysis of an initial randomized control trial (RCT) that included patients with PAR and healthy volunteers. The analyzed inflammatory markers represented secondary outcomes of the initial study [16]. Seventy-nine patients with PAR (mean age  $30.44 \pm 9.9$  years and sex ratio M:F = 1.02) were included in the experimental group, while 30 healthy volunteers (mean age  $28.92 \pm 8.91$  years and sex ratio M:F = 1) were included in the control one. The study protocol, inclusion and exclusion criteria, and clinical evaluation were similar to the initial study [16]. The protocol was approved by the Ethics Committee of the "Iuliu Hatieganu" University of Medicine and Pharmacy, Cluj-Napoca. All patients signed the informed consent at enrollment.

The diagnosis of AR was done according to international guidelines, based on history and skin prick test (SPT) [1]. The following demographic data were noticed from anamnesis: age, sex, and living area (rural/urban). The severity of AR was established based on severity of specific symptoms: rhinorrhea, nasal congestion, sneezing, and nasal and ocular itching. The severity was analyzed on a scale from 0 to 3 (0 = absent, 1 = mild, 2 = moderate, and 3 = severe), retrospectively, for 12 hours prior to presentation. The total symptom score (TSS) was calculated by adding the score for every symptom. A TSS < 6 means a mild rhinitis, while a TSS > 6 represents a moderate-severe form of disease.

After the baseline evaluation, the patients were randomly divided into two groups using an adaptive biased-coin randomization. The first group included 39 patients, and they received levocetirizine 5 mg/day, while the second group of

40 patients received desloratadine 5 mg/day. The treatment was recommended for 4 weeks. At the end of the four weeks, the patients were similarly evaluated.

**2.2. Skin Prick Test (SPT).** The diagnosis of allergy was established through skin prick test, according to international guidelines [17]. The allergen panel included international recommendation and particularities of exposure to allergens in Romania: house dust mites (*Derm. pteronyssinus* and *Derm. farinae*), grass pollens (mixed grasses), cereal pollens (cereals), Betulaceae pollens (spring trees), cat and dog epithelia, *Alternaria alternata*, and weed pollen (*Artemisia vulgaris* and *Ambrosia elatior*). Standardized allergen extracts (Hal Allergy, Netherlands) were used. SPT was done at the beginning of the study.

**2.3. FeNO Measurement.** The measurement of fractionated exhaled nitric oxide (FeNO) was done in accordance to international recommendations [18], using NIOX MINO® (Aerocrine, Sweden). FeNO was measured before and after 1 month of treatment with H1 antihistamines. The measured values were expressed in parts per billion (ppb). A standardized cutoff value of 25 ppb was considered a normal upper limit.

**2.4. Biological Evaluation.** All the biological parameters were determined before and after 1 month of treatment with H1 antihistamines. Total IgE plasmatic level was done using electrochemiluminescence immunoassay method (ECLIA). The obtained values were expressed as UI/ml. A value below 100 UI/ml was considered normal.

The eosinophils (Eo) were manually counted from the peripheral blood on a slide, and their value was expressed as %. We considered a normal value between 2–4%.

The plasmatic levels of ICAM-1, VCAM-1, and E-selectin were determined using ELISA technique (Quantikine R&D system, USA). The blood sample of 5 ml without anticoagulant was collected and centrifuged within the 1st hour, followed by serum separation. The serum was then stored at  $-80^{\circ}\text{C}$  until the determination was performed. All the aforementioned determinations were done according to the manufacturers' instructions. For each assay, samples were diluted as needed, and protein levels were calculated based on four-parameter logistic (4-PL) curve fit.

**2.5. Statistical Analysis.** The statistical analysis was performed using SPSS version 21 (Chicago, IL, USA). Data were labeled as nominal and expressed as percentage and continuous variables. The normal distribution for continuous variables was done using Kolmogorov-Smirnov test. Variables with normal distribution were expressed as mean and standard deviation, while variables with abnormal distribution were expressed as median and 25–75 percentiles.

The adequate statistic tests according to data distribution were chosen. The differences were assessed within groups by Wilcoxon signed-rank test and between groups by Mann-Whitney test. The influence of different parameters on CAM evolution in time was done using ANOVA test for repeating measurements. The Spearman coefficient of correlation was calculated to highlight differences between



TABLE 1: Patients' demographic data.

Parameter	Desloratadine ( <i>n</i> = 40)	Levocetirizine ( <i>n</i> = 39)	<i>p</i>
Age*	28.05 ± 6.32	32.89 ± 12.17	0.031
Sex <sup>^</sup>			
Male	57.5% (23)	43.6% (17)	0.263
Female	42.5% (17)	56.4% (22)	
Living area <sup>^</sup>			
Urban	85% (34)	82.1% (32)	0.770
Rural	15% (6)	17.9% (7)	
Allergic rhinitis onset (months) <sup>°</sup>	24 (6–60)	36 (7.5–68)	0.532
Allergen sensitization <sup>^</sup>			
Indoor	37.5% (15)	5.1% (2)	0.002
Outdoor	17.5% (7)	35.9% (14)	
Indoor + outdoor	45% (18)	59% (23)	
Severity <sup>^</sup>			
Mild	25% (10)	33.3% (13)	0.465
Moderate-severe	75% (30)	66.7% (26)	

\*Data are expressed as mean ± SD; <sup>^</sup>data are expressed as %, *n*; <sup>°</sup>data are expressed as median, 25–75th percentile. SD: standard deviation; *n*: number.

continuous variables. The level of statistical significance was set at  $p < 0.05$ .

### 3. Results

Patients' demographic data are presented in Table 1.

**3.1. Initial Evaluation.** Fifty-six (70.9%) patients presented persistent moderate-severe forms of AR. The initial TSS proved the severity of AR (median 8 (5–11)). Forty-one patients (51.9%) had multiple sensitizations to both indoor and outdoor allergens. The basal TSS was not correlated with the duration of AR but was significantly higher in patients with sensitization to pollen or multiple sensitizations ( $p = 0.01$ ).

In patients with AR, plasmatic ICAM-1 and VCAM-1 were significantly increased compared to healthy volunteers ( $p < 0.001$  and  $p < 0.001$ , resp.), with no differences between the groups. E-selectin was similar in healthy volunteers and patients with AR (Table 2).

The severity of AR expressed as a high value of TSS was correlated with the plasmatic level of E-selectin ( $R = 0.996$ ,  $p < 0.001$ ), but not with basal levels of ICAM-1 ( $R = -0.051$ ,  $p = 0.657$ ) or VCAM-1 ( $R = -0.056$ ,  $p = 0.622$ ). There is no correlation between the plasmatic level of CAM and patients' age, sex, or type of sensitization ( $p > 0.05$ ). There is a positive correlation between the basal values of ICAM-1 and E-selectin ( $R = 0.353$ ,  $p = 0.001$ ).

Total IgE and Eo were significantly increased at baseline, with no differences between the groups ( $p = 0.408$  and  $p = 0.838$ , resp.). The initial value of peripheral Eo was strongly correlated with total IgE ( $R = 0.853$ ;  $p < 0.001$ ). There was no correlation between basal Eo or total IgE levels and ICM-1, VCAM-1, and E-selectin ( $p > 0.05$ ).

FeNO was increased in patients with AR (median 27 (18–46)) compared to the standardized cutoff value

(25 ppb) ( $p < 0.001$ ). There was no difference between the groups regarding the basal value of FeNO. There was no correlation between initial FeNO and severity of rhinitis' symptoms, type of sensitization, or basal values of CAM ( $p > 0.05$ ).

**3.2. One-Month Evaluation.** H1 antihistamines significantly improved all the symptoms after 1 month of treatment. TSS significantly decreased after treatment (median 8 (5–11) versus median 0 (0–4),  $p = 0.01$ ), with no differences between the investigated drugs ( $p = 0.571$ ).

1-month evaluation revealed a significant decrease of IgE plasmatic level ( $p < 0.001$ ), especially in patients with monosensitization either to indoor or outdoor allergens ( $p = 0.05$ ). The reduction of total IgE was not influenced by the type of treatment; patients' age, sex, and environment; or duration of AR ( $p > 0.05$ ) (Table 3). Total IgE significantly decreased in patients with moderate-severe forms of AR compared to those with mild disease ( $p = 0.05$ ).

Same pattern was noticed also for peripheral Eo, with a significant reduction after treatment ( $p = 0.04$ ). The Eo significantly decreased after 1 month of treatment especially in patients with monosensitization to indoor allergens or mixed sensitization ( $p = 0.002$ ). Eo reduction was also significant in patients with severe forms of AR ( $p = 0.04$ ). The reduction of Eo was not influenced by the type of treatment; patients' age, sex, and environment; or duration of AR ( $p > 0.05$ ).

After the four-week treatment, H1 antihistamines significantly decreased the plasmatic levels of ICAM-1 ( $p = 0.049$ ) and E-selectin ( $p = 0.002$ ), but not VCAM-1 ( $p = 0.310$ ) compared to basal values. There was no difference between levocetirizine and desloratadine in the reduction of adhesion molecule plasmatic levels (Table 3). We noticed a significant reduction of CAM levels in patients with moderate-severe forms compared to patients with mild rhinitis (VCAM-1  $p = 0.037$ , ICAM-1  $p = 0.001$ , and E-selectin  $p = 0.002$ ). The reduction of CAM levels was not influenced by patients'



TABLE 2: Plasmatic values of total IgE and adhesion molecules in healthy volunteers and patients with AR.

Parameter	Healthy volunteers ( $n = 30$ )	Patients with AR ( $n = 79$ )	$p$
Total IgE (UI/l)	<100	115 (45.3–169)	<0.001
ICAM-1 (ng/ml)	111.21 (100–206.30)	218.19 (189.13–266.65)	0.001
VCAM-1 (ng/ml)	557 (249–891)	1004.02 (822.32–1174.68)	<0.001
E-selectin (ng/ml)	32.03 (23.68–45.94)	33.81 (24.61–47.53)	0.404

Data are expressed as median, 25–75th percentile. Significance  $p < 0.05$ .

TABLE 3: Patients' biological parameters before and after treatment.

Parameter		Desloratadine ( $n = 40$ )	Levocetirizine ( $n = 39$ )	$p$
Total IgE	Baseline	116.5 (46.25–269)	115 (45.3–269)	0.212
	4 weeks	65 (28.32–167.5)	75 (30–150)	
Eo	Baseline	5.00 (3.20–6.50)	5.20 (2.70–7.80)	0.04
	4 weeks	4.10 (2.60–5.80)	4 (2.35–6.35)	
VCAM-1	Baseline	1037.8 (878.19–1200.82)	919.32 (818.5–1136.02)	0.202
	4 weeks	1037.98 (897.64–1193.09)	913.56 (703.58–1128.60)	
ICAM-1	Baseline	208.12 (179.95–259.04)	229.81 (195.75–275.21)	0.355
	4 weeks	205.58 (170.93–256.01)	206.13 (182.74–270.14)	
E-selectin	Baseline	33.54 (25.72–46.57)	33.81 (23.95–50)	0.459
	4 weeks	33.07 (24.46–44.89)	31.90 (22.08–49.5)	
FeNO	Baseline	38 (19–49)	23 (16.25–43)	0.05
	4 weeks	14 (11–21)	17.5 (14–22.5)	

Data are expressed as median, 25–75th percentile. Significance  $p < 0.05$ .

age, sex, and type of sensitization. We also analyzed the improvement of symptoms in correlation with inflammatory markers. The reduction of TSS was positively correlated with the reduction of ICAM-1 ( $R = 0.238$ ,  $p = 0.035$ ), but it was not correlated with VCAM-1 and E-selectin evolutions. ICAM-1 reduction was positively correlated with E-selectin ( $R = 0.504$ ,  $p < 0.001$ ) and VCAM-1 ( $R = 0.711$ ,  $p < 0.001$ ) evolutions.

FeNO was significantly reduced after 1-month treatment with AH1, desloratadine being more effective than levocetirizine (Table 3). The reduction was not influenced by patients' age, severity of allergic rhinitis or number of sensitization ( $p > 0.05$ ), or the type of it ( $p > 0.05$ ). FeNO had a more significant reduction in male compared to female patients ( $p = 0.036$ ). The reduction of FeNO did not correlate with basal plasmatic levels of CAMs. The reduction of FeNO was not correlated with symptoms' improvement. The reduction of FeNO was minimal in patients sensitized to pollen compared with patients with multiple sensitization or with sensitization to indoor allergens, but the difference did not reach the level of statistical significance (median  $-6$  ( $-32$  to  $-3$ ) versus median  $-12$  ( $-35$  to  $-1.5$ ) versus median  $-11$  ( $-35$  to  $-2$ ),  $p > 0.05$ ).

#### 4. Discussion

This study assessed the effect of H1 antihistamines from the 2nd generation, showing that both levocetirizine and desloratadine improved symptoms and reduced the level of inflammation in allergic rhinitis. We also characterized

the plasmatic profile of adhesion molecules in patients with persistent allergic rhinitis.

AR is characterized by the presence of inflammation in the nasal mucosa. The exposure to allergens mediates the release of mediators from mast cells, especially histamine, which are responsible for the characteristic symptoms of AR (sneezing, nasal itching, and rhinorrhea) [19]. But these mediators will also stimulate infiltration of the nasal mucosa with inflammatory cells, including eosinophils [20]. The chronic inflammatory response with eosinophil infiltration in the nasal mucosa is the pattern of allergic inflammation [1, 19]. These cells continue to produce cytokines, chemokines, and other inflammatory mediators, which leads to persistent symptoms and tissue structural changes and damages. Thus, rhinitis progression and persistence become more dependent on mediators which promote infiltration of cells, such as eosinophils and TH lymphocytes [21]. AR is a risk factor for asthma development and may appear before or after asthma onset. Allergic inflammation is the key to understand both diseases and the mechanisms of rhinitis progression to asthma [5, 19].

The eosinophils migrate at the inflammation site due to the high expression of the adhesion molecules on the endothelial cell surfaces [22]. The role of adhesion molecules in the pathogenesis of allergic diseases was investigated in many studies [10, 23–29]. Most of them showed an increase of ICAM-1 and VCAM-1 in nasal lavage fluid, mucosa biopsies, and serum in patients with AR versus healthy subjects, after allergen challenge tests or in conditions of natural exposure [10, 23, 24, 26–28]. On the other hand, some researchers

did not observe an increased level of ICAM-1 and VCAM-1 in serum of patients with allergic rhinitis [25, 29]. In the present study, the plasmatic levels of ICAM-1 and VCAM-1 were significantly increased in patients with PAR compared to healthy volunteers ( $p < 0.001$  and  $p < 0.001$ , resp.), with no differences between the groups. These results confirm previous published data, reflecting a systemic inflammation in patients with PAR.

The kinetics of VCAM-1 and ICAM-1 is different. In patients with AR, ICAM-1 is increased in nasal secretion in both perennial and seasonal AR from the period of onset [26]. On the other hand, the expression of VCAM-1 is upregulated in the nasal mucosa of patients with AR [28, 30], especially in the late phase of allergic response [31]. Our results are similar to those from the above aforementioned studies. Present research included patients with PAR under continuous natural exposure to allergens. The continuous exposure to indoor or/and outdoor allergens may explain a continuous production of mediators which promote eosinophil recruitments, explaining high plasmatic levels of ICAM-1 and VCAM-1.

Gorska-Ciebiada et al. [27] have shown that ICAM-1 values are significantly lower in patients with mild forms compared to those with moderate-severe rhinitis [27]. In the present study, there was no correlation between ICAM-1 and VCAM-1 and the severity of allergic rhinitis or type of sensitization. Another study showed that VCAM-1 and ICAM-1 grow during the pollen season and fall out during off-season [26]. In the present study, we did not investigate the kinetics of ICAM-1 and VCAM-1. Most of the patients have polysensitization to both indoor and outdoor allergens which may explain the high level of CAMs in serum, due to their continuous production.

Interestingly, E-selectin was similar in patients with AR and healthy volunteers. Similarly, Ural et al. found that the E-selectin value did not differ in patients with allergic and nonallergic rhinitis in nasal lavage fluid [23]. E selectin is involved in leukocyte orientation, and it is a light adhesion marker, while ICAM-1 is a leukocyte-binding adhesion marker. The basal level of E-selectin positively correlated with ICAM-1 ( $R = 0.353$ ,  $p = 0.001$ ). This observation might be explained by their involvement at the beginning of cell recruitments. In patients with AR, the level of E-selectin starts to increase within 15 hours after allergen exposure, [32] and it declines after 24 hours [23, 33]. These data may explain not only the low level of E-selectin in our patients but also the correlation between E-selectin and severity of symptoms ( $R = 0.996$ ,  $p < 0.001$ ), generated mainly by histamine release. As we mentioned before, we did not investigate the kinetics of CAMs in serum, and the patients were under natural exposure not after a controlled allergen challenge exposure. It might be interesting to investigate CAM and cytokine levels in patients with AR at different time points to analyze their kinetics in conditions of natural exposure to allergens.

IgE is the central molecule in the pathogenesis of allergic diseases. It increases after sensitization and binds to mast cells through specific receptors, but a soluble portion remains in the serum and can be determined. In different clinical

studies, the IgE level did not correlate with ICAM-1 or TNF- $\alpha$  values, which are higher in asthmatics but not in those with AR [29]. In our study, there was a significant correlation between the Eo count and total IgE ( $p < 0.001$ ), but the total IgE values did not correlate with other markers of inflammation, such as CAMs or FENO. Although CAMs are involved in Eo migration at the site of inflammation, the serum values of Eo did not correlate with ICAM-1 and VCAM-1 in our study. It is interesting to evaluate the level of CAMs in the nasal mucosa and to correlate with local infiltration of Eo, but in our study we did not perform such kind of investigation.

There is hypothesis suggesting that Eo recruited by CAMs can induce nitric oxide synthase in the epithelial cells of the bronchial mucosa. Nitric oxide (NO) in the exhaled air is known as the marker of eosinophilic inflammation in the lower respiratory tract. IgE-mediated inflammation results in elevated NO in the expired air [34, 35]. Studies have also shown that patients with AR during pollination have elevated NO levels in the air, even if their asthma symptoms are missing or mild [36]. Other studies showed elevated levels of exhaled NO and adenosine in patients with AR versus healthy subjects [34, 35], suggesting that a subclinical inflammation in the lower airways could exist in AR. In our group of patients, FeNO was increased in patients with AR and did not correlate with any of the studied markers. There was no correlation between the initial FeNO and the severity of rhinitis' symptoms, type of sensitization, or basal values of CAM ( $p > 0.05$ ). But this lack of correlations cannot exclude a possible minimal inflammatory process in both the nasal and lower airway mucosa, other factors having an additional contribution to progression of inflammation in lower airways, like TNF- $\alpha$ -stimulation [37]. It might be interesting to monitor the evolution of patients in order to investigate if basal values of FeNo and CAMs could predict the occurrence of asthma after a period of time.

In this study, we also assessed the efficacy of H1 antihistamines, desloratadine and levocetirizine, in the therapy of AR. We also investigated a possible anti-inflammatory effect of both drugs, demonstrated by reduction of CAMs and FeNO. Several studies showed the efficacy of H1 antihistamines in allergic rhinitis [1, 2]. H1 antihistamines are now considered the first-line treatment in AR [1]. In our study, we observed that both desloratadine and levocetirizine improved nasal symptoms, reducing significantly TSS after 1 month of treatment, similar to previous published data [2, 19, 38]. TSS significantly decreased after treatment, with no differences between the investigated drugs ( $p = 0.571$ ).

In our study, we evaluated the effect of desloratadine and levocetirizine on E-selectin, ICAM-1, and VCAM-1. After the four-week treatment, H1 antihistamines significantly decreased the plasmatic levels of ICAM-1 ( $p = 0.049$ ) and E-selectin ( $p = 0.002$ ), but not VCAM-1 ( $p = 0.310$ ) compared to basal values. There was no difference between levocetirizine and desloratadine in reduction of CAM plasmatic levels. In the present study, we also noticed a significant reduction of CAM levels in patients with moderate-severe forms compared to patients with mild rhinitis (VCAM-1  $p = 0.037$ , ICAM-1  $p = 0.001$  and E-selectin  $p = 0.002$ ).

But the reduction of CAM levels was not influenced by patients' age, sex, and type of sensitization.

*In vitro* studies demonstrated that not all 2nd-generation H1 antihistamines had anti-inflammatory effect. Cetirizine did not influence E-selectin, ICAM-1, and VCAM-1 *in vitro* studies although the authors noted an underexpression of ICAM-1 in epithelial cells of patients with AR treated with cetirizine [11]. Loratadine was seen to influence the level of VCAM-1 but not ICAM-1 in patients with monosensitization to house dust mites [12]. Regarding fexofenadine (an active metabolite of terfenadine), several studies showed its similar efficiency to cetirizine [39], loratadine [40], desloratadine, and levocetirizine [38] in improving rhinitis symptoms. But Schäper et al. [13] also demonstrated its anti-inflammatory effect, due to reduction of ICAM-1 in nasal secretions after 14 days of treatment [13]. *In vitro* studies revealed that levocetirizine inhibited ICAM-1 [15] and downregulated the activity of P-selectins [41] and the expression of VCAM-1 [42]. Desloratadine induced downregulation of ICAM-1 [43]. In most of these studies, the used concentrations of AH1 were higher than the therapeutic ones [41]. There are also *in vivo* studies that revealed the anti-inflammatory effect of H1 antihistamines. Both desloratadine and levocetirizine reduced ICAM-1 and nasal Eo [44], similar to present results. In the present study, VCAM-1 was not reduced by AH1, only ICAM-1 and E-selectin. Probably, the expression of ICAM-1 and E-selectin, markers of initial allergic response, is related to histamine release from mast cells, while other new synthesized cytokines and chemokines are probably involved in the expression of VCAM-1.

One-month evaluation revealed a significant decrease of IgE plasmatic level ( $p < 0.001$ ) especially in patients with monosensitization either to indoor or outdoor allergens ( $p = 0.05$ ). Total IgE significantly decreased in patients with moderate-severe forms of AR compared to those with mild disease ( $p = 0.05$ ). The same pattern was also noticed also for peripheral Eo, with a significant reduction after treatment ( $p = 0.04$ ). These results are similar to previous reported data [16, 44–46], for rupatadine, levocetirizine, and desloratadine, after 2–4 weeks of treatment.

The effect of H1 antihistamines on lower airway subclinical inflammation in patients with AR has been demonstrated in few studies [19]. *In vitro* studies have shown that NO synthase activity can be downregulated by H1 antihistamine therapy [47]. Animal studies have demonstrated that histamine released by mast cell plays an important role in the production of FeNO and in the enhancement of bronchial hyperreactivity [48]. *In vivo*, it has been demonstrated that levocetirizine lowers the FeNO values after 3 months of treatment in children with mite allergy [42]. In our study, we observed that FeNO was significantly reduced after 1-month treatment with H1 antihistamines, and desloratadine was more effective than levocetirizine. This observation could be explained by the differences between investigated subgroups in relation with patient sensitization. The group treated with levocetirizine had a lower basal value of FeNO than desloratadine group, so the room for improvement of FeNO was more limited. To establish the clear role of each

H1 antihistamines in reducing FeNO level, further extensive studies are required. But, this observation might open a new strategy in limiting subclinical inflammation using AH1. The continuous treatment with H1 antihistamines in patients with PAR might reduce the occurrence of asthma, confirming the previous published data [42].

There are some limitations of this study. Firstly, a small number of patients were included in the study, sensitized to both indoor and outdoor allergens. The randomization of the patients took into account the treatment, not the type of sensitization, which may explain the differences between investigated subgroups, more patients sensitized to pollen being included in levocetirizine subgroup. The study has another limitation, the lack of information regarding different anti-inflammatory effects of H1 antihistamines according to allergen exposure. It might be interesting to analyze the effect of AH1 on CAMs and other related mediators (cytokines and chemokines) and to differentiate the results according to the type of sensitization.

The present study emphasized the anti-inflammatory role of H1 antihistamines from 2nd generation, demonstrated by reduction of CAM plasmatic levels in patients with PAR. The reduction of CAMs was noticed in the plasma not in the nasal mucosa, in conditions of natural continuous exposure to allergens. Also, the research investigates two H1 antihistamines from 2nd generation in order to establish if there are significant differences between them in improving both clinical symptoms and inflammatory parameters.

## 5. Conclusions

Patients with PAR have high serum levels of ICAM-1 and VCAM-1. FeNO as a marker of subclinical inflammation is increased in patients with PAR. H1 antihistamines improve allergic rhinitis symptoms and reduce the markers of inflammations after 1 month of treatment. Desloratadine has a better anti-inflammatory effect in reducing FeNO. Baseline values of CAMs did not predict the response to therapy.

## Data Availability

The data used to support the findings of this study are available from the corresponding author upon request.

## Conflicts of Interest

The authors declare no conflict of interest regarding the publication of this article.

## Authors' Contributions

Ioana Adriana Muntean and Ioana Corina Bocsan contributed equally to this work.

## Acknowledgments

This work was partially funded by POSDRU Grant (no. 159/1.5/S/138776) entitled "Model colaborativ instituțional pentru translația cercetării științifice biomedicale în practica

clinică-TRANSCENT” and by a research Grant (no. 27020/48/2011) of the Iuliu Hațieganu University of Medicine and Pharmacy, Cluj Napoca.

## References

- [1] J. Bousquet, N. Khaltaev, A. A. Cruz et al., “Allergic rhinitis and its impact on asthma (ARIA) 2008,” *Allergy*, vol. 63, pp. 8–160, 2008.
- [2] J. Bousquet, H. J. Schünemann, T. Zuberbier et al., “Development and implementation of guidelines in allergic rhinitis – an ARIA-Ga<sup>2</sup>len paper,” *Allergy*, vol. 65, no. 10, pp. 1212–1221, 2010.
- [3] B. Leynaert, C. Neukirch, S. Kony et al., “Association between asthma and rhinitis according to atopic sensitization in a population-based study,” *The Journal of Allergy and Clinical Immunology*, vol. 113, no. 1, pp. 86–93, 2004.
- [4] R. H. Schwartz, “T cell anergy,” *Annual Review of Immunology*, vol. 21, no. 1, pp. 305–334, 2003.
- [5] M. L. Kowalski and R. Alam, “Signal transduction mechanisms as new targets for allergists,” *Allergy*, vol. 56, no. 3, pp. 199–203, 2001.
- [6] M. F. Kramer, T. R. Jordan, C. Klemens et al., “Factors contributing to nasal allergic late phase eosinophilia,” *American Journal of Otolaryngology*, vol. 27, no. 3, pp. 190–199, 2006.
- [7] H. Tachimoto, S. A. Hudson, and B. S. Bochner, “Acquisition and alteration of adhesion molecules during cultured human mast cell differentiation,” *The Journal of Allergy and Clinical Immunology*, vol. 107, no. 2, pp. 302–309, 2001.
- [8] B. S. Bochner, *Adhesion Molecules in Allergic Disease*, Marcel Dekker, New York, 1997.
- [9] B. S. Bochner, D. A. Klunk, S. A. Sterbinsky, R. L. Coffman, and R. P. Schleimer, “IL-13 selectively induces vascular cell adhesion molecule-1 expression in human endothelial cells,” *The Journal of Immunology*, vol. 154, no. 2, pp. 799–803, 1995.
- [10] Y. Ohashi, Y. Nakai, A. Tanaka et al., “Soluble vascular cell adhesion molecule-1 in perennial allergic rhinitis,” *Acta Otolaryngologica*, vol. 118, no. 1, pp. 105–109, 1998.
- [11] G. M. Walsh, “The effects of cetirizine on the function of inflammatory cells involved in the allergic response,” *Clinical and Experimental Allergy*, vol. 27, Supplement 2, pp. 47–53, 1997.
- [12] M. Branco-Ferreira, M. C. dos Santos, M. L. Palma-Carlos, and A. G. Palma-Carlos, “Antihistamines and serum adhesion molecule levels,” *Allergie et Immunologie*, vol. 33, no. 6, pp. 233–236, 2001.
- [13] C. Schäper, B. Gustavus, B. Koch et al., “Effects of fexofenadine on inflammatory mediators in nasal lavage fluid in intermittent allergic rhinitis,” *Journal of Investigational Allergology & Clinical Immunology*, vol. 19, no. 6, pp. 459–464, 2009, 20128420.
- [14] J. Mullol, F. de Borja Callejas, M. A. Martínez-Antón et al., “Mometasone and desloratadine additive effect on eosinophil survival and cytokine secretion from epithelial cells,” *Respiratory Research*, vol. 12, no. 1, p. 23, 2011.
- [15] D. Tworek, M. Bocheńska-Marciniak, M. Kupczyk, P. Górski, and P. Kuna, “The effect of 4 weeks treatment with desloratadine (5mg daily) on levels of interleukin (IL)-4, IL-10, IL-18 and TGF beta in patients suffering from seasonal allergic rhinitis,” *Pulmonary Pharmacology & Therapeutics*, vol. 20, no. 3, pp. 244–249, 2007.
- [16] C. I. Bocşan, A. I. Bujor, N. Miron, Ş. C. Vesa, D. Deleanu, and A. D. Buzoianu, “In vivo anti-inflammatory effect of H1 antihistamines in allergic rhinitis: a randomized clinical trial,” *Balkan Medical Journal*, vol. 32, no. 4, pp. 352–358, 2015.
- [17] L. Heinzerling, A. Mari, K. C. Bergmann et al., “The skin prick test - European standards,” *Clinical and Translational Allergy*, vol. 3, no. 1, p. 3, 2013.
- [18] American Thoracic Society and European Respiratory Society, “ATS/ERS recommendations for standardized procedures for the online and offline measurement of exhaled lower respiratory nitric oxide and nasal nitric oxide, 2005,” *American Journal of Respiratory and Critical Care Medicine*, vol. 171, no. 8, pp. 912–930, 2005.
- [19] G. W. Canonica and E. Compalati, “Minimal persistent inflammation in allergic rhinitis: implications for current treatment strategies,” *Clinical & Experimental Immunology*, vol. 158, no. 3, pp. 260–271, 2009.
- [20] A. Togias, “Unique mechanistic features of allergic rhinitis,” *The Journal of Allergy and Clinical Immunology*, vol. 105, no. 6, Part 2, pp. S599–S604, 2000.
- [21] L. Borish, “Allergic rhinitis: systemic inflammation and implications for management,” *The Journal of Allergy and Clinical Immunology*, vol. 112, no. 6, pp. 1021–1031, 2003.
- [22] D. J. Adamko, S. O. Odemuyiwa, D. Vethanayagam, and R. Moqbel, “The rise of the phoenix: the expanding role of the eosinophil in health and disease,” *Allergy*, vol. 60, no. 1, pp. 13–22, 2005.
- [23] A. Ural, M. S. Tezer, A. Yücel, H. Atilla, and F. Ileri, “Interleukin-4, interleukin-8 and E-selectin levels in intranasal polypoid patients with and without allergy: a comparative study,” *The Journal of International Medical Research*, vol. 34, no. 5, pp. 520–524, 2006.
- [24] M. Turgay, G. Keskin, G. Kminkli et al., “Soluble intercellular adhesion molecule-1 (sICAM-1) in patients with allergic rhinoconjunctivitis,” *Allergol Immunopathol (Madr)*, vol. 24, no. 3, pp. 129–131, 1996.
- [25] C. M. Liu, C. T. Shun, and Y. K. Cheng, “Soluble adhesion molecules and cytokines in perennial allergic rhinitis,” *Annals of Allergy, Asthma & Immunology*, vol. 81, no. 2, pp. 176–180, 1998.
- [26] L. Håkansson, C. Heinrich, S. Rak, and P. Venge, “Priming of eosinophil adhesion in patients with birch pollen allergy during pollen season: effect of immunotherapy,” *The Journal of Allergy and Clinical Immunology*, vol. 99, no. 4, pp. 551–562, 1997.
- [27] M. Gorska-Ciebiada, M. Ciebiada, M. M. Gorska, P. Gorski, and I. Grzelewska-Rzymowska, “Intercellular adhesion molecule 1 and tumor necrosis factor  $\alpha$  in asthma and persistent allergic rhinitis: relationship with disease severity,” *Annals of Allergy, Asthma & Immunology*, vol. 97, no. 1, pp. 66–72, 2006.
- [28] B. J. Lee, R. M. Naclerio, B. S. Bochner, R. M. Taylor, M. C. Lim, and F. M. Baroody, “Nasal challenge with allergen upregulates the local expression of vascular endothelial adhesion molecules,” *The Journal of Allergy and Clinical Immunology*, vol. 94, no. 6, Part 1, pp. 1006–1016, 1994.
- [29] M. Ciebiada, M. Gorska-Ciebiada, and P. Gorski, “sICAM-1 and TNF- $\alpha$  in asthma and rhinitis: relationship with the presence of atopy,” *The Journal of Asthma*, vol. 48, no. 7, pp. 660–666, 2011.
- [30] Y. Li, Y. Wang, and Q. Zhang, “Expression of cell adhesion molecule and nitric oxide synthase in nasal mucosa in allergic



- rhinitis," *Lin Chuang Er Bi Yan Hou Ke Za Zhi*, vol. 20, no. 7, pp. 315–318, 2006.
- [31] T. R. Jordan, E. Pfrogner, G. Rasp, and M. F. Kramer, "Clinical symptoms and mediators in the allergic early and late phase reaction," *Laryngo- Rhino- Otologie*, vol. 85, no. 2, pp. 113–123, 2006.
  - [32] T. Matsui, K. Asakura, H. Shirasaki, A. Kataura, and T. Himi, "Relationship between infiltrating cells and adhesion molecules in the nasal mucosa of patients with allergic rhinitis," *Acta Oto-Laryngologica*, vol. 120, no. 8, pp. 973–980, 2000.
  - [33] R. M. Naclerio, "Pathophysiology of perennial allergic rhinitis," *Allergy*, vol. 52, Supplement 36, pp. 7–13, 1997.
  - [34] D. Aronsson, E. Tufvesson, and L. Björmer, "Allergic rhinitis with or without concomitant asthma: difference in perception of dyspnoea and levels of fractional exhaled nitric oxide," *Clinical & Experimental Allergy*, vol. 35, no. 11, pp. 1457–1461, 2005.
  - [35] C. Gratziau, M. Lignos, M. Dassiou, and C. Roussos, "Influence of atopy on exhaled nitric oxide in patients with stable asthma and rhinitis," *The European Respiratory Journal*, vol. 14, no. 4, pp. 897–901, 1999.
  - [36] R. Mösges and L. Klimek, "Today's allergic rhinitis patients are different: new factors that may play a role," *Allergy*, vol. 62, no. 9, pp. 969–975, 2007.
  - [37] H. Widegren, J. Erjefält, M. Korsgren, M. Andersson, and L. Greiff, "Effects of intranasal TNFalpha on granulocyte recruitment and activity in healthy subjects and patients with allergic rhinitis," *Respiratory Research*, vol. 9, no. 1, p. 15, 2008.
  - [38] C. Bachert, "A review of the efficacy of desloratadine, fexofenadine, and levocetirizine in the treatment of nasal congestion in patients with allergic rhinitis," *Clinical Therapeutics*, vol. 31, no. 5, pp. 921–944, 2009.
  - [39] P. H. Howarth, M. A. Stern, L. Roi, R. Reynolds, and J. Bousquet, "Double-blind, placebo-controlled study comparing the efficacy and safety of fexofenadine hydrochloride (120 and 180 mg once daily) and cetirizine in seasonal allergic rhinitis," *The Journal of Allergy and Clinical Immunology*, vol. 104, no. 5, pp. 927–933, 1999.
  - [40] Van Cauwenberge, Juniper, and The STAR study investigating group, "Comparison of the efficacy, safety and quality of life provided by fexofenadine hydrochloride 120 mg, loratadine 10 mg and placebo administered once daily for the treatment of seasonal allergic rhinitis," *Clinical and Experimental Allergy*, vol. 30, no. 6, pp. 891–899, 2000.
  - [41] D. K. Agrawal, "Anti-inflammatory properties of desloratadine," *Clinical and Experimental Allergy*, vol. 34, no. 9, pp. 1342–1348, 2004.
  - [42] F. Marcucci, L. Giovanna Sensi, P. Abate et al., "Anti-inflammatory activity and clinical efficacy of a 3-month levocetirizine therapy in mite-allergic children," *Inflammation & Allergy Drug Targets*, vol. 10, no. 1, pp. 32–38, 2011.
  - [43] J. L. Brozek, C. E. Baena-Cagnani, S. Bonini et al., "Methodology for development of the allergic rhinitis and its impact on asthma guideline 2008 update," *Allergy*, vol. 63, no. 1, pp. 38–46, 2008.
  - [44] M. Ciebiada, M. Barylski, and M. G. Ciebiada, "Nasal eosinophilia and serum soluble intercellular adhesion molecule 1 in patients with allergic rhinitis treated with montelukast alone or in combination with desloratadine or levocetirizine," *American Journal of Rhinology & Allergy*, vol. 27, no. 2, pp. 58–62, 2013.
  - [45] R. Maiti, J. Rahman, J. Jaida, U. Allala, and A. Palani, "Rupatadine and levocetirizine for seasonal allergic rhinitis: a comparative study of efficacy and safety," *Archives of Otolaryngology – Head & Neck Surgery*, vol. 136, no. 8, pp. 796–800, 2010.
  - [46] A. Muntean, I. C. Bocsan, and D. M. Deleanu, "The effect of H1-antihistamines on allergic inflammation in patients with allergic rhinitis," *Human & Veterinary Medicine*, vol. 8, no. 4, pp. 161–165, 2016.
  - [47] J. Králová, L. Račková, M. Pekarová et al., "The effects of H1-antihistamines on the nitric oxide production by RAW 264.7 cells with respect to their lipophilicity," *International Immunopharmacology*, vol. 9, no. 7–8, pp. 990–995, 2009.
  - [48] L. Bennedich Kahn, L. E. Gustafsson, and C. Olgart Höglund, "Nerve growth factor enhances neurokinin A-induced airway responses and exhaled nitric oxide via a histamine-dependent mechanism," *Pulmonary Pharmacology & Therapeutics*, vol. 21, no. 3, pp. 522–532, 2008.



## Research Article

# Ganoderma Triterpenoids Exert Antiatherogenic Effects in Mice by Alleviating Disturbed Flow-Induced Oxidative Stress and Inflammation

Pei-Ling Hsu,<sup>1,2</sup> Yung-Ching Lin,<sup>1,2</sup> Hao Ni,<sup>1</sup> and Fan-E Mo <sup>1,2</sup>

<sup>1</sup>Department of Cell Biology and Anatomy, College of Medicine, National Cheng Kung University, Tainan, Taiwan

<sup>2</sup>Institute of Basic Medical Sciences, College of Medicine, National Cheng Kung University, Tainan, Taiwan

Correspondence should be addressed to Fan-E Mo; [femo@mail.ncku.edu.tw](mailto:femo@mail.ncku.edu.tw)

Received 6 November 2017; Accepted 15 February 2018; Published 11 April 2018

Academic Editor: Raluca M. Pop

Copyright © 2018 Pei-Ling Hsu et al. This is an open access article distributed under the Creative Commons Attribution License, which permits unrestricted use, distribution, and reproduction in any medium, provided the original work is properly cited.

Ganoderma mushrooms, used in traditional Chinese medicine to promote health and longevity, have become widely accepted as herbal supplements. *Ganoderma lucidum* (GL), a commonly seen ganoderma species, is commercially cultivated under controlled conditions for more consistent chemical composition. The medicinal properties of GL are attributable to its antioxidant and anti-inflammatory activities. We intended to assess the effect of GL in atherosclerosis, an arterial condition associated with chronic oxidative stress and inflammation, using a carotid-artery-ligation mouse model. Flow turbulence created in the ligated artery induces oxidative stress and neointimal hyperplasia, a feature of early atherogenesis. Daily oral GL prevented neointimal thickening 2 weeks after ligation. Moreover, the ganoderma triterpenoid (GT) crude extract isolated from GL abolished ligation-induced neointima formation. Mechanistically, endothelial dysfunction was observed 3 days after ligation before any structural changes could be detected. GTs alleviated the oxidative stress and restored the atheroresistant status of endothelium by inhibiting the induction of a series of atherogenic factors, including endothelin-1, von Willebrand factor, and monocyte chemoattractant protein-1 after 3-day ligation. The anti-inflammatory activity of GTs was tested in cultured human umbilical vein endothelial cells (HUVECs) exposed to disturbed flow in an *in vitro* perfusion system. GTs abolished the induction of proinflammatory VCAM-1, TNF- $\alpha$ , and IL-6 by oscillatory shear stress. Moreover, the antioxidant activity of GTs was tested in HUVECs against the insult of H<sub>2</sub>O<sub>2</sub>. GTs dissipated the cellular superoxide accumulation imposed by H<sub>2</sub>O<sub>2</sub>, thereby mitigating H<sub>2</sub>O<sub>2</sub>-induced cell damage and proatherogenic response. Our results revealed the atheroprotective properties of ganoderma mushrooms and identified triterpenoids as the critical constituents for those effects. GTs prevent atherogenesis by eliminating disturbed flow-induced oxidative stress and inflammation.

## 1. Introduction

Atherosclerotic disease remains a leading cause of death in the world based on a most recent survey by the World Health Organization. The complication of atherosclerosis gives rise to coronary artery disease leading to myocardial infarction or cerebrovascular disease leading to stroke. The progression of atherosclerosis involves the development of atheromatous plaques in the intima of arteries. The formation of atheroma is accelerated by dysfunctional endothelium via recruiting circulating monocytes and increasing the uptake of low-density lipoproteins (LDLs)

[1]. Monocytes transmigrate into the intima and differentiate into macrophages. The macrophages ingest oxidized LDL and become foam cells. Oxidized lipoproteins and fatty acids trigger a sustained oxidative burst and apoptosis of foam cells, which leads to the formation of atheroma consisting of a lipid core, apoptotic cells, debris, and many inflammatory cells [2]. The dysfunction of the endothelium, in the context of atherosclerotic cardiovascular disease, encompasses a wide range of maladaptation in its normal functional phenotypes for the regulation of thrombosis, local vascular tone, redox balance, and inflammatory response [1].

Endothelial dysfunction can be induced by inflammatory cytokines, oxidative stress, hypertension, hypercholesterolemia, and diabetes [1]. Though these risk factors exist in the entire arterial system, atherosclerosis preferentially develops at arterial branches or curvatures, where the local flow is disturbed [3]. Disturbed flow imposes low and oscillatory shear stress, which downregulates the nitric oxide production and causes other maladaptive alterations in endothelial functional phenotype [3–5]. Current therapy for atherosclerosis primarily targets hypercholesterolemia, thrombosis, or inflammation, however, lacks a good strategy for restoring endothelial function under disturbed flow. Here, we used a disturbed flow-induced atherogenic mouse model by ligating the carotid artery to evaluate potential new treatments.

Ganoderma mushrooms (Lingzhi in Chinese) are a traditional Chinese herbal medicine that have been widely accepted as a nutritional supplement. Among many species of the mushrooms, *Ganoderma lucidum* (GL) is most commonly seen and is commercially cultivated under controlled conditions to obtain mushrooms with more consistent chemical composition. GL possesses antihypertensive and hypocholesterolemic activities among other medicinal benefits [6]. The primary bioactive compounds in GL include triterpenoids and polysaccharides [6]. GL prevents cardiac damage in animal models by alleviating the oxidative stress associated with myocardial injury [7]. The triterpenoid fraction of ganoderma, consisting of more than 300 lanostane-tetracyclic compounds [8], provides antioxidant activities to prevent myocardial injury [9]. Ganoderma triterpenoids (GTs) also suppress inflammatory response [10] by directly scavenging the free radicals or systemically enhancing the antioxidant enzymes [11], thereby lowering lipid peroxidation in mice [12]. Inflammation and oxidized LDL are two major risk factors driving the progression of atherosclerosis. We intended to evaluate the atheroprotective activities of GL and its triterpenoid constituents using the carotid-artery-ligation mouse model.

## 2. Materials and Methods

**2.1. Animals.** This study was carried out in accordance with the recommendations of the *Guide for the Care and Use of Laboratory Animals* published by the United States National Institutes of Health. All animal use protocols were approved by the Institutional Animal Care and Use Committee of the National Cheng Kung University. The animal sample size ( $n$ ) was estimated by a power analysis of the pilot study using the G\*Power program. We first tested the atheroprotective property of GL in a disturbed flow-induced atherogenesis mouse model. We followed by identifying the constituents contributing to the atheroprotective property of GL by using GT extracts. Furthermore, we tested deferred GTs treatment to assess the potential for using GT to treat existing conditions. Mice were anesthetized with chloral hydrate (300 mg/kg; i.p.) before surgery. If pain or distress was observed after surgery, nalbuphine (1.2 mg/kg; s.c.) was administered to the mice. Male BALB/c mice between 2 and 5 months old were used in this study. To induce

neointima formation, a ligature was made at the end of the left common carotid artery (LCA) near the carotid bifurcation (Figure 1(a)). Granules of GL (300 mg/kg/day Shuang Hor Superfine Lingzhi; Double Crane, Taiwan) derived from concentrated aqueous-ethanolic extract of the fruiting body of GL suspended in water or water vehicle control were delivered orally via a gavage needle 2 h before ligation and daily for the remainder of the waiting period. Alternatively, GTs (300 mg/kg/day; a generous gift from the Biotechnology Research and Development Institute of Double Crane Group, Taiwan) or DMSO vehicle control was subcutaneously injected immediately after ligation and daily for the remainder of the waiting period. Blood flow was monitored with pulsed wave Doppler imaging using the VisualSonics Vevo 770 with a 40 MHz probe.

**2.2. Histological Analysis.** Mice were euthanized 3, 14, or 17 days after surgery. LCAs and right common carotid arteries (RCAs) were harvested and cryopreserved in OCT compound. Eight micrometer cryosections of the artery tissue from the segment between 1.5 and 2 mm from the ligature were stained with hematoxylin and eosin (H&E) or TUNEL staining (Millipore). For immunofluorescence staining, sections of arterial tissue were incubated with the antibodies as indicated, including anti-CD31 (Abcam ab28364, 1:50), anti-F4/80 (Abcam ab6640, 1:100), anti-endothelin-1 (ET-1) (Abcam ab2786, 1:250), anti-von Willebrand factor (vWF) (Abcam ab68545, 1:50), and anti-monocyte chemoattractant protein-1 (MCP-1) (Abcam ab8101, 1:20). The number of cells displaying specific staining was scored in a blinded manner.

**2.3. Dihydroethidium (DHE) Staining.** DHE after being oxidized by superoxides intercalates into DNA and generates red fluorescence. Eight serial arterial sections were incubated with DHE (2  $\mu$ M) at 37°C for 30 min and then immunostained for endothelial-specific CD31 (green) and counterstained with DAPI (blue) for nuclei. The numbers of DHE<sup>+</sup> and total endothelial cells on each artery section were scored in a blinded manner.

**2.4. Cell Culture.** Human umbilical vein endothelial cells (HUVECs) were purchased from the Bioresource Collection and Research Center (Hsinchu, Taiwan). Cells were cultured on gelatin-coated plates in medium 199 (Gibco) supplemented with 10% FBS, 25 U/ml heparin (Sigma), 30  $\mu$ g/ml endothelial cell growth supplement (Millipore), 1x GlutaMax (Gibco), and 1.5 g/l sodium bicarbonate at 37°C and 5% CO<sub>2</sub>.

**2.5. Annexin V/Propidium Iodide (PI) Staining for Apoptosis.** HUVECs were pretreated with GTs (500  $\mu$ g/ml) or DMSO vehicle control for 1 h before H<sub>2</sub>O<sub>2</sub> (400  $\mu$ M) was added, and incubated for additional 24 h. Treated cells were harvested and incubated with an FITC-conjugated annexin V antibody (BD Biosciences 556419, 1:20) and PI at room temperature for 15 min before fluorescence was measured by flow cytometry. The FlowJo software was used to analyze the results. The concentration of 500  $\mu$ g/ml GTs was determined in a dose-response assessment of GTs against

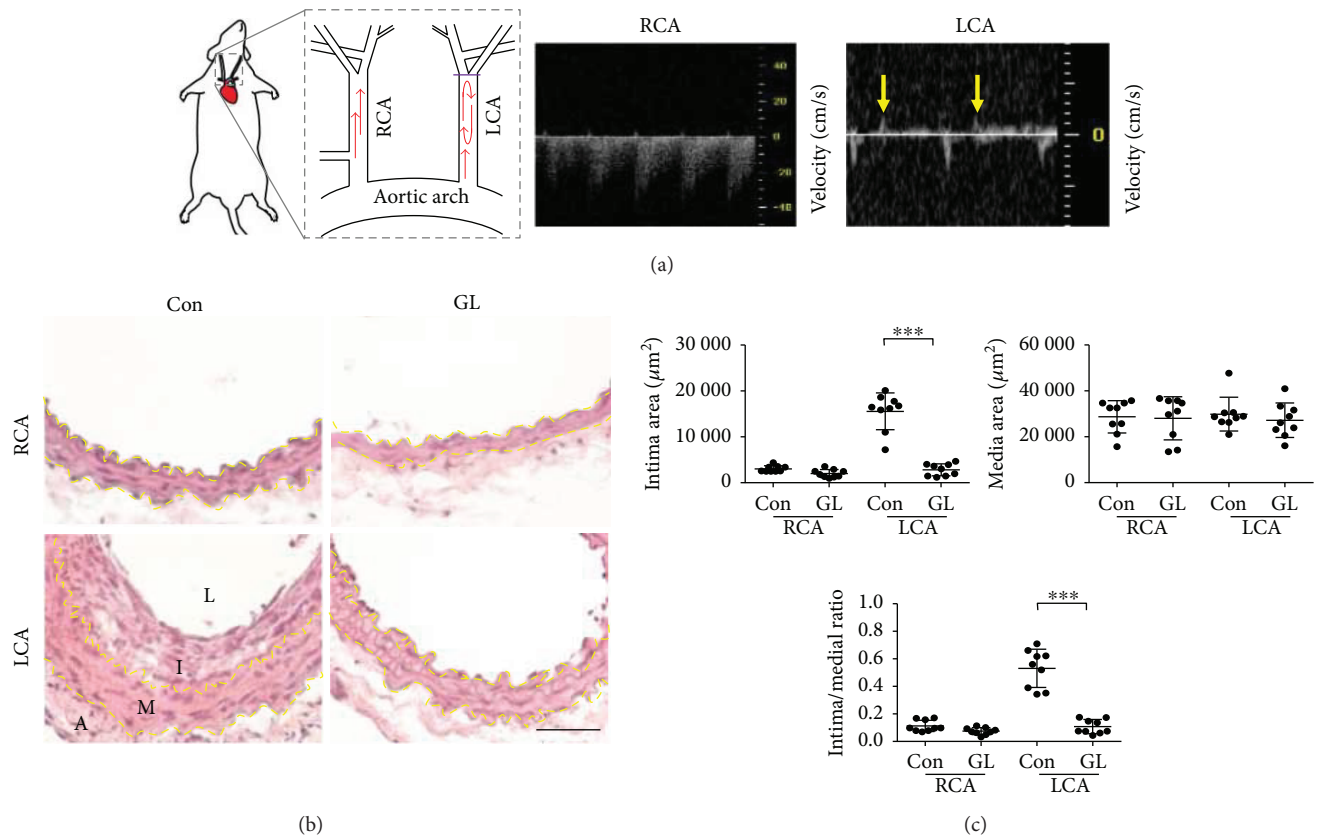


FIGURE 1: *Ganoderma lucidum* (GL) protected the carotid artery from disturbed flow-induced atherogenesis. (a) The diagram illustrates the carotid-artery-ligation model. A purple bar indicates the blockage in the ligated left common carotid artery (LCA). Oscillatory blood flow was generated by arterial ligation. Yellow arrows indicate the flow recirculation in the ligated LCA observed in the pulsed wave Doppler image. The unligated right common carotid artery (RCA) served as the sham control. (b) Carotid arteries were excised 14 days after ligation from mice fed with GL (300 mg/kg/day) or water vehicle control (Con) ( $n = 9$  for each group) and processed for H&E staining. Yellow dashed lines delineate the internal or external elastic lamellae. A: adventitia; I: intima; L: lumen; M: media. Bar: 50  $\mu\text{m}$ . (c) The intima and media areas of each arterial tissue section were quantified using the Nikon NIS-Elements D program. Data are means  $\pm$  SEM from 6 to 8 serial sections from each artery. Statistical significance was calculated using two-way ANOVA and post hoc Tukey's tests, \*\*\*  $p < 0.001$ .

$\text{H}_2\text{O}_2$ -induced apoptosis by counting nuclear condensation after DAPI staining (data not shown).

**2.6. Reactive Oxygen Species (ROS) Measurements.** HUVECs were treated with  $\text{H}_2\text{O}_2$  (400  $\mu\text{M}$ ) in the presence of or no GTs (500  $\mu\text{g}/\text{ml}$ , 1 h pretreatment) for 30 min. To measure cytosolic ROS, live cells were loaded with the ROS dye CM-H2DCFDA (5  $\mu\text{M}$ ) 15 min prior to the end of  $\text{H}_2\text{O}_2$  treatment. Cells were then harvested and resuspended in cold PBS containing 5% FBS. Fluorescence was measured by flow cytometry and analyzed using the FlowJo software.

**2.7. Immunocytochemistry.** HUVECs were treated with  $\text{H}_2\text{O}_2$  (400  $\mu\text{M}$ ) in the presence of or no GTs (500  $\mu\text{g}/\text{ml}$ , 1 h pretreatment) for 5 h. Treated cells were fixed and permeabilized with 0.1% Tween 20 in PBS washing buffer for 30 min at room temperature. Cells were then stained with anti-ET-1 (Abcam ab2786, 1:200) or anti-MCP-1 (Abcam ab8101, 1:200) antibodies.

**2.8. In Vitro Perfusion System for Simulation of Blood Flow.** HUVECs seeded on microslides (ibidi 80186) were

perfused with unidirectional flow to generate laminar shear stress (LSS, 12  $\text{dyn}/\text{cm}^2$ ), or oscillating flow to generate oscillatory shear stress (OSS,  $\pm 5$   $\text{dyn}/\text{cm}^2$ ), or static control for 24 h using the ibidi pump system in the presence of or no GTs (500  $\mu\text{g}/\text{ml}$ ). Total RNA was extracted from treated cells and was subjected to quantitative RT-PCR using the Applied Biosystems StepOne Real-Time PCR Systems. The following gene-specific primer sets were used: (1) Il-6: 5'-GGACGGCTTTTACTTAAACGCCAA GG-3' (sense) and 5'-ATCTTCCCTAGTTACCCAGGT TCAGC-3' (antisense); (2) Tnf $\alpha$ : 5'-AAGAGTTCGCCAGG GACCTCT-3' (sense) and 5'-CCTGGGAGTAGATGAG GTACA-3' (antisense); (3) Vcam-1: 5'-CATTGACTTGC AGCACCACA-3' (sense) and 5'-AGATGTGGTCCCCTCA TTCG-3' (antisense); (4) Gapdh: 5'-GAAGGTGAAGG TCGGAGTC-3' (sense) and 5'-GAAGATGGTGATGGGA TTTC-3' (antisense). The amplification conditions were 10 min at 95°C, 40 cycles of 10 sec/95°C–1 min/60°C. The expression values of individual genes were normalized to Gapdh using the comparative cycle threshold method ( $2^{-\Delta\Delta\text{CT}}$ ).

**2.9. Statistical Analysis.** All assays were repeated at least 3 times and yielded similar patterns. Values are means  $\pm$  SEM. Comparisons were made using two-way ANOVA and post hoc Tukey's tests. Significance was set at  $p < 0.05$  and indicated as \* $p < 0.05$ ; \*\* $p < 0.01$ ; or \*\*\* $p < 0.001$ .

### 3. Results

**3.1. GL Protected the Carotid Artery from Disturbed Flow-Induced Atherogenesis.** We evaluated the effect of GL using a disturbed flow-induced atherogenic mouse model by carotid artery ligation. The blockage of the LCA after ligation was confirmed with pulsed wave Doppler imaging (Figure 1(a)). A unidirectional (away from the heart) pulsatile blood flow pattern was detected in the unligated RCA (Figure 1(a)). By contrast, the flow rate was much reduced after ligation in the LCA and flow recirculation (back to the heart displayed as positive velocities) was detected (Figure 1(a), arrows). The straight part of the healthy common carotid arteries is resistant to atherogenesis. However, low/reciprocating flow shear stress created by the ligation induces intimal hyperplasia, thereby the formation of neointima (Figure 1(b)). To test the atheroprotectivity of GL, mice were treated with oral GL (300 mg/kg/day) or water vehicle control after LCA ligation ( $n = 9$  for each group). The unligated RCA was used as a sham control. Both intima areas and intima/media ratios in the LCA were increased 14 days after ligation in the control (Con) mice (Figure 1(c)). Media layers were not affected by the ligation. Remarkably, GL-treated mice were resistant to ligation-induced intimal hyperplasia (Figures 1(b) and 1(c)), demonstrating the atheroprotective property of GL.

**3.2. GTs Prevented Carotid Artery Ligation-Induced Neointima Formation.** To test the effect of GTs in mice, we used the crude triterpenoids isolated from the acidic ethyl acetate-soluble material of the fruiting body of GL, which consists of >90% of total triterpenoid compounds, including ganoderic acids A (21%), B (8%), C (4%), C5 (3%), C6 (1%), D (10%), E (2%), G (5.5%), and ganoderenic acid D (7.5%), in addition to other minor triterpenoid components analyzed with the reverse phase HPLC fingerprinting as previously described [13]. Mice were subcutaneously injected with GTs (300 mg/kg/day) or vehicle control DMSO ( $n = 5$  for each group). Subcutaneous administration of GTs dissolved in DMSO was more effective than oral delivery in our initial testing (data not shown). GT-treated mice displayed similar resistance against ligation-induced intimal thickening (Figures 2(a) and 2(b)) as observed in mice receiving GL. The oxidative stress, identified with a superoxide indicator (DHE<sup>+</sup>, red, arrowheads), in the endothelium (CD31<sup>+</sup>, green) of the LCA was ameliorated by GTs (Figure 3(a)). Furthermore, the endothelial apoptosis (TUNEL<sup>+</sup>, red, curved arrows) in the LCA was abolished by GTs (Figure 3(b)). The recruitment of monocytes/macrophages (F4/80<sup>+</sup>, red, arrows) to the neointima was increased by ligation, and was eliminated by GTs (Figure 3(c)), demonstrating the anti-inflammatory benefit provided by GTs.

**3.3. GTs Alleviated Disturbed Flow-Induced Oxidative Stress and Proatherogenic Response in Endothelial Cells.** Alteration in endothelial function precedes the structural changes in atherogenesis [1]. We investigated the effect of GTs in regulating endothelial function in mice 3 days after ligation before any structural changes could be detected. We found that oxidative stress was elevated in the intima of the LCA and ~25% of the endothelial cells (CD31<sup>+</sup>, green) were DHE<sup>+</sup> (red) (Figure 4, arrow). Sustained oxidative stress leads to endothelial dysfunction and the induction of atherogenic factors [3]. Indeed, ET-1 (green in Figure 5(a), arrowheads), vWF (red in Figure 5(b), curved arrows), and MCP-1 (red in Figure 5(c), arrows) were induced in the endothelium of the control LCA 3 days after ligation. ET-1 induces vasoconstriction and is overexpressed in atherosclerosis [14]. vWF triggers thrombosis by mediating the initial adhesion of platelets at sites of vascular injury [15]. MCP-1 promotes vascular inflammation by recruiting circulating monocytes to the lesion sites [16]. The induction of ET-1, vWF, and MCP-1 was suppressed in the LCA of GT-treated mice (Figure 5). Together, these results indicated that GTs ameliorate the disturbed flow-induced oxidative stress and proatherogenic response to prevent the progression of atherogenesis.

**3.4. GTs Suppressed Oscillating Flow-Induced Inflammatory Response in Endothelial Cells.** To test the anti-inflammatory activity of GTs directly, HUVECs were exposed to unidirectional laminar flow (LSS) or slower and oscillating flow (OSS) in an *in vitro* perfusion system for 24 h to simulate different hemodynamic patterns in blood vessels. We then used qRT-PCR to measure the expression of a set of pro-inflammatory genes in the treated cells. We found that OSS upregulated the expression of vascular cell adhesion molecule-1 (VCAM-1) (Figure 6(a)), tumor necrotic factor- $\alpha$  (TNF- $\alpha$ ) (Figure 6(b)), and interleukin-6 (IL-6) (Figure 6(c)), compared with the levels in cells under LSS or static control. GTs (500  $\mu$ g/ml) abrogated the induction of VCAM-1, TNF- $\alpha$ , and IL-6 by OSS (Figure 6), demonstrating the anti-inflammatory activity of GTs.

**3.5. GTs Protected Endothelial Cells against Oxidative Insults.** To test the antioxidant activity of GTs, we challenged HUVECs with H<sub>2</sub>O<sub>2</sub> and measured their cellular ROS levels after 30 min H<sub>2</sub>O<sub>2</sub> treatment (400  $\mu$ M) with or without GTs (500  $\mu$ g/ml, 1 h pretreatment). The induction of intracellular ROS by H<sub>2</sub>O<sub>2</sub> was significantly reduced by GTs (Figure 7(a)). Consequently, H<sub>2</sub>O<sub>2</sub>-induced (400  $\mu$ M, 24 h) apoptosis was abolished by GTs (500  $\mu$ g/ml, 1 h pretreatment) in HUVECs. Apoptosis was measured with flow cytometry after annexin V/PI staining. Cells in the early (lower right quadrants, Q3) or late (upper right quadrants, Q2) stages of apoptosis were scored (Figure 7(b)). Oxidative stress leads to endothelial cell dysfunction prior to apoptosis. We found that both ET-1 (red in Figure 7(c)) and MCP-1 (red in Figure 7(c)) intensities were elevated by 5 h H<sub>2</sub>O<sub>2</sub> treatment (400  $\mu$ M). The induction of atherogenic ET-1 and MCP-1 by H<sub>2</sub>O<sub>2</sub> was abolished by GTs (Figure 7(c)), suggesting that the atheroprotective



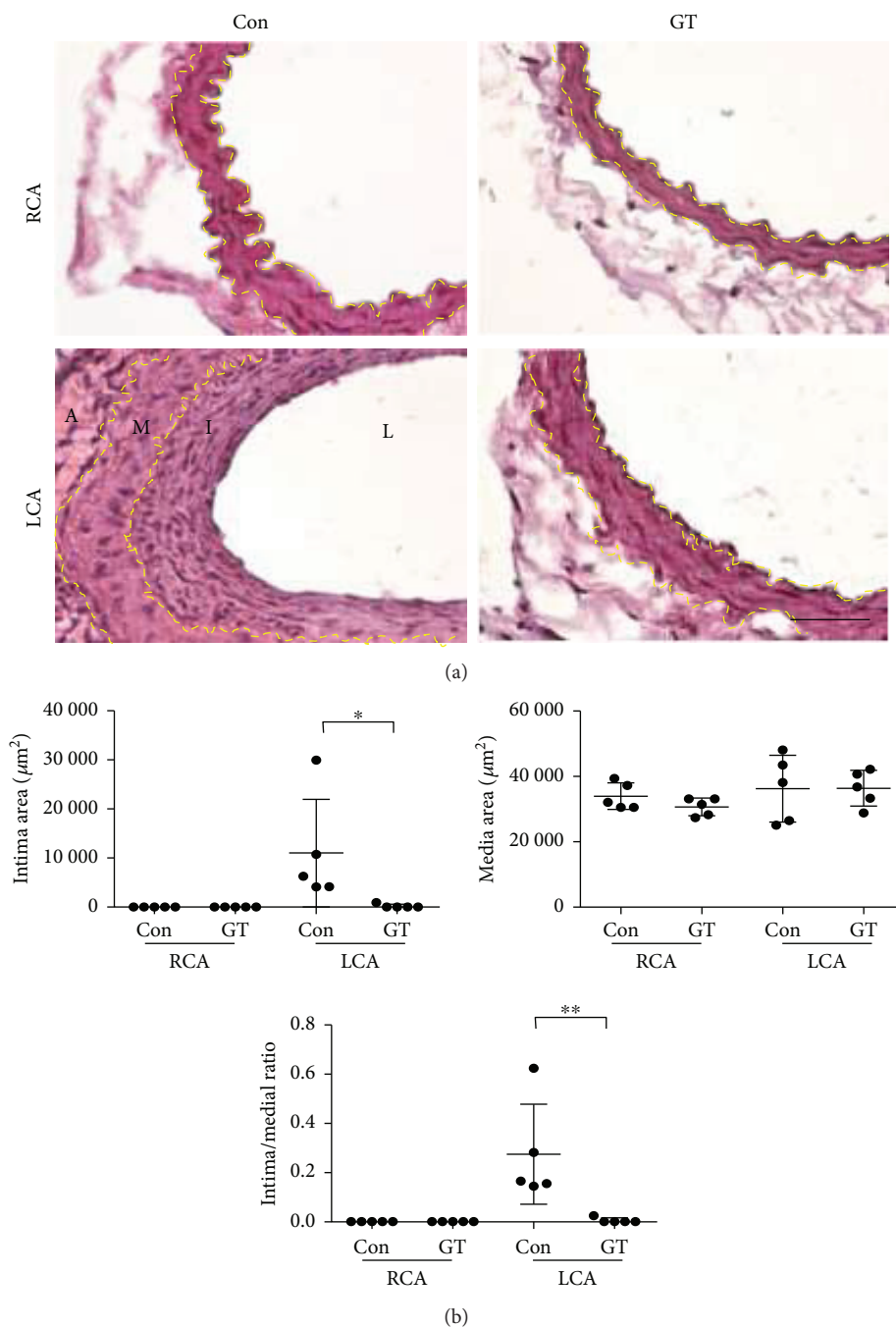


FIGURE 2: Ganoderma triterpenoids (GTs) prevented neointimal hyperplasia after carotid artery ligation. (a) LCAs were excised 14 days after ligation from mice receiving subcutaneous injections of GTs (300 mg/kg/day) or DMSO vehicle control (Con) ( $n = 5$  for each group) immediately after ligation and processed for H&E staining. Unligated RCAs served as the sham control. Yellow dashed lines delineate the internal or external elastic lamellae. A: adventitia; I: intima; L: lumen; M: media. Bar: 50  $\mu\text{m}$ . (b) The intima and media areas were quantified as described in Figure 1. Data are means  $\pm$  SEM from 6 to 8 serial sections from each artery ( $n = 5$ ). Statistical significance was calculated using two-way ANOVA and post hoc Tukey's tests, \* $p < 0.05$ , \*\* $p < 0.01$ .

property of endothelial cells was preserved by GTs attributable to their antioxidant activity.

**3.6. Deferred GT Treatment Effectively Inhibited Atherogenesis.** To assess the therapeutic potential of GTs on preexisting conditions, GT treatment was deferred for 3 days after ligation when endothelial function had been compromised.

We examined the arteries 14 days after the start of GT treatment and found that deferred GT treatment effectively blocked neointima formation (Figure 8(a)). Deferred GT treatment also alleviated the oxidative stress ( $\text{DHE}^+$ , arrowheads in Figure 8(b)) and suppressed the endothelial induction of ET-1 (arrows in Figure 8(b)) in the LCA. These findings suggested that GTs restored endothelial cells



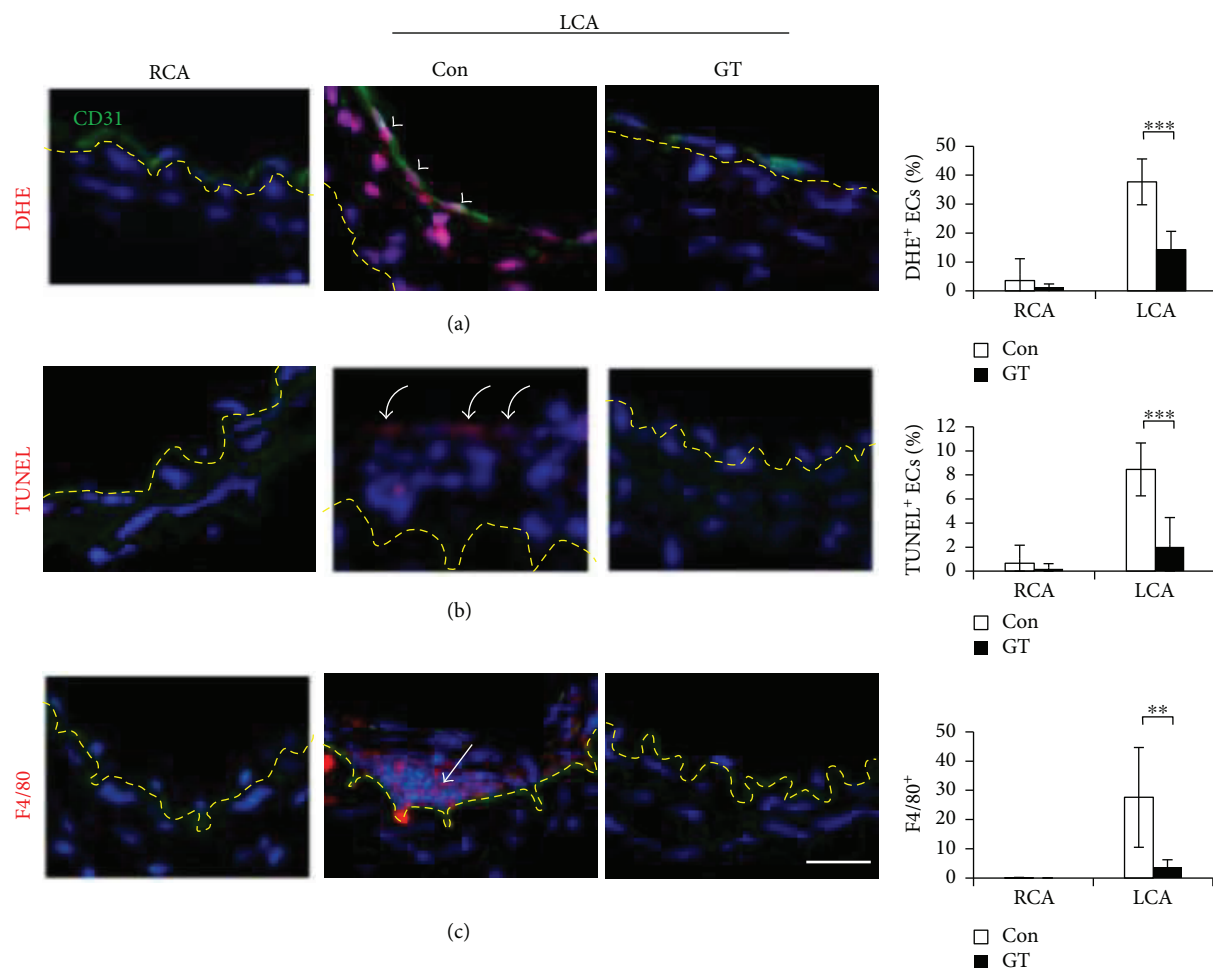


FIGURE 3: GTs inhibited atherogenesis in the ligated artery. Arterial sections, collected from mice treated with GTs (300 mg/kg/day; s.c.) or DMSO vehicle control (Con) 14 days after ligation as described in Figure 2, were stained with the superoxide indicator dihydroethidium (DHE, red in (a)), TUNEL (for apoptosis, red in (b)), an anti-CD31 (an endothelial cell marker, green) antibody, or an anti-F4/80 antibody (a monocyte/macrophage marker, red in (c)), and counterstained with DAPI for nuclei. Yellow dashed lines delineate the internal elastic lamellae. The tissue above the yellow dashed line is the intima. (a) Arrowheads indicate the superoxide-accumulated endothelial cells (DHE<sup>+</sup>/CD31<sup>+</sup> ECs with white nuclei) in the Con LCA. Numbers are the percentage of DHE<sup>+</sup> ECs. (b) Curved arrows indicate the apoptotic ECs (TUNEL<sup>+</sup>, inner lining cells with pink nuclei). Numbers are the percentage of TUNEL<sup>+</sup> ECs. (c) An arrow indicates the infiltrating macrophages (F4/80<sup>+</sup>, pink nuclei) in the intima. Numbers are the F4/80<sup>+</sup> cells in the intima of each arterial section. All the numbers in (a), (b), and (c) are means  $\pm$  SEM from 8 (a, b) or 4 (c) serial sections from each artery ( $n = 5$  for each group). Bar: 25  $\mu$ m. Statistical significance was calculated using two-way ANOVA and post hoc Tukey's tests, \*\* $p < 0.01$ , \*\*\* $p < 0.001$ .

from acquired proatherogenic phenotype after ligation and reversed the progression of atherosclerosis, reinforcing the therapeutic properties of GTs.

#### 4. Discussion

Ganoderma mushrooms have long been used in traditional Chinese medicine. Because of its long-term safety and tolerance, ganoderma is widely accepted as a nutritional supplement in the world. GL has a diverse blend of medicinal properties [6]. In particular, the antihypertensive, antiplatelet aggregation, and hypocholesterolemic properties of GL directly counteract many of the major atherogenic risk factors. Here we tested a new atheroprotective effect of GL using the carotid-artery-ligation mouse model. The ligation of the artery generates disturbed blood flow, a critical

atherogenic factor currently with no cure. We found that GL protected arteries from disturbed flow-induced atherosclerosis and the triterpenoid fraction is the critical constituents for these effects. GTs alleviated oxidative stress and inflammation, thereby preventing neointimal hyperplasia in the ligated arteries.

For atherosclerosis studies, the hyperlipidemic *apolipoprotein E*-null (*ApoE*<sup>-/-</sup>) mice on a high-fat diet are frequently used to generate vascular lesions. Here we used wild-type mice on a regular diet to avoid the complication involving LDL and to focus on the regulation of endothelial function by flow shear stress. Our finding herein defines a novel atheroprotective activity of GL directly on arterial endothelial cells independent of its lipid-lowering property. Without hyperlipidemia, neointimal hyperplasia is induced by arterial ligation, representing the initial feature

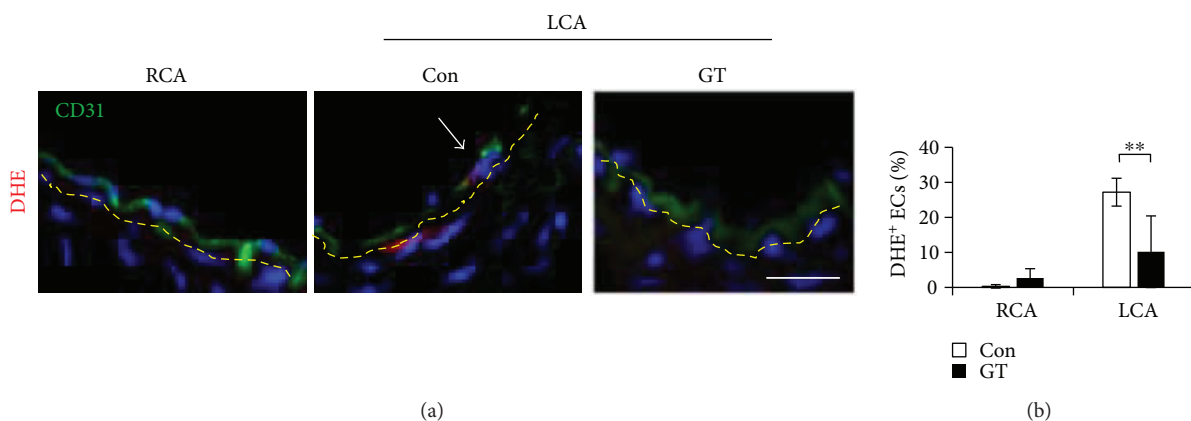


FIGURE 4: GTs alleviated the initial oxidative stress in the endothelium after ligation. (a) LCA and RCA from mice receiving Con (DMSO) or GT (300 mg/kg/day; s.c.) treatment were excised 3 days after ligation before any structural change occurred. Arterial tissue sections were processed for DHE staining. An arrow indicates a DHE<sup>+</sup> (red)/CD31<sup>+</sup> (green) EC. Yellow dashed lines delineate the internal elastic lamellae. Bar: 25  $\mu$ m. (b) The percentages of DHE<sup>+</sup> ECs are means  $\pm$  SEM from 8 serial sections from each artery ( $n = 5$  for each group). Statistical significance was calculated using two-way ANOVA and post hoc Tukey's tests, \*\* $p < 0.01$ .

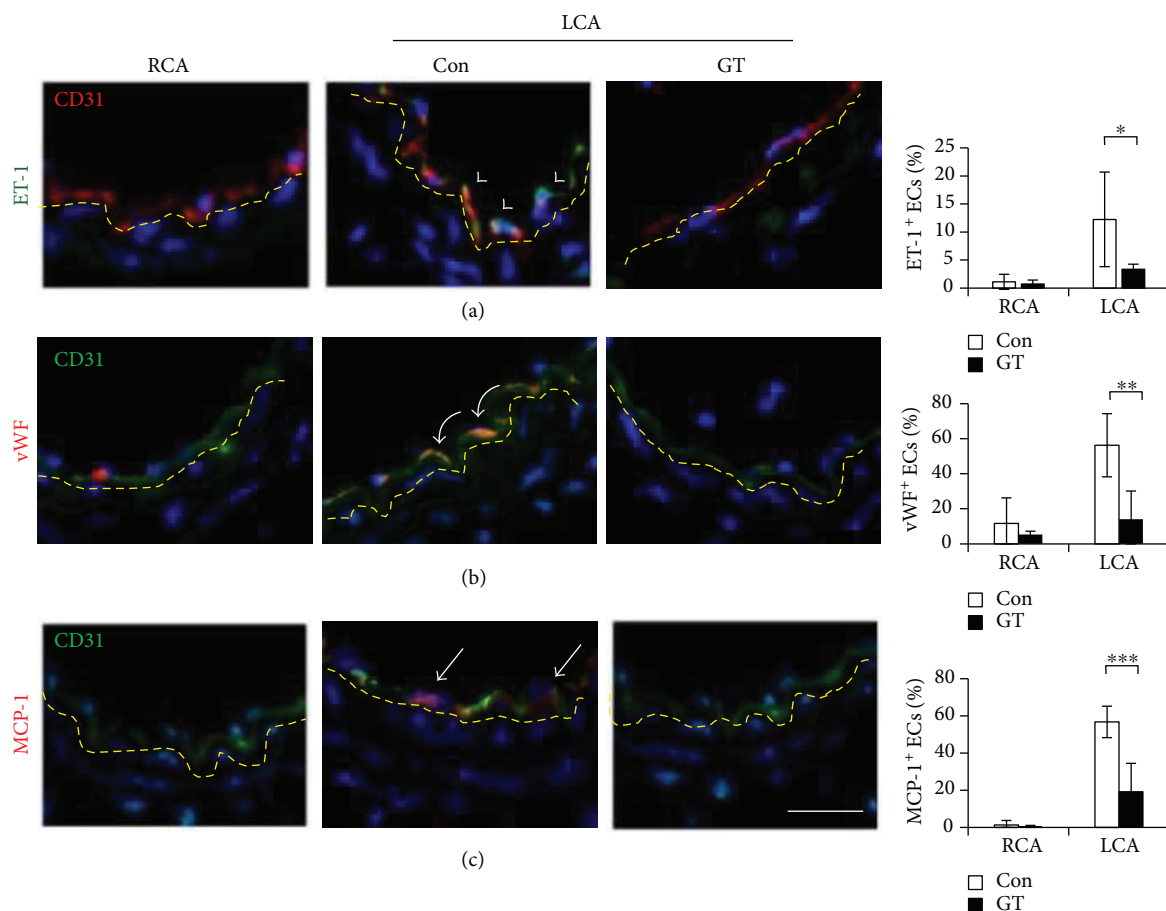


FIGURE 5: GTs preserved the atheroprotective property of endothelial cells in the ligated artery. LCA and RCA tissue sections, collected 3 days after ligation from mice receiving Con (DMSO) or GT (300 mg/kg/day; s.c.) treatment immediately after ligation and daily for the remainder of waiting period, were immunostained for proatherogenic factors ET-1, vWF, or MCP-1 as indicated. (a) Arrowheads indicate the ET-1<sup>+</sup> (green)/CD31<sup>+</sup> (red) ECs. (b) Curved arrows indicate the vWF<sup>+</sup> (red)/CD31<sup>+</sup> (green) ECs. (c) Arrows indicate the MCP-1<sup>+</sup> (red)/CD31<sup>+</sup> (green) ECs. The percentages of the positive ECs are means  $\pm$  SEM from 4 serial sections from each artery ( $n = 5$  for each group). Statistical significance was calculated using two-way ANOVA and post hoc Tukey's tests, \* $p < 0.05$ , \*\* $p < 0.01$ , \*\*\* $p < 0.001$ . Yellow dashed lines delineate the internal elastic lamellae. Bar: 25  $\mu$ m.

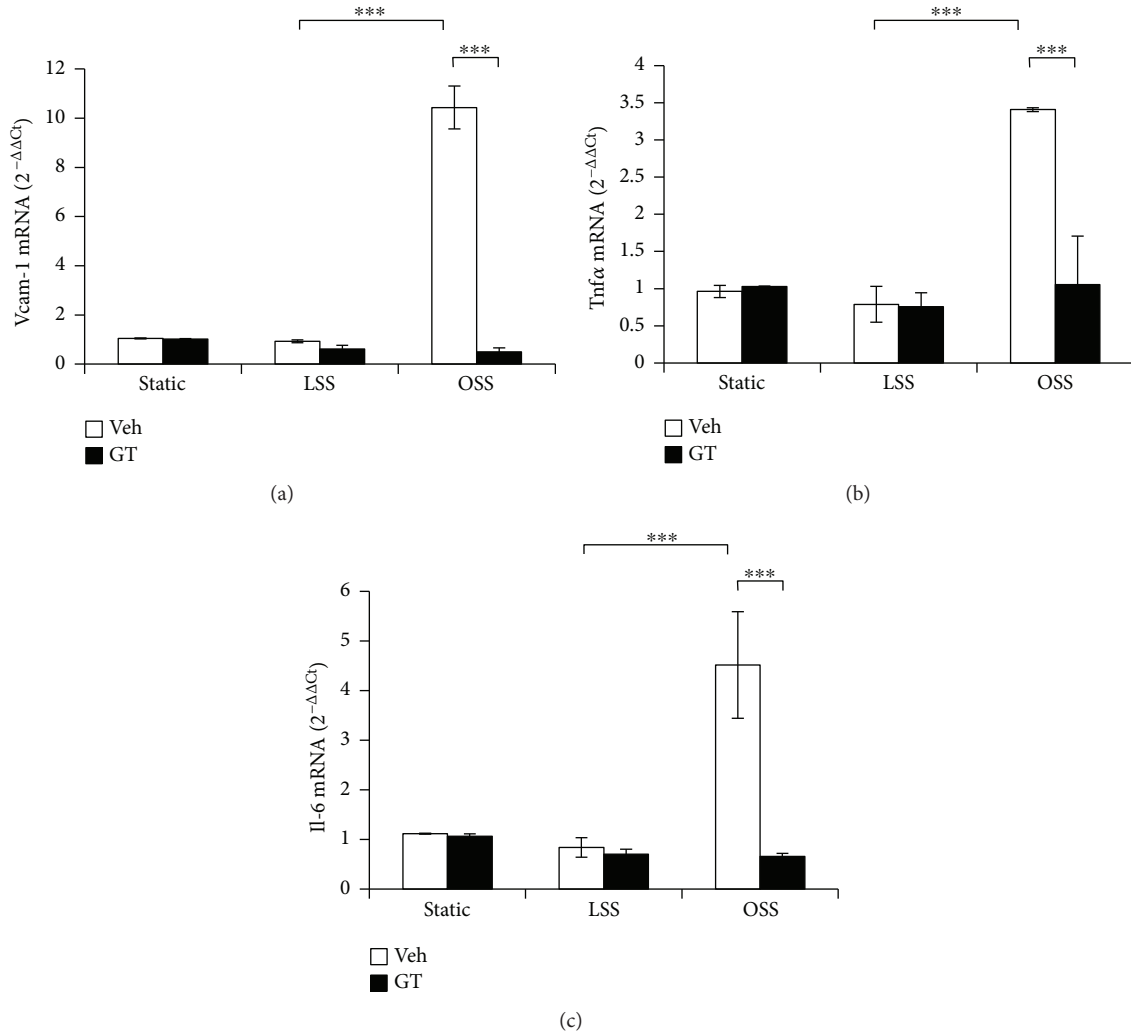
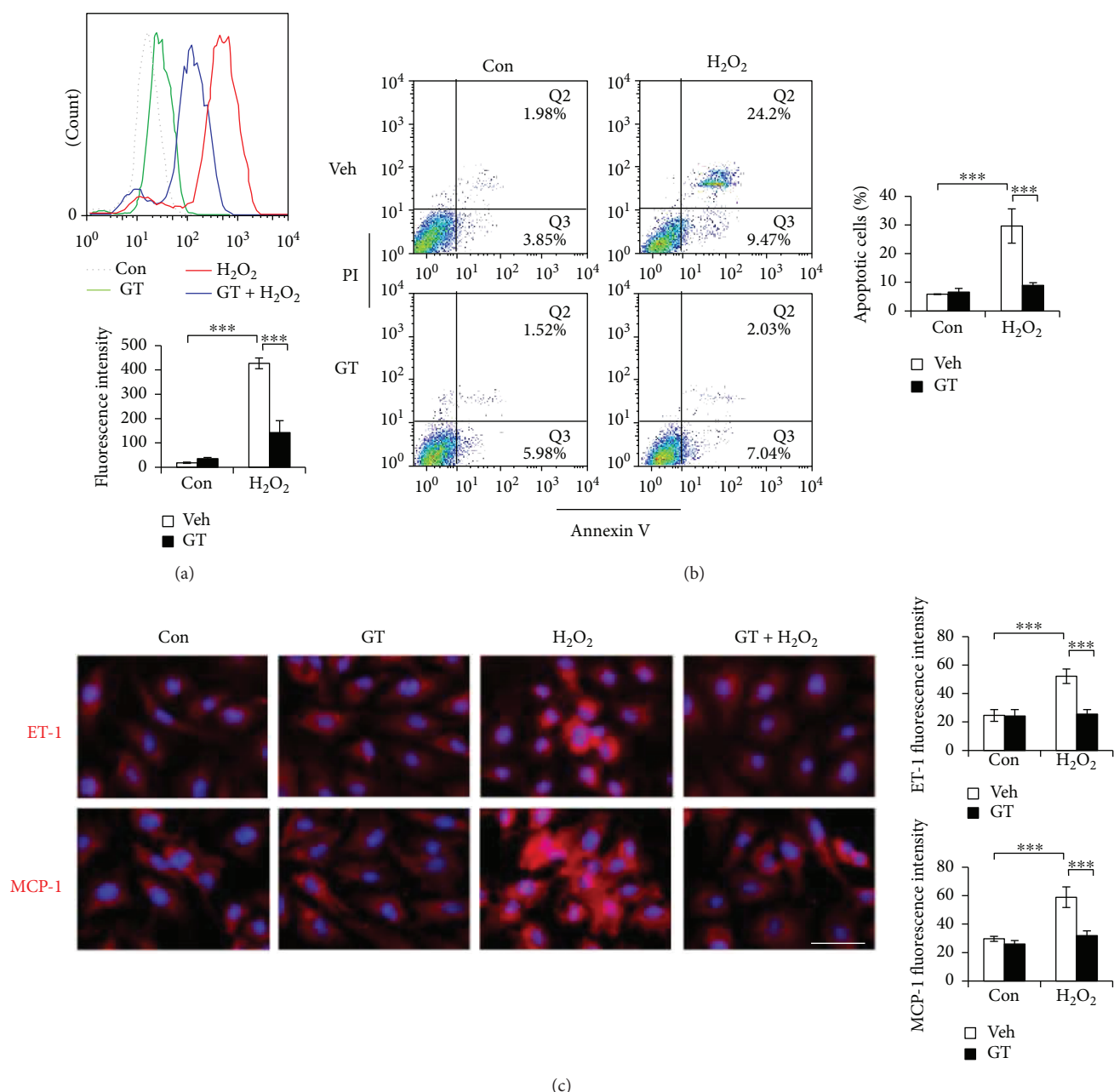


FIGURE 6: GTs suppressed disturbed flow-induced inflammatory response in ECs. Human umbilical vein endothelial cells (HUVECs) cultured on  $\mu$ -slides were exposed to laminar shear stress (LSS, 12 dyn/cm<sup>2</sup>), oscillatory shear stress (OSS,  $\pm 5$  dyn/cm<sup>2</sup>), or static control for 24 h in the presence of GTs (500  $\mu$ g/ml) or DMSO vehicle control (Veh). mRNA from treated cells was isolated and examined for the expression levels of proinflammatory genes (a) Vcam-1, (b) Tnf $\alpha$ , or (c) Il-6 using quantitative RT-PCR. Data are shown as mean  $\pm$  SEM of triplicate experiments. Statistical significance was calculated using two-way ANOVA and post hoc Tukey's tests, \*\*\* $p < 0.001$ .

of atherogenesis. To further develop the complete clinical feature of atherosclerotic lesions, such as lipid deposits and necrotic cores, *ApoE*<sup>-/-</sup> mice (on a regular diet) can be used in the carotid-artery-ligation model to generate atherosclerotic plaques [17]. Our findings here support a further study to test the atheroprotective characteristics of GL against disturbed flow under hyperlipidemic conditions in *ApoE*<sup>-/-</sup> mice.

The atheroprotective effect of GTs is attributable to their anti-inflammatory and antioxidant activities, suggested by the reduction of macrophage infiltration and oxidative stress in the ligated arteries of GT-treated mice. More direct evidence was shown in the *in vitro* assays, in which GTs inhibited the inflammatory response by OSS and reduced the cellular ROS accumulation and the induction of ET-1 and MCP-1 by H<sub>2</sub>O<sub>2</sub> in HUVECs. The anti-inflammatory and antioxidant activities of GTs

maintain endothelial function under stressed conditions, thereby promoting atheroresistance, anti-inflammation, and antithrombosis via downregulating ET-1, MCP-1, and vWF. These atheroprotective effects require separate medications according to current clinical treatment regimens. Furthermore, by promoting vascular health and not interfering with systemic physiology, GTs can be used with less potential side effects, such as the antithrombotic therapy-associated bleeding risks. The effectiveness of the deferred GT treatment indicates that GTs can reverse preexisting endothelial conditions and restore the atheroresistent status of endothelial cells, further strengthening the therapeutic use of GTs. Patients with the conditions, such as existing atherosclerotic plaque, in-stent restenosis, bypass graft occlusion, transplant vasculopathy, or aortic valve calcification, are prone to further development of atherosclerotic lesion due to endothelial dysfunction caused by disturbed



**FIGURE 7: GTs ameliorated H<sub>2</sub>O<sub>2</sub>-induced oxidative stress in the ECs.** (a) HUVECs were preincubated with GTs (500  $\mu$ g/ml) or vehicle (Veh) control DMSO for 1 h before treated with or without H<sub>2</sub>O<sub>2</sub> (400  $\mu$ M, 30 min). Cells were loaded with the fluorescent dye DCFDA for measuring the levels of reactive oxygen species (ROS) using flow cytometry. The upper panel shows a representative histogram overlay of the ROS fluorescent intensities. Quantitative fluorescence intensities are means  $\pm$  SEM of triplicate experiments. (b) Cells were preincubated with GTs (500  $\mu$ g/ml) or Veh (DMSO) for 1 h before treated with or without H<sub>2</sub>O<sub>2</sub> (400  $\mu$ M) for 24 h. Cells were then stained with annexin V/PI and analyzed for apoptosis. The percentage of the apoptotic cells includes the numbers shown in the lower right Q3 (early apoptosis) and in the upper right Q2 (late apoptosis) quadrants. Data are means  $\pm$  SEM of triplicate experiments. (c) HUVECs pretreated with GTs (500  $\mu$ g/ml, 1 h) or Veh (DMSO) were treated with or without H<sub>2</sub>O<sub>2</sub> (400  $\mu$ M) for 5 h, and followed by immunostaining with anti-ET-1 (red) or anti-MCP-1 (red) antibodies as indicated, and counterstaining with DAPI. The fluorescence intensity was quantified using the NIH ImageJ program. Data are means  $\pm$  SEM of triplicate experiments. Bar: 25  $\mu$ m. Statistical significance was calculated using two-way ANOVA and post hoc Tukey's tests, \*\*\* $p$  < 0.001.

blood flow in the affected vascular segments [3]. GTs may promote normal endothelial function and prevent atherosclerosis in these high-risk patients.

Though more than 316 GTs have been identified [8], the triterpenoid constituents of natural ganoderma mushrooms

are in low abundance (<3%) [13]. Nonetheless, the most abundant triterpenoids, including ganoderic acids A, B, C, and D, have been demonstrated for their antioxidant properties [18]. Accumulating evidence on the medicinal properties of GTs has promoted the advancement in the

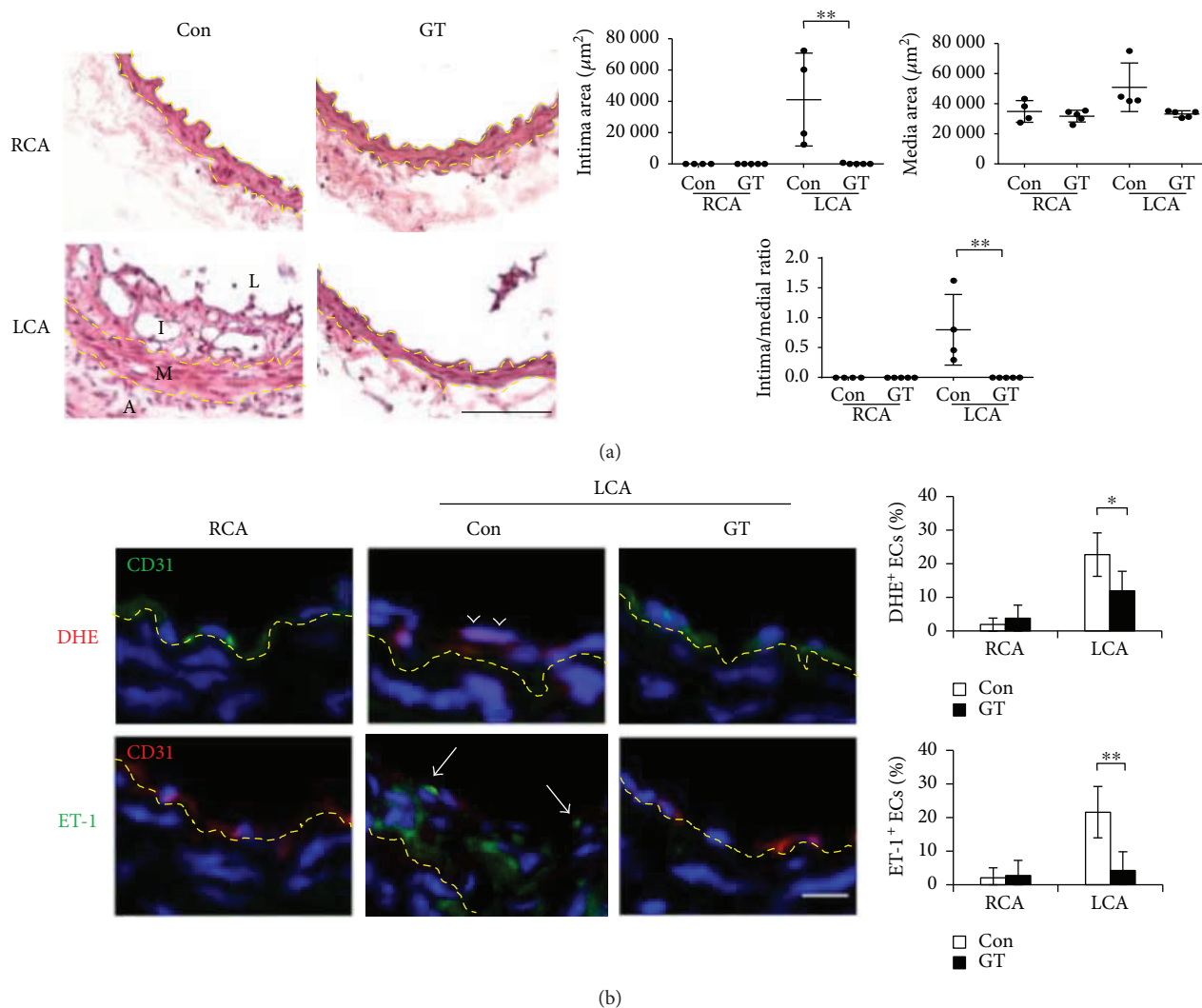


**FIGURE 8: Deferred GT treatment dissipated the oxidative stress and ET-1 induction in endothelial cells and prevented neointima formation in the ligated arteries.** GT (300 mg/kg/day; s.c.;  $n = 5$ ) or Con (DMSO;  $n = 4$ ) treatment was deferred for 3 days after ligation and continued for additional 14 days before the arteries were excised and analyzed. (a) LCA and RCA were processed for H&E staining. The quantitation of intima and media areas was as described in Figure 1. Data are means  $\pm$  SEM from 6 to 8 serial sections from each artery. (b) Arterial tissue sections were subjected to DHE (red) staining, or ET-1 (green) immunostaining, in addition to CD31 immunostaining (green or red as indicated) and DAPI counterstaining. Arrow heads indicate the DHE<sup>+</sup> ECs with pink nuclei. Arrows indicate the green ET-1<sup>+</sup> ECs. Quantitation was done as described in Figure 1. The percentages of the positive ECs are means  $\pm$  SEM from 8 (DHE) or 4 (ET-1) serial sections from each artery. Statistical significance was calculated using two-way ANOVA and post hoc Tukey's tests, \* $p < 0.05$ , \*\* $p < 0.01$ . Yellow dashed lines delineate the internal or external elastic lamellae. Bars in (a) 100  $\mu\text{m}$  and in (b) 25  $\mu\text{m}$ .

industrialized GT isolation technique [19], which allows the development of triterpenoid-enriched ganoderma extracts. Certain over-the-counter ganoderma extracts contain more than 30% of triterpenoid contents based on manufacturer data. It is worth noting that the relatively poor bioavailability of GTs via oral administration can be improved by preconjugating with solid lipid nanoparticles [20]. Therefore, solid lipid nanoparticles can be used to facilitate the absorption of GTs into the circulation to treat atherosclerosis.

Our findings provide evidence that triterpenoids contribute to the atheroprotection of ganoderma and can be used to enhance the efficacy of ganoderma supplements.

Nonetheless, the involvement of other constituents, such as polysaccharides, is not excluded by this study. We are currently testing the correlation between triterpenoid contents and the atheroprotective efficacy of ganoderma extracts by comparing a series of ganoderma products with different levels of triterpenoid contents using the carotid-artery-ligation mouse model.

## Conflicts of Interest

The authors declare that there are no conflicts of interest.



## Authors' Contributions

Pei-Ling Hsu designed the study, established the animal model, performed the *in vitro* studies, and prepared the figures for the manuscript. Yung-Ching Lin performed the GT-related animal works. Hao Ni performed the GL-related animal works. Fan-E Mo designed and coordinated the study. Pei-Ling Hsu and Fan-E Mo wrote the manuscript. All authors approved the final version of the manuscript.

## Acknowledgments




The authors thank Dr. Deng-Hai Chen for providing the GT crude extract and suggestions. The work was supported by the Microbiological Research Foundation, Taiwan.

## References

- [1] M. A. Gimbrone Jr. and G. Garcia-Cardena, "Endothelial cell dysfunction and the pathobiology of atherosclerosis," *Circulation Research*, vol. 118, no. 4, pp. 620–636, 2016.
- [2] N. Ruparelia, J. T. Chai, E. A. Fisher, and R. P. Choudhury, "Inflammatory processes in cardiovascular disease: a route to targeted therapies," *Nature Reviews Cardiology*, vol. 14, no. 3, pp. 133–144, 2017.
- [3] J. J. Chiu and S. Chien, "Effects of disturbed flow on vascular endothelium: pathophysiological basis and clinical perspectives," *Physiological Reviews*, vol. 91, no. 1, pp. 327–387, 2011.
- [4] J. P. Berman, M. E. Farkouh, and R. S. Rosenson, "Emerging anti-inflammatory drugs for atherosclerosis," *Expert Opinion on Emerging Drugs*, vol. 18, no. 2, pp. 193–205, 2013.
- [5] A. Ghattas, H. R. Griffiths, A. Devitt, G. Y. H. Lip, and E. Shantsila, "Monocytes in coronary artery disease and atherosclerosis: where are we now?," *Journal of the American College of Cardiology*, vol. 62, no. 17, pp. 1541–1551, 2013.
- [6] B. Boh, M. Berovic, J. Zhang, and L. Zhi-Bin, "*Ganoderma lucidum* and its pharmaceutically active compounds," *Biotechnology Annual Review*, vol. 13, pp. 265–301, 2007.
- [7] N. P. Sudheesh, T. A. Ajith, and K. K. Janardhanan, "*Ganoderma lucidum* ameliorate mitochondrial damage in isoproterenol-induced myocardial infarction in rats by enhancing the activities of TCA cycle enzymes and respiratory chain complexes," *International Journal of Cardiology*, vol. 165, no. 1, pp. 117–125, 2013.
- [8] Q. Xia, H. Zhang, X. Sun et al., "A comprehensive review of the structure elucidation and biological activity of triterpenoids from *Ganoderma* spp.," *Molecules*, vol. 19, no. 12, pp. 17478–17535, 2014.
- [9] Q. Y. Kuok, C. Y. Yeh, B. C. Su et al., "The triterpenoids of *Ganoderma tsugae* prevent stress-induced myocardial injury in mice," *Molecular Nutrition & Food Research*, vol. 57, no. 10, pp. 1892–1896, 2013.
- [10] S. Dudhgaonkar, A. Thyagarajan, and D. Sliva, "Suppression of the inflammatory response by triterpenes isolated from the mushroom *Ganoderma lucidum*," *International Immunopharmacology*, vol. 9, no. 11, pp. 1272–1280, 2009.
- [11] T. P. Smina, J. Mathew, K. K. Janardhanan, and T. P. A. Devasagayam, "Antioxidant activity and toxicity profile of total triterpenes isolated from *Ganoderma lucidum* (Fr.) P. Karst occurring in South India," *Environmental Toxicology and Pharmacology*, vol. 32, no. 3, pp. 438–446, 2011.
- [12] T. P. Smina, J. Joseph, and K. K. Janardhanan, "*Ganoderma lucidum* total triterpenes prevent  $\gamma$ -radiation induced oxidative stress in Swiss albino mice *in vivo*," *Redox Report*, vol. 21, no. 6, pp. 254–261, 2016.
- [13] D. H. Chen, W. Y. Shiou, K. C. Wang et al., "Chemotaxonomy of triterpenoid pattern of HPLC of *Ganoderma lucidum* and *Ganoderma tsugae*," *Journal of the Chinese Chemical Society*, vol. 46, no. 1, pp. 47–51, 1999.
- [14] M. W. Li, M. O. R. Mian, T. Barhoumi et al., "Endothelin-1 overexpression exacerbates atherosclerosis and induces aortic aneurysms in apolipoprotein E knockout mice," *Arteriosclerosis, Thrombosis, and Vascular Biology*, vol. 33, no. 10, pp. 2306–2315, 2013.
- [15] W. Miesbach and E. Berntorp, "Von Willebrand disease – the 'Dos' and 'Don'ts' in surgery," *European Journal of Haematology*, vol. 98, no. 2, pp. 121–127, 2017.
- [16] S. Pervin, R. Singh, M. E. Rosenfeld, M. Navab, G. Chaudhuri, and L. Nathan, "Estradiol suppresses MCP-1 expression *in vivo*: implications for atherosclerosis," *Arteriosclerosis, Thrombosis, and Vascular Biology*, vol. 18, no. 10, pp. 1575–1582, 1998.
- [17] D. Nam, C. W. Ni, A. Rezvan et al., "Partial carotid ligation is a model of acutely induced disturbed flow, leading to rapid endothelial dysfunction and atherosclerosis," *American Journal of Physiology-Heart and Circulatory Physiology*, vol. 297, no. 4, pp. H1535–H1543, 2009.
- [18] M. Zhu, Q. Chang, L. K. Wong, F. S. Chong, and R. C. Li, "Triterpene antioxidants from *Ganoderma lucidum*," *Phytotherapy Research*, vol. 13, no. 6, pp. 529–531, 1999.
- [19] D. H. Chen and K. D. Chen, "Determination of ganoderic acids in triterpenoid constituents of *Ganoderma tsugae*," *Journal of Food and Drug Analysis*, vol. 11, no. 3, pp. 195–201, 2003.
- [20] C. R. Cheng, M. Yang, S. H. Guan et al., "Pharmacokinetics of ganoderic acid D and its main metabolite by liquid chromatography–tandem mass spectrometry," *Journal of Chromatography B*, vol. 930, pp. 1–6, 2013.

## Research Article

# Chemerin, Inflammatory, and Nitrooxidative Stress Marker Changes Six Months after Sleeve Gastrectomy

Adriana Florinela Cătoi <sup>1</sup>, Alina Elena Pârnu <sup>1</sup>, Aurel Mironiuc,<sup>2</sup> Ștefan Chiorescu,<sup>2</sup> Alexandra Crăciun,<sup>3</sup> Ioana Delia Pop <sup>4</sup>, and Cornel Cătoi<sup>5</sup>

<sup>1</sup>Pathophysiology Department, Faculty of Medicine, “Iuliu Hațieganu”, University of Medicine and Pharmacy, Cluj-Napoca, Romania

<sup>2</sup>Second Surgical Clinic, Faculty of Medicine, “Iuliu Hațieganu”, University of Medicine and Pharmacy, Cluj-Napoca, Romania

<sup>3</sup>Biochemistry Department, Faculty of Medicine, “Iuliu Hațieganu”, University of Medicine and Pharmacy, Cluj-Napoca, Romania

<sup>4</sup>Exact Sciences Department, Faculty of Horticulture, University of Agricultural Sciences and Veterinary Medicine Cluj-Napoca, Cluj-Napoca, Romania

<sup>5</sup>Pathology Department, Faculty of Veterinary Medicine, University of Agricultural Sciences and Veterinary Medicine Cluj-Napoca, Cluj-Napoca, Romania

Correspondence should be addressed to Alina Elena Pârnu; [parvualinaelena@umfcluj.ro](mailto:parvualinaelena@umfcluj.ro)

Received 12 November 2017; Accepted 6 February 2018; Published 11 April 2018

Academic Editor: Ada Popolo

Copyright © 2018 Adriana Florinela Cătoi et al. This is an open access article distributed under the Creative Commons Attribution License, which permits unrestricted use, distribution, and reproduction in any medium, provided the original work is properly cited.

**Background.** Chemerin is a chemokine known to be increased in morbidly obese (MO) patients and correlated with markers of inflammation and nitrooxidative stress. We aimed to evaluate the changes of serum chemerin six months after laparoscopic sleeve gastrectomy (SG) and to assess if these changes are accompanied by variations of inflammatory and nitrooxidative stress markers. **Material and Methods.** We investigated the levels of chemerin, high-sensitive C-reactive protein (hsCRP), tumor necrosis factor alpha (TNF- $\alpha$ ), nitrite and nitrate (NOx), total oxidant status (TOS), total antioxidant response (TAR), and oxidative stress index (OSI) in a group of 24 MO patients submitted to SG before and six months after surgery. The MO group was compared with 20 controls. **Results.** hsCRP ( $p < 0.001$ ), NOx ( $p < 0.001$ ), TOS ( $p < 0.001$ ), TAR ( $p = 0.007$ ), and OSI ( $p = 0.001$ ) were significantly different between the two groups. Six months after surgery, we noticed significant changes (42.28% decrease) of hsCRP ( $p = 0.044$ ) and OSI ( $p = 0.041$ ) (31.81% decrease), while no significant changes were observed for chemerin ( $p = 0.605$ ), TNF- $\alpha$  ( $p = 0.287$ ), NOx ( $p = 0.137$ ), TOS ( $p = 0.158$ ), and TAR ( $p = 0.563$ ). **Conclusions.** Our study showed no significant changes of chemerin, and except for hsCRP and OSI, no other inflammatory and nitrooxidative stress markers changed six months after surgery.

## 1. Introduction

Mounting evidence has demonstrated that excess adipose tissue is a source and a cause of chronic inflammation, oxidative stress, and adipokine dysregulation which are all interrelated and involved in development of metabolic complications [1, 2]. The first acute-phase protein to be described, C-reactive protein (CRP), produced by the liver and the adipose tissue, is a sensitive marker of inflammation known to be increased in obesity and involved in the pathogenesis of coronary heart disease and diabetes mellitus [3–5]. Tumor necrosis factor alpha (TNF- $\alpha$ ) is a well-known inflammatory

marker produced by the macrophages of the stromal vascular tissue from the adipose tissue and has increased circulating levels in obesity-inducing insulin resistance [2, 3]. Furthermore, TNF- $\alpha$  determines oxidative stress leading to endothelial dysfunction and atherogenesis. High levels of TNF- $\alpha$  have been shown to increase the activity of inducible/inflammatory nitric oxide synthase (iNOS), the enzyme that induces large amounts of nitric oxide (NO) production that has cytotoxic effects and promotes apoptosis [6]. On the other hand, it has been shown that reactive oxygen species (ROS) enhance the production of proinflammatory cytokines and adhesion molecules [2, 7, 8].

Chemerin is a recently discovered chemokine known as a regulator of adipogenesis, inflammation, and glucose metabolism. The bulk of human data shows that obese patients display elevated chemerin levels which are positively correlated with markers of inflammation such as TNF- $\alpha$  and CRP, and thereby it might be used as an inflammatory marker. Also, chemerin seems to have a disruptive effect on glucose homeostasis and might be involved in the occurrence of type 2 diabetes and of other comorbidities [9–11]. Moreover, some authors have shown that insulin resistance seems to be a predictor of chemerin levels, independent of BMI [12].

Sleeve gastrectomy (SG) is a safe and effective as a standalone bariatric procedure with good weight loss results and effects on comorbidities explained by the reduction in adipose tissue mass and consecutive improvement of the inflammatory profile [13–15]. Studies that have addressed the dynamic of chemerin in relation with inflammatory markers, glucose homeostasis, and surgical weight loss have demonstrated various results. Some authors showed that the elevated plasma chemerin levels in morbidly obese (MO) patients decreased during the first year after gastric bypass, most prominently in the first 3 months when weight and fat mass loss, improvement of insulin sensitivity, and inflammatory markers were the strongest [16], while others showed no changes six months after both sleeve gastrectomy (SG) and Roux-en-Y gastric bypass (RYGB) [17]. As for the other inflammatory markers, while the change in TNF- $\alpha$  remains a controversial topic, CRP levels seem to improve significantly at 1 month after SG [15, 18].

The aims of this study were to assess the changes of chemerin 6 months after SG and to find out if these changes are accompanied by variations of inflammation and oxidative stress markers. We hypothesized that significant weight loss would be associated with reduction in inflammatory markers leading to diminished cardiovascular risk.

## 2. Materials and Methods

**2.1. Study Groups.** A group of 24 MO (16 female and 8 male) was recruited in a prospective manner from patients referred to bariatric surgery at the Second Surgical Clinic of Cluj-Napoca, Romania, between years 2014 and 2016. They all fulfilled the surgical criteria for bariatric procedures (BMI over 40 kg/m<sup>2</sup> or BMI between 35 kg/m<sup>2</sup> and 40 kg/m<sup>2</sup> with associated comorbidities) and were submitted to laparoscopic SG. The inclusion criteria were both sexes, age between 20 and 59 years, patients eligible for bariatric surgery with several dietary failures, and acceptance to participate to the study. Patients with inflammatory and infectious diseases or use of anti-inflammatory drugs, severe endocrine diseases (other than diabetes), hepatic or renal failure, mental illness, and malignancies were excluded from the study. In the MO group, 8 patients carried the diagnosis of type 2 diabetes, 9 had impaired fasting glucose, and the rest of them were within normal range of fasting blood glucose. None of the patients were on insulin treatment. A second group formed out of 20 normal-weight healthy subjects matched for age and gender with the first group was selected as a control group.

The study was approved by the Ethics Committee (number 503/15.12.2011), and written informed consent was obtained from all individual participants included in the study. The study was conducted in accordance with the ethical principles of the Helsinki declaration.

**2.2. Study Design.** The morbidly obese patients were evaluated anthropometrically and biochemically before and 6 months after SG. Anthropometrical measurements consisted of weight and height. Blood samples were collected after overnight fast and serum was obtained through centrifugation. The samples were run immediately or stored until analysis at –80°C. The study design included the measurements of chemerin, high-sensitive CRP (hsCRP), TNF- $\alpha$ , markers of nitrooxidative stress, fasting blood glucose, insulin, total cholesterol (TC), triglycerides, and HDL-C (high-density lipoprotein cholesterol). Low-density lipoprotein cholesterol (LDL-C) concentration was calculated by Friedewald formula [19].

**2.3. Anthropometric and Laboratory Measurements.** BMI was calculated according to the following formula: weight (in kilograms)/squared height (in square meters). The percent of excess BMI loss (%EBMIL) was calculated according to the following formula: %EBMIL = [(initial BMI – postop BMI)/(initial BMI – 25)]  $\times$  100 [20]. Homeostasis model assessment of insulin resistance (HOMA-IR) was used to evaluate insulin resistance using the following formula: HOMA-IR = (fasting insulin  $\mu$ U/ml  $\times$  fasting glucose mg/dl)/22.5  $\times$  18 [21]. A normal value was considered to be <2.5.

Fasting serum hsCRP levels were assayed using an automated system for chemiluminescence method (Immulate 1000, Siemens) and a commercially Immulate hsCRP kit (Siemens, Germany). Chemerin levels were determined using an ELISA kit (Abcam, Cambridge, United Kingdom), serum insulin using an ELISA kit (EMD Millipore, Burlington, Massachusetts, USA), and TNF- $\alpha$  levels using an ELISA method (Thermo Scientific, Waltham, Massachusetts, USA) according to the specific protocol of the manufacturer using an ELISA plate reader (Organon 230S, Netherlands). Coefficients of variation intra- and interassay for the tests were under 10%.

Nitrooxidative stress was evaluated by measuring serum nitric oxide (NO), total oxidative status (TOS), and total antioxidant response (TAR). NO concentration was measured indirectly using a colorimetric method for nitrite and nitrate (NOx) as final stable products. The principle of this method is the reduction of nitrate by vanadium (III) combined with detection by Griess reaction [22–24]. TOS and TAR as oxidative stress markers were analyzed using colorimetric methods, as well. TOS results were expressed in  $\mu$ mol H<sub>2</sub>O<sub>2</sub> equiv./l [25, 26]. For TAR, the assay was calibrated with Trolox, and the results were expressed as mmol Trolox equiv./l [24–26]. The oxidative stress index (OSI) is an indicator of the degree of oxidative stress and is calculated by the ratio of the TOS to TAR [27].

Fasting blood glucose, TC, HDL-C, and triglycerides were measured using the standard enzymatic colorimetric method on an automatic analyzer (Prestige 24i, Tokyo Boeki, Japan).

**2.4. Surgical Procedure.** The greater curvature and fundus of the stomach were resected starting from the distal antrum, 2–3 cm cranial to the pylorus, to the angle of His. We used an Endo GIATM (Covidien, Medtronic, Minneapolis, MN, USA) laparoscopic stapler, with a 60 mm cartridge in order to divide the stomach and create a gastric tube parallel to and alongside a 34 CH bougie. The resected part of the stomach was extracted through the middle abdominal 15 mm port site.

**2.5. Statistical Analysis.** The normal distribution for each of continuous variables was verified separately for the control and MO group by quantile-quantile plot and normality tests (Shapiro-Wilk test, D'Agostino skewness test, and Anscombe-Glynn kurtosis test). In the descriptive statistics, we used the mean  $\pm$  standard deviation for variables with Gaussian distribution and median/interquartile interval (25th percentile–75th percentile) for variables with non-Gaussian distribution. The comparison between the groups (control and MO) was performed by parametric or nonparametric tests (Student *t*-test or Mann–Whitney *U* test). The analysis of repeated measures was performed using the Student *t*-test for the dependent groups or Wilcoxon signed-ranked test for the repeated measures of non-Gaussian characteristics. Because of the missing data, the number of subjects at every follow-up point being different, we used pairwise deletion in all the tests.

We used the multivariate analysis of variance (MANOVA) for repeated measures to evaluate the statistical significance of mean difference adjusted for variance-covariance of the studied characteristics. The independent factors were as follows: two studied time points (before and 6 months after surgery) and groups (control and MO patients). As post hoc analysis, we used univariate ANOVA test. The significance of linear correlations between the variables was tested by Pearson's coefficient.

The level of statistical significance for all two-sided tests was set at  $p < 0.05$ .

The statistical analysis was performed with the IBM SPSS v.19 (Armonk, NY: IBM Corp) and Statistica, version 6.

### 3. Results

Table 1 shows the anthropometric and biochemical characteristics of the controls and MO at baseline. As expected, we found significant differences, that is, higher levels in MO versus controls regarding mean weight ( $t(23.43) = 11.74$ ,  $p < 0.001$ ), BMI ( $t(26) = 8.07$ ,  $p < 0.001$ ), TC ( $t(23) = 2.28$ ,  $p = 0.032$ ), triglycerides (Mann–Whitney *U* test,  $Z = 2.78$ ,  $p = 0.004$ ), and HOMA-IR (Mann–Whitney *U* test,  $Z = 2.52$ ,  $p = 0.008$ ). The mean values of hsCRP (Mann–Whitney *U* test,  $Z = 3.57$ ,  $p < 0.001$ ), NOx (Mann–Whitney *U* test,  $Z = 3.56$ ,  $p < 0.001$ ), TOS (Mann–Whitney *U* test,  $Z = 3.87$ ,  $p < 0.001$ ), TAR (Mann–Whitney *U* test,  $Z = 2.60$ ,  $p = 0.007$ ), and OSI (Mann–Whitney *U* test,  $Z = 3.03$ ,  $p = 0.001$ ) were significantly different between the groups, that is, elevated mean values of hsCRP, NOx, TOS, and OSI in MO subjects as compared to the control group. Moreover and interestingly, mean values of TAR were higher in MO as compared

to controls. Regarding the mean values of chemerin (Mann–Whitney *U* test,  $Z = 1.83$ ,  $p = 0.07$ ) and TNF- $\alpha$  (Mann–Whitney *U* test,  $Z = 1.84$ ,  $p = 0.06$ ), we identified a tendency towards statistical significance between the two groups (increased levels in MO). There were no statistically significant differences of mean values of fasting blood glucose ( $t(26) = 1.74$ ,  $p = 0.093$ ), insulin ( $t(22) = 1.27$ ,  $p = 0.215$ ), HDL-C ( $t(20) = 1.55$ ,  $p = 0.135$ ), and LDL-C ( $t(20) = 1.20$ ,  $p = 0.242$ ) between controls and MO patients.

Six months after SG, we observed a significant change (a decrease was noticed) of the BMI ( $t(17) = 7.41$ ,  $p < 0.001$ ), hsCRP (Wilcoxon test,  $Z = 2.01$ ,  $p = 0.044$ ), and of OSI (Wilcoxon test,  $Z = 2.04$ ,  $p = 0.041$ ) mean values. The %EBMIL value was  $64.36 \pm 19.58$ . However, we noticed no significant change of chemerin (Wilcoxon test,  $Z = 0.51$ ,  $p = 0.605$ ), TNF- $\alpha$  (Wilcoxon test,  $Z = 1.06$ ,  $p = 0.287$ ), NOx ( $t(12) = 1.59$ ,  $p = 0.137$ ), TOS (Wilcoxon test,  $Z = 1.41$ ,  $p = 0.158$ ), and TAR values (Wilcoxon test,  $Z = 0.57$ ,  $p = 0.563$ ) by the end of the study (Figures 1 and 2).

Using a 1 (group)  $\times$  2 (time) design for MANOVA with repeated measures, we found no statistically significant time point changes (6 months after surgery versus baseline) on the blood lipids levels—TC, HDL-C, LDL-C, and triglycerides (Pillai's trace test:  $F(3, 7) = 1.2$ ,  $p = 0.37 > 0.05$ ). When individual effect of each serum lipid were analyzed, we found no significant differences for TC (univariate ANOVA test,  $F(1, 9) = 0.12$ ,  $p = 0.91 > 0.05$ ), HDL-C ( $F(1, 9) = 4.13$ ,  $p = 0.73 > 0.05$ ), LDL-C ( $F(1, 9) = 0.86$ ,  $p = 0.37 > 0.05$ ), and triglycerides ( $F(1, 9) = 0.029$ ,  $p = 0.87 > 0.05$ ).

There was a statistically significant effect of time on the variables associated with blood glucose in general (MANOVA, Pillai's trace test:  $F(3, 12) = 7.6$ ,  $p = 0.04 < 0.05$ ). Using post hoc analysis, we revealed a significant time effect on fasting blood glucose variable ( $F(1, 14) = 4.53$ ,  $p = 0.052$ ), fasting insulin ( $F(1, 14) = 6.28$ ,  $p = 0.025$ ), and HOMA-IR ( $F(1, 14) = 24.23$ ,  $p < 0.001$ ) (Figure 2).

We observed a statistically significant linear correlation between changes of chemerin and those of TAR at 6 months after surgery ( $r = 0.545$ ,  $p = 0.04$ ), but no correlations were identified between chemerin variations and changes of BMI, TNF- $\alpha$ , hsCRP, NOx, TOS, and OSI.

### 4. Discussion

The present study was designed to analyze the hypothesis that increased levels of chemerin in a group of MO patients change 6 months after SG and that these changes run in parallel with changes of other inflammatory markers such as hsCRP, TNF- $\alpha$ , and nitrooxidative stress thus leading to a reduction of the cardiovascular risk. First of all, our results showed an important reduction of BMI (from  $48.54 \text{ kg/m}^2$  to  $34.69 \text{ kg/m}^2$ ) and a %EBMIL of 64.36% six months after SG. We observed no significant change in circulating chemerin and of TNF- $\alpha$ , NOx, TOS, and TAR, while a significant reduction of hsCRP and OSI was identified after surgery. Moreover, changes of chemerin correlated with changes of TAR, but they were independent of the variations of BMI, hsCRP, TNF- $\alpha$ , NOx, TOS, or OSI. Concerning



TABLE 1: Comparison of anthropometric and laboratory characteristics between groups.

Variables	Control*	Morbidly obese*	<i>p</i> value**
Age (years)	36.38 ± 6.3	42.15 ± 6.86	0.05
Weight (kg)	57.38 ± 6.74	136.85 ± 28.32	<0.001
BMI (kg/m <sup>2</sup> )	21.34 ± 2.73	48.54 ± 9.27	<0.001
TC (mg/dl)	150 ± 22.82	187.35 ± 43.08	0.032
HDL-C (mg/dl)	40.18 ± 8.71	49.66 ± 15.81	0.135
LDL-C (mg/dl)	93.80 ± 19.34	112 ± 39.83	0.242
Triglycerides (mg/dl)	80.50 (69.50–89)	122 (116–173)	0.004
Fasting blood glucose (mg/dl)	90.75 ± 7.19	104.15 ± 21.06	0.093
Insulin (μU/ml)	6.84 ± 3.64	19.28 ± 19.09	0.215
HOMA-IR	1.43 (0.78–2.08)	3.31(2.66–5.05)	0.008
hsCRP (mg/l)	0.26 (0.10–0.48)	16.98(11.30–18.30)	<0.001
TNF-α (pg/ml)	19.52 (12.17–25.65)	25.64 (23.21–52.60)	0.06
Chemerin (ng/ml)	25.13 (21.73–29.95)	47.44(26.63–65.73)	0.07
NOx (μmol/l)	48.51 (44.80–53.74)	71.94 (68.46–76.91)	<0.001
TOS (μmol H2O2 equiv./l)	19.26 (16.33–24.67)	93.19 (52.37–117.83)	<0.001
TAR (mmol trolox equiv./l)	0.62 (0.60–0.63)	0.88 (0.63–1.10)	0.007
OSI	31.39 (26.42–41.48)	142.27 (47.72–185.49)	0.001

BMI: body mass index; %EBMIL: excess body mass index loss; TC: total cholesterol; HDL-C: high-density lipoprotein cholesterol; LDL-C: low-density lipoprotein cholesterol; HOMA-IR: homeostasis model assessment of insulin resistance; hsCRP: high-sensitivity C-reactive protein; TNF-α: tumor necrosis factor alpha; NOx: nitrites/nitrates; TOS: total oxidative status; TAR: total antioxidant response; OSI: oxidative stress index. \*Mean ± standard deviation or median (interquartile interval: Q1–Q3); \*\*Student for independent groups or Mann–Whitney’s test.

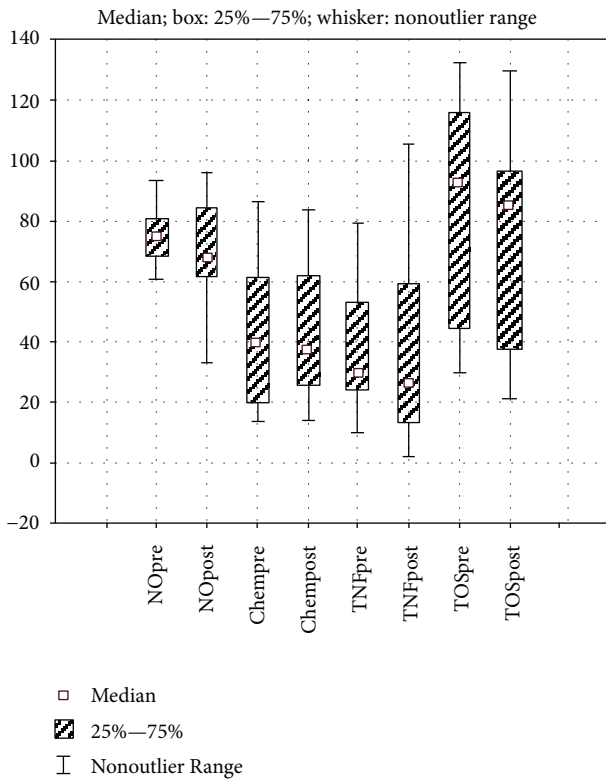


FIGURE 1: Evaluation of the changes of NOx, chemerin, TNF-α, and TOS values.

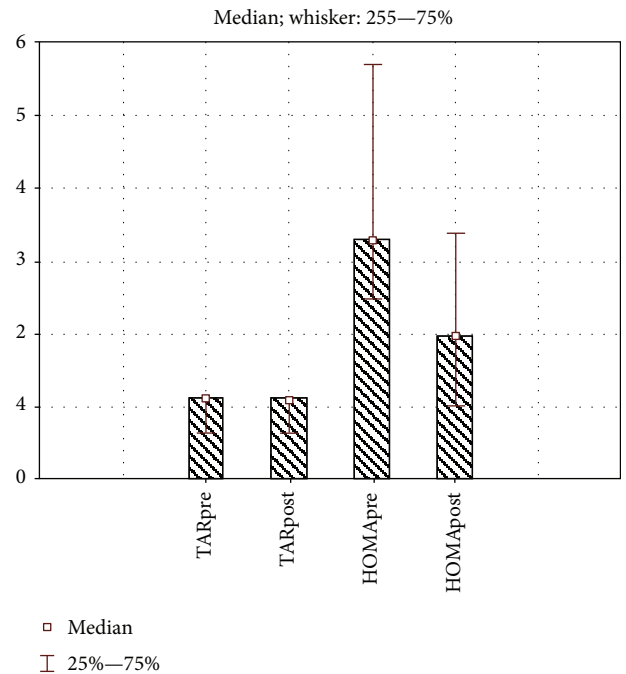


FIGURE 2: Evaluation of the changes of TAR and HOMA-IR values.

changes of fasting blood glucose, insulin, and HOMA-IR, they displayed a significant decrease six months after SG.

Emerging data has demonstrated that chemerin levels are elevated in obese patients [12, 16, 28–30]. Chemerin is a chemoattractant protein for macrophages being produced as a response to inflammation and may induce a positive

feedback for a continuous chronic inflammation. Still, precise data on the conditions that drive the increase of chemerin remain to be elucidated. Regarded as a marker of inflammation, chemerin is considered to be a possible link between obesity and the development of its metabolic comorbidities. Although it seems that chemerin might play a role in insulin sensitivity, the results remain conflicting [9].

Considering that chemerin is an inflammatory marker, we presumed that a postsurgical chemerin change/decrease would result in a reduced recruitment of macrophages in the adipose tissue leading to a diminished proinflammatory state and a lower cardiovascular risk. Still, in our study, six months after surgery, circulating chemerin levels which were increased at baseline as compared to the controls (with a tendency towards statistical significance between the two groups) did not change/decrease significantly and alongside with the important reduction of BMI. There were no correlations between the changes of BMI and those of chemerin. In agreement with our results, other authors showed in a group of MO with similar values of BMI and HOMA-IR as in our group of patients that did not change chemerin levels significantly 6 months after SG, but an important reduction was exhibited one year after surgery [17]. On the other hand, a significant early decrease of circulating chemerin levels, that is, at 3 months after RYGB, was demonstrated by some authors, showing that the reduction was correlated with a decrease in glucose and HOMA-IR [16]. Furthermore, Sell et al. demonstrated that the decrease of chemerin could still be observed between the first and the second year after surgery in the absence of further change in BMI, fat mass, HOMA-IR, leptin, or adiponectin [16]. Consistent with these data, Chakaroun et al. showed that besides an important surgical weight loss (1 year after RYGB) that induced a 25% reduction in chemerin serum concentrations, even a moderate weight loss as a result of a 6-month hypocaloric diet and furthermore even 12 weeks of exercise training before any appreciable changes in body weight induced a decrease of chemerin levels [12]. This reduction was independent of BMI changes and was predicted by reduced hsCRP and improved insulin sensitivity. Taken together, these results suggest that chemerin and inflammation may be associated independently of BMI [12].

Inflammatory cytokines seem to be involved in the upregulation of chemerin [31]. In this respect, Catalán et al. pointed out that elevated chemerin levels did not change one year after RYGB, but TNF- $\alpha$  treatment significantly enhanced the mRNA levels of chemerin in human visceral adipocytes [32]. In line with these results, we might speculate that the lack of significant change of TNF- $\alpha$  together with NOx despite the important decrease of hsCRP might explain the absence of chemerin variations.

Circulating CRP levels have been demonstrated to be significantly decreased at six months after SG [33], and some authors underlined the fact that the change in BMI was correlated with the difference between preoperative and postoperative CRP levels [34, 35]. However, in our group of patients, we did not observe such a correlation. On the other hand, decreased levels of CRP have been demonstrated by other authors to be present even earlier after SG, that is, after

one month, and these values were maintained at 6 months after surgery [15].

As for TNF- $\alpha$  circulating levels, medical data showed that the changes following bariatric surgery remain controversial and should be investigated through randomized trials [3]. We found no significant changes 6 months after restrictive surgery, which is in line with other studies that have demonstrated that reductions in BMI values between 40 kg/m<sup>2</sup> and 30 kg/m<sup>2</sup> slightly affect TNF- $\alpha$  levels in MO [36, 37]. In our group of patients, six months after surgery, the BMI mean value was 34.7 kg/m<sup>2</sup>. However, we did notice a correlation between %EBMIL and changes of TNF- $\alpha$ . Hand in hand with our data, Pardina et al. showed that the expression of TNF- $\alpha$  did not vary with weight loss in the adipose tissue and liver despite the improvement in body weight and in most of the parameters associated with obesity comorbidities (insulin resistance and dyslipidemia), underlining that TNF- $\alpha$  does not reflect the improvement of inflammation during the first year after bariatric surgery [4]. Moreover, another study showed that there was a significant transitory increase of TNF- $\alpha$  levels at 3 months and a trend to increased levels at 6 and 12 months after gastric bypass, explained by the authors by the fact that TNF- $\alpha$  produced in the adipose tissue is not released into the circulation and therefore does not significantly contribute to the circulating TNF- $\alpha$  levels [18]. Furthermore, they underlined that the low levels of vitamin D (commonly noted following gastric bypass) might be another factor contributing to the elevated levels of TNF- $\alpha$  [18]. Last but not least, Pardina et al. explained that although the number of monocytes, the predominant source of TNF- $\alpha$ , decreases with weight loss, there is no correlation between this reduction and the changes in TNF- $\alpha$  [4]. Furthermore, as showed by the same authors, it seems that TNF- $\alpha$  is not involved in the lowering of hsCRP in plasma since it did not appear to be affected by the weight loss [4].

When examined 6 months after SG, besides a significant reduction of BMI and weight, our MO patients underwent no significant changes of nitrooxidative stress markers (NOx, TOS, and TAR). There was, however, a significant decrease of OSI. The levels of NOx as an expression of iNOS activity highly stimulated within the increased number of macrophages, and as an inflammatory marker, were demonstrated elsewhere to be elevated in MO patients [24]. Previously, we showed a slight transitory tendency of NOx to increase and of TAR to decrease 6 months after bariatric surgery but with no significant changes by the first year after the surgical intervention as compared to the baseline. The lack of significant change of nitrooxidative markers observed in our present study (except for OSI) might be explained by the persisting elevated levels of TNF- $\alpha$  6 months after SG. On the other hand, a recent study showed that an improvement of weight and metabolic profile after laparoscopic SG was accompanied in parallel by a progressive recovery of antioxidant enzyme activities and the decline of oxidative byproducts. More precisely, they observed significant changes in antioxidant enzymes and in other markers of oxidative stress with some mean values reaching control levels as early as 3 months postsurgery [38]. We may conclude that there is no unique pattern for the nitrooxidative stress after SG, but it

is worth evaluating it in order to try to reduce it with exogenous antioxidant therapy when necessary.

The main limitation of the present study was that it addressed a small sample of patients. Because of the missing data, the conclusions concerning the changes of the studied parameters must be regarded with precaution. Further studies with a larger number of obese/MO subjects and a longer follow-up time are needed in order to confirm the trend of the repeated measures and correlations between the changes of the studied variables.

In conclusion, we observed that 6-month surgical weight loss through SG was not associated with significant changes of the inflammatory marker chemerin. Furthermore, except for hsCRP and OSI, there were no important variations of other markers of inflammation and oxidative stress.

## Ethical Approval

All procedures involving human participants were in accordance with the ethical standards of the institutional research committee and with the 1964 Helsinki declaration.

## Consent

Informed consent was obtained from all participants included in the study.

## Conflicts of Interest

The authors declare that they have no conflicts of interest.

## Acknowledgments

The first author was supported by the European Social Fund, Human Resources Development Operational Programme 2007-2013, Project no. POSDRU/159/1.5/S/138776, and by the Internal Research Grant no. 27020/39/15.11.2011 of “Iuliu Hațieganu” University of Medicine and Pharmacy Cluj-Napoca, Romania.

## References

- [1] E. Maury and S. M. Brichard, “Adipokine dysregulation, adipose tissue inflammation and metabolic syndrome,” *Molecular and Cellular Endocrinology*, vol. 314, no. 1, pp. 1–16, 2010.
- [2] A. Fernández-Sánchez, E. Madrigal-Santillán, M. Bautista et al., “Inflammation, oxidative stress, and obesity,” *International Journal of Molecular Sciences*, vol. 12, no. 12, pp. 3117–3132, 2011.
- [3] S. R. Rao, “Inflammatory markers and bariatric surgery: a meta-analysis,” *Inflammation Research*, vol. 61, no. 8, pp. 789–807, 2012.
- [4] E. Pardina, R. Ferrer, J. A. Baena-Fustegueras et al., “Only C-reactive protein, but not TNF- $\alpha$  or IL6, reflects the improvement in inflammation after bariatric surgery,” *Obesity Surgery*, vol. 22, no. 1, pp. 131–139, 2012.
- [5] G. M. Hirschfield and M. B. Pepys, “C-reactive protein and cardiovascular disease: new insights from an old molecule,” *QJM: An International Journal of Medicine*, vol. 96, no. 11, pp. 793–807, 2003.
- [6] A. Avogaro and S. V. de Kreutzenberg, “Mechanisms of endothelial dysfunction in obesity,” *Clinica Chimica Acta*, vol. 360, no. 1-2, pp. 9–26, 2005.
- [7] K. Bedard and K. H. Krause, “The NOX family of ROS-generating NADPH oxidases: physiology and pathophysiology,” *Physiological Reviews*, vol. 87, no. 1, pp. 245–313, 2007.
- [8] M. Picklo, K. J. Claycombe, and M. Meydani, “Adipose dysfunction, interaction of reactive oxygen species, and inflammation,” *Advances in Nutrition*, vol. 3, no. 5, pp. 734–735, 2012.
- [9] J. L. Rourke, H. J. Dranse, and C. J. Sinal, “Towards an integrative approach to understanding the role of chemerin in human health and disease,” *Obesity Reviews*, vol. 14, no. 3, pp. 245–262, 2013.
- [10] M. C. Ernst and C. J. Sinal, “Chemerin: at the crossroads of inflammation and obesity,” *Trends in Endocrinology & Metabolism*, vol. 21, no. 11, pp. 660–667, 2010.
- [11] A. A. Roman, S. D. Parlee, and C. J. Sinal, “Chemerin: a potential endocrine link between obesity and type 2 diabetes,” *Endocrine*, vol. 42, no. 2, pp. 243–251, 2012.
- [12] R. Chakaroun, M. Raschpichler, N. Klötting et al., “Effects of weight loss and exercise on chemerin serum concentrations and adipose tissue expression in human obesity,” *Metabolism - Clinical and Experimental*, vol. 61, no. 5, pp. 706–714, 2012.
- [13] B. Wölnerhanssen and R. Peterli, “State of the art: sleeve gastrectomy,” *Digestive Surgery*, vol. 31, no. 1, pp. 40–47, 2014.
- [14] D. Eisenberg, A. Bellatorre, and N. Bellatorre, “Sleeve gastrectomy as a stand-alone bariatric operation for severe, morbid, and super obesity,” *Journal of the Society of Laparoendoscopic Surgeons*, vol. 17, no. 1, pp. 63–67, 2013.
- [15] A. Mallipedhi, S. L. Prior, J. D. Barry, S. Caplin, J. N. Baxter, and J. W. Stephens, “Changes in inflammatory markers after sleeve gastrectomy in patients with impaired glucose homeostasis and type 2 diabetes,” *Surgery for Obesity and Related Diseases*, vol. 10, no. 6, pp. 1123–1128, 2014.
- [16] H. Sell, A. Divoux, C. Poitou et al., “Chemerin correlates with markers for fatty liver in morbidly obese patients and strongly decreases after weight loss induced by bariatric surgery,” *The Journal of Clinical Endocrinology & Metabolism*, vol. 95, no. 6, pp. 2892–2896, 2010.
- [17] X. Terra, T. Auguet, E. Guiu-Jurado et al., “Long-term changes in leptin, chemerin and ghrelin levels following different bariatric surgery procedures: Roux-en-Y gastric bypass and sleeve gastrectomy,” *Obesity Surgery*, vol. 23, no. 11, pp. 1790–1798, 2013.
- [18] F. Illán-Gómez, M. González-Ortega, I. Orea-Soler et al., “Obesity and inflammation: change in adiponectin, C-reactive protein, tumour necrosis factor- $\alpha$  and interleukin-6 after bariatric surgery,” *Obesity Surgery*, vol. 22, no. 6, pp. 950–955, 2012.
- [19] W. T. Friedewald, R. I. Levy, and D. S. Fredrickson, “Estimation of the concentration of low-density lipoprotein cholesterol in plasma, without use of the preparative ultracentrifuge,” *Clinical Chemistry*, vol. 18, no. 6, pp. 499–502, 1972.
- [20] S. A. Brethauer, J. Kim, M. el Chaar et al., “Standardized outcomes reporting in metabolic and bariatric surgery,” *Surgery for Obesity and Related Diseases*, vol. 11, no. 3, pp. 489–506, 2015.
- [21] D. R. Matthews, J. P. Hosker, A. S. Rudenski, B. A. Naylor, D. F. Treacher, and R. C. Turner, “Homeostasis model assessment: insulin resistance and  $\beta$ -cell function from fasting

- plasma glucose and insulin concentrations in man," *Diabetologia*, vol. 28, no. 7, pp. 412–419, 1985.
- [22] A. Ghasemi, M. Hedayati, and H. Biabani, "Protein precipitation methods evaluated for determination of serum nitric oxide end products by the Griess assay," *Journal of Medical Science Research*, vol. 2, pp. 29–32, 2007.
  - [23] K. M. Miranda, M. G. Espey, and D. A. Wink, "A rapid, simple spectrophotometric method for simultaneous detection of nitrate and nitrite," *Nitric Oxide*, vol. 5, no. 1, pp. 62–71, 2001.
  - [24] A. F. Cătoi, A. Pârvu, R. F. Galea, I. D. Pop, A. Mureșan, and C. Cătoi, "Nitric oxide, oxidant status and antioxidant response in morbidly obese patients: the impact of 1-year surgical weight loss," *Obesity Surgery*, vol. 23, no. 11, pp. 1858–1863, 2013.
  - [25] O. Erel, "A new automated colorimetric method for measuring total oxidant status," *Clinical Biochemistry*, vol. 38, no. 12, pp. 1103–1111, 2005.
  - [26] O. Erel, "A novel automated method to measure total antioxidant response against potent free radical reactions," *Clinical Biochemistry*, vol. 37, no. 2, pp. 112–119, 2004.
  - [27] M. Harma, M. Harma, and O. Erel, "Increased oxidative stress in patients with hydatidiform mole," *Swiss Medical Weekly*, vol. 133, no. 41–42, pp. 563–566, 2003.
  - [28] A. F. Cătoi, Ș. Suciu, A. E. Pârvu et al., "Increased chemerin and decreased omentin-1 levels in morbidly obese patients are correlated with insulin resistance, oxidative stress and chronic inflammation," *Clujul Medical*, vol. 87, no. 1, pp. 19–26, 2014.
  - [29] K. Bozaoglu, K. Bolton, J. McMillan et al., "Chemerin is a novel adipokine associated with obesity and metabolic syndrome," *Endocrinology*, vol. 148, no. 10, pp. 4687–4694, 2007.
  - [30] S. S. Fatima, K. Bozaoglu, R. Rehman, F. Alam, and A. S. Memon, "Elevated chemerin levels in Pakistani men: an interrelation with metabolic syndrome phenotypes," *PLoS One*, vol. 8, no. 2, article e57113, 2013.
  - [31] S. Kralisch, S. Weise, G. Sommer et al., "Interleukin-1 $\beta$  induces the novel adipokine chemerin in adipocytes in vitro," *Regulatory Peptides*, vol. 154, no. 1–3, pp. 102–106, 2009.
  - [32] V. Catalán, J. Gómez-Ambrosi, A. Rodríguez et al., "Increased levels of chemerin and its receptor, chemokine-like receptor-1, in obesity are related to inflammation: tumor necrosis factor- $\alpha$  stimulates mRNA levels of chemerin in visceral adipocytes from obese patients," *Surgery for Obesity and Related Diseases*, vol. 9, no. 2, pp. 306–314, 2013.
  - [33] H. Shimizu, F. Hatao, K. Imamura, K. Takanishi, and M. Tsujino, "Early effects of sleeve gastrectomy on obesity-related cytokines and bile acid metabolism in morbidly obese Japanese patients," *Obesity Surgery*, vol. 27, no. 12, pp. 3223–3229, 2017.
  - [34] V. Gumbau, M. Bruna, E. Canelles et al., "A prospective study on inflammatory parameters in obese patients after sleeve gastrectomy," *Obesity Surgery*, vol. 24, no. 6, pp. 903–908, 2014.
  - [35] H. A. Hakeam, P. J. O'Regan, A. M. Salem, F. Y. Bamehriz, and L. F. Jomaa, "Inhibition of C-reactive protein in morbidly obese patients after laparoscopic sleeve gastrectomy," *Obesity Surgery*, vol. 19, no. 4, pp. 456–460, 2009.
  - [36] G. D. Miller, B. J. Nicklas, and A. Fernandez, "Serial changes in inflammatory biomarkers after Roux-en-Y gastric bypass surgery," *Surgery for Obesity and Related Diseases*, vol. 7, no. 5, pp. 618–624, 2011.
  - [37] M. Laimer, C. F. Ebenbichler, S. Kaser et al., "Markers of chronic inflammation and obesity: a prospective study on the reversibility of this association in middle-aged women undergoing weight loss by surgical intervention," *International Journal of Obesity*, vol. 26, no. 5, pp. 659–662, 2002.
  - [38] L. Monzo-Beltran, A. Vazquez-Tarragón, C. Cerdà et al., "One-year follow-up of clinical, metabolic and oxidative stress profile of morbid obese patients after laparoscopic sleeve gastrectomy. 8-oxo-dG as a clinical marker," *Redox Biology*, vol. 12, pp. 389–402, 2017.



## Research Article

# Polyphenolic Compounds, Antioxidant, and Cardioprotective Effects of Pomace Extracts from Fetească Neagră Cultivar

Ștefania Silvia Balea,<sup>1</sup> Alina Elena Pârvu ,<sup>2</sup> Nastasia Pop,<sup>1</sup> Fernando Zamora Marín,<sup>3</sup> and Marcel Pârvu<sup>4</sup>

<sup>1</sup>Department of Horticulture and Landscaping, Faculty of Horticulture, University of Agricultural Sciences and Veterinary Medicine, No. 3-5 Calea Mănăștur Street, Cluj-Napoca 400372, Romania

<sup>2</sup>Department of Pathophysiology, Faculty of Medicine, “Iuliu Hatieganu” University of Medicine and Pharmacy, No. 4-6 Victor Babeș Street, Cluj-Napoca 400012, Romania

<sup>3</sup>Department of Biochemistry and Biotechnology, Faculty of Oenology, Rovira i Virgili University, C/Marcel·li Domingo s/n Street, Tarragona 43007, Spain

<sup>4</sup>Department of Biology, Faculty of Biology and Geology, Babes-Bolyai University, No. 42 Republicii Street, Cluj-Napoca 400015, Romania

Correspondence should be addressed to Alina Elena Pârvu; [parvualinaelena@umfcluj.ro](mailto:parvualinaelena@umfcluj.ro)

Received 6 December 2017; Accepted 31 January 2018; Published 22 March 2018

Academic Editor: Ada Popolo

Copyright © 2018 Ștefania Silvia Balea et al. This is an open access article distributed under the Creative Commons Attribution License, which permits unrestricted use, distribution, and reproduction in any medium, provided the original work is properly cited.

Grape pomace is a potential source of natural antioxidant agents. Phenolic compounds and antioxidant and cardioprotective properties of fresh and fermented pomace extracts obtained from *Vitis vinifera* L. red variety Fetească neagră grown in Romania in 2015 were investigated. Grape pomace extracts total phenolic index, total tannins, total anthocyanins, proanthocyanidins, flavan-3-ol monomers, stilbenes, and DPPH free radical scavenger were measured. The effect of a seven-day pretreatment with grape pomace extracts on the isoprenaline-induced infarct-like lesion in rats was assessed by ECG monitoring, serum levels of creatine kinase, aspartate transaminase, and alanine transaminase. Total serum oxidative status, total antioxidant response, oxidative stress index, malondialdehyde, total thiols, and nitric oxide have been also assessed. Higher phenolic content and antioxidant activity were found in fermented pomace extracts when compared to fresh pomace extracts. Pretreatment with grape pomace extracts significantly improved cardiac and oxidative stress parameters. In conclusion, Fetească neagră pomace extracts had a good *in vitro* antioxidant activity due to an important phenolic content. *In vivo*, the extracts had cardioprotective effects against isoprenaline-induced infarct-like lesion by reducing oxidative stress, fresh pomace extracts having a better effect.

## 1. Introduction

Cardiovascular diseases are the first cause of death worldwide. The role of oxidative stress in the pathophysiology of cardiovascular diseases is well documented [1]. Moreover, in cardiovascular pathophysiology, oxidative stress became a promising disease biomarker [1] and an important therapeutic target [2].

Oxidative stress is defined as a misbalance between the oxidants and antioxidants in favour of oxidants that promote

damage on biological molecules like lipids, proteins, and DNA. Reactive oxygen species (ROS) and nitrogen reactive species (RNS) have been suggested to increase oxidative stress and to cause diseases such as heart attack, stroke, neurodegenerative diseases, diabetes, and cancer [3]. ROS include the superoxide anion ( $O_2^-$ ),  $H_2O_2$ , and the hydroxyl radical. Initially, they cause mitochondrial depolarization and then activate a positive feedback loop of ROS-induced ROS release [4]. RNS include NO and peroxynitrite ( $ONOO^-$ ), the coupling product of  $O_2^-$  with transient excessive NO. Many

studies pointed to the role of peroxynitrite in many cardiovascular diseases by inducing oxidative, nitrative, and nitro-stress [5].

The failure of antioxidant therapy in human diseases was called the antioxidant paradox, and several explanations have been proposed [6]. One explanation was that oxidative stress was not the cause of specific human diseases but a consequence thereof, another theory was that antioxidants had no tissue- or cell-specific effect, and a third explanation was the lack of an appropriate method to measure oxidative stress. The latest opinion is that antioxidants do not simultaneously inhibit both oxidative stress and inflammation [3].

Many natural products proved to have antioxidant and cardioprotective properties [7] by reducing inflammation and oxidative and nitrative stress [3]. The low incidence of cardiovascular diseases in southern France despite a diet rich in saturated fat, known as the “French Paradox,” was attributed to the antioxidant effect of the regular red wine drinking [8].

A recent point of interest in the winemaking industry is waste management [9]. About 80% of the worldwide grape production is used in winemaking industry. During the winemaking process, after alcoholic fermentation, about 25% of the processed grape weight remains as organic solid waste, the grape pomace (GP). It consists mainly of skin residues, broken cells with pulp remains, stalks and seeds. Large quantities of GP are produced annually, and it is used mainly for animal food, organic fertilizers, and ethanol production [10]. In Romania, GP is disposed as a waste. Grapes, GP, and wines from red varieties of *Vitis vinifera* L. are important sources of natural antioxidants, because of their high concentration of different phenolic compounds [11]. About 70% of the phenolic compounds were reported to remain in the pomace [12]. The majority of grape polyphenols come from the skin and seeds. They comprise two main classes: flavonoids (anthocyanins, flavonols, flavan-3-ols, flavones, and chalcones) and nonflavonoids (phenolic acids, stilbenes, tannins, coumarins, and neolignans) [10].

Moreover, in the case of the polyphenolic compounds, it has been found that they have antioxidant properties but they may also act as prooxidants because they may induce free radical production [13]. Another opinion is that the prooxidant effect of grape pomace extract might be beneficial because it triggers the preconditioning mechanisms [14].

Considering all these previous findings, in this paper, we present the results of performing a phytochemical analysis and investigation of the antioxidant and cardioprotective effects of GP obtained from *Vitis vinifera* L. red variety Fetească neagră (FN) grown in Romania. To the best of our knowledge, there is no research published on the antioxidant and cardioprotective effects of Fetească neagră GP.

## 2. Materials and Methods

**2.1. Chemicals and Reagents.** All solvents were of HPLC quality, and all chemicals were of analytical grade (>99%). Methanol, ethanol (96.5%), deionised water, acetonitrile, formic acid, absolute ethanol, and hydrochloric acid (37%) were purchased from Panreac (Barcelona, Spain). The commercial

standards transresveratrol, transpiceid, and (–)-epicatechin were bought from Phytolab (Vestenbergsgreuth, Germany) and Extrasynthese (Genay, France), respectively. The trans-isomers of resveratrol and piceid (resveratrol-3-glucoside) were transformed into their respective cis isomers by UV irradiation (366 nm light for 5 min in quartz vials) of 25% MeOH solutions of the trans-isomers. Trolox (6-hydroxy-2,5,7,8-tetramethylchroman-2-carboxylic acid), N-(1-Naphthyl)ethylenediamine dihydrochloride (NEDD), xylenol orange [o-cresosulfonphthalein-3,3-bis (sodium methyliminodiacetate)], ortho dianisidine, vanadium (III) chloride (VCl<sub>3</sub>), hydrogen peroxide (H<sub>2</sub>O<sub>2</sub>), methanol, diethyl ether sulphanilamide (SULF) and ferrous ammonium sulphate, thiobarbituric acid, trichloroacetic acid (TCA), ethylenediaminetetraacetic acid, sodium dodecylsulphate, butylated hydroxytoluene, 1,1,3,3-tetraethoxypropane, 5,5'-dithiobis (2-nitrobenzoic acid) (DTNB), and glutathione (GSH) were purchased from Sigma-Aldrich (Germany) and Merck (Germany). All chemicals were of analysis grade.

**2.2. Grape Sample.** The grape *Vitis vinifera* (L.) var. Fetească neagră (clone 762, *Vitis* L., port graft: S.O.4, Austria) planted in 2006, from Mureş county, Mica parish, part of Târnavelor Plateau (46°21'44.5"N and 24°23'55.7"E; 330–350 m above sea level), was used in our studies. Grapes were harvested manually at full maturity level, during the 2015 vintage. The GP samples were collected in two winemaking stages: one was supplied immediately after pressing the grapes, the fresh unfermented GP (FNFs), and the other was supplied after 20 days of fermentation at 20°C and must separation, the fermented GP (FNFr). The samples were stored in vacuum bags at –22°C prior to the analysis and were used in the experiments.

**2.3. Sample Preparation for Phytochemical Analysis.** The GP was submitted to the freeze-drying process and then ground with a domestic blender (Sinbo, model number SCM 2923). The extracts were prepared by adding 50 mL of ethanol 50% and 1 mL of metabisulphite (MBS) 5.25% to 5 g of GP sample. All extracts were placed in a water bath at 50°C for 7 days and stirred daily. Prior to each analysis, the extracts were centrifuged and the supernatants were further used. All samples were processed in 3 repetitions.

**2.4. Total Phenolic Index, Total Tannins, and Total Anthocyanin Determination.** The total phenolic index (TPI) was determined by measuring 280 nm absorbance of a 1:200 dilution of GP extracts [15]. The condensed tannin concentration (TC) was estimated by precipitation with methyl cellulose [16]. The absorbance was read at 280 nm, and TC was calculated as the difference between the total polyphenols and the quantity of tannins precipitated by methyl cellulose. Aqueous (–)-epicatechin solutions were used to establish a standard curve, and TPI and TC were expressed as epicatechin mg/g d.w. The total anthocyanin content (TAC) was determined spectrophotometrically using the method described by [17]. The absorbance was read at 520 nm. A standard curve was made using malvidin-3-O-

glucoside chloride, and results were expressed as malvidin-3-O-glucoside mg/g d.w. Spectrophotometric measurements for TPI, TT, and TAC were performed with a Helios Alpha UV-Vis spectrophotometer, Thermo Fisher Scientific Inc., Waltham, MA, USA.

**2.5. HPLC-DAD Determination of Proanthocyanidins and Flavan-3-ol Monomers.** The proanthocyanidins of the GP were extracted and analyzed by acid depolymerization in the presence of an excess of phloroglucinol [18]. The products of the reaction were separated by RP-HPLC-DAD. The proanthocyanidins were analyzed with an Agilent 1200 Series HPLC equipped with a G1362A refractive index detector (RID), a G1315D DAD, a G1311A quaternary pump, a G1316A column oven, and a G1329A autosampler (Agilent Technologies, Santa Clara, CA, USA). The chromatographic system was managed by an Agilent Chem Station (version B.01.03) data processing station. The number of terminal subunits was considered to be the difference between the total monomers measured in normal conditions (with phloroglucinol) and thus obtained when the analysis was performed without phloroglucinol addition. The number of extension subunits was considered as the addition of all the phloroglucinol adducts. Because acid catalysis with phloroglucinol is not completely efficient, the real yield of the reaction was measured using a pure B2 proanthocyanidin dimer [(-)-epicatechin-(4 → 8)-(-)-epicatechin]. This output was used to calculate the total proanthocyanidin concentration from extracts. The mean degree of polymerization (mDP) was calculated by adding terminal and extension subunits (in moles) and dividing by the terminal subunits. The percentage of prodelphinidins (PD%) was computed by dividing the total (-)-epigallocatechin units by the total monomeric units and converting the result to a %. Similarly, the percentage of galloylation (G%) was computed by dividing the total (-)-epicatechin-3-gallate units by the total monomeric units and converting the result to a %. In order to quantify the flavan-3-ol monomers, (+)-catechin, (-)-epicatechin, and (-)-epicatechin-3-O-gallate in GP, the assay was also carried out without the addition of phloroglucinol and the retention times were compared with those of pure compounds. All analyses were performed in three repetitions.

**2.6. HPLC-DAD-ESI-MS/MS Determination of Stilbenes.** HPLC identification of GP stilbenes was performed using an Agilent 1200 series system equipped with DAD (Agilent, Germany) and coupled to an AB Sciex 3200 Q TRAP (Applied Biosystems) electrospray ionization mass spectrometry system (ESI-MS/MS) [19]. The chromatographic conditions used were conditions that had been previously reported [20]. The chromatographic system was managed by an Agilent Chem Station (version B.01.03) data process in G station. The mass spectral data was processed with the Analyst MDS software (Applied Bio-systems, version 1.5) [21].

**2.7. DPPH Radical Scavenging Activity.** The antioxidant capacities of the GP samples were measured in terms of their radical scavenging activity (RSA), using the DPPH method

[22, 23]. Briefly, a 3 ml aliquot of the extract solution was added to 1 mL of methanol solution of DPPH 0.1 mM. The mixture was then homogenized and kept in the dark at room temperature for 30 min prior to analysis. The absorbance was measured at 517 nm against a blank. The following equation was used to determine the percentage of the radical scavenging activity of each extract:  $RSA (\%) = [1 - (A_{\text{sample}} - A_{\text{blank}}) / A_{\text{control}}] \times 100$ , where  $A_{\text{control}}$  is the absorbance of DPPH radical + methanol,  $A_{\text{sample}}$  is the absorbance of DPPH radical + sample, and  $A_{\text{blank}}$  is the absorbance of methanol + sample. The  $IC_{50}$  (half maximal inhibitory concentration) was calculated graphically, using a calibration curve, in the linear range by plotting the extract concentration versus the corresponding scavenging effect (RSA%), over 30 min. Trolox was used as a positive antioxidant control. The percentage of DPPH consumption was converted to trolox equivalents (TE) using a calibration curve ( $R^2 = 0.985$ ) of Trolox standard solutions (0.5–5  $\mu\text{g/mL}$ ). An  $IC_{50} < 50 \mu\text{g TE/mL}$  is a very good antioxidant activity; an  $IC_{50}$  of 50–100  $\mu\text{g TE/mL}$  is a good antioxidant activity; an  $IC_{50}$  of 100–200  $\mu\text{g TE/mL}$  is a weak antioxidant activity; an  $IC_{50} > 200 \mu\text{g TE/mL}$  means no antioxidant activity. Assay was performed in triplicate.

**2.8. Plant Extract Preparation for In Vivo Study.** Fetească neagră fresh GP extract (FNFs) and Fetească neagră-fermented GP extract (FNFr) were obtained with 70% ethanol (Merck, Bucuresti, Romania) by a modified Squibb repercolation method (1/1 g/ml) [24].

**2.9. Animals.** The experiments were carried out on male albino Wistar rats, weighing 200–250 g, that were bred in the Animal Facility of the Iuliu Hațieganu University of Medicine and Pharmacy. The animals were housed in standard polypropylene cages (five per cage) under controlled conditions (12 h light/dark cycle, at an average temperature of 21–22°C) and with ad libitum access to standard pellet diet (Cantacuzino Institute, Bucharest, Romania) and water.

Experimental protocols have been approved by the Ethics Committee (nr. 26/16.12.2015) of the Faculty of Veterinary Medicine, University of Agricultural Sciences and Veterinary Medicine from Cluj-Napoca and the Ethics Committee of the Iuliu Hațieganu University of Medicine and Pharmacy. The experiments were performed in triplicate. All experimental groups began with 3 days of acclimatization to the housing facility, and animals were used only once. At the end of the experiments under anaesthesia using a combination of ketamine (60 mg/kg bw) and xylazine (15 mg/kg bw) [25], blood was withdrawn by retroorbital puncture, serum was separated and stored at –80°C until use, and then animals were killed by cervical dislocation.

**2.10. Experimental Myocardial Ischemia.** The animals were divided into 4 groups ( $n = 5$ ). The negative control group (CONTROL) and the isoprenaline-induced (ISO) myocardial infarction group received 0.9% saline (1 mL/day p.o.) for 7 days. In FNFs and FNFr groups, each extract was administered orally by gavage (1 mL/day p.o.) for 7 days. In day 8 and day 9, rats were injected with ISO dissolved in

normal saline (150 mg/kg, s.c.) at an interval of 24 h to induce experimental MI [26], excepting CONTROL animals. ECG was recorded in days one, 7, and 10. In day 10, after ECG registration, blood samples were collected for estimation of cardiac markers and oxidative stress markers.

**2.11. Electrocardiography.** The overnight-fasted rats were anaesthetized with ketamine (80 mg/kg, i.p.) and xylazine (8 mg/kg, i.p.). At 15 min after anesthesia, animals were placed in the supine position on a board, electrodes were bound on the paw pads of each rat, and ECG was recorded from the limb lead at position II (right forelimb to left hind limb) with a Biopac MP150 system. The ECG apparatus was calibrated at 1 mV/1 cm with a speed of 50 mm/s.

Analysis of ECG waves was done to calculate heart rate (beats/min), RR intervals (msec), QT interval (msec), and ST segment changes (mV). QT interval was measured from the beginning of QRS complex to the end of T wave, and it was calculated in msec. Corrected QT interval (QTc), which is used to rectify the influence of the heart rate on QT interval, according to Bazett formula, is equal to QT interval divided by the square root of RR interval and was also calculated [27].

**2.12. Cardiac Marker Enzymes.** The creatine kinase-MB (CK-MB), aspartate transaminase (AST), and alanine transaminase (ALT) activities were measured by using commercial kits.

**2.13. In Vivo Antioxidant Effect Evaluation.** The total oxidative status (TOS) of the serum was measured using a colorimetric assay [28]. Assay measurements were standardized using hydrogen peroxide ( $\text{H}_2\text{O}_2$ ) as the oxidative species, and the assay results are expressed in  $\mu\text{mol H}_2\text{O}_2$  equiv/L.

The total antioxidant response (TAR) was measured in serum using a colorimetric assay [29]. This assay is calibrated using trolox, and results are expressed as mmol trolox equiv/L.

The ratio of the TOS to the TAR represents the oxidative stress index (OSI), an indicator of the degree of oxidative stress:  $\text{OSI (arbitrary unit)} = \text{TOS (mol H}_2\text{O}_2 \text{ equiv/L)}/\text{TAR (mmol trolox equiv/L)}$  [30].

Malondialdehyde (MDA) was assessed as a lipid peroxidation marker, using thiobarbituric acid, as previously described [31]. The absorbance of the supernatant was measured at 532 nm. A standard curve was generated with a 1,1,3,3-tetraethoxypropane standard (0.3–10 nmol/mL). Serum MDA concentration was expressed as nmol/mL of serum.

Total thiols (SH) were estimated using Ellman's reagent [32]. Supernatant absorbance was measured at 412 nm. To create a standard curve, solutions of glutathione (GSH) concentration, ranging from 0.25 to 2 mM GSH, were used. Serum SH concentration was expressed as mmol GSH/mL.

The Griess reaction was used to indirectly determine NO synthesis (NOx). First serum proteins were removed by extraction with a 3:1 (v:v) solution of methanol/diethyl ether [33]. The sample absorbance was read at 540 nm. The

concentration of serum NOx was determined using a sodium nitrite-based curve and expressed as nitrite  $\mu\text{mol/L}$  [34].

All serum spectrophotometric measurements were performed using a Jasco V-530 UV-Vis spectrophotometer (Jasco International Co. Ltd., Tokyo, Japan).

**2.14. Statistical Analyses.** Results were expressed as means and standard deviations and were analyzed statistically using the SPSS (version 20) software. Data were compared by one-way ANOVA and post hoc Bonferroni-Holm test. Pearson's correlation coefficient ( $r$ ) was used to evaluate relationships between parameters of the same group. The level of significance was set at  $p < 0.05$ .

### 3. Results

**3.1. Total Phenolic Index, Total Tannins, and Total Anthocyanin Content.** The TPI, TAC, and TC obtained from Fetească neagră GP are shown in Table 1. In the present study, FNFr pomace had significantly higher polyphenol extraction ( $161.58 \pm 3.42$  mg catechin equivalent/g d.w.) than FNFs ( $114.71 \pm 15.86$  mg catechin equivalent/g d.w.) ( $p < 0.05$ ). TC in GP ranged from  $63.15 \pm 7.12$  mg epicatechin/g d.w. in FNFs to  $113.98 \pm 4.39$  mg epicatechin/g d.w. in FNFr, the difference being very significant ( $p < 0.001$ ). Higher TAC was found in FNFs ( $184.84 \pm 17.13$  mg malvidin-3-O-glucoside/g d.w.) than in FNFr ( $47.67 \pm 5.0$  mg malvidin-3-O-glucoside/g d.w.). Between TAC of FNFs and FNFr, the difference was highly significant ( $p < 0.001$ ).

**3.2. HPLC-DAD Determination of Proanthocyanidins and Flavan-3-ol Monomers.** The results of analyzing GP proanthocyanidins obtained by acid depolymerization in the presence of excess phloroglucinol are shown in Table 2. The total proanthocyanidin concentration is higher in FNFr than in FNFs ( $p < 0.05$ ). As shown in Table 1, the mDP of FNFr and FNFs were not significantly different ( $p > 0.05$ ), PD% in FNFs was significantly bigger than that in FNFr ( $p < 0.01$ ), and G% in FNFr was higher than that in FNFs but not significant ( $p > 0.05$ ).

The flavan-3-ol monomeric compositions from the whole Fetească neagră GP were described in a detailed form in Table 1. With respect to the total flavan-3-ol monomer concentration, we found that it was higher in the FNFr sample than in the FNFs sample ( $p < 0.01$ ). The analysis of individual flavan-3-ol monomers showed that the difference in total monomers concentrations was due to the higher content of (+)-catechin and (–)-epicatechin in the FNFr samples ( $p < 0.01$ ). The epicatechin-3-O-gallate concentration was not significantly different between the FNFr and FNFs samples ( $p > 0.05$ ).

**3.3. HPLC-DAD-ESI-MS/MS Determination of Stilbenes.** The transresveratrol was in a higher amount in the FNFs ( $p < 0.01$ ) than in the FNFr and cis-resveratrol in a higher amount in the FNFr ( $p < 0.01$ ) than in the FNFs. In both FNFs and FNFr samples, the concentration of cis-resveratrol was higher than the concentration of transresveratrol. Piceid was the most abundant stilbenes in GP from both FNFs and FNFr, and both isomers cis- and transpiceid were in



TABLE 1: Phytochemical analysis of grape pomace from cv. Fetească neagră 2015.

GP	TPI (mg catechin equivalent/g d.w.)	TC (mg epicatechin/g d.w.)	TAC (malvidin-3-O-glucoside mg/g d.w.)
FNFs	114.71 ± 15.86	63.15 ± 7.12	184.84 ± 17.13***
FNFr	161.58 ± 3.42**	113.98 ± 4.39***	47.67 ± 5.0
	Proanthocyanidins (mg/g d.w.)	mDP	PD%
FNFs	25.57 ± 3.82	6.29 ± 0.16 <sup>n.s.</sup>	8.18 ± 0.49**
FNFr	28.71 ± 9.78*	5.64 ± 1.33	3.91 ± 1.12
	∑ flavan-3-ol monomers (mg/g d.w.)	(+)-catechin (mg/g d.w.)	(-)-epicatechin (mg/g d.w.)
FNFs	2.05 ± 0.21	1.12 ± 0.10	0.87 ± 0.09
FNFr	4.71 ± 0.17**	2.59 ± 0.01**	2.05 ± 0.16**
	Transresveratrol (μg/g d.w.)	cis-resveratrol (μg/g d.w.)	Transpiceid (μg/g d.w.)
FNFs	3.22 ± 1.91**	5.03 ± 1.09	53.54 ± 10.53**
FNFr	0.58 ± 1.01	12.27 ± 3.07**	14.31 ± 2.25
			cis-Piceid (μg/g d.w.)
FNFs			33.04 ± 8.14**
FNFr			7.67 ± 1.99

Values are expressed as average ± standard deviation ( $n = 3$ ) <sup>n.s.</sup>  $p > 0.05$ , \*  $p < 0.05$ , \*\*  $p < 0.01$ , and \*\*\*  $p < 0.001$ . GP: grape pomace; Fs: fresh; Fr: fermented; FN: Fetească neagră; TPI: total phenolic index; TC: tannins concentration; TAC: total anthocyanin content; mDP: mean degree of polymerization; PD: prodelphinidins; G%: galloylation.

TABLE 2: RR interval, QT interval, QTc, heart rate, and ST segment of rats, day 10 ECG.

	RR (ms)	QT (ms)	QTc (ms)	HR (bpm)	ST (mV)
CONTROL	238 ± 22.80	80 ± 14.14	198 ± 36.33	213.31 ± 22.18	00
ISO	256* ± 21.90	136** ± 16.73	274** ± 43.35	195.71 <sup>n.s.</sup> ± 19.55	0.64** ± 0.01
FNFs	224# ± 21.90	120# ± 14.14	254* ± 19.49	269.79# ± 24.80	0.12## ± 0.01
FNFr	228# ± 22.80	136 <sup>n.s.</sup> ± 35.77	268 <sup>n.s.</sup> ± 45.11	265.24# ± 26.17	0.11## ± 0.01

Values are expressed as mean ± SEM,  $n = 6$ . \*  $p < 0.05$ , \*\*  $p < 0.01$  versus control group; #  $p < 0.05$ , ##  $p < 0.01$  versus ISO group. GP: grape pomace; Fs: fresh; Fr: fermented; FN: Fetească neagră; ISO: isoprenaline; QTc: corrected QT interval; HR: heart rate.

a greater quantity in the FNFs samples as compared to the FNFr samples ( $p < 0.001$ ) (Table 1).

**3.4. Radical Scavenging Activity toward DPPH.** The ethanol extracts of FNFs and FNFr showed very good RSA by having an increased absorbance with increased concentration at 517 nm (Figure 1). Compared to trolox ( $IC_{50} = 11.18 \mu\text{g/ml}$ ), FNFr ( $IC_{50} = 9.95 \mu\text{g TE/ml}$ ) exhibits a better antioxidant activity than FNFs ( $IC_{50} = 36.99 \mu\text{g TE/ml}$ ), and there was a statistically significant difference between these extracts ( $p < 0.001$ ). For FNFs, DPPH test results exhibited significant, positive correlations with TC, TAC, flavan-3-ol monomers, and stilbene results ( $r = 0.80-0.99$ ). The FNFr DPPH test correlated with proanthocyanidins, PD, mDP, and cis-stilbenes ( $r = 0.76-0.90$ ).

**3.5. Effect of Fetească Neagră Grape Pomace Extracts on ECG Parameters.** ECG recording from days one and 7 had no significant changes in all groups. The ECG patterns of normal and experimental group rats in day 10 are shown in Figure 2 and Table 2. Isoprenaline injection was seen to induce significant alterations in ECG patterns such as decreased heart rate, increased RR, QT and QTc intervals,

and ST segment depression coupled with marked T wave inversion that reflect isoprenaline-induced infarct-like lesion. Pretreatment with FNFs produced protective effects on ECG by reducing RR, QT, and QTc increase, by increasing the HR and reducing ST depression as compared to ISO-treated group (Table 2). Pretreatment with FNFr reduced just RR interval, increased the HR, and reduced ST depression as compared to ISO-treated group.

**3.6. Effect of Fetească Neagră Grape Pomace Extracts on Cardiac Marker Enzymes.** The cardioprotective effects of Fetească neagră GP extracts revealed by the serum cardiac marker enzyme AST, ALT, and CK-MB levels are summarized in Table 3. Serum levels of cardiac marker enzymes, AST, ALT, and CK-MB, increased significantly in ISO-treated rats ( $p < 0.001$ ). FNFs and FNFr extract pretreatment produced protective effects by reducing significantly AST, ALT, and CK-MB levels. On AST, FNFs effect ( $p < 0.01$ ) was better than that of FNFr ( $p < 0.05$ ). ALT was significantly reduced by both pretreatments, FNFs and FNFr ( $p < 0.01$ ), and the results were almost similar. FNFr lowered CK-MB more than FNFs did ( $p < 0.001$ ). The cardioprotective effects

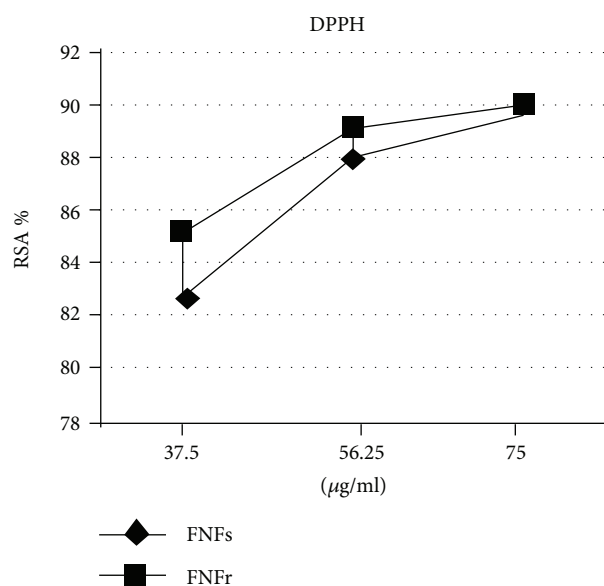


FIGURE 1: Fetească neagră grape pomace radical scavenging activity toward DPPH. Fs: fresh, Fr: fermented, FN: Fetească neagră, RSA: radical scavenging activity.

of FNFs and FNFr on cardiac enzymes were correlated with ST segment changes.

**3.7. In Vivo Antioxidant Effect of Fetească Neagră Grape Pomace Extracts.** Oxidative stress tests are summarized in Table 4. Significant increases in serum OSI ( $p < 0.001$ ) and TOS ( $p < 0.001$ ) with concomitant decrease in TAR ( $p < 0.01$ ) were seen in the ISO-induced MI rats. In contrast, individual preadministration of FNFs and FNFr resulted in a significant decrease in the levels of TOS ( $p < 0.001$ ) and OSI ( $p < 0.001$ ) as well as significant increases in TAR ( $p < 0.01$ ). However, when FNFs and FNFr groups were compared to each other, the ANOVA analysis revealed that the decrease in TOS and OSI levels and the increase in TAR were not significantly different. Furthermore, OSI, TOS, and TAR changes were correlated. ISO-induced ischemia was associated with a significant elevation of MDA ( $p < 0.01$ ), and FNFs and FNFr pretreatments reduced MDA production ( $p < 0.05$ ). FNFs and FNFr were equally efficient on MDA ( $p > 0.05$ ). SH was reduced by the ISO-induced ischemia ( $p < 0.001$ ), and pretreatment with FNFs and FNFr extracts had no important effect on SH ( $p > 0.05$ ). Serum NOx was significantly elevated in the ISO group ( $p < 0.001$ ) as compared to the control rats. Pretreatment with FNFs and FNFr extracts induced no significant reduction of nitric oxide production ( $p > 0.05$ ). There was no significant statistical difference between FNFs and FNFr extracts in terms of NOx production ( $p > 0.05$ ).

## 4. Discussion

In the present study, polyphenolic composition and antioxidant and cardioprotector effects of fresh and fermented FN GP were analysed. The FNFs and FNFr demonstrated to be

rich sources of phenolic compounds. It is already known that phenolic compounds represent one of the largest and important groups of natural plant products, having physiological properties such as antiallergenic, anti-inflammatory, antimicrobial, antioxidant, antithrombotic, cardioprotective, and vasodilatory effects [35]. There is a growing consensus that a combination of antioxidants, rather than single entities, may be more effective over the long term [36].

As in other studies, FNFs and FNFr phenolic contents were high [37]. The differences between GP phenolic contents are related to the grape variety, grape ripeness, environmental factors, and technological procedures used during winemaking. In wine, the total phenolic content was higher when the maceration time was longer [10]. In our samples, the higher TPI in the fermented compared to the fresh FN GP may be attributed to the maceration process.

Tannins are localized mainly in the skin and seeds of grapes. Tannin content in FN GP followed the same trend as TPI, FNFr having a higher tannin yield than FNFs. These results were in accordance with reports that found tannin extraction efficiency from unfermented grape skins in a hydroalcoholic solution lower than 38% [38]. The cell wall degradation during fermentation enhances tannin recovery [39]. When samples were compared with other studies from six red wine cultivars from France, after vinification, GP total tannin contents were comparable [40].

Between different cultivars, there are differences of TAC [41]. Moreover, anthocyanins accumulate gradually in the grape skin because their synthesis begins during veraison and continues during the ripening process [42], and after GP maceration, the anthocyanin concentration decreases [43]. It was appreciated that 77% of the anthocyanins are released in this process, resulting in a GP with a low content of these pigments. Furthermore, within the anthocyanin family, due to structural differences, they have different extractabilities [38]. Additionally, the formation of polymeric pigments decreases the amount of free anthocyanins [43]. Furthermore, anthocyanins may be degraded and/or absorbed by yeasts and the tank surface [42]. All these processes explain why TAC diminished in the FNFr sample. The result was in accordance with other studies [44].

The total proanthocyanidin of wines is affected by maturity and maceration. Proanthocyanidin concentration is higher at veraison, decreases until ripeness, and then remains relatively constant. Then, a longer maceration increases the proanthocyanidin content [42]. By putting together the two changes, we may explain why there were small differences between the FNFs and FNFr samples, proanthocyanidin concentrations, namely the maturity-induced lowering being masked by the maceration-induced increase.

Proanthocyanidin structures differ according to their origin. In wines, the proanthocyanidin mean degree of polymerization (mDP) and the percentage of PD increased with maturity, whereas the G% decreased. Furthermore, maceration length also has a significant effect on the proanthocyanidin mDP of wines. Throughout maceration time, the proportion of PD tends to decrease [42], but the G% increases because skin (–)-epigallocatechin is released more quickly [42]. The results obtained for FN GP were in accordance with

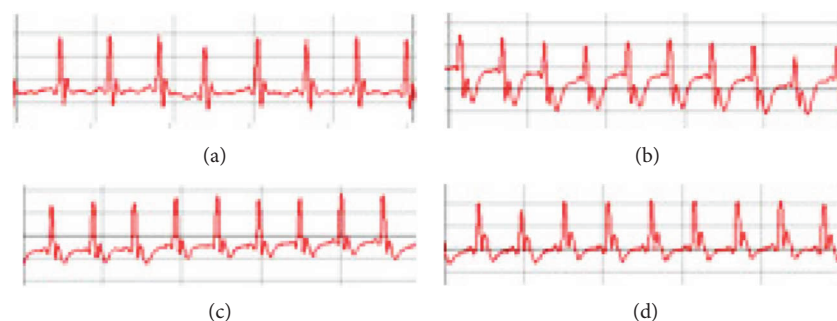


FIGURE 2: Chart records showing the effect of Fetească neagră grape pomace fresh extract (FNFs) and Fetească neagră grape pomace fermented extract (FNFr) pretreatments on ECG tracings: (a) normal control, (b) isoproterenol (ISO), (c) FNFs, and (d) FNFr. The electrocardiogram was recorded from limb leads II in each group. The sensitivity was 1 mV, and the chart speed was 50 mm/sec.

TABLE 3: Serum cardiac marker enzymes.

	AST (UI/L)	ALT (UI/L)	CK-MB (UI/L)
CONTROL	51.36 ± 7.04	47.27 ± 3.17	213.10 ± 46.48
ISO	131.50*** ± 20.72	113.27*** ± 13.17	562.50*** ± 105.20
FNFs	98.52## ± 8.18	86.00## ± 8.14	375.30## ± 33.61
FNFr	103.73# ± 9.34	86.74## ± 5.59	295.20## ± 66.49

Values are expressed as mean ± SEM ( $n = 6$ ). \*\*\* $p < 0.001$  versus control; # $p < 0.05$ , ## $p < 0.01$  versus ISO group. AST: aspartate transaminase; ALT: alanine transaminase; CK-MB: creatine kinase-MB; Fs: fresh; Fr: fermented; FN: Fetească neagră; ISO: isoprenaline.

TABLE 4: Serum oxidative stress markers.

GP	TOS ( $\mu\text{M H}_2\text{O}_2$ equiv/L)	TAR (mM trolox equiv/L)	OSI	MDA (nM/L)	SH (mM/L)	NOx ( $\mu\text{M/L}$ )
CONTROL	26.92 ± 7.30	1.090 ± 0.001	0.25 ± 0.02	1.09 ± 0.22	0.54 ± 0.06	33.31 ± 4.50
ISO	47.95* ± 2.70	1.089* ± 0.001	0.44* ± 0.02	5.25*** ± 0.64	0.51 <sup>n.s.</sup> ± 0.10	69.78*** ± 3.06
FNFs	29.77## ± 4.86	1.091# ± 0.001	0.27## ± 0.04	4.64# ± 0.39	0.50 <sup>n.s.</sup> ± 0.11	65.22 <sup>n.s.</sup> ± 4.04
FNFr	32.53# ± 4.77	1.091# ± 0.001	0.30## ± 0.04	4.46# ± 0.20	0.54 <sup>n.s.</sup> ± 0.07	66.3 <sup>n.s.</sup> ± 3.18

Values are expressed as average ± standard deviation ( $n = 3$ ). <sup>n.s.</sup> $p > 0.05$ , \* $p < 0.05$ , \*\* $p < 0.01$ , and \*\*\* $p < 0.001$  versus control; <sup>n.s.</sup> $p > 0.05$ , # $p < 0.05$ , ## $p < 0.01$ , and ### $p < 0.01$  versus ISO group. GP: grape pomace; Fs: fresh; Fr: fermented; FN: Fetească neagră; ISO: isoprenaline; TOS: total oxidative status; TAR: total antioxidant reactivity; OSI: oxidative stress index; MDA: malondialdehyde; SH: total thiols; NOx: nitrites and nitrates.

the observations on wine, mDP, and PD% being higher in FNFs and G% being higher in FNFr.

Flavan-3-ols are extracted from grapes during the vinification process, but not completely, remaining in great amounts in the winemaking residue. Like in other studies, analysing red GP flavan-3-ol monomers [45], in FN GP extracts epicatechin-3-O-gallate were in lower concentration than (+)-catechin and (−)-epicatechin. The higher (+)-catechin and (−)-epicatechin concentrations in FNFr compared to FNFs were attributed to the better extraction of the flavan-3-ols from the skins during the maceration.

Stilbenes are among the main polyphenols involved in the health protection effects of drinking wine. The main grape stilbenes are trans- and cis-resveratrol, glycosylated derivatives of resveratrol trans- and cis-piceid, piceatannol, and resveratrol dimers (viniferins) [46]. Several *in vitro* studies have shown that resveratrol has antioxidant, anti-inflammatory, cardioprotective, and platelet antiaggregant activities, and glycosylated stilbenes have antioxidant effects [47]. Significant

stilbene concentration differences were also observed between GP and skin [48] and between GP, wine, must, and grapes [49]. In FNFs and FNFr, resveratrol and piceid were found in the form of trans- and cis-isomers as previously described for other red GP [50, 51]. Total stilbene content from FNFr agreed with other studies [52], but FNFs stilbenes were above the values found in other fresh GP. The considerably higher cis-resveratrol in FNFr may be explained by the observation that during vinification trans-resveratrol is isomerized to the cis-form [53]. Because piceid has greater bioavailability than resveratrol [54] and may be hydrolyzed releasing resveratrol [55], high piceid concentration from FNFs and FNFr may represent an important health benefit.

An actual trend is to reduce oxidative stress by using herbal supplements or functional foods rich in natural antioxidants. FNFs and FNFr *in vitro* antioxidant activities were evaluated with the most frequently used method, the DPPH test [36]. The high content of phenolic compounds from

the FNFs and FNFr samples explained the good antioxidant activity evaluated by DPPH test. FNFr had a better DPPH IC<sub>50</sub> than FNFs. This observation is consistent with other studies indicating that the fermentation process increases polyphenol releases from the pomace cells [56]. As phenolic compounds are the most important grape secondary metabolites with antioxidant properties, a high and significant correlation between FNFs and FNFr *in vitro* antioxidant activities and TPI was found. The different structure of each phenolic compound explains their specific efficiency to scavenge different free radicals [10].

The antioxidant capacity of plant extracts cannot be evaluated by using a single test. Studies comparing the *in vitro* and *in vivo* antioxidant effects of a plant extract have shown that some extracts exhibit antioxidant activity both *in vitro* and *in vivo*, but for other extracts, the *in vitro* antioxidant activity does not apply to *in vivo* models [14]. Due to those observations, after demonstrating the promising antioxidant capacity by DPPH test, the FN GP extracts were examined in terms of their *in vivo* cardioprotective and antioxidant effects in experimental rat ISO-induced MI [26].

When injected in rats, isoprenaline undergoes autooxidation and induces myocardial cell membrane injury [57]. ISO induced ECG infarct-like changes, such as heart rate reduction, RR, QT and QTc interval increase, T wave inversion, and ST segment depression. It was considered that such alterations could be due to the consecutive loss of cell membrane potential in the injured myocardium as a result of oxidative stress. Pretreatments with FN GP extracts had cardioprotective effects because they reduced ISO-induced ECG ischemic changes. According to ECG effects, FNFs was a better cardioprotective treatment than FNFr.

Myocardial injury leads to loss of cell membrane structural integrity, with increased permeability and enzyme leakage. The degree of AST, ALT, and CK-MB increase in serum reflects the severity of myocardial injury [58]. Like in other reports, the increase of AST, ALT, and CK-MB correlated well with ST depression in ISO-treated group [57]. FNFs and FNFr pretreatments were cardioprotective by causing a correlated reduction of cardiac enzyme markers and ECG improvements.

The myocardium is vulnerable to oxidative damage because it has limited antioxidant defence possibilities [59]. In MI, the leading cause of myocardial injury is the imbalance between oxidant and antioxidant defences [60]. It was also proved that oxidative stress is coupled with an inflammatory response [61]. Because ROS can freely cross intracellular membranes, plasma can be significantly exposed to ROS leading to systemic consequences [62].

In the present study, oxidative stress was evaluated systematically by measuring serum oxidative stress markers. As a result, an increased oxidative stress, characterized by the TOS, OSI, and MDA elevation associated with TAR lowering, has been found. Both FNFs and FNFr had cardioprotective effects by reducing oxidative stress markers, but FNFs had better *in vivo* activity. The antioxidant activity of plant extracts is the result of the combined effects of many different compounds. It was demonstrated that the antioxidant *in vitro* activity does not always apply to *in vivo* models.

Moreover, it was proved that *in vitro* and *in vivo* antioxidant effects may not correspond because polyphenols may also act as prooxidants via Fenton reaction [14].

Nitric oxide (NO) is an important signalling messenger known to play important roles in many physiological and pathological conditions. Endogenous NO is generated from L-arginine by three major nitric oxide synthases: endothelial, neural, and inducible nitric oxide synthases (iNOS). NO plays an important role in host defence and homeostasis when generated at a low level for a brief period of time, whereas the high level or prolonged induction of NO may contribute to a variety of pathological phenomena associated with inflammatory processes [63]. In the present study, ISO-induced myocardial ischemia was associated with an increase of NOx. Preconditioning myocardium with resveratrol has been shown to be related to the stimulation of iNOS [64] with increased NO synthesis acting as an antioxidant [65]. FNFs and FNFr pretreatments had no important effect on NOx concentration after ISO administration. Although enhanced peroxynitrite formation contributes to the pathophysiology of cardiovascular diseases, it was demonstrated that nanomolar concentrations of peroxynitrite inhibit leukocyte-endothelial cell interaction, which improves postischemic myocardial function [66]. Moreover, it was reported that peroxynitrite plays a role in triggering ischemic preconditioning and ischemic postconditioning [67].

## 5. Conclusion

In conclusion, fresh or fermented Fetească neagră grape pomace extract had a good *in vitro* antioxidant activity due to an important phenolic content. *In vivo* Fetească neagră grape pomace extracts had cardioprotective effects against ISO-induced myocardial ischemia by reducing oxidative stress. The *in vitro* and *in vivo* antioxidant effects were different, respectively, fermented Fetească neagră grape pomace had a better *in vitro* antioxidant activity, and fresh Fetească neagră grape pomace had a stronger *in vivo* antioxidant activity. Overall, the findings presented in this study suggest for the first time that Fetească neagră grape pomace extract pretreatment may be an option for heart preconditioning. Further studies are required to investigate the cardioprotective effects of Fetească neagră grape pomace extracts over a longer period.

## Conflicts of Interest

The authors declare no conflicts of interest in the present study.

## References

- [1] E. Ho, K. Karimi Galougahi, C.-C. Liu, R. Bhindi, and G. A. Figtree, "Biological markers of oxidative stress: applications to cardiovascular research and practice," *Redox Biology*, vol. 1, no. 1, pp. 483–491, 2013.
- [2] N. Vaisman and E. Niv, "Daily consumption of red grape cell powder in a dietary dose improves cardiovascular parameters: a double blind, placebo-controlled, randomized study,"



- International Journal of Food Sciences and Nutrition*, vol. 66, no. 3, pp. 342–349, 2015.
- [3] S. K. Biswas, “Does the interdependence between oxidative stress and inflammation explain the antioxidant paradox?,” *Oxidative Medicine and Cellular Longevity*, vol. 2016, 9 pages, 2016.
- [4] N. He, J. J. Jia, J. H. Li et al., “Remote ischemic preconditioning prevents liver transplantation-induced ischemia/reperfusion injury in rats: role of ROS/RNS and eNOS,” *World Journal of Gastroenterology*, vol. 23, no. 5, pp. 830–841, 2017.
- [5] D. A. Butterfield and M. Perluigi, “Redox proteomics: a key tool for new insights into protein modification with relevance to disease,” *Antioxidants & Redox Signaling*, vol. 26, no. 7, pp. 277–279, 2017.
- [6] B. Halliwell, “The antioxidant paradox: less paradoxical now?,” *British Journal of Clinical Pharmacology*, vol. 75, no. 3, pp. 637–644, 2013.
- [7] J. Zhu, X. Yi, J. Zhang, S. Chen, and Y. Wu, “Chemical profiling and antioxidant evaluation of Yangxinshi tablet by HPLC–ESI–Q–TOF–MS combined with DPPH assay,” *Journal of Chromatography B*, vol. 1060, pp. 262–271, 2017.
- [8] B. Fuhrman, N. Volkova, R. Coleman, and M. Aviram, “Grape powder polyphenols attenuate atherosclerosis development in apolipoprotein E deficient ( $E^0$ ) mice and reduce macrophage atherogenicity,” *The Journal of Nutrition*, vol. 135, no. 4, pp. 722–728, 2005.
- [9] R. Apolinar-Valiente, I. Romero-Cascales, E. Gómez-Plaza, J. M. López-Roca, and J. M. Ros-García, “Cell wall compounds of red grapes skins and their grape marcs from three different winemaking techniques,” *Food Chemistry*, vol. 187, pp. 89–97, 2015.
- [10] Y. Xu, S. Burton, C. Kim, and E. Sismour, “Phenolic compounds, antioxidant, and antibacterial properties of pomace extracts from four Virginia-grown grape varieties,” *Food Science & Nutrition*, vol. 4, no. 1, pp. 125–133, 2016.
- [11] C. Manach, A. Scalbert, C. Morand, C. Rémésy, and L. Jiménez, “Polyphenols: food sources and bioavailability,” *The American Journal of Clinical Nutrition*, vol. 79, no. 5, pp. 727–747, 2004.
- [12] G. N. Mattos, R. V. Tonon, A. A. L. Furtado, and L. M. C. Cabral, “Grape by-product extracts against microbial proliferation and lipid oxidation: a review,” *Journal of the Science of Food and Agriculture*, vol. 97, no. 4, pp. 1055–1064, 2017.
- [13] M. Cotoras, H. Vivanco, R. Melo, M. Aguirre, E. Silva, and L. Mendoza, “*In vitro* and *in vivo* evaluation of the antioxidant and prooxidant activity of phenolic compounds obtained from grape (*Vitis vinifera*) pomace,” *Molecules*, vol. 19, no. 12, pp. 21154–21167, 2014.
- [14] A. S. Veskoukis, A. Kyparos, M. G. Nikolaidis et al., “The antioxidant effects of a polyphenol-rich grape pomace extract *in vitro* do not correspond *in vivo* using exercise as an oxidant stimulus,” *Oxidative Medicine and Cellular Longevity*, vol. 2012, 14 pages, 2012.
- [15] P. Ribéreau-Gayon, Y. Glories, A. Maujean, D. Dubourdieu, and P. Compounds, *Handbook of Enology, the Chemistry of Wine: Stabilization and Treatments*, Vol. 2, .
- [16] C. J. Sarneckis, R. G. Damberg, P. Jones, M. Mercurio, M. J. Herderich, and P. A. Smith, “Quantification of condensed tannins by precipitation with methyl cellulose: development and validation of an optimised tool for grape and wine analysis,” *Australian Journal of Grape and Wine Research*, vol. 12, no. 1, pp. 39–49, 2006.
- [17] J. Bakker and C. F. Timberlake, “The distribution and content of anthocyanins in young port wines as determined by high performance liquid chromatography,” *Journal of the Science of Food and Agriculture*, vol. 36, no. 12, pp. 1325–1333, 1985.
- [18] J. A. Kennedy and G. P. Jones, “Analysis of proanthocyanidin cleavage products following acid-catalysis in the presence of excess phloroglucinol,” *Journal of Agricultural and Food Chemistry*, vol. 49, no. 4, pp. 1740–1746, 2001.
- [19] E. S. Lago-Vanzela, R. Da-Silva, E. Gomes, E. García-Romero, and I. Hermosín-Gutiérrez, “Phenolic composition of the Brazilian seedless table grape varieties BRS Clara and BRS Morena,” *Journal of Agricultural and Food Chemistry*, vol. 59, no. 15, pp. 8314–8323, 2011.
- [20] N. Castillo-Muñoz, S. Gómez-Alonso, E. García-Romero, M. V. Gómez, A. H. Velders, and I. Hermosín-Gutiérrez, “Flavonol 3-O-glycosides series of *Vitis vinifera* Cv. Petit Verdot red wine grapes,” *Journal of Agricultural and Food Chemistry*, vol. 57, no. 1, pp. 209–219, 2009.
- [21] M. L. Muncaciu, F. Zamora Marin, N. Pop, and A. C. Babeş, “Comparative polyphenolic content of grape pomace flours from ‘Fetească neagră’ and ‘Italian Riesling’ Cultivars,” *Notulae Botanicae Horti Agrobotanici Cluj-Napoca*, vol. 45, no. 2, p. 532, 2017.
- [22] C. Sanchez-Moreno, J. A. Larrauri, and F. Saura-Calixto, “Free radical scavenging capacity and inhibition of lipid oxidation of wines, grape juices and related polyphenolic constituents,” *Food Research International*, vol. 32, no. 6, pp. 407–412, 1999.
- [23] J. D. Choudhury, D. Sharma, V. Mayank, S. Behera, and S. Hamid, “Evaluation of antioxidant activity of ethanolic extract of *Ocimum canum* in prevention of renal ischemia,” *International Journal of Pharmaceutical Sciences and Research*, vol. 3, no. 9, pp. 3259–3266, 2012.
- [24] A. E. Parvu, M. Parvu, L. Vlase, P. Miclea, A. C. Mot, and R. Silaghi-Dumitrescu, “Anti-inflammatory effects of *Allium schoenoprasum* L. leaves,” *Journal of Physiology and Pharmacology*, vol. 65, no. 2, pp. 309–315, 2014.
- [25] J. N. Francisci, T. I. C. Frade, M. P. A. d. Almeida, B. F. G. d. Queiroz, and Y. S. Bakhle, “Ketamine-xylazine anaesthesia and orofacial administration of substance P: a lethal combination in rats,” *Neuropeptides*, vol. 62, pp. 21–26, 2017.
- [26] K. H. Lim, D. Ko, and J.-H. Kim, “Cardioprotective potential of Korean red ginseng extract on isoproterenol-induced cardiac injury in rats,” *Journal of Ginseng Research*, vol. 37, no. 3, pp. 273–282, 2013.
- [27] M. Ziaee, A. Khorrami, M. Ebrahimi et al., “Cardioprotective effects of essential oil of *Lavandula angustifolia* on isoproterenol-induced acute myocardial infarction in rat running title : cardioprotective effects of *Lavandula angustifolia*,” *Iranian Journal Pharmaceutical Research*, vol. 14, pp. 1–27, 2015.
- [28] O. Erel, “A new automated colorimetric method for measuring total oxidant status,” *Clinical Biochemistry*, vol. 38, no. 12, pp. 1103–1111, 2005.
- [29] O. Erel, “A novel automated method to measure total antioxidant response against potent free radical reactions,” *Clinical Biochemistry*, vol. 37, no. 2, pp. 112–119, 2004.

- [30] M. Harma, M. Harma, and O. Erel, "Increased oxidative stress in patients with hydatidiform mole," *Swiss Medical Weekly*, vol. 133, no. 41-42, pp. 563–566, 2003.
- [31] H. H. Draper, E. J. Squires, H. Mahmoodi, J. Wu, S. Agarwal, and M. Hadley, "A comparative evaluation of thiobarbituric acid methods for the determination of malondialdehyde in biological materials," *Free Radical Biology & Medicine*, vol. 15, no. 4, pp. 353–363, 1993.
- [32] M.-L. Hu, "[41] Measurement of protein thiol groups and glutathione in plasma," *Methods in Enzymology*, vol. 233, no. C, pp. 380–385, 1994.
- [33] A. Ghasemi, M. Hedayati, and H. Biabani, "Protein precipitation methods evaluated for determination of serum nitric oxide end products by the Griess assay," *Journal of Medical Sciences Research*, vol. 2, pp. 29–32, 2007.
- [34] K. M. Miranda, M. G. Espey, and D. A. Wink, "A rapid, simple spectrophotometric method for simultaneous detection of nitrate and nitrite," *Nitric Oxide*, vol. 5, no. 1, pp. 62–71, 2001.
- [35] S. R. F. Iora, G. M. Maciel, A. A. F. Zielinski et al., "Evaluation of the bioactive compounds and the antioxidant capacity of grape pomace," *International Journal of Food Science and Technology*, vol. 50, no. 1, pp. 62–69, 2015.
- [36] M. N. Alam, N. J. Bristi, and M. Rafiquzzaman, "Review on *in vivo* and *in vitro* methods evaluation of antioxidant activity," *Saudi Pharmaceutical Journal*, vol. 21, no. 2, pp. 143–152, 2013.
- [37] G. M. Reis, H. Faccin, C. Viana, M. B. da Rosa, and L. M. de Carvalho, "*Vitis vinifera* L. cv Pinot noir pomace and lees as potential sources of bioactive compounds," *International Journal of Food Sciences and Nutrition*, vol. 67, no. 7, pp. 789–796, 2016.
- [38] D. Fournand, A. Vicens, L. Sidhoum, J. M. Souquet, M. Moutounet, and V. Cheynier, "Accumulation and extractability of grape skin tannins and anthocyanins at different advanced physiological stages," *Journal of Agricultural and Food Chemistry*, vol. 54, no. 19, pp. 7331–7338, 2006.
- [39] R. L. Hanlin, M. Hrmova, J. F. Harbertson, and M. O. Downey, "Review: condensed tannin and grape cell wall interactions and their impact on tannin extractability into wine," *Australian Journal of Grape and Wine Research*, vol. 16, no. 1, pp. 173–188, 2010.
- [40] I. Ky, B. Lorrain, N. Kolbas, A. Crozier, and P. L. Teissedre, "Wine by-products: phenolic characterization and antioxidant activity evaluation of grapes and grape pomaces from six different French grape varieties," *Molecules*, vol. 19, no. 12, pp. 482–506, 2014.
- [41] Y. Li, R. Ma, Z. Xu et al., "Identification and quantification of anthocyanins in Kyoho grape juice-making pomace, Cabernet Sauvignon grape winemaking pomace and their fresh skin," *Journal of the Science of Food and Agriculture*, vol. 93, no. 6, pp. 1404–1411, 2013.
- [42] M. Gil, N. Kontoudakis, E. González et al., "Influence of grape maturity and maceration length on color, polyphenolic composition, and polysaccharide content of Cabernet Sauvignon and Tempranillo wines," *Journal of Agricultural and Food Chemistry*, vol. 60, no. 32, pp. 7988–8001, 2012.
- [43] J. R. Vergara-Salinas, P. Bulnes, M. C. Zúñiga et al., "Effect of pressurized hot water extraction on antioxidants from grape pomace before and after oenological fermentation," *Journal of Agricultural and Food Chemistry*, vol. 61, pp. 6929–6936, 2013.
- [44] M. J. Otero-Pareja, L. Casas, M. T. Fernández-Ponce, C. Mantell, and E. J. M. De La Ossa, "Green extraction of antioxidants from different varieties of red grape pomace," *Molecules*, vol. 20, no. 12, pp. 9686–9702, 2015.
- [45] M. S. Lingua, M. P. Fabani, D. A. Wunderlin, and M. V. Baroni, "*In vivo* antioxidant activity of grape, pomace and wine from three red varieties grown in Argentina: its relationship to phenolic profile," *Journal of Functional Foods*, vol. 20, pp. 332–345, 2016.
- [46] X. Vitrac, A. Bornet, R. Vanderlinde et al., "Determination of stilbenes ( $\delta$ -viniferin, trans-astringin, trans-piceid, cis- and trans-resveratrol,  $\epsilon$ -viniferin) in Brazilian wines," *Journal of Agricultural and Food Chemistry*, vol. 53, no. 14, pp. 5664–5669, 2005.
- [47] R. Flamini, F. Mattivi, M. De Rosso, P. Arapitsas, and L. Bavaresco, "Advanced knowledge of three important classes of grape phenolics: anthocyanins, stilbenes and flavonols," *International Journal of Molecular Sciences*, vol. 14, no. 12, pp. 19651–19669, 2013.
- [48] S. Vincenzi, D. Tomasi, F. Gaiotti et al., "Comparative study of the resveratrol content of twenty-one italian red grape varieties," *South African Journal of Enology and Viticulture*, vol. 34, no. 1, pp. 30–35, 2013.
- [49] P. Iacopini, M. Baldi, P. Storch, and L. Sebastiani, "Catechin, epicatechin, quercetin, rutin and resveratrol in red grape: content, *in vitro* antioxidant activity and interactions," *Journal of Food Composition and Analysis*, vol. 21, no. 8, pp. 589–598, 2008.
- [50] A. Teixeira, N. Baenas, R. Dominguez-Perles et al., "Natural bioactive compounds from winery by-products as health promoters: a review," *International Journal of Molecular Sciences*, vol. 15, no. 9, pp. 15638–15678, 2014.
- [51] E. I. Geana, O. R. Dinca, R. E. Ionete, V. Artem, and V. C. Niculescu, "Monitoring trans-resveratrol in grape berry skins during ripening and in corresponding wines by HPLC," *Food Technology and Biotechnology*, vol. 53, no. 1, pp. 73–80, 2015.
- [52] M. Gil, M. Esteruelas, E. González et al., "Effect of two different treatments for reducing grape yield in *Vitis vinifera* cv Syrah on wine composition and quality: berry thinning versus cluster thinning," *Journal of Agricultural and Food Chemistry*, vol. 61, no. 20, pp. 4968–4978, 2013.
- [53] B. Sun, A. M. Ribes, M. C. Leandro, A. P. Belchior, and M. I. Spranger, "Stilbenes: quantitative extraction from grape skins, contribution of grape solids to wine and variation during wine maturation," *Analytica Chimica Acta*, vol. 563, no. 1-2, pp. 382–390, 2006.
- [54] S. Potdar, M. S. Parmar, S. D. Ray, and J. E. Cavanaugh, "Protective effects of the resveratrol analog piceid in dopaminergic SH-SY5Y cells," *Archives of Toxicology*, 2017.
- [55] J. Garrido and F. Borges, "Wine and grape polyphenols - a chemical perspective [food research international 44 (2011) 3134-3148]," *Food Research International*, vol. 54, no. 2, p. 1843, 2013.
- [56] J. G. F. Albuquerque, V. L. Assis, A. J. P. O. Almeida et al., "Antioxidant and vasorelaxant activities induced by northeastern Brazilian fermented grape skins," *BMC Complementary and Alternative Medicine*, vol. 17, no. 1, p. 376, 2017.
- [57] O. A. El-Gohary and M. M. Allam, "Effect of vitamin D on isoprenaline-induced myocardial infarction in rats: possible role of peroxisome proliferator-activated receptor- $\gamma$ ," *Canadian Journal of Physiology and Pharmacology*, vol. 95, no. 6, pp. 641–646, 2017.

- [58] I. R. Mohanty, D. S. Arya, A. Dinda, and S. K. Gupta, "Comparative cardioprotective effects and mechanisms of vitamin E and lisinopril against ischemic reperfusion induced cardiac toxicity," *Environmental Toxicology and Pharmacology*, vol. 35, no. 2, pp. 207–217, 2013.
- [59] K. Ozdogan, E. Taskin, and N. Dursun, "Protective effect of carnosine on adriamycin-induced oxidative heart damage in rats," *Anadolu Kardiyoloji Dergisi/The Anatolian Journal Cardiology*, vol. 11, no. 1, pp. 3–10, 2011.
- [60] Z. Makazan, H. K. Saini, and N. S. Dhalla, "Role of oxidative stress in alterations of mitochondrial function in ischemic-reperfused hearts," *American Journal of Physiology. Heart and Circulatory Physiology*, vol. 292, no. 4, pp. H1986–H1994, 2007.
- [61] M. Dallak, "A synergistic protective effect of selenium and taurine against experimentally induced myocardial infarction in rats," *Archives of Physiology and Biochemistry*, vol. 123, no. 5, pp. 344–355, 2017.
- [62] E. Taskin, E. K. Kindap, K. Ozdogan, M. B. Y. Aycan, and N. Dursun, "Acute adriamycin-induced cardiotoxicity is exacerbated by angiotension II," *Cytotechnology*, vol. 68, no. 1, pp. 33–43, 2016.
- [63] D. A. Ribeiro, J. B. Buttros, C. T. F. Oshima, C. T. Bergamaschi, and R. R. Campos, "Ascorbic acid prevents acute myocardial infarction induced by isoproterenol in rats: role of inducible nitric oxide synthase production," *Journal of Molecular Histology*, vol. 40, no. 2, pp. 99–105, 2009.
- [64] G. Imamura, A. A. Bertelli, A. Bertelli, H. Otani, N. Maulik, and D. K. Das, "Pharmacological preconditioning with resveratrol : an insight with iNOS knockout mice," *American Journal of Physiology-Heart and Circulatory Physiology*, vol. 282, no. 6, pp. H1996–H2003, 2002.
- [65] L. Rochette, J. Lorin, M. Zeller et al., "Nitric oxide synthase inhibition and oxidative stress in cardiovascular diseases: possible therapeutic targets?," *Pharmacology & Therapeutics*, vol. 140, no. 3, pp. 239–257, 2013.
- [66] D. J. Lefer, R. Scalia, B. Campbell et al., "Peroxynitrite inhibits leukocyte – endothelial cell interactions and protects against ischemia-reperfusion injury in rats," *Journal of Clinical Investigation*, vol. 99, no. 4, pp. 684–691, 1997.
- [67] M. Pipicz, G. F. Kocsis, L. Sárváry-Arantes et al., "Low-dose endotoxin induces late preconditioning, increases peroxynitrite formation, and activates STAT3 in the rat heart," *Molecules*, vol. 22, no. 3, 2017.

## Review Article

# SIRT3: A New Regulator of Cardiovascular Diseases

Wei Sun,<sup>1</sup> Caixia Liu,<sup>2</sup> Qiuhui Chen,<sup>3</sup> Ning Liu,<sup>1</sup> Youyou Yan,<sup>1</sup> and Bin Liu <sup>1</sup>

<sup>1</sup>Department of Cardiology, The Second Hospital of Jilin University, 218 Ziqiang Road, Changchun 130041, China

<sup>2</sup>Department of Neurology, The Liaoning Province People's Hospital, 33 Wenyi Road, Shenyang 110016, China

<sup>3</sup>Department of Neurology, The Second Hospital of Jilin University, 218 Ziqiang Road, Changchun 130041, China

Correspondence should be addressed to Bin Liu; [liubin3333@vip.sina.com](mailto:liubin3333@vip.sina.com)

Received 1 November 2017; Revised 20 December 2017; Accepted 4 January 2018; Published 13 February 2018

Academic Editor: Ada Popolo

Copyright © 2018 Wei Sun et al. This is an open access article distributed under the Creative Commons Attribution License, which permits unrestricted use, distribution, and reproduction in any medium, provided the original work is properly cited.

Cardiovascular diseases (CVDs) are the leading causes of death worldwide, and defects in mitochondrial function contribute largely to the occurrence of CVDs. Recent studies suggest that sirtuin 3 (SIRT3), the mitochondrial NAD<sup>+</sup>-dependent deacetylase, may regulate mitochondrial function and biosynthetic pathways such as glucose and fatty acid metabolism and the tricarboxylic acid (TCA) cycle, oxidative stress, and apoptosis by reversible protein lysine deacetylation. SIRT3 regulates glucose and lipid metabolism and maintains myocardial ATP levels, which protects the heart from metabolic disturbances. SIRT3 can also protect cardiomyocytes from oxidative stress-mediated cell damage and block the development of cardiac hypertrophy. Recent reports show that SIRT3 is involved in the protection of several heart diseases. This review discusses the progress in SIRT3-related research and the role of SIRT3 in the prevention and treatment of CVDs.

## 1. Introduction

Cardiovascular diseases (CVDs) are the leading causes of death worldwide, with >80% CVD-related deaths in low- and middle-income countries. Globally, the incidence of CVD-related deaths increased by 14.5% (95% confidence interval (95%CI): 12.1%–17.1%) between 2006 and 2016, although age-standardized death rates due to CVD decreased by 14.5% (95%CI: 12.5%–16.2%) over this time period [1]. By 2030, almost 23.6 million people are predicted to die from CVDs, mainly from heart disease and stroke [2, 3]. The molecular mechanisms of CVD include accumulation of reactive oxygen species (ROS), imbalance of vasoconstriction/vasodilation, chronic inflammation, and premature senescence, which are closely related to sirtuin-mediated regulation [4].

Sirtuins are a family of nicotinamide adenine dinucleotide- (NAD<sup>+</sup>-) dependent histone deacetylases, which are highly conserved across species from bacteria to humans [5–7]. It was first discovered in yeast as “silent mating type information regulator 2” (SIR2) in 1979 [8]. In mammals, seven SIR2 homologs (SIRT1–7) were identified, which differ

in subcellular localization and mechanisms of biological regulation. SIRT3 is located in the mitochondrial matrix [9]; however, several studies suggest that it is also located in the nucleus and cytoplasm [10–12]. SIRT3 is a deacetylase that regulates the majority of mitochondrial lysine acetylation [13–15]. Recent studies show that SIRT3 plays important roles in cardiovascular physiology and pathology and describe the mechanisms via which SIRT3 regulates cardiac processes [16–25]. In this review, we will discuss current opinions on the role of SIRT3 in CVDs and speculate on its prospects for clinical application.

## 2. SIRT3: Function and Targets

**2.1. SIRT3 and Energy Metabolism.** More than 90% of ATP in the normal myocardium is derived from mitochondrial oxidative phosphorylation, followed by anaerobic glycolysis of glucose. Fatty acid beta oxidation is the main source of mitochondrial oxidative phosphorylation, followed by glucose, lactic acid, and ketone body aerobic oxidation [26]. SIRT3 regulates the enzymatic activity of the key enzymes of



oxidative phosphorylation via deacetylation, thereby regulating mitochondrial energy metabolism (Table 1).

Reduced SIRT3 levels promote glycolysis via two mechanisms. First, the peptidylprolyl isomerase D (cyclophilin D) is in a highly acetylated state in the absence of SIRT3, which activates hexokinase II (HK2), a key glycolytic enzyme in the mitochondrial outer membrane. HK2 phosphorylates glucose to produce glucose-6-phosphate (G6P), the first step in most glucose metabolism pathways [27, 28]. Second, loss of Sirt3 increases ROS production, which stabilizes hypoxia-inducible factor-1 $\alpha$  (HIF-1 $\alpha$ ), a transcription factor that regulates glycolytic gene expression [29, 30].

SIRT3-mediated deacetylation modifies and activates long-chain acyl-CoA dehydrogenase (LCAD), which is the key enzyme of fatty acid  $\beta$  oxidation, to promote fatty acid metabolism. Compared to wild-type mice, *Sirt3* knockout (*Sirt3*-KO) mice exhibit hallmarks of fatty acid oxidation disorders during fasting, including reduced ATP levels and intolerance to cold exposure [31]. In addition, SIRT3 can regulate other enzymes of fatty acid oxidation, such as medium chain-specific acyl-CoA dehydrogenase (ACADM) and acyl-glycerol kinase (AGK) [32]. Acyl-CoA synthetase short-chain family member 2 (ACSS2) plays a key role in lipogenesis by converting acetate to acetyl-CoA, which enters the tricarboxylic acid cycle (TCA) to promote oxidative phosphorylation and produce energy. Previous studies show that SIRT3 deacetylates and activates ACSS2 [33, 34]. In addition, SIRT3 regulates ketone body production by deacetylating and activating 3-hydroxy-3-methylglutaryl-CoA synthase 2 (HMGCS2), which is the rate-limiting enzyme in ketone-body biosynthesis [35, 36].

Most amino acids are decomposed by aminotransferase-mediated transfer of an  $\alpha$ -amino moiety to  $\alpha$ -ketoglutarate to form glutamate. SIRT3-mediated deacetylation activates glutamate dehydrogenase 1 (GLUD1), the enzyme that produces  $\alpha$ -ketoglutarate from glutamate and is involved in both TCA cycle and ammonia metabolism [15]. SIRT3 can also upregulate the urea cycle (UC) through deacetylation and activation of ornithine transcarbamylase (OTC), the key enzyme of UC, suggesting that SIRT3 increases amino acid catabolism and ammonia detoxification during periods of metabolic stress [37]. Furthermore, SIRT3 regulates mitochondrial protein synthesis by deacetylation of the ribosomal protein MRPL10 [38].

The TCA cycle and electron transport chain (ETC) couple redox balance with ATP generation [39]. SIRT3-mediated deacetylation activates the components of the ETC complex, including NDUFA9 (complex I) [40] and SDHA (complex II) [41, 42]. SIRT3 also regulates ATP synthase activity [43]. Moreover, SIRT3 deacetylates IDH2, a key enzyme of TCA, which promotes oxidation of isocitrate to  $\alpha$ -ketoglutarate and produces NADPH [44].

**2.2. SIRT3 and Oxidative Stress.** Oxidative stress causes extensive accumulation of intracellular ROS; destruction of proteins, lipids, and nucleic acids; membrane phospholipid peroxidation; and mitochondrial DNA mutations, which lead to severe cell damage and death. It is closely related to cardiac hypertrophy [17, 45–47], coronary atherosclerosis

[48, 49], hyperlipidemia [37, 50], diabetes [51, 52], and other diseases. The mitochondrial ETC is the main source of ROS, and SIRT3 enhances the ability of the mitochondria to cope with ROS in multiple ways. The key superoxide scavenger, Mn superoxide dismutase (SOD2), can reduce superoxide production and protect against oxidative stress. SIRT3 directly regulates the activity of SOD2 by deacetylation [53–57]. Moreover, SIRT3 can sequester forkhead box O3a (FOXO3A) in the nucleus to increase the transcription of SOD2 and other key genes involved in antioxidation. Human serum FOXO3A and SIRT3 can be used as markers for ageing, with therapeutic potential for maintenance of healthy ageing [17, 58]. Second, SIRT3 deacetylates and activates the TCA cycle enzyme IDH2 and helps replenish the mitochondrial pool of NADPH [44]. NADPH is a key reducing factor that affects glutathione reductase, a part of the antioxidant defense system against cellular oxidative stress [44]. In addition, SIRT3 promotes effective electron transport via deacetylation of ETC complex components, which indirectly reduces ROS production [57].

**2.3. SIRT3 and Apoptosis.** Currently, the relationship between SIRT3 and apoptosis is not clear, and whether SIRT3 promotes or inhibits apoptosis is still controversial. However, SIRT3 was shown to mainly inhibit cardiomyocyte apoptosis in most studies. As mentioned previously, SIRT3 can inhibit apoptosis by regulating oxidative stress. In addition, SIRT3 also inhibits apoptosis by the following route: first, SIRT3 deacetylates and activates optic atrophy 1 (OPA1). Loss of OPA1 impairs mitochondrial fusion, perturbs cristae structure, and increases the susceptibility of cells toward apoptosis [59, 60]. Second, SIRT3 activates Ku70 by deacetylation. The activated Ku70 binds to Bax, which inhibits Bax-induced cardiomyocyte apoptosis [58]. Third, SIRT3 deacetylates cyclophilin D and closes the mitochondrial permeability transition pore (mPTP) to maintain the normal morphology of mitochondria, thereby inhibiting apoptosis [45, 61, 62].

### 3. SIRT3 in Cardiovascular Disease

**3.1. SIRT3 in Ischemic Heart Disease.** Ischemic heart disease (IHD) and cerebrovascular disease (stroke) together accounted for more than 85.1% of all CVD deaths in 2016. Total deaths from IHD increased by 19.0% (95%CI: 16.2%–22.1%), which contributed largely to the overall increase in total deaths from CVD in 2016 [1]. Severe ischemia can lead to a variety of pathological processes, including metabolic disorders and myocardial cell ultrastructure damage, which can be catastrophic for myocardial cells [63].

SIRT3 downregulation increases the susceptibility of cardiac-derived cells and adult hearts to ischemia-reperfusion (IR) injury and may contribute to a higher level of IR injury in the aged heart [22, 64]. *SIRT3* knockout leads to coronary microvascular dysfunction and impairs cardiac recovery post myocardial ischemia [18, 65]. Klishadi et al. reported that SIRT3 levels decreased after IR induced by left anterior descending artery occlusion [66]. The renin-angiotensin-aldosterone system (RAAS) is involved in ischemic injury

TABLE 1: Known targets of SIRT3 and function.

Function	Gene symbol	Gene name	References
<i>Energy metabolism</i>			
Glycolysis	PPID	Peptidylprolyl isomerase D (cyclophilin D)	[27]
Fatty acid oxidation	ACADL	Long-chain Acyl-CoA dehydrogenase (LCAD)	[31]
Ketone body synthesis	HMGCS2	3-Hydroxy-3-methylglutaryl-CoA synthase 2, mitochondrial	[35]
Acetate metabolism	ACSS2	Acyl-CoA synthetase short-chain family member 2	[33,34]
Urea cycle	OTC	Ornithine transcarbamylase	[37]
Amino acid catabolism	GLUD1	Glutamate dehydrogenase 1 (GDH)	[15]
Mitochondrial protein synthesis	MRPL10	Mitochondrial ribosomal protein L10	[38]
	NDUFA9	NADH dehydrogenase (ubiquinone) 1 $\alpha$ subcomplex 9	[40]
Oxidative phosphorylation	SDHA	Succinate dehydrogenase complex, subunit A, flavoprotein	[41,42]
	ATP5a	F <sub>1</sub> F <sub>0</sub> -ATPase subunit $\alpha$	[43]
TCA cycle	IDH2	Isocitrate dehydrogenase 2, mitochondrial	[44]
<i>Oxidative stress</i>			
Transcriptional activation	FOXO3a	Forkhead box O3a	[17,58]
ROS	SOD2	Superoxide dismutase 2, mitochondrial (MnSOD)	[53–57]
<i>Apoptosis</i>	OPA1	Optic atrophy 1	[59,60]
	XRCC6	X-ray repair cross-complementing 6 (Ku70)	[58]

[67, 68]. Angiotensin II downregulates SIRT3 [69], and drugs directly inhibiting RAAS normalized SIRT3 levels in the ischemic myocardium and improved cardiac function [40, 66, 70]. However, data on the instant effect of RAAS on SIRT3 during the acute ischemia is not available.

Atherosclerosis caused by vascular inflammation is also one of the pathophysiological mechanisms of IHD. Many studies have shown that SIRT3 is involved in the regulation of vascular inflammation. Trimethylamine-N-oxide (TMAO) activates nucleotide-binding oligomerization domain-like receptor family pyrin domain containing 3 (NLRP3) inflammasomes to induce vascular inflammation, which promotes atherosclerosis. TMAO was found to promote ROS generation, especially mitochondrial ROS, and inhibit SOD2 activation and SIRT3 expression in HUVECs and aortas from ApoE<sup>-/-</sup> mice. Overexpression of SIRT3 resulted in protection against TMAO-induced activation of NLRP3 inflammasomes in endothelial cells. TMAO can also not further inhibit SOD2 and activate NLRP3 inflammasome in SIRT3 siRNA-treated HUVECs and aortas from SIRT3<sup>-/-</sup> mice [71].

Moreover, a study of aerobic interval training showed that compared to the control group, *Sirt3* expression was reduced in the myocardium of rats with acute myocardial injury, while the interval of aerobic breathing resulted in increased *Sirt3* expression and protected against myocardial infarction-induced oxidative injury [72]. However, Winnik et al. observed that *SIRT3* knockout did not affect the progression of atherosclerotic lesions and plaque stability [73]. Therefore, the role of SIRT3 in atherosclerosis remains to be elucidated.

**3.2. SIRT3 in Hypertrophy and Heart Failure.** Hypertrophy is a compensatory response that results in cardiomyocyte death, fibrosis, and cardiac pressure or volume overload-induced heart failure because of structural changes in

myocardial cells [74]. An increasing number of studies revealed that poor SIRT3 activity is one of the causes of cardiac hypertrophy and heart failure [17, 45, 75].

Four weeks after a transverse aortic constriction, the ejection fraction in *Sirt3*-KO mice was lesser than that in wild-type mice, which was accompanied by an increase in cardiac hypertrophy and fibrosis [19, 76]. *Sirt3*-KO mice showed a decreasing trend for palmitate oxidation, glucose oxidation, oxygen consumption, respiratory capacity, and ATP synthesis, whereas glycolytic rates were increased [19]. *Sirt3*-KO mice also showed abnormal lipid accumulation [77]. SIRT3 levels are reduced, and mitochondrial protein lysine acetylation is elevated in models of hypertensive heart failure, suggestive of impaired SIRT3 activity [78]. The low SIRT3 levels may be associated with the downregulation of PGC-1 $\alpha$  [79]. Moreover, as a DNA repair enzyme, poly(ADP-ribose)-polymerase 1 (PARP-1) also uses NAD<sup>+</sup> as a cosubstrate [80]. Overactivation of PARP-1 in failing hearts increases the competition between SIRT3 and NAD<sup>+</sup>, which leads to large-scale consumption of cellular NAD<sup>+</sup> and a decrease in SIRT3 activity [80, 81]. In addition, RIP140, which is involved in the pathogenesis of cardiac hypertrophy and heart failure, also inhibits SIRT3 [82].

Recent studies show that SIRT3 regulates energy metabolism [30, 32], resists oxidative stress [17, 45, 47, 58], and prevents cardiac hypertrophy. Nicotinamide mononucleotide adenylyltransferase 3 (NMNAT3) is the only known enzyme of the NAD<sup>+</sup> synthesis pathway that is localized in the mitochondrial matrix [83]. NMNAT3 is a SIRT3 substrate, deacetylation of which enhances its activity. Subsequently, NMNAT3 contributes to SIRT3-mediated antihypertrophic effects in cardiomyocytes by supplying NAD<sup>+</sup> [84, 85]. Moreover, a study showed that SIRT3-LKB1-AMPK pathway activation improved cardiac hemodynamics and preserved the ejection fraction [25, 86]. SIRT3 can also protect against

cardiac fibrosis by inhibiting myofibroblast transdifferentiation via the STAT3-NFATc2 [87] and  $\beta$ -catenin/PPAR- $\gamma$  [88] signaling pathways.

In addition, emerging evidence indicates that impaired angiogenesis may contribute to hypertension-induced cardiac remodeling. A mouse myocardial fibrosis model induced by angiotensin II confirmed that SIRT3 enhanced mitochondrial autophagy, mediated by Pink/Parkin, and attenuated the production of mitochondrial ROS, restored vascular budding and tube formation, and improved myocardial fibrosis and cardiac function [89].

**3.3. SIRT3 in Drug-Induced Cardiotoxicity.** Drug-induced cardiotoxicity is now a common clinical practice. In particular, chemotherapeutic drug-induced cardiotoxicity has spawned the emergence of the interdisciplinary field of cardio-oncology. Recently, practice guidelines were published to guide clinical work in this interdisciplinary area [90].

Anthracycline chemotherapeutics such as doxorubicin (DOX) are commonly used for the clinical treatment of tumors. DOX induces cardiotoxicity via mitochondrial dysfunction [91]. A study showed that DOX reduced SIRT3 expression and correspondingly increased mitochondrial protein acetylation, an effect that was more pronounced in SIRT3-KO mice [23, 92, 93]. SIRT3 overexpression deacetylates and activates OPA1, which regulates mitochondrial dynamics and protects cardiomyocytes from doxorubicin-induced cardiotoxicity [23, 60, 93, 94]. Moreover, SIRT3 may also attenuate doxorubicin-induced cardiac hypertrophy and mitochondrial dysfunction via suppression of BNIP3 [95].

**3.4. SIRT3 in Diabetic Cardiomyopathy and Cardiac Lipotoxicity.** Diabetes and obesity are important risk factors for CVD. Studies show that the mitochondrial sirtuin family is involved in insulin resistance with diabetes mellitus [19, 20, 24].

SIRT3 can prevent and even reverse diabetes-induced retinal [96–98], skeletal [99–101], and cardiac damage [102, 103]. The SIRT3-FOXO3A-Parkin signaling pathway may play a vital role in the development of diabetic cardiomyopathy [102]. Melatonin protects against diabetic cardiomyopathy through MST1/SIRT3 signaling [104], and garlic protects patients with diabetic cardiomyopathy from oxidative stress by enhancing SIRT3 activity [105]. Moreover, APLN gene therapy increases angiogenesis and improves cardiac functional recovery in diabetic cardiomyopathy via upregulation of the SIRT3 pathway [103].

SIRT3 levels were low in the hearts of high-fat diet (HFD-) fed obese mice, and cardiac lipotoxicity was high in Sirt3 knockout mice [19, 20, 24]. SIRT3 possibly regulates lipotoxicity by promoting lipid metabolism, reducing fatty acid accumulation and oxidative stress injury [31, 32, 106], and restoring cardiac remodeling function [20, 24].

Oxidative stress is the common pathophysiology of diabetic cardiomyopathy and cardiac lipotoxicity [107, 108]. SIRT3 protects pancreatic beta cells from lipotoxicity by antagonizing oxidative stress-induced cell damage [109].

Thus, SIRT3 can inhibit diabetic cardiomyopathy and cardiac lipotoxicity.

**3.5. SIRT3 in Hypertension.** Hypertension, a common risk factor for diseases, such as cardiovascular, cerebrovascular, and kidney disease, has become a major risk factor for premature death and disability worldwide [110]. The roles of SIRT3 in hypertension are well documented. Waypa et al. first demonstrated that Sirt3 deletion does not augment hypoxia-induced ROS signaling or its consequences in the cytosol of pulmonary arterial smooth muscle cells, nor the development of pulmonary arterial hypertension (PAH) [111]. However, Paulin et al. more recently reported that SIRT3 is downregulated in a rat PAH model and in human PAH tissues. SIRT3<sup>-/-</sup> and SIRT3<sup>+/-</sup> mice develop PAH in a gene dose-dependent manner. Sirt3 gene therapy even reverses PAH in rats in vivo and human vascular cells in vitro [30]. Recently, Dikalova et al. showed that downexpression and redox inactivation of Sirt3 lead to SOD2 inactivation and contribute to the pathogenesis of hypertension [55]. These data suggest that Sirt3 responses may be cell type specific or restricted to certain genetic backgrounds.

## 4. Therapeutic Application

SIRT3 plays an important role in the development and progression of CVDs. Therefore, promotion of SIRT3 expression and activity via pharmacological pathways can delay the development of CVDs (Table 2).

**4.1. Traditional Chinese Medicine.** Components extracted from traditional Chinese medicine promoted SIRT3-mediated cardioprotective effects [112]. Resveratrol, which is abundant in grapes and blueberries, is the first compound that was shown to activate SIRT3 [113, 114]. A study demonstrated that resveratrol activates SIRT3 and downregulates the TGF- $\beta$ /Smad3 pathway to improve myocardial fibrosis [115]. Polydatin, a monocrystalline and a polyphenolic drug extracted from the traditional Chinese herb *Polygonum cuspidatum*, protects cardiomyocytes against myocardial infarction injury by upregulating autophagy and improving mitochondrial biogenesis via SIRT3 activity [116]. Berberine decreases DOX-induced cardiotoxicity by activating SIRT3 [117]. Honokiol, a natural biphenolic compound derived from the bark of magnolia trees, blocks and reverses cardiac hypertrophy by activating SIRT3 [76, 118]. Pomegranin A activates SOD2 through SIRT3-mediated deacetylation and reduces intracellular ROS [119]. Oroxylin A (OA), which is derived from the root of *Scutellaria baicalensis*, was found to be a SIRT3 activator in an in vitro model of cardiac myocyte insulin resistance [120] and plays roles in preventing myocardial contractile function and improving myocardial fibrosis and heart failure [121]. Curcumin, a phenolic compound extracted from the natural herb turmeric, can activate the PGC-1 $\alpha$ /SIRT3 signaling pathway to protect against mitochondrial impairment, and it can also stimulate SIRT1 to have cardioprotective effects [122].

**4.2. Small Molecule Activators of SIRT3.** Inactivation of PIK-FYVE, an evolutionarily conserved lipid kinase that regulates

TABLE 2: Therapeutic application of SIRT3.

Categories	Representatives	Mechanism	References
Traditional Chinese medicine	Resveratrol	↑SIRT3 ↓TGF- $\beta$ /Smad3	[113–115]
	Polydatin	↑SIRT3	[116]
	Berberine	↑SIRT3	[117]
	Honokiol	↑SIRT3	[76,118]
	Pomegranin A	↑SIRT3/SOD2	[119]
	Oroxylin A	↑SIRT3	[120,121]
	Curcumin	↑PGC-1 $\alpha$ /SIRT3	[122]
Small molecule activators of SIRT3	↓PIKFYVE	↑SIRT3	[123]
	Melatonin	↑SIRT3	[79, 104, 124, 125]
	Adjudin	↑SIRT3	[126]
	Minocycline	↑SIRT3/PHD2 ↓HIF-1 $\alpha$	[127]
	MIPEP	↑SIRT3	[128]
	Metformin	↑SIRT3	[129]
	NMNAT3	↑NAD <sup>+</sup> /SIRT3	[84]
Signaling pathways	C12	↑SIRT3/MnSOD	[138]
	EphB2 signaling	↑SIRT3/MnSOD	[139]
	cAMP/PKA signaling	↑SIRT3/OPA1	[59]
	AMPK	↑SIRT3	[140]
	SIRT1	↑SIRT3	[141]
	PLGA-PNIPAM-NaB	↑SIRT3	[142]
	PGC-1 $\alpha$ -HO-1	↑SIRT3	[143]
MicroRNAs	MicroRNA-210	↓SIRT3	[144]
	MicroRNA-92a	↓SIRT2 ( <i>Drosophila</i> , homologous to human SIRT2 and SIRT3)	[145]
	MicroRNA28-5p	↓SIRT3	[146]
	MicroRNA-421	↓SIRT3/FOXO3	[147]

pleiotropic cellular functions, suppresses excessive mitochondrial ROS production and apoptosis through a SIRT3-dependent pathway in cardiomyoblasts [123]. Moreover, melatonin treatment alleviated cardiac dysfunction and ameliorated myocardial ischemia-reperfusion injury via SIRT3-dependent regulation of oxidative stress and apoptosis [79, 104, 124, 125]. Adjudin, which functions as an antispermatogenic agent, was found to attenuate oxidative stress and cellular senescence by activating SIRT3 [126]. Minocycline inhibited HIF-1 $\alpha$ -mediated cellular responses and protected the blood-brain barrier and hypoxic brain injuries via activation of the SIRT3-PHD2 pathway. It implied that minocycline may have roles in IHD [127]. Mitochondrial intermediate peptidase (MIPEP), a mitochondrial signal peptidase (MtSPase), may promote the maintenance of mitochondrial quality during caloric restriction (CR), which extends lifespan and suppresses age-associated pathophysiology in various animal models by activating SIRT3 [128]. Metformin, a common drug for diabetes treatment, was found to modulate the appearance of atherosclerosis and reduce vascular events by increasing SIRT3 expression [129]. SIRT3 activity is dependent on the

levels of cellular NAD<sup>+</sup> and exogenous supplementation of NAD<sup>+</sup> [78, 130–134]. Therefore, an increase in the levels of NMNAT3, the rate-limiting enzyme for mitochondrial NAD<sup>+</sup> biosynthesis, also enhances the myocardium-protective role of SIRT3 [84]. Moreover, a variety of SIRT3-specific small molecules is being developed [135–137]. A recent study identified a novel SIRT3 activator, 7-hydroxy-3-(4'-methoxyphenyl) coumarin (C12), which binds to SIRT3 with high affinity, promotes deacetylation of MnSOD, and modulates mitochondrial protein acetylation and ROS [138].

**4.3. Signaling Pathways.** In addition, other signaling paths can also increase SIRT3 activity. EphB2 signaling-mediated SIRT3 expression promotes MnSOD-mediated mtROS scavenging [139]. Mitochondrial cAMP/PKA signaling controls SIRT3 levels and proteolytic processing of OPA1 [59]. AMPK attenuates the cardiac remodeling parameters and improves cardiac function via the SIRT3/oxidative stress signaling pathway [140]. SIRT1 activation induces SIRT3 and the combined functions of the nuclear-mitochondrial triad switch glycolysis to fatty acid oxidation and immunity from activation to repression in acute inflammation [141]. A study



that is expected to be used in clinical trials showed that PLGA-PNIPAM microspheres loaded with the gastrointestinal nutrient NaB specifically binds to SIRT3 and activates its deacetylase function, thereby inhibiting ROS generation and autophagy, promoting angiogenesis and protecting cardiomyocytes in acute myocardial infarction (AMI) [142]. The peroxisome proliferator-activated receptor gamma coactivator 1- $\alpha$ - (PGC-1 $\alpha$ -) heme oxygenase- (HO-1-) SIRT3 pathway increases mitochondrial viability and provides metabolic protection [143].

**4.4. MicroRNAs.** MicroRNAs are single-stranded, noncoding small molecule RNAs that inhibit translation or induce target molecule degradation. Our previous study found that microRNA-210 can indirectly regulate the expression and activity of SIRT3 and promote cellular energy metabolism [144]. A study of *Drosophila* circadian rhythms found that microRNA-92a modulates neuronal excitability by suppressing the expression of SIRT2, which is homologous to human SIRT2 and SIRT3 [145]. Poulsen et al. found that high glucose levels coupled with oxidative stress resulted in the upregulation of microRNA28-5p, which directly inhibited expression of SIRT3 [146]. To date, the only microRNA for which SIRT3 was identified as a functionally relevant target was microRNA-421. MicroRNA-421 acts upstream of the SIRT3/FOXO3 pathway to modulate oxidant stress and lipid metabolism [147]. Although the study of the regulation of SIRT3 by microRNAs has only just begun, it may provide a new approach for the application of SIRT3.

## 5. Conclusion and Outlook

An important pathophysiological mechanism of cardiovascular disease is mitochondrial damage and dysfunction. As shown in Table 1, SIRT3 plays important roles in cellular energy metabolism, oxidative stress, and apoptosis. Moreover, it can potentially be used for protection against CVDs. Currently, small molecule drug screening for SIRT3 constitutes an important research direction. We believe that, in the near future, studies on SIRT3 will generate new approaches for the prevention and treatment of CVDs. SIRT3 can also regulate systemic inflammation, improving the whole body's metabolic balance. Although much progress has been made in the study of SIRT3, there are still many problems to be clarified: (1) the sirtuin family plays an important role in cardiovascular regulation; however, the physiological and pathological effects of SIRT4 and SIRT5 are unclear. (2) Sirtuins are the sentries of mitochondrial homeostasis; however, the interactomes of mitochondrial sirtuins are quite different from each other, which suggests that there is a diversity and complexity of sirtuin functions within the mitochondrion. A better understanding of the mechanism of mitochondrial regulation of CVD will be further advanced by studies of the regulatory networks acting among the sirtuin family members. (3) SIRT3, named "the longevity gene," is closely related to the ageing of the human body. However, there is currently little data on the function of SIRT3 in ageing-related decline in cardiovascular functions. Further research to address these questions will be helpful

in advancing our understanding of the roles of SIRT3 in CVD in order to facilitate the development of clinical diagnostic therapies.

## Conflicts of Interest

The authors declare that they have no conflict of interests.

## Authors' Contributions

Wei Sun and Caixia Liu contributed equally to this work.

## Acknowledgments

This study was supported by grants from the National Natural Science Foundation of China (no. 81570250), the Ph.D. Outstanding Personnel Development Program of Bethune Medical Department (yb201503), and the National Clinical Key Specialty Project.

## References

- [1] M. Naghavi, A. A. Abajobir, C. Abbafati et al., "Global, regional, and national age-sex specific mortality for 264 causes of death, 1980-2016: a systematic analysis for the Global Burden of Disease Study 2016," *The Lancet*, vol. 390, no. 10100, pp. 1151-1210, 2017.
- [2] M. Dehghan, A. Mente, X. Zhang et al., "Associations of fats and carbohydrate intake with cardiovascular disease and mortality in 18 countries from five continents (PURE): a prospective cohort study," *The Lancet*, vol. 390, no. 10107, pp. 2050-2062, 2017.
- [3] S. Yusuf, S. Rangarajan, K. Teo et al., "Cardiovascular risk and events in 17 low-, middle-, and high-income countries," *The New England Journal of Medicine*, vol. 371, no. 9, pp. 818-827, 2014.
- [4] V. Conti, M. Forte, G. Corbi et al., "Sirtuins: possible clinical implications in cardio and cerebrovascular diseases," *Current Drug Targets*, vol. 18, no. 4, pp. 473-484, 2017.
- [5] Y. Lu, Y. D. Wang, X.y. Wang, H. Chen, Z.j. Cai, and M.x. Xiang, "SIRT3 in cardiovascular diseases: emerging roles and therapeutic implications," *International Journal of Cardiology*, vol. 220, pp. 700-705, 2016.
- [6] R. A. Frye, "Phylogenetic classification of prokaryotic and eukaryotic Sir2-like proteins," *Biochemical and Biophysical Research Communications*, vol. 273, no. 2, pp. 793-798, 2000.
- [7] B. Osborne, N. L. Bentley, M. K. Montgomery, and N. Turner, "The role of mitochondrial sirtuins in health and disease," *Free Radical Biology & Medicine*, vol. 100, pp. 164-174, 2016.
- [8] J. Rine, J. N. Strathern, J. B. Hicks, and I. Herskowitz, "A suppressor of mating-type locus mutations in *Saccharomyces cerevisiae*: evidence for and identification of cryptic mating-type loci," *Genetics*, vol. 93, no. 4, pp. 877-901, 1979.
- [9] B. Schwer, B. J. North, R. A. Frye, M. Ott, and E. Verdin, "The human silent information regulator (Sir)2 homologue hSIRT3 is a mitochondrial nicotinamide adenine dinucleotide-dependent deacetylase," *The Journal of Cell Biology*, vol. 158, no. 4, pp. 647-657, 2002.
- [10] J. Bao, Z. Lu, J. J. Joseph et al., "Characterization of the murine SIRT3 mitochondrial localization sequence and

- comparison of mitochondrial enrichment and deacetylase activity of long and short SIRT3 isoforms," *Journal of Cellular Biochemistry*, vol. 110, no. 1, pp. 238–247, 2010.
- [11] M. B. Scher, A. Vaquero, and D. Reinberg, "SirT3 is a nuclear NAD<sup>+</sup>-dependent histone deacetylase that translocates to the mitochondria upon cellular stress," *Genes & Development*, vol. 21, no. 8, pp. 920–928, 2007.
  - [12] H. M. Cooper and J. N. Spelbrink, "The human SIRT3 protein deacetylase is exclusively mitochondrial," *Biochemical Journal*, vol. 411, no. 2, pp. 279–285, 2008.
  - [13] C. Peng, Z. Lu, Z. Xie et al., "The first identification of lysine malonylation substrates and its regulatory enzyme," *Mol Cell Proteomics*, vol. 10, no. 12, article M111 012658, 2011.
  - [14] M. J. Rardin, J. C. Newman, J. M. Held et al., "Label-free quantitative proteomics of the lysine acetylome in mitochondria identifies substrates of SIRT3 in metabolic pathways," *Proceedings of the National Academy of Sciences of the United States of America*, vol. 110, no. 16, pp. 6601–6606, 2013.
  - [15] D. B. Lombard, F. W. Alt, H. L. Cheng et al., "Mammalian Sir2 homolog SIRT3 regulates global mitochondrial lysine acetylation," *Molecular and Cellular Biology*, vol. 27, no. 24, pp. 8807–8814, 2007.
  - [16] H. Bugger, C. N. Witt, and C. Bode, "Mitochondrial sirtuins in the heart," *Heart Failure Reviews*, vol. 21, no. 5, pp. 519–528, 2016.
  - [17] N. R. Sundaresan, M. Gupta, G. Kim, S. B. Rajamohan, A. Isbatan, and M. P. Gupta, "Sirt3 blocks the cardiac hypertrophic response by augmenting Foxo3a-dependent antioxidant defense mechanisms in mice," *The Journal of Clinical Investigation*, vol. 119, no. 9, pp. 2758–2771, 2009.
  - [18] C. Koentges, K. Pfeil, M. Meyer-Steenbuck et al., "Preserved recovery of cardiac function following ischemia-reperfusion in mice lacking SIRT3," *Canadian Journal of Physiology and Pharmacology*, vol. 94, no. 1, pp. 72–80, 2016.
  - [19] C. Koentges, K. Pfeil, T. Schnick et al., "SIRT3 deficiency impairs mitochondrial and contractile function in the heart," *Basic Res Cardiol*, vol. 110, no. 4, p. 36, 2015.
  - [20] O. A. Alrob, S. Sankaralingam, C. Ma et al., "Obesity-induced lysine acetylation increases cardiac fatty acid oxidation and impairs insulin signalling," *Cardiovascular Research*, vol. 103, no. 4, pp. 485–497, 2014.
  - [21] J. M. Chinawa and A. T. Chinawa, "Assessment of primary health care in a rural health centre in Enugu South East Nigeria," *Pakistan Journal of Medical Sciences*, vol. 31, no. 1, pp. 60–64, 2015.
  - [22] G. A. Porter, W. R. Urciuoli, P. S. Brookes, and S. M. Nadtochiy, "SIRT3 deficiency exacerbates ischemia-reperfusion injury: implication for aged hearts," *American Journal of Physiology Heart and Circulatory Physiology*, vol. 306, no. 12, pp. H1602–H1609, 2014.
  - [23] K. G. Cheung, L. K. Cole, B. Xiang et al., "Sirtuin-3 (SIRT3) protein attenuates doxorubicin-induced oxidative stress and improves mitochondrial respiration in H9c2 cardiomyocytes," *The Journal of Biological Chemistry*, vol. 290, no. 17, pp. 10981–10993, 2015.
  - [24] H. Zeng, V. R. Vaka, X. He, G. W. Booz, and J. X. Chen, "High-fat diet induces cardiac remodelling and dysfunction: assessment of the role played by SIRT3 loss," *Journal of Cellular and Molecular Medicine*, vol. 19, no. 8, pp. 1847–1856, 2015.
  - [25] V. B. Pillai, N. R. Sundaresan, G. Kim et al., "Exogenous NAD blocks cardiac hypertrophic response via activation of the SIRT3-LKB1-AMP-activated kinase pathway," *The Journal of Biological Chemistry*, vol. 285, no. 5, pp. 3133–3144, 2010.
  - [26] W. C. Stanley, F. A. Recchia, and G. D. Lopaschuk, "Myocardial substrate metabolism in the normal and failing heart," *Physiological Reviews*, vol. 85, no. 3, pp. 1093–1129, 2005.
  - [27] L. Wei, Y. Zhou, Q. Dai et al., "Oroxylin A induces dissociation of hexokinase II from the mitochondria and inhibits glycolysis by SIRT3-mediated deacetylation of cyclophilin D in breast carcinoma," *Cell Death & Disease*, vol. 4, no. 4, article e601, 2013.
  - [28] P. L. Pedersen, S. Mathupala, A. Rempel, J. F. Geschwind, and Y. H. Ko, "Mitochondrial bound type II hexokinase: a key player in the growth and survival of many cancers and an ideal prospect for therapeutic intervention," *Biochimica et Biophysica Acta (BBA) - Bioenergetics*, vol. 1555, no. 1–3, pp. 14–20, 2002.
  - [29] L. W. S. Finley, A. Carracedo, J. Lee et al., "SIRT3 opposes reprogramming of cancer cell metabolism through HIF1 $\alpha$  destabilization," *Cancer Cell*, vol. 19, no. 3, pp. 416–428, 2011.
  - [30] R. Paulin, P. Dromparis, G. Sutendra et al., "Sirtuin 3 deficiency is associated with inhibited mitochondrial function and pulmonary arterial hypertension in rodents and humans," *Cell Metabolism*, vol. 20, no. 5, pp. 827–839, 2014.
  - [31] M. D. Hirschey, T. Shimazu, E. Goetzman et al., "SIRT3 regulates mitochondrial fatty-acid oxidation by reversible enzyme deacetylation," *Nature*, vol. 464, no. 7285, pp. 121–125, 2010.
  - [32] W. Yang, K. Nagasawa, C. Münch et al., "Mitochondrial sirtuin network reveals dynamic SIRT3-dependent deacetylation in response to membrane depolarization," *Cell*, vol. 167, no. 4, pp. 985–1000.e21, 2016.
  - [33] B. Schwer, J. Bunkenborg, R. O. Verdin, J. S. Andersen, and E. Verdin, "Reversible lysine acetylation controls the activity of the mitochondrial enzyme acetyl-CoA synthetase 2," *Proceedings of the National Academy of Sciences of the United States of America*, vol. 103, no. 27, pp. 10224–10229, 2006.
  - [34] W. C. Hallows, S. Lee, and J. M. Denu, "Sirtuins deacetylate and activate mammalian acetyl-CoA synthetases," *Proceedings of the National Academy of Sciences of the United States of America*, vol. 103, no. 27, pp. 10230–10235, 2006.
  - [35] T. Shimazu, M. D. Hirschey, L. Hua et al., "SIRT3 deacetylates mitochondrial 3-hydroxy-3-methylglutaryl CoA synthase 2 and regulates ketone body production," *Cell Metabolism*, vol. 12, no. 6, pp. 654–661, 2010.
  - [36] W. Yi, X. Xie, M. Y. Du et al., "Green tea polyphenols ameliorate the early renal damage induced by a high-fat diet via ketogenesis/SIRT3 pathway," *Oxidative Medicine and Cellular Longevity*, vol. 2017, Article ID 9032792, 14 pages, 2017.
  - [37] W. C. Hallows, W. Yu, B. C. Smith et al., "Sirt3 promotes the urea cycle and fatty acid oxidation during dietary restriction," *Molecular Cell*, vol. 41, no. 2, pp. 139–149, 2011.
  - [38] Y. Yang, H. Cimen, M. J. Han et al., "NAD<sup>+</sup>-dependent deacetylase SIRT3 regulates mitochondrial protein synthesis by deacetylation of the ribosomal protein MRPL10," *The Journal of Biological Chemistry*, vol. 285, no. 10, pp. 7417–7429, 2010.
  - [39] L. Zhong and R. Mostoslavsky, "Fine tuning our cellular factories: sirtuins in mitochondrial biology," *Cell Metabolism*, vol. 13, no. 6, pp. 621–626, 2011.

- [40] B.-H. Ahn, H.-S. Kim, S. Song et al., "A role for the mitochondrial deacetylase Sirt3 in regulating energy homeostasis," *Proceedings of the National Academy of Sciences of the United States of America*, vol. 105, no. 38, pp. 14447–14452, 2008.
- [41] L. W. S. Finley, W. Haas, V. Desquiere-Dumas et al., "Succinate dehydrogenase is a direct target of sirtuin 3 deacetylase activity," *PLoS One*, vol. 6, no. 8, article e23295, 2011.
- [42] H. Cimen, M.-J. Han, Y. Yang, Q. Tong, H. Koc, and E. C. Koc, "Regulation of succinate dehydrogenase activity by SIRT3 in mammalian mitochondria," *Biochemistry*, vol. 49, no. 2, pp. 304–311, 2010.
- [43] J. Bao, I. Scott, Z. Lu et al., "SIRT3 is regulated by nutrient excess and modulates hepatic susceptibility to lipotoxicity," *Free Radical Biology & Medicine*, vol. 49, no. 7, pp. 1230–1237, 2010.
- [44] S. Someya, W. Yu, W. C. Hallows et al., "Sirt3 mediates reduction of oxidative damage and prevention of age-related hearing loss under caloric restriction," *Cell*, vol. 143, no. 5, pp. 802–812, 2010.
- [45] A. V. Hafner, J. Dai, A. P. Gomes et al., "Regulation of the mPTP by SIRT3-mediated deacetylation of CypD at lysine 166 suppresses age-related cardiac hypertrophy," *Aging*, vol. 2, no. 12, pp. 914–923, 2010.
- [46] E. S. Park, J. C. Kang, Y. C. Jang et al., "Cardioprotective effects of rhamnetin in H9c2 cardiomyoblast cells under H<sub>2</sub>O<sub>2</sub>-induced apoptosis," *Journal of Ethnopharmacology*, vol. 153, no. 3, pp. 552–560, 2014.
- [47] V. B. Pillai, N. R. Sundaresan, and M. P. Gupta, "Regulation of Akt signaling by sirtuins its implication in cardiac hypertrophy and aging," *Circulation Research*, vol. 114, no. 2, pp. 368–378, 2014.
- [48] C. Dong, D. Della-Morte, L. Wang et al., "Association of the sirtuin and mitochondrial uncoupling protein genes with carotid plaque," *PLoS One*, vol. 6, no. 11, article e27157, 2011.
- [49] L. Li, H. Zeng, X. Hou, X. He, and J. X. Chen, "Myocardial injection of apelin-overexpressing bone marrow cells improves cardiac repair via upregulation of Sirt3 after myocardial infarction," *PLoS One*, vol. 8, no. 9, 2013.
- [50] A. Giralt, E. Hondares, J. A. Villena et al., "Peroxisome proliferator-activated receptor- $\gamma$  coactivator-1 $\alpha$  controls transcription of the *Sirt3* gene, an essential component of the thermogenic brown adipocyte phenotype," *The Journal of Biological Chemistry*, vol. 286, no. 19, pp. 16958–16966, 2011.
- [51] O. M. Palacios, J. J. Carmona, S. Michan et al., "Diet and exercise signals regulate SIRT3 and activate AMPK and PGC-1 $\alpha$  in skeletal muscle," *Aging*, vol. 1, no. 9, pp. 771–783, 2009.
- [52] M. D. Hirschey, T. Shimazu, E. Jing et al., "SIRT3 deficiency and mitochondrial protein hyperacetylation accelerate the development of the metabolic syndrome," *Molecular Cell*, vol. 44, no. 2, pp. 177–190, 2011.
- [53] R. Tao, M. C. Coleman, J. D. Pennington et al., "Sirt3-mediated deacetylation of evolutionarily conserved lysine 122 regulates MnSOD activity in response to stress," *Molecular Cell*, vol. 40, no. 6, pp. 893–904, 2010.
- [54] X. Qiu, K. Brown, M. D. Hirschey, E. Verdin, and D. Chen, "Calorie restriction reduces oxidative stress by SIRT3-mediated SOD2 activation," *Cell Metabolism*, vol. 12, no. 6, pp. 662–667, 2010.
- [55] A. E. Dikalova, H. A. Itani, R. R. Nazarewicz et al., "Sirt3 impairment and SOD2 hyperacetylation in vascular oxidative stress and hypertension," *Circulation Research*, vol. 121, no. 5, pp. 564–574, 2017.
- [56] X. Xie, L. Wang, B. Zhao, Y. Chen, and J. Li, "SIRT3 mediates decrease of oxidative damage and prevention of ageing in porcine fetal fibroblasts," *Life Sciences*, vol. 177, pp. 41–48, 2017.
- [57] R. A. H. van de Ven, D. Santos, and M. C. Haigis, "Mitochondrial sirtuins and molecular mechanisms of aging," *Trends in Molecular Medicine*, vol. 23, no. 4, pp. 320–331, 2017.
- [58] N. R. Sundaresan, S. A. Samant, V. B. Pillai, S. B. Rajamohan, and M. P. Gupta, "SIRT3 is a stress-responsive deacetylase in cardiomyocytes that protects cells from stress-mediated cell death by deacetylation of Ku70," *Molecular and Cellular Biology*, vol. 28, no. 20, pp. 6384–6401, 2008.
- [59] A. Signorile, A. Santeramo, G. Tamma et al., "Mitochondrial cAMP prevents apoptosis modulating Sirt3 protein level and OPA1 processing in cardiac myoblast cells," *Biochimica et Biophysica Acta-Molecular Cell Research*, vol. 1864, no. 2, pp. 355–366, 2017.
- [60] S. A. Samant, H. J. Zhang, Z. Hong et al., "SIRT3 deacetylates and activates OPA1 to regulate mitochondrial dynamics during stress," *Molecular and Cellular Biology*, vol. 34, no. 5, pp. 807–819, 2014.
- [61] A. Cheng, Y. Yang, Y. Zhou et al., "Mitochondrial SIRT3 mediates adaptive responses of neurons to exercise and metabolic and excitatory challenges," *Cell Metabolism*, vol. 23, no. 1, pp. 128–142, 2016.
- [62] T. Bochaton, C. Crola-Da-Silva, B. Pillot et al., "Inhibition of myocardial reperfusion injury by ischemic postconditioning requires sirtuin 3-mediated deacetylation of cyclophilin D," *Journal of Molecular and Cellular Cardiology*, vol. 84, pp. 61–69, 2015.
- [63] R. M. Bell and D. M. Yellon, "There is more to life than revascularization: therapeutic targeting of myocardial ischemia/reperfusion injury," *Cardiovascular Therapeutics*, vol. 29, no. 6, pp. e67–e79, 2011.
- [64] R. M. Parodi-Rullán, X. Chapa-Dubocq, P. J. Rullan, S. Jang, and S. Javadov, "High sensitivity of SIRT3 deficient hearts to ischemia-reperfusion is associated with mitochondrial abnormalities," *Frontiers in Pharmacology*, vol. 8, p. 275, 2017.
- [65] X. He, H. Zeng, and J.-X. Chen, "Ablation of SIRT3 causes coronary microvascular dysfunction and impairs cardiac recovery post myocardial ischemia," *International Journal of Cardiology*, vol. 215, pp. 349–357, 2016.
- [66] M. S. Klishadi, F. Zarei, S. H. Hejazian, A. Moradi, M. Hemati, and F. Safari, "Losartan protects the heart against ischemia reperfusion injury: sirtuin3 involvement," *Journal of Pharmacy & Pharmaceutical Sciences*, vol. 18, no. 1, pp. 112–123, 2015.
- [67] K. M. Baker, G. W. Booz, and D. E. Dostal, "Cardiac actions of angiotensin II: role of an intracardiac renin-angiotensin system," *Annual Review of Physiology*, vol. 54, no. 1, pp. 227–241, 1992.
- [68] B. C. Yang, M. I. Phillips, P. E. J. Ambuehl, L. P. Shen, P. Mehta, and J. L. Mehta, "Increase in angiotensin II type 1 receptor expression immediately after ischemia-reperfusion in isolated rat hearts," *Circulation*, vol. 96, no. 3, pp. 922–926, 1997.



- [69] A. Benigni, D. Corna, C. Zoja et al., "Disruption of the Ang II type 1 receptor promotes longevity in mice," *The Journal of Clinical Investigation*, vol. 119, no. 3, pp. 524–530, 2009.
- [70] R. Parodi-Rullan, G. Barreto-Torres, L. Ruiz, J. Casasnovas, and S. Javadov, "Direct renin inhibition exerts an anti-hypertrophic effect associated with improved mitochondrial function in post-infarction heart failure in diabetic rats," *Cellular Physiology and Biochemistry*, vol. 29, no. 5-6, pp. 841–850, 2012.
- [71] M. Chen, X. Zhu, L. Ran, H. Lang, L. Yi, and M. Mi, "Trimethylamine-N-oxide induces vascular inflammation by activating the NLRP3 inflammasome through the SIRT3-SOD2-mtROS signaling pathway," *Journal of the American Heart Association*, vol. 6, no. 9, article e006347, 2017.
- [72] H. K. Jiang, Y. Miao, Y. H. Wang et al., "Aerobic interval training protects against myocardial infarction-induced oxidative injury by enhancing antioxidant system and mitochondrial biosynthesis," *Clinical and Experimental Pharmacology and Physiology*, vol. 41, no. 3, pp. 192–201, 2014.
- [73] S. Winnik, D. S. Gaul, F. Preitner et al., "Deletion of Sirt3 does not affect atherosclerosis but accelerates weight gain and impairs rapid metabolic adaptation in LDL receptor knock-out mice: implications for cardiovascular risk factor development," *Basic Research in Cardiology*, vol. 109, no. 1, p. 399, 2014.
- [74] N. Frey, H. A. Katus, E. N. Olson, and J. A. Hill, "Hypertrophy of the heart: a new therapeutic target?," *Circulation*, vol. 109, no. 13, pp. 1580–1589, 2004.
- [75] N. R. Sundaresan, S. Bindu, V. B. Pillai et al., "SIRT3 blocks aging-associated tissue fibrosis in mice by deacetylating and activating glycogen synthase kinase 3 $\beta$ ," *Molecular and Cellular Biology*, vol. 36, no. 5, pp. 678–692, 2015.
- [76] V. B. Pillai, S. Samant, N. R. Sundaresan et al., "Honokiol blocks and reverses cardiac hypertrophy in mice by activating mitochondrial Sirt3," *Nature Communications*, vol. 6, p. 6656, 2015.
- [77] T. Chen, J. Liu, N. Li et al., "Mouse SIRT3 attenuates hypertrophy-related lipid accumulation in the heart through the deacetylation of LCAD," *PLoS One*, vol. 10, no. 3, article e0118909, 2015.
- [78] J. M. Grillon, K. R. Johnson, K. Kotlo, and R. S. Danziger, "Non-histone lysine acetylated proteins in heart failure," *Biochimica et Biophysica Acta (BBA) - Molecular Basis of Disease*, vol. 1822, no. 4, pp. 607–614, 2012.
- [79] L. Yu, B. Gong, W. Duan et al., "Melatonin ameliorates myocardial ischemia/reperfusion injury in type 1 diabetic rats by preserving mitochondrial function: role of AMPK-PGC-1 $\alpha$ -SIRT3 signaling," *Scientific Reports*, vol. 7, article 41337, 2017.
- [80] P. Pacher and C. Szabo, "Role of poly(ADP-ribose) polymerase 1 (PARP-1) in cardiovascular diseases: the therapeutic potential of PARP inhibitors," *Cardiovascular Drug Reviews*, vol. 25, no. 3, pp. 235–260, 2007.
- [81] H. Yang, T. Yang, J. A. Baur et al., "Nutrient-sensitive mitochondrial NAD<sup>+</sup> levels dictate cell survival," *Cell*, vol. 130, no. 6, pp. 1095–1107, 2007.
- [82] J. You, Z. Yue, S. Chen et al., "Receptor-interacting protein 140 represses sirtuin 3 to facilitate hypertrophy, mitochondrial dysfunction and energy metabolic dysfunction in cardiomyocytes," *Acta Physiologica*, vol. 220, no. 1, pp. 58–71, 2017.
- [83] A. Nikiforov, C. Dolle, M. Niere, and M. Ziegler, "Pathways and subcellular compartmentation of NAD biosynthesis in human cells: from entry of extracellular precursors to mitochondrial NAD generation," *The Journal of Biological Chemistry*, vol. 286, no. 24, pp. 21767–21778, 2011.
- [84] Z. Yue, Y. Ma, J. You et al., "NMNAT3 is involved in the protective effect of SIRT3 in Ang II-induced cardiac hypertrophy," *Experimental Cell Research*, vol. 347, no. 2, pp. 261–273, 2016.
- [85] X. Tang, X.-F. Chen, H.-Z. Chen, and D.-P. Liu, "Mitochondrial sirtuins in cardiometabolic diseases," *Clinical Science*, vol. 131, no. 16, pp. 2063–2078, 2017.
- [86] Y. C. Lai, D. M. Tabima, J. J. Dube et al., "SIRT3-AMP-activated protein kinase activation by nitrite and metformin improves hyperglycemia and normalizes pulmonary hypertension associated with heart failure with preserved ejection fraction," *Circulation*, vol. 133, no. 8, pp. 717–731, 2016.
- [87] X. Guo, F. Yan, J. Li, C. Zhang, and P. Bu, "SIRT3 attenuates AngII-induced cardiac fibrosis by inhibiting myofibroblasts transdifferentiation via STAT3-NFATc2 pathway," *American Journal of Translational Research*, vol. 9, no. 7, pp. 3258–3269, 2017.
- [88] X. Guo, F. Yan, X. Shan et al., "SIRT3 inhibits Ang II-induced transdifferentiation of cardiac fibroblasts through  $\beta$ -catenin/PPAR- $\gamma$  signaling," *Life Sciences*, vol. 186, pp. 111–117, 2017.
- [89] T. Wei, G. Huang, J. Gao et al., "Sirtuin 3 deficiency accelerates hypertensive cardiac remodeling by impairing angiogenesis," *Journal of the American Heart Association*, vol. 6, no. 8, article e006114, 2017.
- [90] J. L. Zamorano, P. Lancellotti, D. Rodriguez Muñoz et al., "2016 ESC Position Paper on cancer treatments and cardiovascular toxicity developed under the auspices of the ESC Committee for Practice Guidelines The Task Force for cancer treatments and cardiovascular toxicity of the European Society of Cardiology (ESC)," *European Journal of Heart Failure*, vol. 19, no. 1, pp. 9–42, 2017.
- [91] S. Zhang, X. Liu, T. Bawa-Khalife et al., "Identification of the molecular basis of doxorubicin-induced cardiotoxicity," *Nature Medicine*, vol. 18, no. 11, pp. 1639–1642, 2012.
- [92] I. Marques-Aleixo, E. Santos-Alves, D. Mariani et al., "Physical exercise prior and during treatment reduces sub-chronic doxorubicin-induced mitochondrial toxicity and oxidative stress," *Mitochondrion*, vol. 20, pp. 22–33, 2015.
- [93] V. B. Pillai, S. Bindu, W. Sharp et al., "Sirt3 protects mitochondrial DNA damage and blocks the development of doxorubicin-induced cardiomyopathy in mice," *American Journal of Physiology-Heart and Circulatory Physiology*, vol. 310, no. 8, pp. H962–H972, 2016.
- [94] V. W. Dolinsky, "The role of sirtuins in mitochondrial function and doxorubicin-induced cardiac dysfunction," *Biological Chemistry*, vol. 398, no. 9, pp. 955–974, 2017.
- [95] Q. Du, B. Zhu, Q. Zhai, and B. Yu, "Sirt3 attenuates doxorubicin-induced cardiac hypertrophy and mitochondrial dysfunction via suppression of Bnip3," *American Journal of Translational Research*, vol. 9, no. 7, pp. 3360–3373, 2017.
- [96] J. B. Lin, S. Kubota, N. Ban et al., "NAMPT-mediated NAD<sup>+</sup> biosynthesis is essential for vision in mice," *Cell Reports*, vol. 17, no. 1, pp. 69–85, 2016.
- [97] Y. Zeng, K. Yang, F. Wang et al., "The glucagon like peptide 1 analogue, exendin-4, attenuates oxidative stress-induced



- retinal cell death in early diabetic rats through promoting Sirt1 and Sirt3 expression," *Experimental Eye Research*, vol. 151, pp. 203–211, 2016.
- [98] S. Balaiya, K. K. Abu-Amero, A. A. Kondkar, and K. V. Chalam, "Sirtuins expression and their role in retinal diseases," *Oxidative Medicine and Cellular Longevity*, vol. 2017, Article ID 3187594, 11 pages, 2017.
- [99] E. Jing, B. Emanuelli, M. D. Hirschey et al., "Sirtuin-3 (Sirt3) regulates skeletal muscle metabolism and insulin signaling via altered mitochondrial oxidation and reactive oxygen species production," *Proceedings of the National Academy of Sciences of the United States of America*, vol. 108, no. 35, pp. 14608–14613, 2011.
- [100] Y. Guan, Z.-J. Cui, B. Sun, L.-P. Han, C.-J. Li, and L.-M. Chen, "Celastrol attenuates oxidative stress in the skeletal muscle of diabetic rats by regulating the AMPK-PGC1 $\alpha$ -SIRT3 signaling pathway," *International Journal of Molecular Medicine*, vol. 37, no. 5, pp. 1229–1238, 2016.
- [101] L. Shi, T. Zhang, Y. Zhou et al., "Dihydromyricetin improves skeletal muscle insulin sensitivity by inducing autophagy via the AMPK-PGC-1 $\alpha$ -Sirt3 signaling pathway," *Endocrine*, vol. 50, no. 2, pp. 378–389, 2015.
- [102] W. Yu, B. Gao, N. Li et al., "Sirt3 deficiency exacerbates diabetic cardiac dysfunction: role of Foxo3A-Parkin-mediated mitophagy," *Biochimica et Biophysica Acta-Molecular Basis of Disease*, vol. 1863, no. 8, pp. 1973–1983, 2017.
- [103] X. Hou, H. Zeng, X. He, and J.-X. Chen, "Sirt3 is essential for apelin-induced angiogenesis in post-myocardial infarction of diabetes," *Journal of Cellular and Molecular Medicine*, vol. 19, no. 1, pp. 53–61, 2015.
- [104] M. Zhang, J. Lin, S. Wang et al., "Melatonin protects against diabetic cardiomyopathy through Mst1/Sirt3 signaling," *Journal of Pineal Research*, vol. 63, no. 2, 2017.
- [105] M. R. Sultana, P. K. Bagul, P. B. Katare, S. Anwar Mohammed, R. Padiya, and S. K. Banerjee, "Garlic activates SIRT-3 to prevent cardiac oxidative stress and mitochondrial dysfunction in diabetes," *Life Sciences*, vol. 164, pp. 42–51, 2016.
- [106] S. S. Vadvalkar, S. Matsuzaki, C. A. Eyster et al., "Decreased mitochondrial pyruvate transport activity in the diabetic heart role of mitochondrial pyruvate carrier 2 (MPC2) acetylation," *The Journal of Biological Chemistry*, vol. 292, no. 11, pp. 4423–4433, 2017.
- [107] A. Faria and S. J. Persaud, "Cardiac oxidative stress in diabetes: mechanisms and therapeutic potential," *Pharmacology & Therapeutics*, vol. 172, pp. 50–62, 2017.
- [108] W. C. Stanley, E. R. Dabkowski, R. F. Ribeiro, and K. A. O'Connell, "Dietary fat and heart failure: moving from lipotoxicity to lipoprotection," *Circulation Research*, vol. 110, no. 5, pp. 764–776, 2012.
- [109] Y. Zhou, A. C. K. Chung, R. Fan et al., "Sirt3 deficiency increased the vulnerability of pancreatic beta cells to oxidative stress-induced dysfunction," *Antioxidants & Redox Signaling*, vol. 27, no. 13, pp. 962–976, 2017.
- [110] M. H. Forouzanfar, A. Afshin, L. T. Alexander et al., "Global, regional, and national comparative risk assessment of 79 behavioural, environmental and occupational, and metabolic risks or clusters of risks, 1990–2015: a systematic analysis for the Global Burden of Disease Study 2015," *The Lancet*, vol. 388, no. 10063, pp. 1659–1724, 2016.
- [111] G. B. Waypa, S. W. Osborne, J. D. Marks, S. K. Berkelhamer, J. Kondapalli, and P. T. Schumacker, "Sirtuin 3 deficiency does not augment hypoxia-induced pulmonary hypertension," *American Journal of Respiratory Cell and Molecular Biology*, vol. 49, no. 6, pp. 885–891, 2013.
- [112] N. Trevino-Saldana and G. Garcia-Rivas, "Regulation of sirtuin-mediated protein deacetylation by cardioprotective phytochemicals," *Oxidative Medicine and Cellular Longevity*, vol. 2017, Article ID 1750306, 16 pages, 2017.
- [113] B. N. M. Zordoky, I. M. Robertson, and J. R. B. Dyck, "Pre-clinical and clinical evidence for the role of resveratrol in the treatment of cardiovascular diseases," *Biochimica et Biophysica Acta-Molecular Basis of Disease*, vol. 1852, no. 6, pp. 1155–1177, 2015.
- [114] G. Han, J. Xia, J. Gao, Y. Inagaki, W. Tang, and N. Kokudo, "Anti-tumor effects and cellular mechanisms of resveratrol," *Drug Discoveries & Therapeutics*, vol. 9, no. 1, pp. 1–12, 2015.
- [115] T. Chen, J. Li, J. Liu et al., "Activation of SIRT3 by resveratrol ameliorates cardiac fibrosis and improves cardiac function via the TGF- $\beta$ /Smad3 pathway," *American Journal of Physiology-Heart and Circulatory Physiology*, vol. 308, no. 5, pp. H424–H434, 2015.
- [116] M. Zhang, Z. Zhao, M. Shen et al., "Polydatin protects cardiomyocytes against myocardial infarction injury by activating Sirt3," *Biochimica et Biophysica Acta (BBA) - Molecular Basis of Disease*, vol. 1863, no. 8, pp. 1962–1972, 2017.
- [117] A. R. Coelho, T. R. Martins, R. Couto et al., "Berberine-induced cardioprotection and Sirt3 modulation in doxorubicin-treated H9c2 cardiomyoblasts," *Biochimica et Biophysica Acta (BBA) - Molecular Basis of Disease*, vol. 1863, no. 11, pp. 2904–2923, 2017.
- [118] V. B. Pillai, A. Kanwal, Y. H. Fang et al., "Honokiol, an activator of Sirtuin-3 (SIRT3) preserves mitochondria and protects the heart from doxorubicin-induced cardiomyopathy in mice," *Oncotarget*, vol. 8, no. 21, pp. 34082–34098, 2017.
- [119] C. Zhao, T. Sakaguchi, K. Fujita et al., "Pomegranate-derived polyphenols reduce reactive oxygen species production via SIRT3-mediated SOD2 activation," *Oxidative Medicine and Cellular Longevity*, vol. 2016, Article ID 2927131, 9 pages, 2016.
- [120] N. Hu, J. Ren, and Y. Zhang, "Mitochondrial aldehyde dehydrogenase obliterates insulin resistance-induced cardiac dysfunction through deacetylation of PGC-1 $\alpha$ ," *Oncotarget*, vol. 7, no. 47, pp. 76398–76414, 2016.
- [121] J. Liu, Y. Tang, Z. Feng et al., "Acetylated FoxO1 mediates high-glucose induced autophagy in H9c2 cardiomyoblasts: regulation by a polyphenol (–)-epigallocatechin-3-gallate," *Metabolism-Clinical and Experimental*, vol. 63, no. 10, pp. 1314–1323, 2014.
- [122] J. Xiao, X. Sheng, X. Zhang, M. Guo, and X. Ji, "Curcumin protects against myocardial infarction-induced cardiac fibrosis via SIRT1 activation in vivo and in vitro," *Drug Design Development and Therapy*, vol. 10, pp. 1267–1277, 2016.
- [123] H. Tronchere, M. Cinato, A. Timotin et al., "Inhibition of PIKfyve prevents myocardial apoptosis and hypertrophy through activation of SIRT3 in obese mice," *EMBO Molecular Medicine*, vol. 9, no. 6, pp. 770–785, 2017.
- [124] M. Zhai, B. Li, W. Duan et al., "Melatonin ameliorates myocardial ischemia reperfusion injury through SIRT3-dependent regulation of oxidative stress and apoptosis," *Journal of Pineal Research*, vol. 63, no. 2, 2017.
- [125] J. Hu, L. Zhang, Y. Yang et al., "Melatonin alleviates postinfarction cardiac remodeling and dysfunction by inhibiting Mst1," *Journal of Pineal Research*, vol. 62, no. 1, 2017.

- [126] W. Xia and K. Geng, "A sirtuin activator and an anti-inflammatory molecule—multifaceted roles of adjuvin and its potential applications for aging-related diseases," *Seminars in Cell & Developmental Biology*, vol. 59, pp. 71–78, 2016.
- [127] F. Yang, L. Zhou, D. Wang, Z. Wang, and Q. Y. Huang, "Minocycline ameliorates hypoxia-induced blood–brain barrier damage by inhibition of HIF-1 $\alpha$  through SIRT-3/PHD-2 degradation pathway," *Neuroscience*, vol. 304, pp. 250–259, 2015.
- [128] M. Kobayashi, K. Takeda, T. Narita et al., "Mitochondrial intermediate peptidase is a novel regulator of sirtuin-3 activation by caloric restriction," *FEBS Letters*, vol. 591, no. 24, pp. 4067–4073, 2017.
- [129] N. Diaz-Morales, S. Rovira-Llopis, C. Bañuls et al., "Does metformin protect diabetic patients from oxidative stress and leukocyte-endothelium interactions?," *Antioxidants & Redox Signaling*, vol. 27, no. 17, pp. 1439–1445, 2017.
- [130] R. H. Houtkooper and J. Auwerx, "Exploring the therapeutic space around NAD<sup>+</sup>," *Journal of Cell Biology*, vol. 199, no. 2, pp. 205–209, 2012.
- [131] J. Yoshino, K. F. Mills, M. J. Yoon, and S. Imai, "Nicotinamide mononucleotide, a key NAD<sup>+</sup> intermediate, treats the pathophysiology of diet- and age-induced diabetes in mice," *Cell Metabolism*, vol. 14, no. 4, pp. 528–536, 2011.
- [132] W. T. Harkcom, A. K. Ghosh, M. S. Sung et al., "NAD<sup>+</sup> and SIRT3 control microtubule dynamics and reduce susceptibility to antimicrotubule agents," *Proceedings of the National Academy of Sciences of the United States of America*, vol. 111, no. 24, pp. E2443–E2452, 2014.
- [133] A. P. Gomes, N. L. Price, A. J. Y. Ling et al., "Declining NAD<sup>+</sup> induces a pseudohypoxic state disrupting nuclear-mitochondrial communication during aging," *Cell*, vol. 155, no. 7, pp. 1624–1638, 2013.
- [134] K. D. Brown, S. Maqsood, J. Y. Huang et al., "Activation of SIRT3 by the NAD<sup>+</sup> precursor nicotinamide riboside protects from noise-induced hearing loss," *Cell Metabolism*, vol. 20, no. 6, pp. 1059–1068, 2014.
- [135] B. R. Sabari, D. Zhang, C. D. Allis, and Y. Zhao, "Metabolic regulation of gene expression through histone acylations," *Nature Reviews Molecular Cell Biology*, vol. 18, no. 2, pp. 90–101, 2017.
- [136] M. Gertz and C. Steegborn, "Using mitochondrial sirtuins as drug targets: disease implications and available compounds," *Cellular and Molecular Life Sciences*, vol. 73, no. 15, pp. 2871–2896, 2016.
- [137] C. Schölz, B. T. Weinert, S. A. Wagner et al., "Acetylation site specificities of lysine deacetylase inhibitors in human cells," *Nature Biotechnology*, vol. 33, no. 4, pp. 415–423, 2015.
- [138] J. Lu, H. Zhang, X. Chen et al., "A small molecule activator of SIRT3 promotes deacetylation and activation of manganese superoxide dismutase," *Free Radical Biology & Medicine*, vol. 112, pp. 287–297, 2017.
- [139] Y. H. Jung, H. J. Lee, J. S. Kim, S. J. Lee, and H. J. Han, "EphB2 signaling-mediated Sirt3 expression reduces MSC senescence by maintaining mitochondrial ROS homeostasis," *Free Radical Biology & Medicine*, vol. 110, pp. 368–380, 2017.
- [140] Y. Chen, C. Chen, B. Dong et al., "AMPK attenuates ventricular remodeling and dysfunction following aortic banding in mice via the Sirt3/oxidative stress pathway," *European Journal of Pharmacology*, vol. 814, pp. 335–342, 2017.
- [141] V. T. Vachharajani, T. Liu, X. Wang, J. J. Hoth, B. K. Yoza, and C. E. McCall, "Sirtuins link inflammation and metabolism," *Journal of Immunology Research*, vol. 2016, Article ID 8167273, 10 pages, 2016.
- [142] P. Cheng, W. Zeng, L. Li et al., "PLGA-PNIPAM microspheres loaded with the gastrointestinal nutrient NaB ameliorate cardiac dysfunction by activating Sirt3 in acute myocardial infarction," *Advanced Science*, vol. 3, no. 12, article 1600254, 2016.
- [143] S. P. Singh, J. Schragenheim, J. Cao, J. R. Falck, N. G. Abraham, and L. Bellner, "PGC-1  $\alpha$  regulates HO-1 expression, mitochondrial dynamics and biogenesis: role of epoxyeicosatrienoic acid," *Prostaglandins & Other Lipid Mediators*, vol. 125, pp. 8–18, 2016.
- [144] W. Sun, L. Zhao, X. Song et al., "MicroRNA-210 modulates the cellular energy metabolism shift during H<sub>2</sub>O<sub>2</sub>-induced oxidative stress by repressing ISCU in H9c2 cardiomyocytes," *Cellular Physiology and Biochemistry*, vol. 43, no. 1, pp. 383–394, 2017.
- [145] X. Chen and M. Rosbash, "MicroRNA-92a is a circadian modulator of neuronal excitability in *Drosophila*," *Nature Communications*, vol. 8, article 14707, Article ID 28276426, 2017.
- [146] R. C. Poulsen, H. J. Knowles, A. J. Carr, and P. A. Hulley, "Cell differentiation versus cell death: extracellular glucose is a key determinant of cell fate following oxidative stress exposure," *Cell Death & Disease*, vol. 5, no. 2, article e1074, 2014.
- [147] Y. Cheng, J. Mai, T. Hou, and J. Ping, "MicroRNA-421 induces hepatic mitochondrial dysfunction in non-alcoholic fatty liver disease mice by inhibiting sirtuin 3," *Biochemical and Biophysical Research Communications*, vol. 474, no. 1, pp. 57–63, 2016.